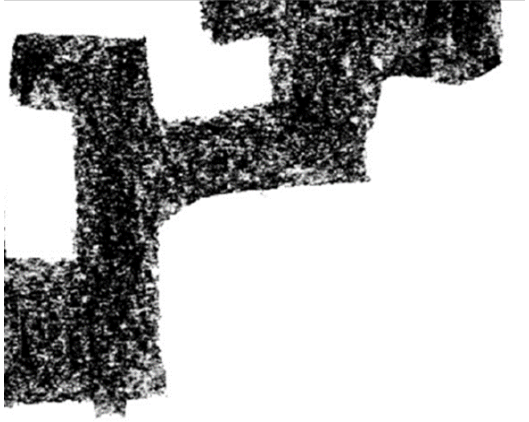

eman ta zabal zazu

Universidad del País Vasco

Euskal Herriko Unibertsitatea

Elucidating Angelman **syndrome**'s molecular mechanisms by identifying the substrates, interactors and counteracting DUBs of UBE3A

NAGORE ELU ARANTZAMENDI

2022

ESKER ONAK

Bidaia oro bezala, amaierara iritsi naiz. Tesi honetan murgildu nintzenean ez nuen inolaz ere pentsatuko horrenbeste bizipen eskainiko zizkidanik, baina halaxe izan da. Ez da izan ikerketa lan huts bat; pertsona, leku eta oroimenez betetako bidaia luze bat baizik, beraz mila esker ibilbide honetan parte hartu duzuen guztioi.

Lehenik eta behin, eskerrik asko Ugo esperientzia hau bizitzeko aukera emateagatik. Pribilegio bat izan da urte hauek zure gidaritzapean ematea eta zientzia zurekin eraikitzea. Eskerrik asko baita ere doktoregoaren alderdi politenak bizitzeko aukera emateagatik; atzerrira zientzia komunikatzera joateko aukera oro aprobetxatzera bultzatu nauzu, eta esperientzia izugarria izan da.

Nerea, mila esker hor egoteagatik. Beti. Edozer gauzatarako. Ezingo nuke imajinatu zuzendarikide hoberik! Ez dakit nola eskertu eman didazun laguntza guztia.

Mila esker baita ere laborategiko kideoi, Juanma, Benoit, Cristina, Unai eta Natalia. Eskerrik asko bidaia honetan zuen laguntza emateagatik, jaso ditudan gomendioengatik, eta egunerokotasuna horren ona egiteagatik. Gustuko lekuan aldaparik ez, ba giro onean, oraindik gutxiago! Eskerrik asko Jabi, primerako auzokidea izan zara, eta urte hauetan pasatu ditugun momentuak altxorra lez gordeta daramatzat.

Jesus Mari, graduan ezagutu ginen, eta gure bizitzak behin baino gehiagotan gurutzatu izan dira zorionez. Zure gomendioengatik ez balitz, ez nintzateke ikerketa talde honetan egongo, beraz mila esker bidea egiteagatik. Espero dut bidegurutze gehiagotan elkar topatzea, eta zientzian ez bada ere, badakit urtean behin elkar ikusiko dugula. Miren Josu eta Kerman, eskerrik asko zuei ere eskainitako laguntza guztiagatik, kafe-tartetxoengatik eta hasieratik horren harrera ona egiteagatik.

Eskerrak eman nahi dizkiet baita ere Ondarru aldeko lagun guztiei, asko zarete, baina zuetariko bakoitzak badakizue zenbat eskertu dudan urte hauetan eman didazuen berotasuna.

Asier, mila esker hor egoteagatik eta bidaia hau gozotzeagatik. Tesia zurea ere bada. Gaian aditua izan gabe eman didazun laguntza guztiagatik, momentu txarrak jasateagatik, eta uneoro irribarre bat ateratzeagatik, eskerrik asko, mundiala zara!

Eta nola ez, eskerrik asko aita, ama eta Aitor. Zuek izan zarete momentu oro hor egon zaretenak, eta Tesi-bidaia hau zuen azalean sentitu duzuenak. Mila esker horren inplikatuta egoteagatik, momentu eskasetan dena ondo joango zela sinestarazteagatik, eta momentu politetan nire poztasuna zuena balitz bezala sentitzeagatik. Ama, orain bai, atera ezazu xanpaina! Matxe-matxe!

EDUKIAK / TABLE OF CONTENTS

I. Laburdurak / Abbreviations 1

II. Figurak eta Taulak / Figures and Tables 7

III. Summary 12

IV. Laburpena 14

V. Sarrera / Introduction 16

1. Ubikitina Proteasoma Sistema 17

1.1 Ubikitina-proteasoma sistemako osagaiak 19

1.2 Ubikitinazio-motak eta funtzioak 35

1.3 UPS: gaixotasunak eta itu terapeutikoak 38

2. Angelman sindromea 41

2.1 Oinarri genetikoa 42

2.2 UBE3A E3 ligasa 45

2.2.1 UBE3Aren substratuak 47

2.2.2 UBE3A: isoformak, egitura eta lokalizazioa 50

2.3 Angelman sindromeari aurre egiteko estrategiak, terapiak eta tratamendu farmakologikoak 53

2.4 Angelman sindromea ikertzeko animalia modeloak 54

2.4.1 Modelo murinoak 55

2.4.2 *Drosophila melanogaster* eulia 57

3. Ubikitinazioa ikertzeko metodologia 62

3.1 Ubikitinatutako materiala aberasteko estrategiak 62

3.1.1 BioUb sistema 65

3.1.2 GFP pull-down estrategia baldintza denaturalizatzaileetan. 67

3.2 Proteinen arteko elkarrekintzak ikertzeko estrategiak 68

3.2.1 BioID2 estrategia 69
3.3 Masa espektrometria 71
VI. Hipotesiak eta Helburuak / Hypothesis and Objectives 75
VII. Material eta metodoak / Materials and Methods 77
1. Biologia molekularra 78
2. Zelulen kultiboak eta transfekzioak 82
2.1 UBE3A substratuen balioztatzea 83
2.2 Ubikitinazio-guneak eta ubikitina kate-motak 84
2.3 Giza DUBen baheketa 84
3. GFP *pull-down* protokoloa 85
3.1 Protokolo zorrotza ubikitinazioa ikertzeko 85
3.2 Protokolo leuna interaktoreak identifikatzeko 85
4. BioID2 *pull-down* protokoloa 86
5. Western plapaketa eta zilar tindaketa 87
5.1 Antigorputzak 87
5.2 Western plapaketa 87
5.3 Zilar tindaketa 88
6. Masa espektrometria: laginen prestaketa, datuen bilketa eta analisia 88
6.1 *In-gel* tripsina bidezko digestioa eta peptioen erauzketa 88
6.2 LC-MS/MS analisia 89
6.3 Datuen prozesamendua eta analisi bioinformatikoa 90
7. *Drosophila melanogaster* eulien igotze-abiaduraren testa 90
8. UBE3Aren purifikazioa eta kristalizazioa 91
8.1 Bakterioen transformazioa eta proteinaren adierazpena 91
8.2 Afinitate purifikazioa eta mozketa 92

8.3 Ioi-trukeko kromatografia 92
8.4 Gel-iragazpeneko kromatografia 92
8.5 Aurre-kristalizazio testa 93
8.6 Kristalizazioa 93
9. Saguen portaera 94
9.1 Ultrasoinu-bokalizazioak 94
9.2 *Elkarganako elkarrekintza sozialaren* testa 94
9.3 *Eremu irekiaren* testa 95
9.4 *Grooming*-a 95
9.5 *Hiru ganberako* testa 95
9.6 *Argi-ilunpe* testa 95
9.7 *Plaka beroaren* testa 96
VIII. Results 97
1. Validation and characterization of candidate UBE3A substrates 98
1.1 Validation of previously identified UBE3A substrates 99
1.1.1 DDI1/DDI2 101
1.1.2 PSMA5 107
1.1.3 MINDY2 110
1.1.4 UBE2L3 113
1.1.5 BLMH 116
1.1.6 TAX1BP1 117
1.1.7 Substrate expression and cellular localization 119
1.1.8 Interaction between UBE3A and validated substrates 121
1.2 Characterization of human DDI1 and DDI2 ubiquitination 122
1.2.1 Ubiquitination sites on hDDI1 127
1.2.2 Ubiquitin chain-types on hDDI1 131

1.2.3 Ubiquitination sites on hDDI2 132
1.2.4 Ubiquitin chain-types on hDDI2 136
1.2.5 hDDI1 vs hDDI2 137
2. Identification and validation of UBE3A counteracting DUBs 139
2.1 Screening for human UBE3A counteracting DUBs 141
2.2 Validation of candidates USP7, USP9X, USP42 and UCHL5 143
2.3 Inhibition of USP9X using WP1130 drug 146
2.4 WP1130 treatment in *Drosophila melanogaster* flies 148
2.5 Changes in protein ubiquitination upon WP1130 treatment in *Drosophila melanogaster* 149
2.6 Inhibition of USP9X using FT709 drug 155
3. *In vivo* identification of UBE3A interactors 158
4. Determination of the human full-length UBE3A structure 171
4.1 hUBE3A expression in bacteria 173
4.2 Purification 174
4.2.1 Affinity purification 174
4.2.2 Cleaveage 176
4.2.3 Q-HP: ion-exchange chromatography 177
4.2.4 Gel filtration chromatography 180
4.3 Crystallization 182
4.3.1 Pre-crystallization test 182
4.3.2 Screening for crystallization conditions 183
4.3.3 Structure determination 184
5. UBE3A gainadierazten duten saguen portaeraren karakterizazioa 185
5.1 Portaera soziala 187

5.2 Aktibitate lokomotorea 190
5.3 Portaera errepikakorrak 192
5.4 Minarekiko sentikortasuna 192
IX. Discussion 194
X. Ondorioak 217
XI. References 220

I.

LABURDURAK

ACC	Acetyl-CoA carboxylase
AHNAK	Neuroblast differentiation-associated protein AHNAK
AIB1	Amplified in breast cancer 1 protein
ALOX12B	Arachidonate 12-lipoxygenase, 12R-type
AMPA	α-amino-3-hydroxy-5-methyl-4-isoxazolepropionic acid
ARFGAP1	ADP-ribosylation factor GTPase-activating protein 1
AS	Angelman syndrome
AS-IC	Angelman syndrome imprinting center
ASPM	Abnormal spindle-like microcephaly-associated protein
ASD	Autism spectrum disorder
ATP	Adenosine 5'-triphosphate
APBB1	Amyloid beta precursor protein binding family B member 1
APF-1	ATP-dependent proteolysis factor 1
Arc	Activity-regulated cytoskeleton-associated protein
AZUL	Amino-terminal Zn-finger of Ube3a Ligase
Bak1	BCL2 antagonist/killer 1
BAP1	BRCA1 associated protein 1
BICD2	Protein bicaudal D homolog 2
BirA	Bifunctional ligase/repressor BirA
BioID	Proximity-dependent biotin identification
BLHM	Bleomycin hydrolase
Blk	B Lymphoid tyrosine kinase
BP	Breaking point
CDK	Cyclin-dependent kinase
CoRest	REST corepressor
CP	Core protein
CTTN	Src substrate cortactin
DBN1	Drebrin
Ddi1	DNA damage inducible protein 1 (yeas)
DDI1	DNA damage inducible 1 homolog 1 (human)
DDI2	DNA damage inducible 1 homolog 2 (human)
DMSO	Dimethyl sulfoxide
Dsk2	Dominant suppressor of kar1
DUB	Deubiquitinase

E1	Ubiquitin-activating enzyme
E2	Ubiquitin-conjugating enzyme
E3	Ubiquitin-ligase enzyme
E6-AP	*E6*-associated protein (see UBE3A)
EPS15L1	Epidermal growth factor receptor substrate 15-like 1
ERAD	Endoplasmic-reticulum-associated protein degradation
ERK	Extracellular signal-regulated kinases
EIF4B	Eukaryotic translation initiation factor 4B
Faf	Probable ubiquitin carboxyl-terminal hydrolase *faf*
FLNA	Filamin-A
GABA	Gamma-aminobutyric acid
GABRA5	Gamma-aminobutyric acid type A receptor subunit Alpha5
GABRB3	Gamma-aminobutyric acid type A receptor subunit Beta3
GABRG3	Gamma-aminobutyric acid type A receptor subunit Gamma3
GAL4	Galactose metabolism transcription factor
GEF	Guanine nucleotide exchange factor
GFP	Green fluorescent protein
GSH	Glutathion
GST	Glutathione S-transferase
HBA1	Hemoglobin subunit alpha
HECT	Homologous to the E6-AP carboxyl terminus
HEK293T	Human embryonic kidney 293 cells
HERC	HECT domain and RCC1-like domain-containing protein
HHR23A	UV excision repair protein RAD23 homolog A
HSPA5	Endoplasmic reticulum chaperone BiP
IGF2R	Cation-independent mannose-6-phosphate receptor
iTRAQ	Isobaric tag for relative and absolute quantitation
JAMM	JAB1/M/PNMOV34 proteases
KIF5B	Kinesin-1 heavy chain
LAMTOR1	Late endosomal/lysosomal adaptor, MAPK and MTOR activator 1
LC-MS/MS	Liquid chromatography-tandem mass spectrometry
LFQ	Label free quantification
LIMD1	LIM domain-containing protein 1
LTV1	Protein LTV1 homolog

MAP4	Microtubule-associated protein 4
MC1R	Melanocortin 1 receptor
MCCC1	Methylcrotonyl-CoA Carboxylase
MEK	Mitogen-activated protein kinase kinase
mGluR	Metabotropic glutamate receptor
MINDY	Motif interacting with Ub containing novel DUB family
MINDY-2	Ubiquitin carboxyl-terminal hydrolase MINDY-2 (see FAM63B)
MJD	Machado-Joseph disease proteases
MS	Mass spectrometry
MS/MS	Tandem mass spectrometry
NEDD4	Neural precursor cell expressed developmentally down-regulated protein 4
NF-kB	Nuclear factor *kappa*-light-chain-enhancer of activated B cells
Nrf1	Endoplasmic reticulum membrane sensor (see NFE2L1)
NTA	Nitrilotriacetic acid
OTU	Ovarian tumour proteases
P27	Cyclin-dependent kinase inhibitor p27
P53	Tumor protein P53
Pbl	Pebble
PC	Piruvate carboxilase
PCT	Pre-crystallization test
PIP	Phosphatidylinositol 5-phosphate 4-kinase type-2 alpha
PPP6R1	Serine/threonine-protein phosphatase 6 regulatory subunit 1
PPP6R3	Serine/threonine-protein phosphatase 6 regulatory subunit 3
PSMA5	Proteasome subunit alpha type-5
PSMD4	Proteasome 26S subunit ubiquitin receptor, non-ATPase 4 (see Rpn10)
PTM	Post-translational modifications
PW-IC	Prader Willi imprinting center
Rad23	Radiation sensitivity abnormal 23
RBR	RING-between-RING
RING	Really interesting new gene
Ring1B	RING finger protein 1B
Rngo	Rings lost

RP	Regulatory particle
Rpn10	Regulatory particle non-ATPase 10 (see PSMD4)
Rpn1, 2, 10, 11, 13	Regulatory particle non-ATPase 1, 2, 10, 11, 13
RPS27	Ribosomal protein S27
Rpt1-6	Proteasome regulatory particle base subunit RPT1-6
RRM2	Ribonucleoside-diphosphate reductase subunit M2
RVP	Aspartyl protease-like domain
S100A11	Protein S100-A11
SDS-PAGE	Sodium dodecyl sulphate–polyacrylamide gel electrophoresis
SEC	Size exclusion chromatography
SENP	Sentrin/SUMO-specific protease
SFN	14-3-3 protein sigma
SH-SY5Y	Human neuroblastoma cell line
SILAC	Stable isotope labeling by amino acids in cell culture
SLC3A2	4F2 cell-surface antigen heavy chain
SLK	STE20-like serine/threonine-protein kinase
SNARE	Soluble NSF attachment protein receptor
SNRPN	Small nuclear ribonucleoprotein polypeptide N
SNURF	SNRPN upstream open reading frame
SRP68	Signal recognition particle subunit SRP68
STAU1	Double-stranded RNA-binding protein Staufen homolog 1
SUMO	Small ubiquitin-like modifier
SYAP1	Synapse-associated protein 1
T6BP	TRAF6-binding protein (see TAX1BP1)
TAX1BP1	Tax1-binding protein 1 (see T6BP)
TBC1D5	TBC1 domain family member 5
TEV	Tobacco Etch Viral protease
TLN1	Talin-1
TMT	Tandem Mass Tag (TMT) system
TNF	Tumor necrosis factor
TOF	Time of Flight
TXLNA	Alpha-taxilin
UAS	Upstream activating sequence

UBA	Ubiquitin associated domain
UBA1	Ubiquitin-like modifier activating enzyme 1
UBA52	Ubiquitin-60S ribosomal protein L40
UBA6	Ubiquitin-like modifier-activating enzyme 6
UBAP2L	Ubiquitin-associated protein 2-like
UBB	Polyubiquitin B
UBC	Polyubiquitin-C
UBC	Ubiquitin-conjugating catalytic domain
UBD	Ubiquitin -binding domain
UBE2L3	Ubiquitin-conjugating enzyme E2 L3 (see UbcH7)
UBE3A	Ubiquitin protein ligase E3A (see E6-AP)
UBE3A-OE	UBE3A over-expression
UBE3A-AS	UBE3A antisense transcript
UBL	Ubiquitin-like domain
UCH	Ubiquitin C-terminal hydrolases
UCH-L1	Ubiquitin C-terminal hydrolase L1
UCH-L3	Ubiquitin C-terminal hydrolase L3
UCH-L5	Ubiquitin C-terminal hydrolase L5
UIM	Ubiquitin-interacting motif
UPD	Paternal uniparental disomy
UPS	Ubiquitin proteosome system
USP	Ubiquitin-specific proteases
Wnt	Wingless-related integration site
WP1130	Degrasyn
Y2H	Yeast Two Hybrid

II.

FIGURAK ETA TAULAK

1. irudia. Ubikitina-proteasoma sistemaren zikloa.
2. irudia. Ugaztunen ubikitina geneak.
3. irudia. RING E3 entzima konjugatzaileen egitura eta funtzionamendua.
4. irudia. HECT motako E3 ligasen egitura eta funtzionamendua.
5. irudia. RING E3 entzima konjugatzaileen egitura eta funtzionamendua.
6. irudia. Deubikitinasen zuhaitz filogenetikoa.
7. irudia. DUBen funtzio nagusiak.
8. irudia. Proteasomaren egitura.
9. irudia. 19S azpiunitate erregulatzailearen egitura.
10. irudia. 20S muinaren egitura.
11. irudia. Ubikitinazio-motak.
12. irudia. Angelman sindromedun indibiduoen ezaugarriak.
13. irudia. UBE3A genearen inpronta-mekanismoa.
14. irudia. Angelman sindromea eragiten duten akats genetikoak.
15. irudia. Legamia, Drosophila, sagu eta gizakien DDI1 homologoen egiturak.
16. irudia. UBE3A proteinaren isoforma ezberdinak sagu eta giza espezieetan.
17. irudia. UBE3A E3 ligasaren egitura.
18. irudia. UBE3A E3 ligasaren AZUL domeinuaren egitura.
19. irudia. *Drosophila melanogaster* euliaren bizi-zikloa.
20. irudia. GAL4/UAS sistema binarioa.
21. irudia. di-Gly sinaduraren sorrera.
22. irudia. BioUb sistema.
23. irudia. GFP *pull-down* estrategia.
24. irudia. BioID2 estrategia.
25. irudia. Proteinen identifikazioa masa-espektrometria bidez.
26. irudia. Thermo Scientific-en Q-Exactive masa espektrometroaren eskema.

Figure 27. Modified GFP pull-down protocol allows the detection of the protein of interest and its ubiquitination pattern.
Figure 28. GFP tag does not disrupt DDI1 ubiquitination.
Figure 29. DDI1 is a UBE3A substrate in HEK293T cells.
Figure 30. DDI1 is a UBE3A substrate in in SH-SY5Y cells.
Figure 31. DDI2 is a UBE3A substrate in HEK293T cells.
Figure 32. PSMA5 is a UBE3A substrate in HEK293T cells.
Figure 33. PSMA5 is a UBE3A substrate in SH-SY5Y cells.

Figure 34. MINDY2 is a UBE3A substrate in HEK293T cells.
Figure 35. MINDY2 is a UBE3A substrate in SH-SY5Y cells.
Figure 36. UBE2L3 is not a UBE3A substrate in HEK293T cells.
Figure 37. UBE2L3 is not a UBE3A substrate in SH-SY5Y cells.
Figure 38. BLMH is not a UBE3A substrate in HEK293T cells.
Figure 39. TAX1BP1 is not a UBE3A substrate in HEK293T cells.
Figure 40. Cellular localization of UBE3A and its validated substrates.
Figure 41. Co-immunoprecipitation of UBE3A and its putative substrates.
Figure 42. Silver and Coomassie staining of DDI1-GFP pull-down elutions.
Figure 43. Schematic diagram of the MS-based procedure used to study ubiquitination sites and ubiquitin chain-types.
Figure 44. Identification of ubiquitinated proteins.
Figure 45. Sequence coverage of hDDI1-GFP sequence.
Figure 46. Representative annotated spectra for K133 hDDI1 diGly modified peptide.
Figure 47. UBE3A ubiquitinates hDDI1 on K133.
Figure 48. UBE3A-dependent ubiquitination of hDDI1-GFP mutants.
Figure 49. UBE3A forms K48 ubiquitin chains on hDDI1.
Figure 50. Sequence coverage for hDDI2.
Figure 51. Representative annotated spectra for K77 DDI2 diGly modified peptide.
Figure 52. UBE3A ubiquitinates hDDI2 on K77.
Figure 53. UBE3A-dependent ubiquitination of hDDI2-GFP mutants.
Figure 54. UBE3A forms K48 chains in hDDI2.
Figure 55. Sequence alignment of human DDI1 and DDI2 sequences.
Figure 56. Screening of 41 human DUBs to search for UBE3A counteracting DUBs.
Figure 57. Candidate DUBs are efficiently silenced.
Figure 58. USP9X deubiquitinates hDDI1.
Figure 59. Time course effect of WP1130 treatment in HEK293T and SH-SY5Y cell lines.
Figure 60. USP9X inhibition by WP1130 enhances DDI1 ubiquitination.
Figure 61. WP1130 treatment in model flies for Angelman syndrome rescues the climbing phenotype.
Figure 62. Isolated ubiquitinated material for mass spectomety analyis.
Figure 63. Ubiquitination of several proteins change in BioUb *Drosophila melanogaster* flies upon WP1130 treatment.

Figure 64. Ubiquitome analysis of WP1130 and DMSO treated Drosophila flies.
Figure 65. USP9X inhibition by FT709 enhances DDI1 poly-ubiquitination.
Figure 66. Biotinylated material for mass spectometry analyis.
Figure 67. Commassie staining and slicing for mass spectrometry analysis.
Figure 68. Overlap between proteins identified in the different conditions.
Figure 69. Multi-correlation graphs of LFQ intensities (in log2 scale) of proteins quantified across the different pull-downs and replicates.
Figure 70. Identification of proteins across different samples.
Figure 71. Experimentally recorded and imputed quantitative data.
Figure 72. Identification of candidate UBE3A interactors in HEK293T cells.
Figure 73. Comparison between UBE3A$^{C\text{-}ter}$ and UBE3A$^{N\text{-}ter}$ conditions to further corroborate UBE3A interactors.
Figure 74. LIMD1 is a UBE3A interactor in HEK293T cells.
Figure 75. Workflow for hUBE3A purification and crystallization.
Figure 76. SDS-PAGE for collected samples during the affinity purification protocol.
Figure 77. SDS-PAGE for samples before and after tag cleaveage.
Figure 78. Ion-exchange chromatography of hUBE3A affinity purified from GST-P2 vector.
Figure 79. Ion-exchange chromatography of hUBE3A affinity purified from His-SUMO vector.
Figure 80. Ion-exchange chromatography of hUBE3A affinity purified from His-P2 vector.
Figure 81. Gel filtration based purification of hUBE3A protein.
Figure 82. Pre-crystallization test of hUBE3A protein.
Figure 83. Alphafold human UBE3A full-length predicted structure.
84. irudia. UBE3A-OE saguek UBE3A emeki gainadierazten dute.
85. irudia. UBE3A-OE saguen ultrasoinu bokalizazio-emisioak normalak dira.
86. irudia. UBE3A-OE saguen elkarrenganako portaera soziala normala da.
87. irudia. Hiru Ganberako testa UBE3A-OE saguen portaera soziala ikertzeko.
88. irudia. UBE3A-OE saguek distantzia luzeagoak egiten dituzte eta abiadura handiagoan mugitzen dira.
89. irudia. UBE3A-OE saguak lehenago pasatzen dira argiztatutako gunera.
90. irudia. UBE3A-OE saguek *grooming* egiteko tendentzia azaltzen dute.
91. irudia. UBE3A-OE saguek minaren aurkako portaera normala dute.

1. taula. UPSko osagai desberdinak eta horiekin erlazionatutako gaixotasun eta ikerketak.

2. taula. Saguen portaera aztertzeko frogarik ohikoenak, zein adin-tartetan burutu behar diren eta horien deskribapena.

3. taula. Tesian zehar erabilitako plasmidoak.

4. taula. Tesian zehar erabilitako abiarazleak.

Table 5. List of putative UBE3A substrates to validate.

Table 6. List of putative UBE3A interactors that fulfill the criteria. A) Criteria to consider UBE3A interactors based on different sample comparison (+++ more abundant, --- less abundant and not detected). B) Putative UBE3A interactors detected by mass spectrometry.

The following supplementary information can be found on the enclosed CD.

Supplementary table 1. hDDI1 ubiquitination sites and ubiquitin chain-types mediated by UBE3A.

Supplementary table 2. hDDI2 ubiquitination sites and ubiquitin chain-types mediated by UBE3A.

Supplementary table 3. Changes in protein ubiquitination upon WP1130 treatment.

Supplementary table 4. Identification of UBE3A interactors using BioID2 strategy.

1. dokumentu osagarria. Kristalizaziorako baldintza ezberdinak: Morpheus, PACT, Amonio sulfato eta Proplex baheketa kitak erabili ditugu.

III.

SUMMARY

Angelman syndrome (AS) is a rare neurological disorder, caused by the lack of functional UBE3A in the brain. UBE3A is an E3 ligase, which ubiquitinates different proteins and determines their function within the cell. Although the gene responsible for the disease was identified years ago, the molecular mechanisms underlying AS have not been yet deciphered. Dr. Mayor's lab has been focused on developing tools to study ubiquitination, and use them to identify UBE3A substrates *in vivo*.

During this Thesis project we have validated UBE3A candidate substrates previously identified in *Drosophila melanogaster* and mice, employing a modified purification strategy –GFP pull-down–. We have further confirmed that this strategy in combination with mass spectrometry can be used to identify ubiquitination sites and ubiquitin chain-types mediated by UBE3A, in any given GFP-tagged substrate. In addition, we have performed a screening of different human deubiquitinases (DUBs) and identified USP9X as an UBE3A counteracting DUB. Upon USP9X inhibition, ubiquitination levels of the UBE3A substrate DDI1 were enhanced, and the phenotype of Angelman syndrome model flies improved significantly. Thus, we suggest USP9X can greatly contribute to the development of future treatments for AS. Moreover, following a mass spectrometry-based approach, we have identified several proteins that changed their ubiquitination upon drug treatment, and could potentially be responsible for improving the AS fly model phenotype. On the other hand, we have identified several UBE3A interactors that may regulate the E3 ligase function. Additionally, we have determined if the interactors bind to either the N-terminal, C-terminal or full length version of UBE3A. Finally, we have established a protocol for successful UBE3A purification with the aim of resolving its full-length structure, and we have characterized the behavior of our mice model that overexpresses UBE3A.

IV.

LABURPENA

Angelman sindromea (AS) gaixotasun neurologiko bakana da, garunean UBE3A funtzionalaren gabeziak sortua. UBE3A E3 ubikitina ligasa bat da, eta bere funtzioa proteina ezberdinak ubikitinatzea da, eta ondorioz, proteina horien patua zehazten du. Gaixotasunaren eragile den genea orain dela urte batzuk identifikatu bazen ere, UBE3Aren gabeziak ASren koadro klinikoa sortzeko mekanismo molekularrak ez dira oraindik argitu. Mayor doktorearen laborategia ubikitinazioa ikertzeko tresnak garatzen zentratu da, horien bidez UBE3Aren substratuak *in vivo* identifikatzeko.

Tesi honetan, aurretiaz *Drosophila melanogaster* eulian eta saguetan identifikatutako UBE3Aren balizko substratuak balioztatu ditugu, horretarako moldatutako purifikazio estrategia bat erabiliz –GFP *pull-down* estrategia–. Halaber, estrategia hori masa espektrometriarekin konbinatuz UBE3Ak edozein substratutan sortutako ubikitina kate-motak eta substratu horien ubikitinazio-guneak identifikatzeko baliogarria dela egiaztatu dugu. Horrez gain, giza deubikitinasa (DUB) ezberdinak testatu ditugu, eta USP9X identifikatu dugu UBE3Aren aurkako funtzioa burutzen duen DUB gisa. USP9Xren inhibizioak UBE3Aren substratu den DDI1 proteinaren ubikitinazioa emendatzen du. Era berean, Angelman sindromearen modelo diren eulien fenotipoa ere hobetzen du, eta horrek, etorkizunean ASrentzako tratamenduak garatzen lagundu dezake. Inhibitzaile horren ondorioz, ubikitinazio-maila aldatzen duten, eta beraz, eulien fenotipoa hobetzearen eragile izan daitezkeen proteinak identifikatu ditugu masa espektrometrian oinarritutako esperimentu baten bidez. UBE3Arekin elkarrekin eta ligasaren funtzioa erregulatu dezaketen hainbat proteina ere identifikatu ditugu, baita proteina horiek UBE3Aren amino muturrarekin, karboxilo muturrarekin edo proteina osoarekin elkarrekiten duten zehaztu ere. Azkenik, UBE3Aren egitura osoa definitzeko helburuarekin, ligasa modu eraginkorrean purifikatzeko protokoloa ezarri dugu, eta UBE3A gainadierazten duten saguen portaera ikertu dugu.

V.

SARRERA

1. Ubikitina-proteasoma sistema

1838an proteinak lehenengoz isolatu zirenetik (Mulder, 1839), urte luzez uste izan da organismoko proteinak molekula egonkorrak zirela, eta soilik dietatik jasotako proteinak degradatzen zirela. Baina 1937an, isotopikoki markatutako konposatuak erabiliz, proteinak etengabe berriztatzen direla behatu zuten. Proteina exogenoek ez ezik, endogenoek ere degradazio-prozesua jasaten dutela ondorioztatu zuten (Schoenheimer et al., 1939). 50. hamarkadan, proteinak degradatzen dituzten lisosomen aurkikuntzarekin batera, ideia berritzaile horrek indarra hartu zuen (de Duve et al., 1955). Hala ere, lisosomen funtzionamenduak ez zuen azaltzen proteinen degradazioan behatutako energia gastu handia (Etlinger eta Goldberg, 1977), ezta ere proteina bakoitzarentzako neurtutako degradazio-abiadura ezberdinak (Goldberg eta St. John, 1976). Hori horrela, lisosometan oinarritzen ez zen, eta ATPren mendekoa zen proteolisi-sistema baten existentzia planteatu zen (Etlinger eta Goldberg, 1977).

80. hamarkadan, Hershkoren laborategiak frogatu zuen proteinak, ATParen mendeko erreakzio baten bidez, beroarekiko egonkorra den peptido batekin (APF-1) kobalenteki eraldatzen direla (Hershko et al., 1980). Gainera, polipeptido hori proteinen degradazioarekin erlazionatu zuten. Hain zuzen ere, aurkikuntza horri esker, 2004. urtean Aaron Ciechanover, Irwin Rose eta Avram Hershko ikerlariek Kimikako Nobel saria jaso zuten (https://www.nobelprize.org/prizes/chemistry/2004/summary/). Aldi berean, beste ikerketa talde batek APF-1 proteina "ubikuoa" zela ikusi zuen, landare- eta animalia-zelulez gain, onddoetan ere aurkitzen baita. Molekula hori da gaur egun ubikitina bezala ezagutzen duguna (Wilkinson et al., 1980).

Ubikitina bidezko proteinen eraldaketari ubikitinazio deritzo, eta zelula barneko proteina gehienak degradaziora bideratzeko mekanismo nagusia da (Ciechanover, 2013). Organismo eukarioto guztietan kontserbatuta dagoen prozesu konplexu horretan hiru proteina motek dihardute modu koordinatuan: E1 ubikitina-aktibatzaileak, E2 ubikitina-konjugatzaileak eta E3 ubikitina-ligasak (Hershko et al., 1980). Lehendabizi, E1 entzimak ubikitina aktibatzen du ATParen mendeko erreakzio baten bidez. Ondoren, aktibatutako ubikitina E2 entzimara transferitzen da, eta azkenik, E2 entzimak, E3 entzimaren laguntzaz, ubikitina

substratura gehitzen du. Kasu batzuetan, zehazki HECT motako E3 ligasen kasuan, ubikitina E2-tik E3-ra pasatzen da, azken horrek substratura gehitu dezan. Aldiz, RING motakoek ez dute ubikitinarekin elkarrekiten; E2 eta substratuarekin batuz ubikitinaren transferentzia errazten dute (1. irudia) (Berndsen eta Wolberger, 2014). Substratura ubikitina bakar bat edo gehiago atxikitzearen arabera, mono- edo poli-ubikitinazioa emango da, hurrenez hurren. Eratutako ubikitina-katearen arabera, proteina horiek zelulako funtzio ezberdinak burutuko dituzte (seinaleztapena, lokalizazioa etab.) (Swatek eta Komander, 2016).

Ubikitinazioa prozesu dinamiko eta itzulgarria da. Zehazki, deubikitinasa (DUB) izenez ezagutzen diren entzimak dira deubikitinazioa katalizatzen dutenak (1. irudia) (Komander, 2009). Hala, ubikitinatutako proteina batek bere funtzioa betetzen duenean, eta deubikitinatu behar denean, DUBak arduratzen dira substratutik ubikitina mozteaz.

Bestalde, proteina horiek gehiago behar ez direnean, proteasomara bideratzen dira, bertan degradatuak izan daitezen. Prozesu horretan ubikitina birziklatu eta ubikitinazio-ziklo berri baterako eskuragarri gelditzen da.

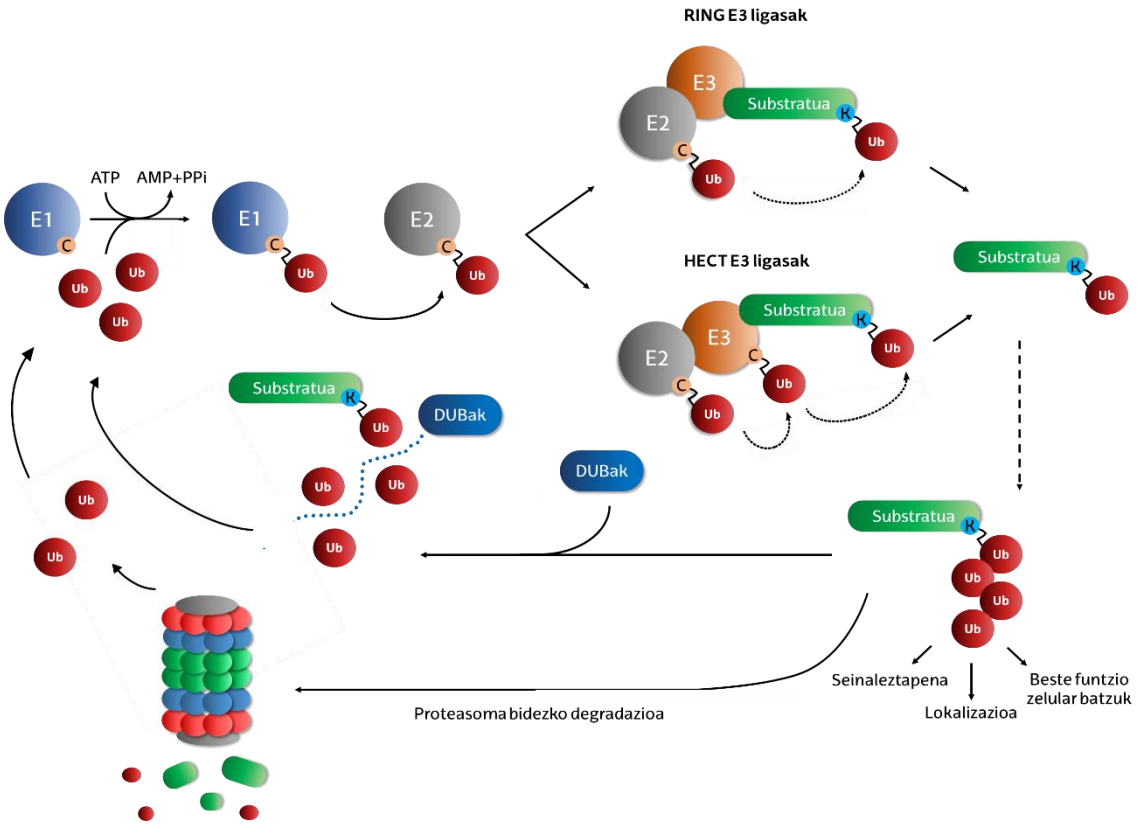

1.irudia. Ubikitina-proteasoma sistemaren zikloa. Ubikitina E1 entzimaren bitartez aktibatzen da ATParen mendeko erreakzio batean. Aktibatutako ubikitina E2 entzima-konjugatzailera transferitzen da. Ubikitinari lotutako E2 entzimak E3 ligasarekin elkarrekiten du ubikitina substratura transferitzeko. Prozesuan parte hartzen duen E3 ligasa motaren arabera, ubikitina zuzenean substratuetara transferitzen da (RING motako E3 ligasen kasuan), edota lehendabizi E3 ligasara batzen da, hortik substratuetara transferitzeko (HECT motako E3 ligasen kasuan). Prozesu horren errepikapen ziklikoen bidez, ubikitina molekula bakar bat (mono-ubikitinazioa) edo gehiago (poli-ubikitinazioa) atxikitzen dira substratuetara. Eratutako poli-ubikitina kate-mota bakoitzak funtzio bat burutzen du; substratuak degradaziora bideratu, seinaleztapen bideak erregulatu, lokalizazioa baldintzatu eta abar. Deubikitinasa entzimak (DUBak) proteinei ubikitina kentzeaz arduratzen dira, eta horri esker ubikuitina birziklatzen da (Ciechanover, 2013-tik moldatuta).

Proteinen ubikitinazioan modu koordinatuan parte hartzen duten entzima guztiek ubikitina-proteasoma sistema (UPS, *Ubiquitin Proteosome System*) osatzen dute, eta bere etengabeko jarduerari esker, zelulako oreka mantentzen da.

Sistema hori deskribatu zenean, ubikitinatutako proteinen patu bakarra proteasoma bidezko degradazioa zela uste zuten (Hershko et al., 1980). Alabaina, gaur egun badakigu proteinen ubikitinazioa gaizki tolestutako edo erabilgarriak ez diren proteinen degradazio eta birziklapenetik haratago doala (Komander and Rape, 2012).

1.1. Ubikitina-proteasoma sistemako osagaiak

1.1.1. Ubikitina

Ubikitina 76 aminoazidoz osatutako polipeptido txikia da (8.5 kDa). Ugaztunen genoman lau gene ezberdinek kodetu dezake, eta kasu guztietan, aintzindari edo pro-proteina bat bezala adierazten da (2. irudia). Lau gene horietatik bik (UBA52 eta RPS27), ubikitina molekula erribosomen biogenesirako ezinbestekoak diren azpiunitate erribosomikoei (L40 eta S27, hurrenez hurren) fusionatuta kodetzen dute (Finley et al., 1989). Aitzitik, beste bi geneek (UBB eta UBC), hurrenez hurren, 3 eta 9 ubikitina molekulaz osatutako poli-ubikitina kate linealak kodetzen dituzte. DUBek (UCHL3, USP5, USP7, USP9X eta Otulin) ubikitinaren aitzindari horiek guztiak digeritu eta zelulan ubikitina molekula bakanak askatzen dituzte (Grou et al., 2015; Kimura eta Tanaka, 2010) (2. irudia).

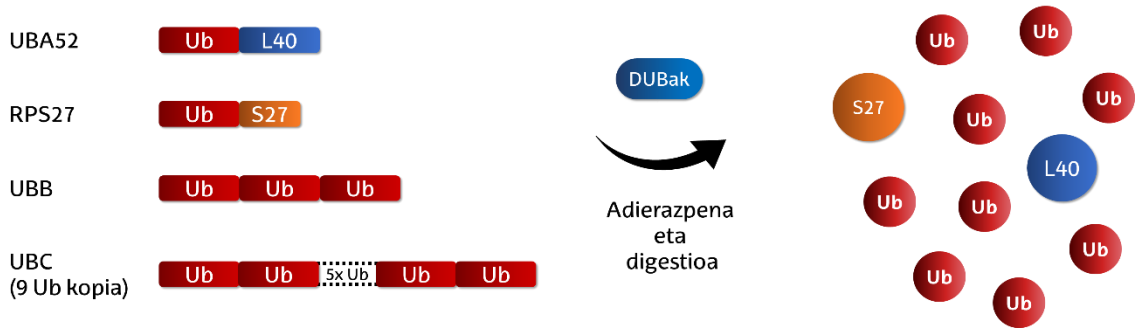

2. irudia. Ugaztunen ubikitina geneak. Ubikitina lau gene ezberdinen bidez kodetzen da. UBA52 geneak ubikitina bakar bat L40 azpiunitate erribosomikoarekin batera kodetzen du. RPS27 geneak, aldiz, ubikitina molekula S27 azpiunitate erribosomikoarekin kodetzen du. UBB eta UBC geneek 3 eta 9 kopiako poli-ubikitina kateak kodetzen dituzte, hurrenez hurren. Lau gene horien adierazpenetik sortutako pro-ubikitina forma guztiak zelularen barneko deubikitinasek digeritu eta berdinak diren ubikitina molekulak askatzen dituzte.

Ubikitina kodetzeko lau gene ezberdin izateak, eta horietako bik poli-ubikitina kateak kodetzeak, agerian uzten du ubikitinaren sintesiak zelularentzako duen garrantzia. Pentsa liteke gene horien artean teilakamendua dagoela, eta guztiak beharrezkoak ez direla. Baina bakar baten gabeziak garapen arazoak, obesitatea edo ubikitina eskasia sor dezake (Ryu et al., 2007, 2008a, 2008b). Are gehiago, UBC genea estresaren mendeko erantzunean ezinbestekoa dela frogatu dute (Pereira et al., 2006; Tsirigotis et al., 2001). Gene erredundantziak zelulan nahi adina ubikitina dagoela ere pentsarazi diezaguke. Alabaina, zelulako ubikitina aske eta erabilgarriaren kantitatea zelularen beharretara estuki doituta dago, nagusiki DUBen bidez (Bianchi et al., 2019; Dantuma et al., 2006; Ryu et al., 2007).

Ubikitina substratuetara lotura isopeptidiko bidez konjugatzen da. Gehienetan, ubikitinaren karboxilo muturra substratuen lisina bateko ε-NH_2-taldearekin lotzen da (Glickman eta Ciechanover, 2002). Halaber, posible da ubikitina lotura peptidikoz substratuen α-NH2 muturrarekin (Ciechanover eta Ben-Saadon, 2004) edo lisinak ez diren beste aminoazido batzuekin –zisteina, serina eta treoninarekin– lotzea (Wang et al., 2012). Ubikitinazio mota horiek ere funtzio biologiko garrantzitsu ugaritan parte hartzen dute, esaterako, erretikulu endoplasmatikoaren bidezko degradazioan (ERAD), kolesterolaren biosintesian, apoptosian edo neuronen endekapenean (McClellan et al., 2019).

Arestian aipatu bezala, ohikoena ubikitina eta lisinen arteko lotura isopeptidikoa da. Ubikitinak berak zazpi lisina eta muturreko amino talde bat dituenez, posible eta ohikoa da poli-ubikitina kateak sortzea, hau da, substratu batera gehitutako ubikitina bati, beste ubikitina bat edo gehiago lotzea. Ubikitina molekula berria aurrez gehitutako ubikitinaren amino muturrarekin edo sekuentziako zazpi lisinetako edozeinekin (K6, K11, K27, K29, K33, K48, K63) batuz, topologia ezberdinetako poli-ubikitina-kateak sor daitezke (Komander eta Rape, 2012). Proteina ubikitinatuen milaka aldaera sortzeko gai den sistema konplexu horri esker, prozesu biologiko ugari erregulatu daitezke (Swatek eta Komander, 2016) (ikusi 1.2. *Ubikitinazioa eta bere funtzioak* atala).

1.1.2. E1 entzima aktibatzailea

Behin ubikuitina prekurtsorea prozesatuta dagoela, ubikitinazio-prozesuko lehen urratsa ubikitina molekula aktibatzean datza. Energia kontsumitzen duen erreakzio hori E1 entzima aktibatzaileak katalizatzen du (Ciechanover et al., 1981; Haas et al., 1982). E1 entzimak legamia eta gizakietan kontserbaturik daude. Alabaina, legamietan Uba1 deritzon gene bakar dagoen bitartean (McGrath et al., 1991), gizakietan bi gene aurki daitezke: UBA1 eta UBA6 (Pelzer et al., 2007).

E1 entzimak katalizatzen duen erreakzioa bi pausutan gauzatzen da; lehenik, E1 entzima ATP molekularekin eta ubikitinarekin batzen da, eta momentuko ubikitina-adenilato bitarteko bat sortzen da. Jarraian, ubikitina E1 entziman kontserbatuta dagoen zisteina hondar katalitikora batzen da tioester lotura bidez (Haas et al., 1982; Schulman eta Harper, 2009).

1.1.3. E2 entzima konjugatzailea

Ubikitinazio-prozesuan parte hartzen duen bigarren entzima E2 entzima konjugatzailea da. E1 proteinak aktibatutako ubikitina, E2 entzimara lotzen da tioester lotura bidez (Glickman eta Ciechanover, 2002; Hershko et al., 1983), eta ondoren, horrek substratura transferitzen du E3 entzima baten laguntzaz.

Eukariotoen genoman E2 proteinak kodetzen dituzten hainbat gene ezagutzen dira. Gizakietan, esaterako, 37 gene deskribatu dira (Michelle et al.,

2009). Hasiera batean garraiatzaile hutsak zirela uste bazen ere, ubikitinazio-prozesuan partaide aktiboak direla frogatu da. Izan ere, substratuetan zein lisina ubikitinatu behar den (David et al., 2010), edo ubikitina-kateen topologia eta luzera zein izan behar diren arautuz, substratuen patua baldintzatzen dute (Ye eta Rape, 2009).

E2 entzimek ubikitina konjugatzeko kontserbatuta dagoen domeinu katalitiko bat dute, UBC (*Ubiquitin-conjugating catalytic)* deritzon 150 aminoazido ingurutako domeinua, hain zuzen. Domeinu horretan kokatzen dira ubikitina lotzeko gakoa den zisteina hondarra (Wijk eta Timmers, 2010), eta baita E1 eta E3 entzimak batzeko guneak ere (Am et al., 2008).

E2 entzima batzuk UBC domeinu katalitikoz soilik daude osatuta. Aldiz, beste zenbait E2 entzimek, UBC domeinutik haratago luzatzen diren muturrak izan ditzakete, eta lau familia bereizten dira mutur horien arabera: bakarrik UBC domeinua dutenak (I motakoak), amino muturreko luzapena dutenak (II motakoak), karboxilo muturreko luzapena dutenak (III motakoak) eta luzapenak bi muturretan dituztenak (IV motakoak) (Wijk eta Timmers, 2010). Luzapen horiek, besteak beste, E2 entzimen zelula barruko lokalizazioa, E1 entzimarekiko loturaren egonkortasuna, edo bikote duten E3 entzimaren aktibitatea baldintzatu dezakete (Wijk eta Timmers, 2010).

1.1.4. E3 ligasa entzima

Ubikitinazio-prozesuko azken urratsa ubikitina-ligasa edo E3 entzimek burutzen dute, E2ek garraiatzen duten ubikitina zuzenean substratuetara atxikiz edo prozesu horretan lagunduz (Glickman eta Ciechanover, 2002; Hershko et al., 1983). Ubikitina-proteasoma sistema osatzen duten entzima guztien artean familiarik handiena da. Izan ere, gizakietan 600dik gora genek osatzen dute (Li et al., 2008). Ubikitinazio-prozesuan substratuarekiko espezifikotasuna bermatzen dute, ubikitinaz kargatutako E2 entzimarekin, eta ubikitina transferituko zaion substratuarekin aldi berean elkarrekiteko gaitasuna baitaukate (Metzger et al., 2014). E3 entzimek, hainbat substratu ubikitinatzeko gai izateaz gain, E2 entzima ezberdinekin elkarrekin dezakete. Ondorioz, E2/E3 bikote ezberdinek proteina

bera ubikitinatu dezakete, eta bikote bakoitzak ubikitinazio-patroi espezifikoa sor dezake (Metzger et al., 2014).

E2/E3 elkarrekintzak gauzatzeko E3 entzimek kontserbatutako domeinu ezberdinak dituzte. Domeinu horien egituraren arabera, eta ubikitina E2 entzimetatik substratuetara transferitzeko mekanismoaren arabera, E3 ligasen hiru familia nagusi bereizten dira: RING (*Really Interesting New Gene*), HECT (*Homologous to the E6-AP Carboxyl Terminus*) eta RBR (*RING-between-RING*) familiak (Berndsen eta Wolberger, 2014).

RING motako E3 entzimen ezaugarri nagusia honakoa da: RING edo U-BOX domeinua izatea. Bi domeinu horiek espezifikoki tartekatutako histidina eta zisteina hondarrak dituzte. Biek gurutze itxura hartzen dute, baina egitura egonkortzeko elkarrekintza ezberdinak erabiltzen dituzte: RING domeinuak Zn^{2+} ioiekin lotzen dira (Metzger et al., 2014), eta U-BOX domeinuek hidrogeno- eta gatz-zubiak eratzen dituzte (3. irudia) (Aravind eta Koonin, 2000; Ohi et al., 2003). Domeinu horien funtzioa ubikitina garraiatzen duten E2 entzimekin lotzea, eta ubikitinaren transferentzia estimulatzea da (Metzger et al., 2014). Zehazki, E2 entzima eta substratua elkarrengana hurbilduz, ubikitina E2 entzimatik zuzenean substratura transferitzea ahalbidetzen dute (Deshaies eta Joazeiro, 2009; Metzger et al., 2014; Petroski eta Deshaies, 2005).

RING-motako ligasen artean azpifamiliarik handiena Cullin E3 ligasena da, zelulako ubikitinazioaren %20az arduratzen dena (Petroski eta Deshaies, 2005). Cullin E3 ligasek monomero, dimero edo azpiunitate ugariko konplexu bezala jardun dezakete (Chew et al., 2007; Choo eta Hagen, 2012; Petroski eta Deshaies, 2005).

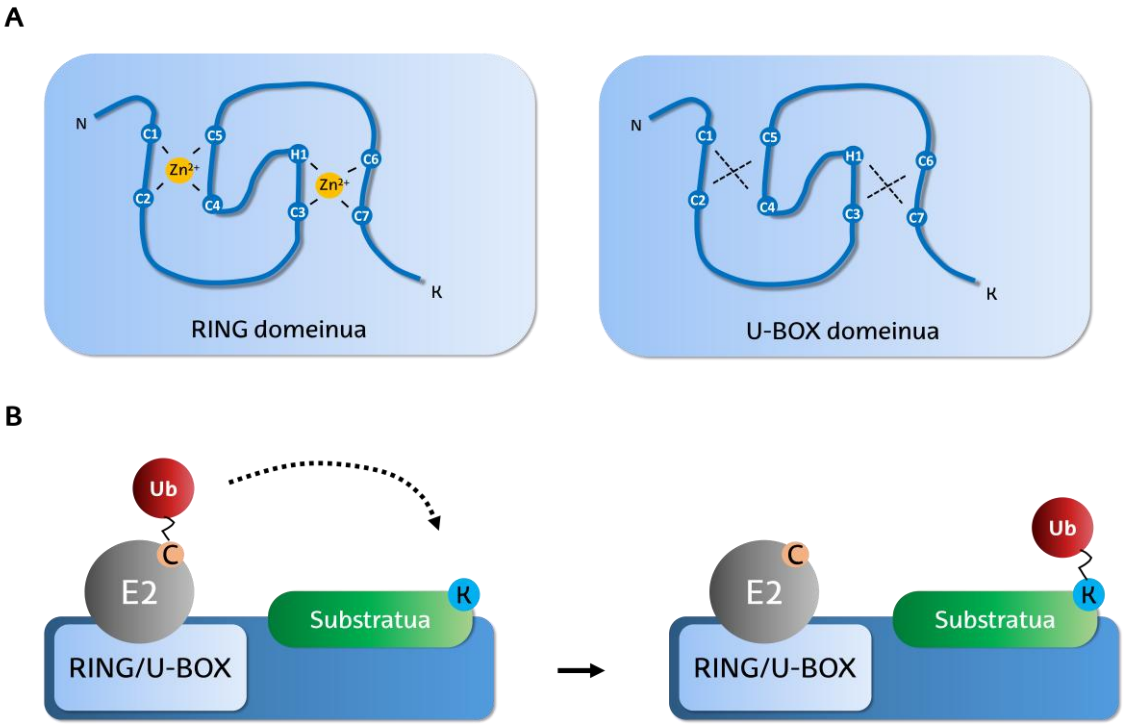

3. irudia. RING E3 entzima konjugatzaileen egitura eta funtzionamendua. A) RING eta U-BOX domeinuek gurutze itxurako egitura dute, histidina eta zisteina hondarrak tartekatuz. RING eta U-BOX domeinuak zink-ioiz eta hidrogeno- eta gatz-zubiz egonkortzen dira, hurrenez hurren. B) RING E3 ligasen familiako proteinetan E2 entzima konjugatzaileak RING edo U-box domeinuetara batzen dira, eta horiek ubikitinaren transferentzia estimulatzen dute substratura. Berndsen eta Wolberger, 2014-tik moldatuta.

HECT motako E3 ligasei dagokienez, karboxilo muturrean HECT deritzon 350 aminoazidotako domeinu bereizgarri bat dute. Ugaztunetan deskribatutako lehen E3 ligasa UBE3A edo E6AP (*E6-Asociated Protein*) da (Huibregtse et al., 1995). Hortik aurrera, ligasa horren domeinuaren homologoak dituzten gainerako E3 ligasak HECT (*Homologous to the E6-AP Carboxyl Terminus*) motako gisa sailkatu dira. Gaur gaurkoz, gizakion HECT-motako E3 ligasen familiak 28 kide ditu. HECT domeinuaren egiturari dagokionez, funtzio ezberdineko bi lobulu ditu: amino muturrekoa (N lobulua) eta karboxilo muturrekoa (K lobulua). N lobulua E2 entzimarekin batzen da, eta K lobulua, gune aktiboko zisteinaren bitartez, ubikitinarekin batu eta substratura transferitzeaz arduratzen da (4. irudia) (Huibregtse et al., 1995; Scheffner eta Kumar, 2014).

Ubikitinatu beharreko substratuaek E3 ligasen HECT domeinutik kanpo geratzen den amino muturrarekin elkarrekiten dute, eta mutur horren arabera, hiru azpifamilia bereizten dira: NEDD4/NEDD4-bezalako E3 ligasak (triptofano-

triptofano domeinua daukatenak), HERC E3 ligasak (*Chromosome Condensation 1-like* domeinua daukatenak) eta gainerako HECT E3 ligasak (domeinu horietako bat ere ez daukatenak) (Scheffner eta Kumar, 2014).

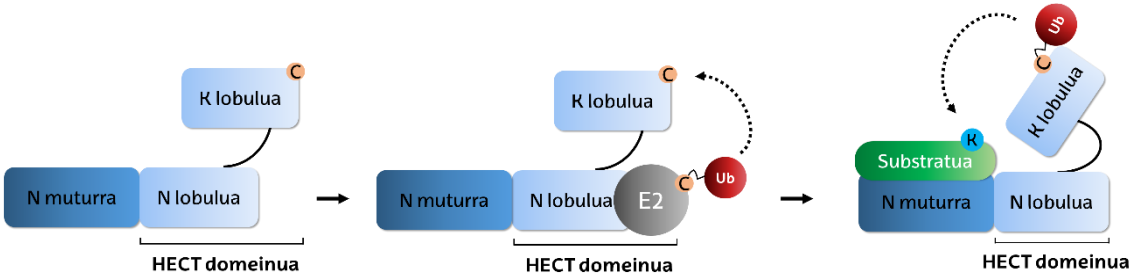

4. irudia. HECT motako E3 ligasen egitura eta funtzionamendua. Mota honetako E3 ligasek HECT domeinua dute karboxilo muturrean. Era berean, domeinu horrek bi lobulu ditu: N eta K lobuluak. Ubikitina garraiatzen duen E2 entzima N lobulura batzen da. Jarraian, ubikitina K lobuluko zisteina katalitikora transferitzen da, eta azkenik ubikitina hori E3 ligasaren amino muturrera batzen den substratuari transferitzen zaio. Berndsen eta Wolberger, 2014-tik moldatuta.

Aurrez aipatutako RING eta HECT domeinuen ezaugarriak azaltzen dituzten E3 ligasak ere badira, RBR (*RING between RING*) E3 ligasa bezala ezagutzen direnak. Horiek bi RING domeinu dituzte (RING1 eta RING2), IBR (*in between RING*) deritzon kontserbatutako sekuentzia batez bananduta (Eisenhaber et al., 2007) (5. irudia). RBR ligasek RING domeinuak izan arren, HECT motakoen antzera, ubikitinarekin tio-ester bitartekari bat sortzeko ahalmena dute (Morreale eta Walden, 2016). Hau da, RING1 domeinua E2 entzimarekin lotzen den bitartean, ubikitina RING2 domeinuaren zisteina katalitikoarekin batzen da, eta hortik substratura konjugatzen da (Berndsen eta Wolberger, 2014). Bestalde, IBR sekuentzia RING1 eta RING2 domeinuak antolatzeaz arduratzen da, substratuen ubikitinazioa errazteko (Beasley et al., 2020). Talde horretako ligasen artean aurki dezakegu, adibidez, Parkinson gaixotasunarekin erlazionatutako Parkin E3 ligasa (Berndsen eta Wolberger, 2014; Shimura et al., 2000).

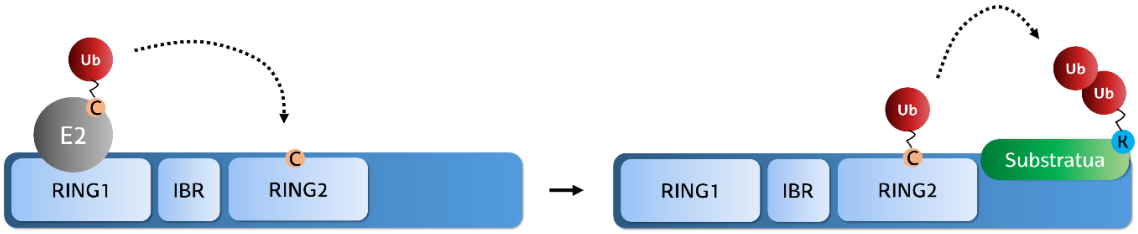

5. irudia. RBR motako E3 ligasen funtzionamendua. RBR motako E3 ligasek bi RING domeinu dituzte IBR sekuentzia baten bidez bananduta. Ubikitinatutako E2 entzima, amino muturrean kokatzen den RING1 domeinura batzen da. Ubikitina, berriz, RING2 domeinuko zisteina hondarrera transferitzen da, eta ondoren, karboxilo muturrera batutako substratura transferitzen da. Berndsen eta Wolberger 2014-tik moldatuta.

1.1.5. Deubikitinasak

80. hamarkadan, ubikitinazioa, proteinen itzulpen osteko aldaketa gehienen antzera, prozesu itzulgarria dela frogatu zen. Izan ere, orduan aurkitu zituzten ubikitinaren eta substratuen arteko lotura isopeptidikoak apurtzeko gai ziren proteinak, hots, deubikitinasak edo entzima deubikitinatzaileak (DUBak) (Matsui et al., 1982). DUBek E3 ligasen aurkako funtzioa burutzen dute, substratuei ubikitina-molekulak kentzeaz arduratzen dira, eta ubikitina aintzindaria aktibatzen dute.

Giza genomak 100 DUB inguru kodetzen ditu, eta beraien domeinu katalitikoaren sekuentzian eta egituran dauzkaten antzekotasunen arabera, sei familia nagusitan banatzen dira. Horietariko bost familia zisteina-proteasak dira: USP (*Ubiquitin-Specific Proteases*), UCH (*Ubiquitin C-terminal Hydrolases*), OTU (*Ovarian Tumour proteases*), MJD (*Machado-Joseph Disease proteases*) eta oraintsu deskribatutako MINDY (*Motif Interacting with Ub containing Novel DUB family*) familia (Abdul Rehman et al., 2016; Amerik eta Hochstrasser, 2004). Seigarren familia JAMM (*JAB1/MPN/MOV34 proteases*) metalo-proteasena da, funtzio katalitikoa burutzeko zink ioien beharra duten entzimez osatua (Amerik eta Hochstrasser, 2004). Horrez gain, badago SUMO deritzon ubikitina-bezalako proteinak kentzeaz arduratzen den DUBen familia bat, SENP deiturikoa (*SENtrin/SUMO-specific Protease*) (6. irudia) (Harrigan et al., 2018).

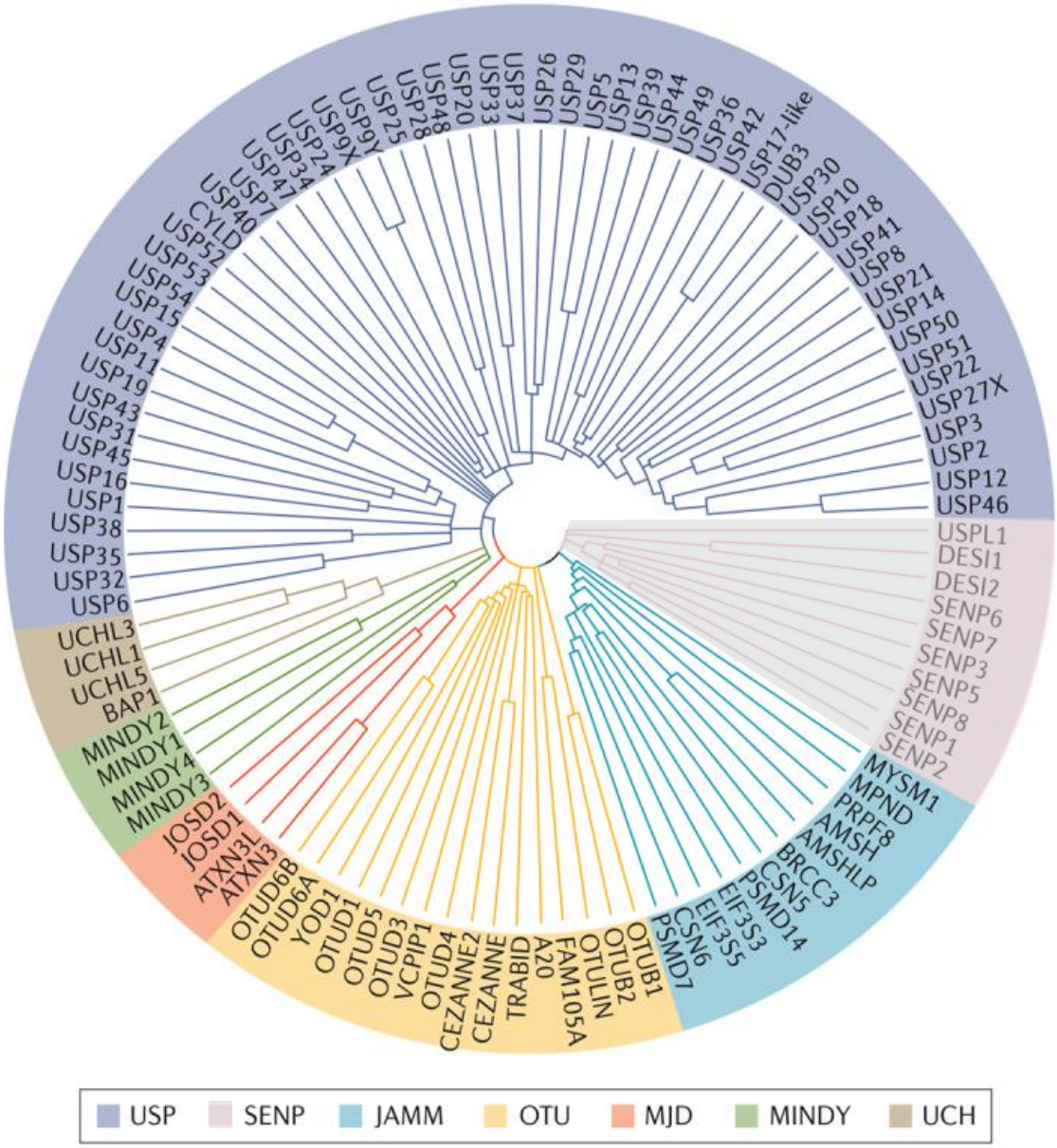

6. irudia. Deubikitinasen zuhaitz filogenetikoa. Sei DUB familia bereizten dira. Talderik handiena, eta ondoen deskribatu izan dena, USP deubikitinasek osatzen dute. UCH familia lehendabizi deskribatu zen familia da, eta OTU, MJD eta JAMM familiek, berriki deskribatutako MINDY familiarekin batera, DUB ezberdinen multzoa osatzen dute. SENP familia SUMO deritzon ubikitina-bezalako molekula kentzeaz arduratzen diren proteinez osatuta dago. Harrigan et al., 2018tik moldatua.

Familia guztien artean, UCH proteasena izan zen deskribaturiko lehena (Rose eta Warms, 1983). Gizakion kasuan, lau kidez osatzen da (UCHL1, UCHL3, BAP1 eta UCHL5) eta guztiek homologia altua erakusten dute gune katalitikoan, aktibo izateko berebizikoa den hirukote katalitikoa guztiz kontserbatuta dutelarik. Batez ere substratu txikiak (20-30 aminoazido) deubikitinatzen dituzte,

substratu handiagoak ezin baitira gune aktibora sartu ezintasun esterikoak direla eta (Amerik eta Hochstrasser, 2004). Beraz, luzera txikiko ubikitina-kateen birziklapenaz, eta ubikitinaren proproteina aitzindarien digestioaz arduratzen dira nagusiki (Larsen et al., 1998). Hala ere, kasu batzuetan substratu handiagoak ere digeritu ditzaketela frogatu da (Misaghi et al., 2005).

USP proteasen familia giza genomak kodetutako DUB familiarik handiena da. Gaur gaurkoz, 50etik gora USP deskribatu dira (Nijman et al., 2005). USP proteasen gune katalitikoa ongi kontserbatutako bi motibok osatzen dute, zisteina- eta histidina-kutxek hain zuzen ere, non katalisirako beharrezko aminoazido hondarrak aurkitzen diren (Hu et al., 2002, 2005; Renatus et al., 2006). Familia horretako kideek substratu handiagoak digeritu ditzakete, eta besteak beste, zelulen-zikloa, apoptosia edo seinaleztapen-bideak erregulatzen dituzte (Young et al., 2019).

OTU proteasen familia analisi bioinformatiko batean identifikatu zen mende honen hasieran (Makarova et al., 2000). Makarovaren taldeak, *Drosophila melanogaster* eulietan oozitoen morfogenesiarekin erlazionatuta dagoen *Otu* genean zuen interesa (Goodrich et al., 2004; Steinhauer et al., 1989). *Otu* genearen funtzioa argitzeko burututako analisi bioinformatikoan, birusen zisteina-proteasen sekuentziekin antzekotasunak zituela konturatu ziren. Horrek OTU deubikitinasen familia berriaren sorrera ekarri zuen. Familia horretan, beste zisteina-proteasetan ez bezala, hirukote katalitikoa ez dago guztiz osatuta, eta gune katalitikoa hidrogeno-zubien bidez egonkortzen da (Nanao et al., 2004). Horrez gain, proteina horien muinak bost beta-orriz osatutako egitura du (Komander eta Barford, 2008; Messick et al., 2008; Nanao et al., 2004). OTU proteasek deubikitinasa funtzioa burutzen dutela frogatu izan den arren, ez dago oraindik argi zelulako zein prozesutan parte hartzen duten (Balakirev et al., 2003; Evans et al., 2003).

Aurreko kasuan bezala, MJD edo Josephin proteasen familia ere ubikitina-proteasa familia ezberdinak bilatzeko ahaleginean egindako analisi bioinformatiko bati esker deskribatu zen (Scheel et al., 2003). Ikerketa horretan ataxina-3 eta ataxina-3-bezalako-proteinak identifikatu zituzten. *In vitro* ikerketek egiaztatu zuten proteina horiek deubikitinasa aktibitatea zutela (Burnett et al., 2003). Egitura aldetik hirukote katalitikoa kontserbatuta dagoen arren (Mao et al., 2005; Nicastro et al., 2005), domeinu katalitikoak sekuentzia-

antzekotasun baxua erakusten du gainerako DUBekin konparatuz (Nijman et al., 2005). Zelulako funtzioei dagokienez, ataxina-3 proteinak transkripzioaren erregulazioarekin erlazioa duela ikusi da. Hala ere, prozesu horretan deubikitinasa aktibitateak parte hartzen ote duen argitzeke dago (Li et al., 2002).

JAMM proteasak metaloproteasak dira, eta ondorioz, deubikitinasa aktibitatea burutzeko metalen bat behar dute, kasu honetan, Zn^{2+} ioiak. Gutxienez lau JAMM domeinu bereizten dira: hiruk ubikitinatutako substratuak prozesatzen dituzte (Abdul Rehman et al., 2016; Maurer eta Wertz, 2016; Verma, 2002; Wauer eta Komander, 2014), eta batek Nedd8 deritzon ubikitina-bezalako proteinen bidez eraldatutako substratuetan jarduten du (Cope et al., 2002). JAMM motako deubikitinasak dira, esaterako, proteasomaren bidezko degradazioan jarduten duten Rpn8 eta Rpn11 proteinak (Wauer eta Komander, 2014).

MINDY deubikitinasen familia oraintsu deskribatutako familia da. Horien funtzio katalitikoa, gainerako DUBekiko homologiarik ez daukan deskribatu gabeko domeinu baten mende dago (Abdul Rehman et al., 2016). Eukarioto guztietan aurkitzen dira, eta K48 motako poli-ubikitina-kateekiko oso selektiboak direla ikusi dute. Horrez gain, ubikitina-kate luzeak mozteaz arduratzen direla frogatu dute (Maurer eta Wertz, 2016).

Hasiera batean DUBen funtzioa proteinen degradazioa saihestea zela uste bazen ere, gaur egun badakigu funtzio biologiko ugari burutzen dituztela. Batetik, ubikitina askearen sorreran parte hartzen dute ubikitinaren gene ezberdinek sortzen dituzten pro-proteinak digerituz (Kimura eta Tanaka, 2010) (7. irudia, 1. atala). Bestetik, ubikitina molekulak kentzen dituzte proteinetatik, esaterako proteina horien funtzioak edo lokalizazioa erregulatzeko (7. irudia, 2. atala), baita integritatea babesteko ere (7. irudia, 3. atala). Horrez gain, proteasomaren bidez degradatzen diren proteinen ubikitina molekulak birziklatzen dituzte (7. irudia, 4. atala) (Yao eta Cohen, 2002). Hortaz, DUBek ubikitina eskuragarriaren mailak estuki doitzen dituzte zelularen beharretara, ubikitinatutako proteinen ubikitinazio-mailak erregulatuz. Beraz, zelulako hainbat funtzio kontrolatzen dituzte (Komander, 2009); esaterako, metafaseko kromosomen kondentsazioa eta neurotransmisorren askapena induzitzen dituzte histonak eta gune pre-sinaptikoko proteinak deubikitinatuz, hurrenez hurren (Fuchs eta Oren, 2014; Rinetti eta Schweizer, 2010).

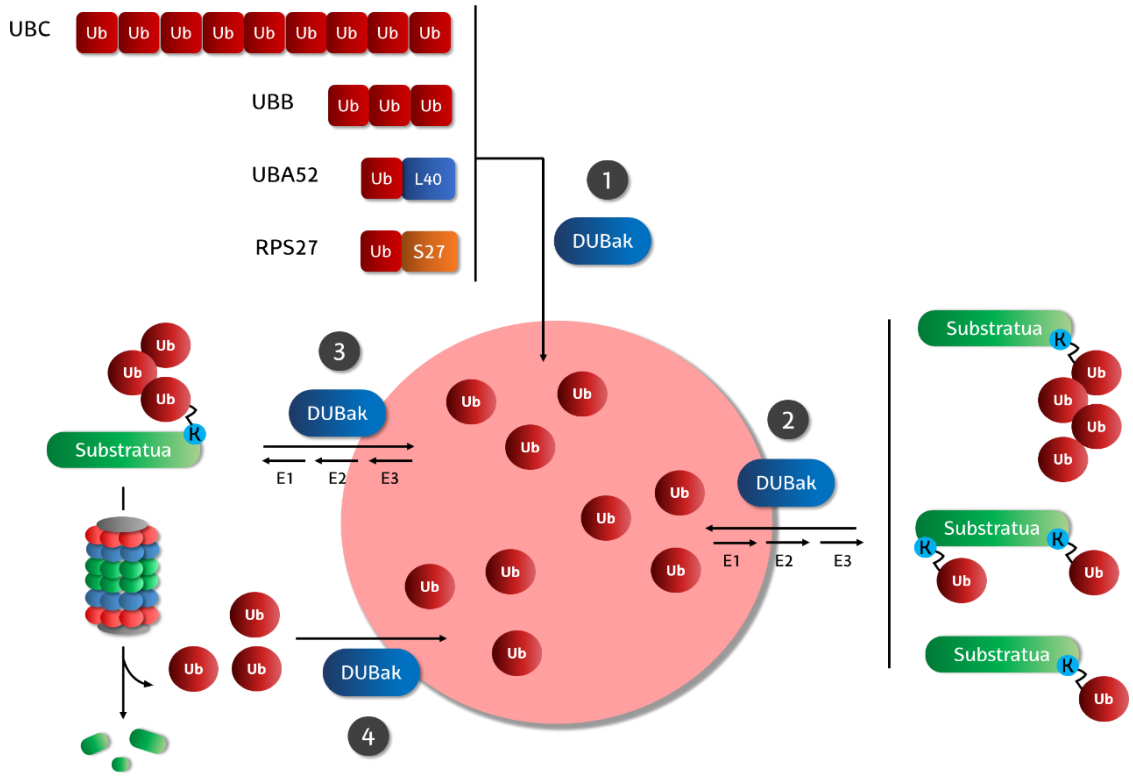

7. irudia. DUBen funtzio nagusiak. 1) Deubikitinasek ubikitina molekula berrien sintesian parte hartzen dute. 4 gene ezberdinek kodetutako proteina prekurtsore multimerikoetatik (bai ubikitina kate linealetatik eta bai proteina erribosomikoekin eratutako fusio-proteinetatik) ubikitina molekula indibidualak askatzen dituzte. 2) Ubikitinatutako proteinen funtzioak erregulatzen dituzte horien ubikitinazioa erregulatuz. 3) Proteinak degradaziotik babesten dituzte, ubikitina moztuz. 4) Ubikitina-mailak mantentzen dituzte, degradatu behar diren proteinetatik ubikitina birziklatuz. Funtzio guzti horiei esker, DUBek zelulak eskuragarri duen ubikitina-maila erregulatu eta baldintzatzen dute.

1.1.6. Ubikitina-hartzaileak

Proteina bati ubikitina gehitzean, mezu jakin bat zehazten zaio. Mezu hori ezberdina izan daiteke proteinaren ubikitinazio-patroiaren arabera. Horrela, proteina bati zehaztutako mezua ondokoek baldintzatzen dute: lotzen zaion ubikitina kopuruak, ubikitina horiek zein aminoazidotan lotzen diren, eta eraikiz gero, ubikitina-kateak nolakoak diren. Kasuan kasu, proteinak jasotzen duen mezua deszifratzeko, ubikitina-hartzaileak daude zelulan, hots, modu ez-kobalentean ubikitinarekin elkarrekiten duten domeinuak (UBD, *Ubiquitin-Binding Domain*) dituzten proteinak. Domeinu horiek beharrezkoak dira ubikitinazio bidez aktibatutako mezua zelula barneko seinale biokimiko bilakatu ahal izateko (Dikic et al., 2009).

UBD domeinuek funtzio berdina duten arren, egitura desberdinak izan ditzakete. Deskribatu ziren lehen UBD domeinuak, proteasomaren azpiunitatea den PSMD4/Rpn10 (*Human Regulatory Particle Non-ATPase 10*) proteinaren UIM (*Ubiquitin-Interacting Motifs*) motiboak izan ziren (Young et al., 1998). Geroago, legamien Ddi1 (*DNA-Damage Inducible protein 1*) eta Rad23 (*Radiation Sensitivity Abnormal 23*) proteinen UBA (*Ubiquitin Associated*) domeinuek ubikitinarekin elkarrekiteko gaitasuna zutela ikusi zuten (Bertolaet et al., 2001). Harrezkero, hogeitik gora UBD familia deskribatu dira, egituraren arabera bost azpifamiliatan sailkatzen direnak (Kliza eta Husnjak, 2020): α-helize egiturak (UIM eta UBA barne), zink-hatzak, plekstrina-bezalakoak, ubikitina-konjugatzaile-bezalakoak eta gainerakoak.

UBD domeinu batzuk poli-ubikitina-kate espezifikoekin elkarrekiten dute (Raasi et al., 2005; Sims eta Cohen, 2009; Trempe et al., 2005). Adibidez, Rad23 proteinako UBA domeinuak K48 motako kateak ezagutzen ditu (Raasi et al., 2005). Aldiz, badira UBD batzuk edozein kate motekin modu promiskuoan batzen direnak (Raasi et al., 2005; Zhang et al., 2008). UBD bakoitzak ubikitina-kateekiko duen espezifikotasuna domeinuaren egituraren eta proteinan duen kokapenaren araberakoa dela uste da (Sims eta Cohen, 2009). Gaur egun, kristalografia bidezko ikerketei esker, ubikitinaren eta UBD mota bakoitzaren arteko lotura nola ematen den dakigu (Dikic et al., 2009; Husnjak eta Dikic, 2012). Alabaina, lotura horren ondorioz zeluletan erantzun biologiko ezberdinak nola sortzen diren oraindik ez da argitu.

Ubikitinatutako proteinen degradazioan parte hartzen duten ubikitina-hartzaile batzuk (Rpn10 eta Rpn13, esaterako) proteasomaren parte dira, eta proteasomatik hurbil kokatzen diren substratuak jaso eta proteasoma barrura bideratzeko (Madura, 2004). Baina badira ere proteasomaren parte ez diren hartzaileak. Horiek proteasoma-anezkak dira, eta proteasomatik urrun kokatzen diren substratuak identifikatu eta proteasomara hurbiltzen dituzte degradatuak izan daitezen (Hartmann-Petersen eta Gordon, 2004). Identifikatu eta karakterizatutako lehen anezka-proteinak *Saccharomyces cerevisiae* edo legamiako Ddi1, Rad23 eta Dsk2 izan ziren (Kaplun et al., 2005; Lambertson et al., 1999; Zientara-Rytter eta Subramani, 2019). Klasikoki, proteasoma-anezkek amino muturrean UBL (*Ubiquitin-Like*) deritzon ubikitina bezalako domeinua daukate. UBL domeinuak proteasomaren 26S azpiunitateko UBL hartzaileekin

elkarrekiten du (Finley, 2009). Bestalde, proteasoma-anezkek karboxilo muturrean UBD domeinua (*ubiquitin-binding domain*) daukate, ubikitinarekin edo poli-ubikitina kateekin lotzen dena (Bertolaet et al., 2001). Beraz, UBD eta UBL domeinuei esker, anezkek substratuak eta ubikitina hartzaileak batzen dituzte aldi berean, eta substratuak proteoasomara hurbiltzen dituzte bertan degradatuak izan daitezen (Finley, 2009).

1.1.7. Proteasoma

Proteinak gehiago behar ez direnean edo birziklatu behar direnean, ubikitinatu egiten dira, klasikoki K48 motako poli-ubikitina-kateen bidez, eta proteasomara bideratzen dira degradatzera (Swatek eta Komander, 2016). Beraz, proteinen degradazioaz arduratzen den makinaria da proteasoma. Zehazki, 26S deritzon ATP-aren mendeko konplexu multi-katalitikoa da (Matthews et al., 1989), eta zelula eukariotoen zitoplasman nahiz nukleoan aurkitzen da (Peters et al., 1994; Wójcik eta DeMartino, 2003). Bi azpiunitate mota ditu; 19S azpiunitate erregulatzailea (RP, *Regulatory Particle*), proteina ubikitinatuak ezagutu eta degradaziorako prestatzen dituena, eta 20S muina (*CP, Core Protein*), proteina horiek degradatzeaz arduratzen dena (8. irudia) (Finley et al., 2016).

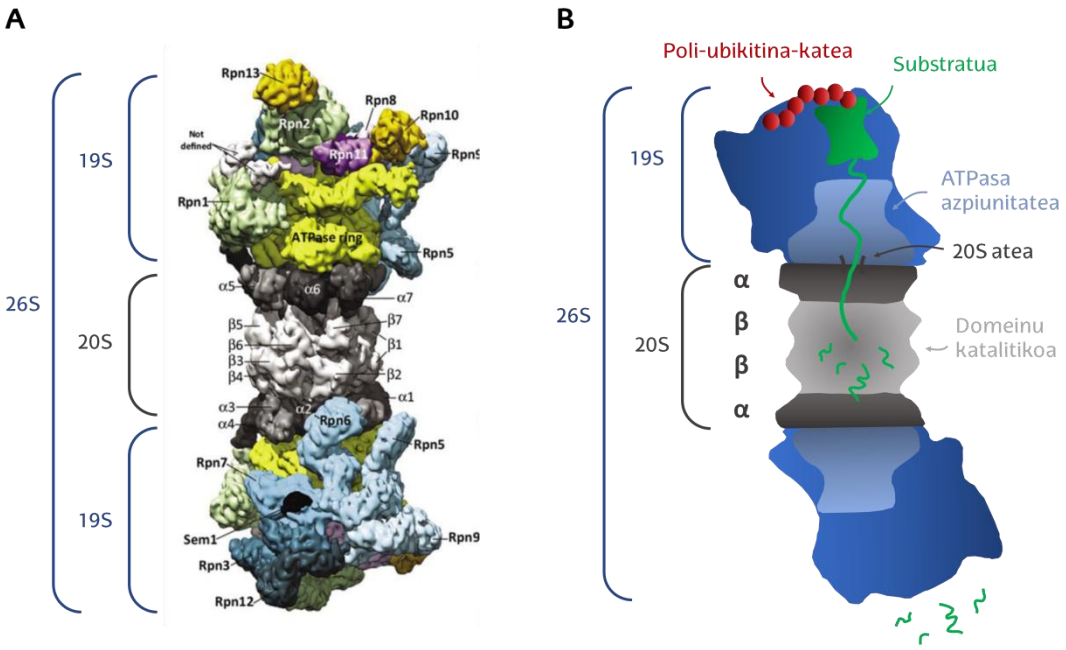

8. irudia. Proteasomaren egitura. A) Legamiaren proteasomaren irudia krioelektroi mikroskopioz. 20S muina bi 19S azpiunitate erregulatzaileren artean kokatzen da, eta guztien artean 26S konplexua eratzen dute. Azpiunitate bakoitza osatzen duten proteinen izenak adierazten dira. Finley et al., 2016tik moldatuta. B) Proteasomaren funtzionamendua erakusten da; poli-ubikitina katea (gorriz) duen substratua (berdez) azpiunitate erregulatzailera sartzen da. ATPasa azpiunitatean destolestu egiten da, eta 20S deritzon atetik pasatuz domeinu katalitikora iristen da. Domeinu hori α eta β egiturez osatuta dago, eta bertan proteina degradatzen da. Azkenik, degradazio produktuak beheko azpiunitate erregulatzailetik ateratzen dira.

Proteasomak bi 19S edo RP azpiunitate-erregulatzaile dauzka, proteasomaren muinaren (20S) alde banatan kokatzen direnak (8. irudia). RP azpiunitate bakoitza 19 proteinaz osatzen da, oinarri eta tapa gisa funtzionatzen duten bi egitura ezberdinetan antolatuta (9. irudia) (Lander et al., 2012). RP azpiunitateko tapa ATPasak ez diren (*non-ATPase*) 9 proteinaz osatzen da: Rpn3, 5–9, 11–12, eta Sem1 legamietan. Guztien artean, metaloproteasen familiako Rpn11 (*Regulatory Particle Non-ATPase 11*) deubikitinasa da gehien ezagutzen dena, substratuen ubikitinak kentzen baititu degradatu behar diren proteinak proteasoma barrura sartzeko (Verma, 2002). Gainerakoek, Rpn11 bere lekuan mantenduz, deubikitinasaren aktibitatea erregulatzen dutela uste da (Dambacher et al.). Bestalde, RP azpiunitateko oinarria den azpi-konplexua sei ATPasaz (Rpt1-6) eta lau ez-ATPasaz (Rpn1, Rpn2, Rpn10 eta Rpn13) dago osatua (Lander et al., 2012). ATPasek eraztun hetero-hexameriko bat eratzen dute. Eraztun horretan, ATParen hidrolisitik lortutako energia erabiltzen da degradatu behar diren proteinak destolestu, eta proteasomaren muinera translokatzeko (Tomko et al., 2010). Aldiz, ez-ATPasen artean, Rpn10 eta Rpn13 proteinak ubikitina-hartzaileak dira, eta poli-ubikitinatutako proteinak ezagutzen dituzte (Deveraux et al., 1994; Husnjak et al., 2008). Rpn1 eta Rpn2 proteinek antzeko funtzioa burutzen dute, normalean ubikitina-hartzaileek dituzten ubikitina-batzeko domeinuetara batuz (Rosenzweig et al., 2012).

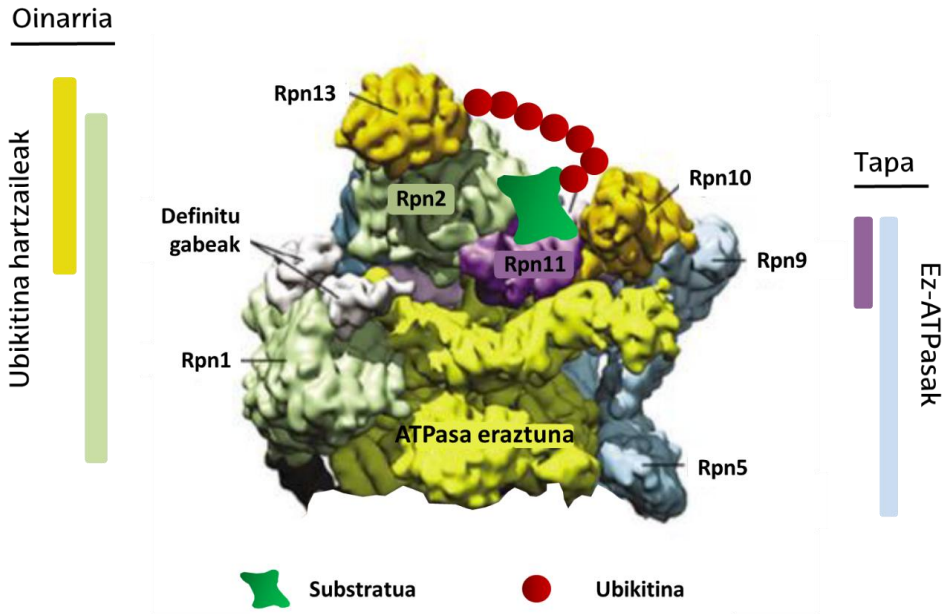

9. irudia. 19S azpiunitate erregulatzailearen egitura. Bi atal bereizten dira, tapa, non ubikitina hartzaileak eta ATPasak ez diren proteinak kokatzen diren, eta oinarria, aktibitate katalitikoa duten ATPasa eraztunez eta ubikitina-hartzailez osatua dagoena. Poli-ubikitinatutako substratuen ubikitina kateak Rpn10 eta Rpn13 proteinek ezagutzen dituzte, eta substratua Rpn11 proteinaren inguruan kokatzen da. Substratuaren destolespena oinarrian kokatzen den ATPasen eraztunak burutzen du, gero 20S azpiunitatean proteina degradatua izan dadin. Finley et al., 2016tik moldatuta.

Behin proteinak RP azpiunitatean deubikitinatu eta destolesten direnean, proteasomaren 20S edo muinera translokatzen dira (Finley et al., 2016). Upel itxurako egitura hori 28 proteinaz osatzen da (10. irudia). Proteina horiek bata bestearen gainean kokatzen diren lau eraztun hetero-heptamerikotan antolatzen dira (Groll et al., 1997). Kanpoaldeko bi eraztunak α-motako egiturak dira, aldiz, barneko biak β-motakoak (Finley et al., 2016; Lowe et al., 1995). β1, β2 eta β5′ posizioko proteinek aktibitate proteolitikoa daukate eta hondar hidrofobiko, basiko eta azidoak prozesatzen dituzte, hurrenez hurren (Finley et al., 2016). Horien gune aktiboak muinaren barnealdera begira kokatzen dira, eta bertara sartzen diren proteinak oso azkar degradatzen dira (Finley et al., 2016; Groll et al., 1997).

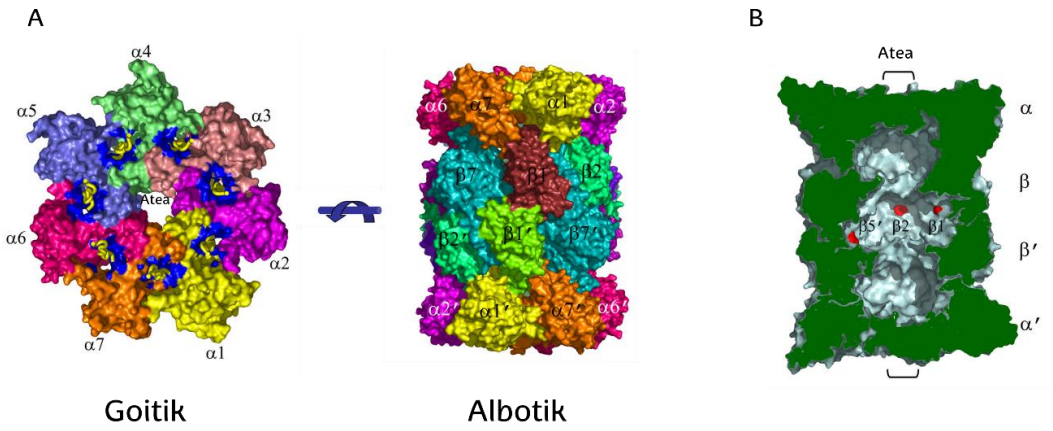

10. irudia. 20S muinaren egitura. A) Eraztun heptamerikoa goitik eta albotik ikusita. Albotiko irudian, lau eraztun hetero-heptamerikoak bata bestearen gainean nola kokatzen diren bereizten da. Finley et al., 2009tik hartuta. B) 20S azpiunitatearen barnealdean proteinen digestioaz arduratzen diren hiru proteina katalitikoak azpimarratu dira (β5′, β2 eta β1). Finley et al., 2009tik hartuta.

1.2. Ubikitinazio-motak eta funtzioak

XX. mende bukaeratik gaur egun arte eginiko ikerketek argi utzi dute ubikitinazioak proteinen degradazioa bideratzeaz gain, prozesu biologiko ugaritan parte hartzen duela (Popovic et al., 2014; Swatek eta Komander, 2016). Ubikitina proteinako aminoazido ezberdinei lotu daiteke, eta konfigurazio-aukerak izugarri handiak direnez, ubikitina-kate ezberdinak sortzen dira. Hain zuzen ere, heterogeneitate horri zor zaio ubikitinazioak horrenbeste funtzio bete ahal izatea, kate mota bakoitzak irakurketa espezifikoa izango baitu zelulan (Swatek eta Komander, 2016).

Ubikitinazio mota guztien artean, mono-ubikitinazioa, alegia, substratuari ubikitina bakar bat gehitzea, da sinpleena (11. irudia)(Hicke, 2001; Kaiser et al., 2011). Mono-ubikitinazioak zelularentzako oinarrizkoak diren hainbat funtziotan parte hartzen du: transkripzioaren erregulazioan (Pham eta Sauer, 2000), mintz-plasmatikoko proteinen eta hartzaileen barneraketan (Haglund et al., 2003; Terrell et al., 1998; Yao eta Xu, 2020), proteinen aktibitatearen erregulazioan (van Delft et al., 1997; Di Fiore et al., 2003) edota zelula barneko proteinen lokalizazioan (Landré et al., 2017; Yao eta Xu, 2020). Mono-ubikitinazioa aldi berean substratuko hainbat lisinetan gertatzen denean, multi-mono-ubikitinazioaz ari gara (11. irudia).

Eraldaketa hori endozitosiarekin edo ubikitinatutako proteinen lisosometarako garraioarekin erlazionatu da (Haglund et al., 2003).

Proteinetan poli-ubikitina kateak ere era daitezke, ubikitinak berak ubikitinatu daitezkeen 8 amino talde baititu; amino muturreko metioninarena (M1) eta sekuentzia barruko zazpi lisinen albo katekoak (K6, K11, K27, K29, K33, K48, K63) (11. irudia). Ubikitina substratuari atxiki ostean, printzipioz, ubikitinaren 8 amino taldetatik edozein ubikitinatu daiteke (Komander eta Rape, 2012; Swatek eta Komander, 2016). Ubikitinak elkarren artean lotzen diren moduaren arabera, konfigurazio ezberdinetako poli-ubikitina-kateak eratzen dira. Poli-ubikitina-katean zehar erabilitako lisinak berdinak badira, katea homogeneoa izango da (adibidez, K48-kateak). Aitzitik, katearen eraikuntzan lisina ezberdinek parte hartzen badute, katea heterogeneoa da (adibidez, K48/K11-katea). Aldi berean ubikitina bakar bateko hainbat lisina eraldatzen badira, kate adarkatuak sortzen dira (11. irudia).

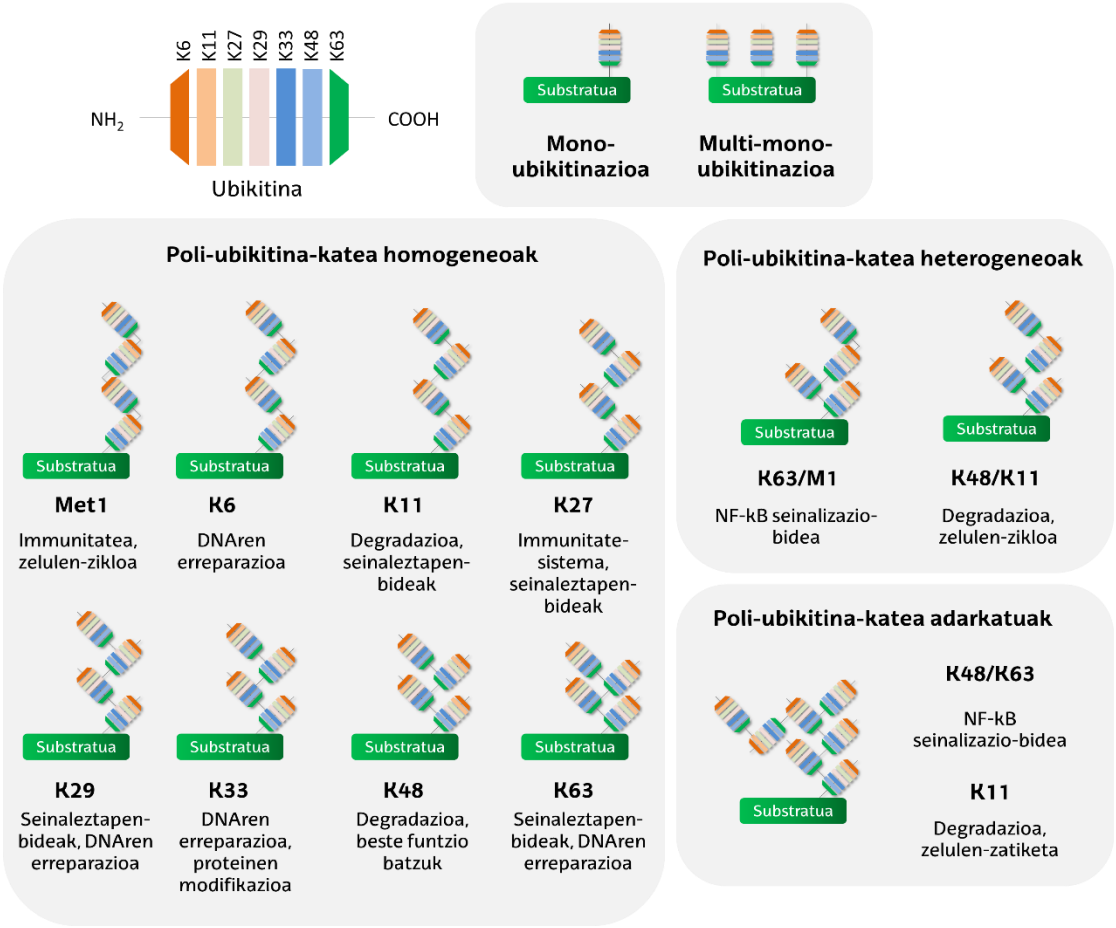

11. irudia. Ubikitinazio-motak. Ubikitina molekularen amino muturra eta barneko zazpi lisinak (K7, K11, K27, K29, K33, K48, K63) ubikitinatu egin daitezke. Hori dela eta, mono-ubikitinazioaz gain, poli-ubikitina kateak eratu daitezke. Ubikitinatzen den barneko lisina beti berdina bada, kate homogeneoak eratzen dira. Aldiz, katean zehar ubikitinaren lisina ezberdinak ubikitinatzen badira, kate heterogeneoak sortzen dira. Bi kasuak batera ematen direnean, kate adarkatuak osatzen dira. Ubikitinazio-motaren eta eratutako poli-ubikitina-kate motaren arabera, proteinari funtzio edo ezaugarri ezberdin bat esleitzen zaio.

Poli-ubikitina-kateen artean homogeneoak dira ikertuenak, eta beraz, hobekien karakterizatutakoak. Horien artean ugariena K48 motako katea da (Kaiser et al., 2011; Swatek eta Komander, 2016). K48 kateek konfigurazio konpaktua daukate (Eddins et al., 2007), eta klasikoki proteinen degradazioarekin erlazionatu izan diren arren (Ciechanover, 2013; Glickman eta Ciechanover, 2002; Grice eta Nathan, 2016; Hu et al., 2021; Thrower et al., 2000), funtzio ez-degradatiboetan ere parte hartzen dute (Flick et al., 2006). Bigarren kate homogeneo mota ugariena K63 motakoa da (Kaiser et al., 2011). K63 kateek konfigurazio irekiagoa dute (Komander, 2009), eta nagusiki degradazioarekin zerikusirik ez duten funtzioekin erlazionatu dira: kinasak aktibatzea (Deng et al., 2000; Newton et al., 2008), DNA-kalteen aurkako erantzuneko proteinak biltzea (Bennett eta Harper, 2008; Hoege et al., 2002; Zhao et al., 2007) edota proteinen lokalizazioa baldintzatzea (Wang et al., 2018b). Gainerako kate-homogeneoak neurri txikiagoan agertzen diren arren, funtzio biologiko garrantzitsuak deskribatu zaizkie. Horien artean, K6 motako kateek, Parkin E3 ligasaren aktibitatea kontrolatuz, mitofagia erregulatzen dute (Durcan et al., 2014). K11 motako kate sinpleek zelulen zatiketa erregulatzen dute (Wickliffe et al., 2011). K6- eta K33-kateek DNA-kalteen aurkako erantzunean (Elia et al., 2015; Swatek eta Komander, 2016) eta TNF bidezko seinaleztapenean hartzen dute parte (Dynek et al., 2010). K27 kate-motek MEK/ERK seinaleztapen bidea (Yin et al., 2019) eta immunitate-sistema erregulatzen dituzte (Wu et al., 2019b). K29 motako kateak estres proteasomikopean detektatu dira, beraz uste da proteasoma bidezko degradazioa kontrolatzen dutela poli-ubikitinatutako proteinen ezagutza oztopatuz (Besche et al., 2014). Horrez gain, K29-kateek Wnt/β-katenina seinalizazioa negatiboki erregulatzen dutela ere ikusi da (Fei et al., 2013). K33 motako kateek konfigurazio irekia azaltzen dute (Michel et al., 2015), eta proteinen trafikoarekin eta DNA-kalteen aurkako erantzunarekin erlazionatu dira (Elia et al., 2015). Azkenik, amino muturreko kate linealek hanturan eta erantzun

immunean parte hartzen dute (Gerlach et al., 2011) eta NF-kB seinaleztapen-bidea erregulatzen dute (Rittinger eta Ikeda, 2017; Tokunaga et al., 2009).

Kate heterogeneoen ikerketak gero eta ugariagoak dira, erronka teknologiko handiagoa suposatzen badute ere. Adibidez, K11/K48 motako kateek proteinen degradazioan (Baur eta Rape, 2020) nahiz zelulen zikloan eta kalitate kontrolean parte hartzen dutela ikusi da (Yau et al., 2017). Are gehiago, M1/K63-kate mixtoek NF-kB seinaleztapen bidearen eta berezko immunitate sistemaren aktibazioan hartzen dute parte (Emmerich et al., 2013, 2016).

Aitzitik, ubikitina kate adarkatuen funtzioa proteinak degradaziora bideratzea dela ikusi dute (Ohtake et al., 2018). K11 motako kate adarkatuek proteasomaren bidezko degradaziorako seinale gisa jarduten dute zelularen zatiketan ubikitinatutako substratuen errekonozimendua erraztuz (Meyer eta Rape, 2014). K48/K63-kate adarkatuek NF-kB seinaleztapen bidea, eta K29/K48 kate adarkatuek autofagia erregulatzen dutela ere baieztatu dute (Chen et al., 2021; Ohtake et al., 2016).

Ubikitinazio-motarik ohikoena substratuen lisinetan ematen den arren, zisteina, serina eta treonina hondarretan, nahiz ubikitinaren amino muturreko amino talde askean ere eman daiteke (Spit et al., 2019; Wang et al., 2012). Ubikitinazio-mota horiek degradazioan, ERAD prozesuetan, seinaleztapenean edota hartzaileen birziklapenean parte hartzen dutela frogatu izan dute (McClellan et al., 2019).

1.3. UPS: gaixotasunak eta itu terapeutikoak

Ubikitina-proteasoma sistemaren funtzionamendu egokia berebizikoa da zelularen biziraupenerako. Sistema horretan prozesu ugari zehatz erregulatu behar dira. Batetik, proteinen ubikitinazioa emateko, E1, E2 eta E3 proteinen arteko koordinazio estua behar da, eta bestetik, zelulako oreka mantentzeko, DUBen jarduera egokia ezinbestekoa da. Sistema horretako osagairen batek gaizki funtzionatzen duenean, arazoak sor daitezke proteinen birziklapenean, seinaleztapen-bideetan, eta oro har, ubikitinazioak erregulatzen dituen prozesu

guztietan. Beraz, ez da harritzekoa UPSren homeostasiaren galera hainbat gaixotasunen etiologiarekin erlazionatuta egotea.

Hori kontuan izanda, azken urteotan UPS itu garrantzitsu bilakatu da gaixotasun horien tratamendura bidean. Taula honetan laburbildu da UPSko osagai ezberdinek zein gaixotasunetan parte hartu dezaketen, eta osagai horiek itu terapeutiko gisa erabili izan dituzten ikerketen erreferentziak (1. taula):

1. taula. UPSko osagai desberdinak eta horiekin erlazionatutako gaixotasun eta ikerketak.

UPSko osagaia	Gaixotasuna	Ikerketak
E1 entzimak	• Bizkarrezurreko muskulu-atrofia (Groen eta Gillingwater, 2015; Shaughnessy et al., 2020) • Minbizia (Xu et al., 2010b)	Muskulu-atrofia: Itoh eta Suzuki, 2018; Powis et al., 2016 Minbizia: Barghout eta Schimmer, 2018; Deng et al., 2020; Hyer et al., 2018; Liu et al., 2015; Yang et al., 2007; Zhuang et al., 2019
E2 entzimak	• Fanconi anemia (Hira et al., 2015; Zhang et al., 2011) • Gaixotasun immunologikoak (Han et al., 2009; Pruneda et al., 2014; Stahl et al., 2010) • Minbizia (Luo et al., 2016; van Ree et al., 2010) • Atrofia muskulu eskeletikoa (Polge et al., 2015) • UBE2A gabeziaren sindromea (de Leeuw et al., 2010; Nascimento et al., 2006) • Gaixotasun neurologikoak (Osinalde et al., 2018) • Huntington gaixotasuna (de Pril et al., 2007; Wang et al., 2018a) • Parkinson gaixotasuna (Fiesel et al., 2014; Geisler et al., 2014) • Adimen urritasuna eta atzerapen mentala (Budny et al., 2010; de Oliveira et al., 2019; Tsurusaki et al., 2017)	Gaixotasun immunologikoak: (Zhou et al., 2020) Fanconi anemia: (Cornwell et al., 2019; Morreale et al., 2017) Minbizia: (Cheng et al., 2014; Deng et al., 2020; Liang et al., 2017; Liu et al., 2015; Ramatenki et al., 2016; Vila et al., 2017; Zhou et al., 2020)

E3 entzimak	• Gaixotasun neurologikoak (George et al., 2018; Osinalde et al., 2018) 1. Angelman sindromea (Khatri eta Man, 2019) • Minbizia (Sala-Gaston et al., 2020; Wang et al., 2020a) • Gaixotasun inflamatorioak (Popovic et al., 2014)	Minbizia: (Deng et al., 2020; Liu et al., 2015) Gaixotasun inflamatorioak: (Goru et al., 2016)
DUBak	• Gaixotasun neurologikoak (Osinalde et al., 2018) • SCA3 (*spinocerebellar ataxia-3*) (Evers et al., 2014; Paulson eta Shakkottai, 1993) • Minbizia (Popovic et al., 2014; Zeng et al., 2020) • Gaixotasun immunologikoak (Sun, 2008)	Minbizia: (Chen et al., 2020; D'Arcy et al., 2015; Deng et al., 2020; Pinto-Fernandez eta Kessler, 2016; Young et al., 2019; Yuan et al., 2018) SCA3: (Evers et al., 2013; Li et al., 2015) Gaixotasun immunologikoak: (Lopez-Castejon eta Edelmann, 2016)
Proteasoma	Proteasomaren aktibitate murriztua • Neuroendekapenezko gaitzak (Thibaudeau et al., 2018) • Gaitz autoimmuneak (Feist et al., 2016) • Minbizia (Chen et al., 2017) Proteasomaren gehiegizko aktibitatea • Muskulu-atrofia (Gomes et al., 2012; Kitajima et al., 2020) • Gaitz autoimmuneak (Feist et al., 2016) • I motako diabetes mellitusa (Alexandrova et al., 2006; Broca et al., 2014) • Minbizia (Chen et al., 2017)	Gaitz autoinmuneak: (Verbrugge et al., 2015; Xiao et al., 2017) Minbizia: (Narayanan et al., 2020; Zhang et al., 2020) Muskulu-atrofia:(Beehler et al., 2006; Caron et al., 2011) Diabetesa: (Otoda et al., 2018) Orokorra: (Wang et al., 2020b)

2. Angelman sindromea

Angelman sindromea (AS, OMIM #105830) populazioan 15.000 pertsonatik batek jasaten duen gaixotasun bakana da (Margolis et al., 2015). Euskadi/Espainia mailan familien elkarteak ere osatu dira azkenengo urteetan (https://angelman-asa.org/). Lehengo kasua 1965ean Harry Angelman doktoreak deskribatu zuen, erlaziorik gabeko hiru haurrek ez-ohiko ezaugarri fisiko berdinak zituztela behatu ostean (Angelman, 1965). Sindrome hori pairatzen duten pertsonek adimenaren garapenaren atzerapena eta hitz egiteko ezintasuna dute (Bird, 2014; Williams et al., 2010). Sarritan ezaugarri horiekin batera epilepsia, arazo gastrointestinalak eta lo egiteko zailtasunak izaten dituzte (Bakke et al., 2018; Bindelsde Heus et al., 2020; Glassman et al., 2017; Samanta, 2021; Spruyt et al., 2018). Gaixotasunaren oinarri genetikoaren arabera, ezaugarri fisikoak desberdinak izan daitezke. Horien artean etengabeko irribarrea da bereizgarriena. Horrez gain, mugitzeko zailtasunak, oinezkera baldarra, eta sarritan, eskuak gorantz igotzeko joera izaten dute (Bindelsde Heus et al., 2020). Haur gehienen aurpegiak morfologia normala izan arren, batzuek aho handia edo ezpain-sudur arteko distantzia txikia daukate eta mihia kanpoan izan ohi dute (Buiting et al., 2016). Mikrozefalia bezalako aberrazio anatomikoak ere ohikoak dira (Bindelsde Heus et al., 2020; Sachdeva et al., 2016) (12. irudia).

12. irudia. Angelman sindromedun indibiduoen ezaugarriak. Gaixotasunaren ezaugarri fisikoak desberdinak izan ohi dira oinarri genetikoaren arabera. Ezaugarrien artean aurkitzen dira; aurpegi alaia eta irribarretsua, eskuak gorantz izateko joera (a eta b), mikrozefalia (a, b, e eta f) eta mihia kanpoan izatea (e, f). Buiting et al., 2016tik hartuta.

Oro har, ezaugarri horiek urtebetetik aurrera azaltzen dira, nahiz eta atzerapen psikomotorra sei hilabeterekin ere detektatu daitekeen (Tan et al., 2011). Hortaz, sindromea normalean urte bat edo bi dituzten haurretan diagnostikatzen da (Margolis et al., 2015). Gaur egun, diagnostiko hori test genetikoen bidez burutzen da, beraz, jaio aurretik burutu daiteke (Beygo et al., 2019; Hu et al., 2016). Urteak pasa ahala, gaixotasuna inoiz desagertu ez arren, ezaugarriak ezkutatu egin daitezke, neurri batean bada ere. Indibiduo horien bizi-itxaropena normala da, baita garapena eta ugalkortasuna ere (Buiting et al., 2016). Edonola ere, bizi osoan zehar zaintzaile baten beharra izaten dute, izaera esploratzailea adimen urritasunarekin konbinatuta, Angelman sindromedun indibiduoek istripu-arrisku handia baitaukate (Bird, 2014).

2.1. Oinarri genetikoa

Angelman sindromea 15q11-q13 kromosoma-eremuan ematen diren aberrazio genetiko eta epigenetikoen ondorioz sortzen da. 1987an elkarren artean erlaziorik ez zuten, eta Angelman sindromearen ezaugarriak azaltzen zituzten bi emakumek kromosoma-eremu horretan delezio bat zutela ikusi zuten (Magenis et al., 1987). Ordura arte eremu horretako delezioa Prader-Willi deritzon sindromearekin erlazionatu zen, alegia, hipotonia eta obesitatea bezalako ezaugarriak dituen gaixotasun genetiko konplexuarekin (Kalsner eta Chamberlain, 2015). Eremu-kromosomiko berdin bateko delezioak sindrome ezberdin bi sortzen zituela ikusirik, ikerketak gune horretan zentratu ziren. Bertan kokatzen diren geneak inpronta genomiko deritzon mekanismo batez isilduta daudela ondorioztatu zuten (Knoll et al., 1989; Magenis et al., 1990). Zehazki, eremu horretako gene batzuk inpronta aitatiarra, eta horrenbestez, adierazpen amatiarra dutela frogatu zuten. Beste batzuk, ordea, inpronta amatiarra dutenez, adierazpen aitatiarra daukate. Eta badaude ere adierazpen bialelikoa duten geneak (Margolis et al., 2015). Hain zuzen ere, adierazpen aitatiarra duten geneen galerak Prader-Willi sindromea sortzen dute. Aldiz, Angelman sindromea, neuronetan adierazpen amatiarra duen, eta 15q11-q13 lokusean kokatzen den *UBE3A* genearen funtzio galerak sortzen du (Buiting et al., 2016; Vu eta Hoffman,

1997). Gene horrek 120 kb eta 16 exoi ditu, eta UBE3A E3 ubikitina-ligasa kodetzen du (Kishino eta Wagstaff, 1998; Kishino et al., 1997).

Geneen inpronta aitarengandik eta amarengandik jasotako kromosometako geneak modu ezberdinean adierazteko mekanismoa da. Normalean, inpronta markaketak zitosina-guanina di-nukleotidoetan aberatsak diren DNA eremuei (CG guneak) metilo talde bat kobalenteki atxikiz sortzen dira. Eremu horiek inpronta-zentru bezala ezagutzen dira, eta zentru horien metilazioak inguruko gene-multzoen adierazpena ekiditzen du. 15q11-q13 kromosoma-eremuan bi inpronta zentru daude, SNURF/SNRPN geneen sustatzaile eremuan kokatzen direnak; Angelman sindromearen inpronta-zentrua (AS-IC, *Angelman Syndrome Imprinting Center*) eta Prader-Willi inpronta-zentrua (PW-IC, *Prader Willi Imprinting Center*)(13. irudia). PW-IC inpronta-zentruaren metilazioak ondoko gene multzo baten adierazpena ekiditen du. Alabaina, UBE3A genearen adierazpena ez da zuzenean metilazioz erregulatzen, baizik eta PW-IC-an hasten den eta UBE3A-AS deritzon transkripto batek erregulatzen du. Hau da, PW-IC inpronta-zentrua metilatu gabe dagoenean (aitaren kromosoman), UBE3A-AS transkribatu egiten da, eta horrek UBE3A genearen adierazpena blokeatzen du. Aldiz, inpronta-zentrua metilatuta dagoenean (amaren kromosoman), ez da AS-UBE3A transkriptoa adierazten, eta ondorioz, UBE3Aren adierazpena normala da. Neuronak ez diren gainerako zeluletan, transkripto hori ez da UBE3A generaino iristen. Hortaz, zelula horietan UBE3A genea inprontapean aurkitzen ez denez, adierazpen bi-alelikoa mantentzen da (Maranga et al.).

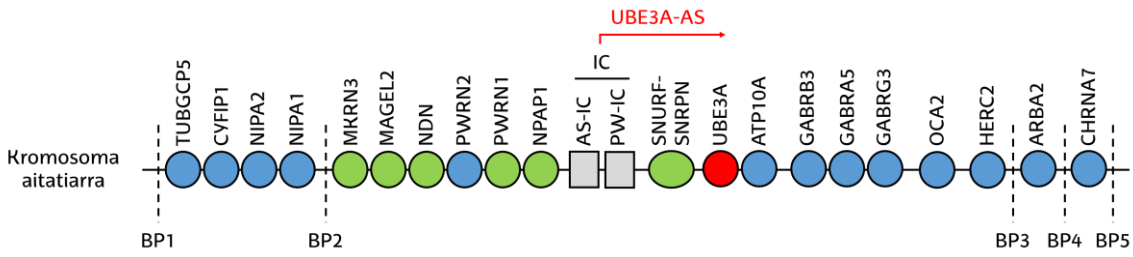

13. irudia. UBE3A genearen inpronta-mekanismoa. Neuronetako kromosoma aitatiarrean PW-IC inpronta-zentrua metilatu gabe dagoenez, UBE3Aren adierazpena ekiditen duen UBE3A-AS transkriptoa kodetzen da. Neuronetako kromosoma amatiarrean, aldiz, inpronta-zentrua metilatuta dagoenez, ez da UBE3A-AS transkriptoa kodetzen, eta UBE3A genea adierazi egiten da. Urdinez adierazpen bi-alelikoa duten geneak, berdez adierazpen aitatiarra duten geneak, grisez inpronta-zentruak eta gorriz isildutako geneak. Biribilak kromosoman kodetzen diren geneak eta karratuak inpronta-zentruak. Marra etenez BP1-BP5 hauste-puntuak. Maranga et al., 2020tik moldatuta.

Hori horrela izanik, Angelman sindromea lau arazo genetikoren ondorioz eman daiteke (14. irudia). Batetik, ohikoenak (kasuen % 75) amaren kromosomako 15q11-q13 delezioak izaten dira (Margolis et al., 2015), alegia inpronta-domeinu osoa eta inprontapean ez dauden zenbait gene ere hartzen dituzten *de novo* sortutako 5-7 Mb arteko delezioak. Delezio horiek errekonbinazio ez-homologoz ematen dira, hauste-puntuetan aurkitzen diren errepikapenezko sekuentzien ondorioz. Normalean, delezioak sei hauste-puntutatik sortzen dira (BP1-BP3, BP4A, BP4B eta BP5) (13. irudia) (Buiting et al., 2016). Angelman sindromedun banakoek bi klasetako delezioak azaltzen dituzte inplikatutako hauste-puntuaren arabera; I klasekoak (BP1 eta BP3 hauste-puntuetatik sortutakoak, delezio-kasuen % 40) eta II klasekoak (BP2 eta BP3 hauste-puntuetatik sortutakoak, delezio-kasuen % 50). Kasu gutxi batzuetan (% 10a baino gutxiago), 10.6 Mb-rainoko delezio handiagoak eman daitezke (BP3tik BP4 edo BP5 hauste-puntuetaraino) (Sahoo et al., 2007). Delezio horiek guztiak GABA hartzaileei dagozkien hiru gene ere barne hartzen dituzte (GABRB3, GABRA5 eta GABRG3).

Angelman sindomea pairatzen duten gaixoen % 5-10ak UBE3A genea mutatuta dauka (Buiting et al., 2015; Kishino et al., 1997; Matsuura et al., 1997). Horien artean gehienek stop kodoi goiztiarren bat daukate (Buiting et al., 2016; Margolis et al., 2015). Amaren aleloan 73 mutazio ezberdin identifikatu dira, gehienak E3 ligasaren HECT domeinu katalitikoari eragiten diotenak (Sadikovic et al., 2014).

Gaixoen % 1-2ak aitarengandik jasotako kromosomen disomia (UPD, *Paternal Uniparental Disomy*) aurkezten du. Horrek esan nahi du 15. kromosoma biek jatorri aitatiarra dutela (Margolis et al., 2015; Nicholls et al., 1992), eta beraz, bi aleloak inprontapean daudenez, adierazpen amatiarreko kopia aktiborik ez daukatela.

AS duten banakoen % 1-3ak inpronta-zentruetako arazoak ditu. Arazoak genetikoak izan daitezke, adibidez, inpronta-zentruen mikrodelezioak ematen direnean (Buiting et al., 1995). Beste kasu batzuetan, arazoak epigenetikoak izaten dira; amarengandik jasotako kromosomako inpronta-zentruaren metilazio faltagatik, UBE3A-AS transkriptoa adierazi eta amaren UBE3A isildu egiten da (Beygo et al., 2020; Buiting et al., 2003, 2016). Edonola ere, arazo horien fenotipoa delezioena baino leunagoa da (Bird, 2014; Williams et al., 2010). Horrek erakusten

du 15q11-q13 lokusean adierazpen bi-alelikoa duten geneek gaixotasunaren larritasunean eragina daukatela (LaSalle et al., 2015).

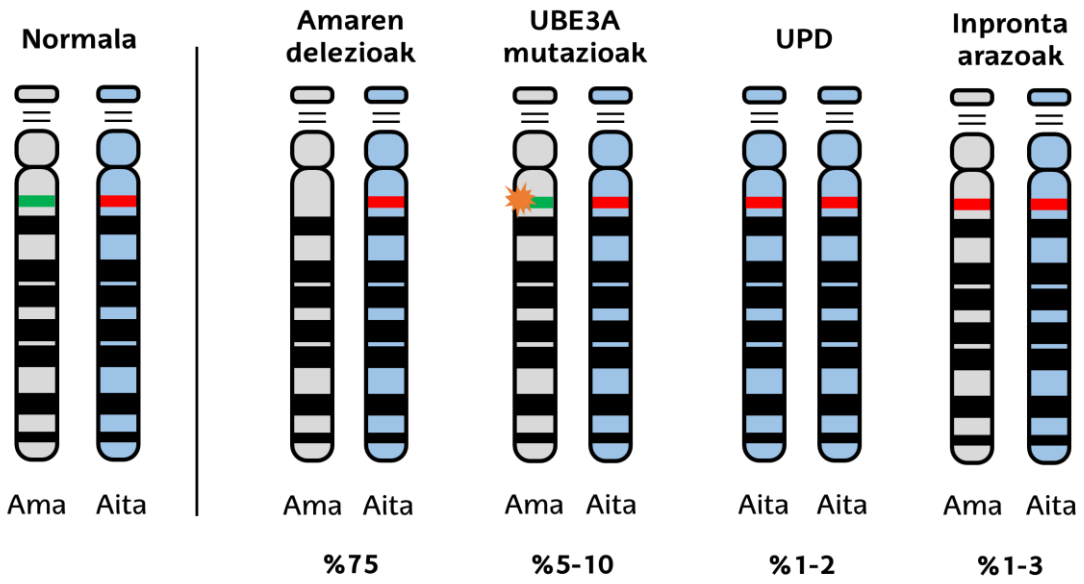

14. irudia. Angelman sindromea eragiten duten akats genetikoak. Neuronetan egoera normalean aurki daitezken kromosomen egitura eta horietan eman daitezkeen lau arazo genetikoak: amaren kromosomako 15q11-q13 eremuaren delezioa (% 75), UBE3A genearen mutazioak (% 5-10), aitarengandik jasotako kromosomen disomia (UPD) (% 1-2) eta inpronta arazoak (% 1-3). Kromosoma amatiarra grisez adierazten da, eta aitatiarra urdinez. Karratu berdea adierazten den UBE3A geneari dagokio, eta gorria, aldiz, inprontapean isilduta dagoen UBE3A geneari. Laranjaz, mutazio puntuala irudikatu da.

Edonola ere, gaixotasunaren arrazoi molekularra anomalia kromosomiko eta epigenetiko guztien azpian dagoen UBE3A proteinaren funtzio-galera da. UBE3A forma trunkatuen sorrera dakarten mutazio puntualak nahikoa dira sindromea garatzeko (Kishino et al., 1997; Matsuura et al., 1997).

2.2. UBE3A E3 ligasa

UBE3A 100 kDa inguruko ubikitina E3 ligasa bat da (Scheffner et al., 1993). Lehenbizi deskribatu zenean behatu zuten UBE3Ak p53 proteinaren ubikitina-bidezko degradazioa bultzatzen zuela, 16 eta 18 motako giza-papilomabirusaren E6 onkoproteinarekin konplexua eratuz (Huibregtse et al., 1991; Scheffner et al., 1993). Horregatik E6AP (*E6-Associated Protein*) izenez ere ezagutzen da

(Huibregtse et al., 1991). UBE3Ak karboxilo muturrean duen zisteina baten bidez ubikitinarekin tioester bitartekari bat eratzen du. Zisteina hori barne hartzen duen 350 aminoazidoko eremua proteina ezberdinen artean kontserbatuta dagoela ikusi zuten, eta HECT (*Homologous to the E6-AP Carboxyl Terminus*) domeinu izendatu zuten (Huibregtse et al., 1991; Scheffner et al., 1993).

Aurrez aipatu bezala, gorputzeko gainerako ataletan ez bezala, neuronetan UBE3aren adierazpena inprontapean dago (Buiting et al., 2016). Entzimaren mailak estuki kontrolatuta egotea ezinbestekoa da garunak modu egokian funtziona dezan. Hori horrela, UBE3Aren gabeziak AS sortzen duen bitartean, gehiegizko dosiak autismoaren espektroko gaixotasunak (*Autism Spectrum Disorders*, ASD) sortzen ditu (Copping et al., 2017; Noor et al., 2015; Smith et al., 2011; Urraca et al., 2013; Yi et al., 2015).

In vitro ikerketek erakutsi dutenez, UBE3Ak K48-motako kateak eraikitzeko joera dauka (Wang eta Pickart, 2005). Hori dela eta, proteinak degradaziora bidaltzea da E3 ligasa horri esleitu zaion funtzio nagusia. Hala ere, gaur egun badakigu UBE3Ak funtzio-aniztasun handiagoa duela. Esaterako, p18/LAMTOR1 ubikitinatuz eta degradaziora bideratuz, plastikotasun sinaptikoa erregulatzen du (Sun et al., 2018; Vatsa eta Jana, 2018), proteasoma inhibituz Wnt/β seinalizazio-bidea aktibatzen du (Yi et al., 2017), eta dendriten morfogenesian ere parte hartzen du (Miao et al., 2013). Horrez gain, ASa duten indibiduoek azaldu ohi duten hipopigmentazioarekin erlazionatutako MC1R proteinaren transkripzioa erregulatzen du (Low eta Chen, 2011), eta 26S proteasoma ubikitinatzen du (Jacobson et al., 2014). Nukleoko hormona hartzaileen ko-aktibatzaile gisa ere jardun dezake (Nawaz et al., 1999). Oraintsu, UBE3Aren galera Alzheimer gaixotasuneko patologia sinaptikoarekin erlazionatuta dagoela ere ikusi dute (Olabarria et al., 2019). Funtzio horiekin guztiekin ez ezik, UBE3A zelulako beste hainbat prozesurekin erlazionatu dute (Lopez et al., 2019; Martínez-Noël et al., 2018), baina ligasa aktibitatea da AS fenotipoaren eragilea. Izan ere, ligasa aktibitatea kaltetua daukaten zelulek, hartzaile aktibitatea bere horretan mantentzen dute (Nawaz et al., 1999; Yi et al., 2015). Hori dela eta, ASren patofisiologia hobeto ulertzeko, ezinbestekoa da ligasa aktibitate horrekin erlazionatutako UBE3Aren neuronetako substratuak identifikatzea.

2.2.1. UBE3Aren substratuak

UBE3A E3 ligasaren gabezia Angelman sindromearen eragilea zela jakin zenetik (Kishino et al., 1997; Matsuura et al., 1997) hainbat saiakera egin dira garunean entzima horren substratuak identifikatzeko, gaixotasunaren mekanismo molekularra hobeto ulertzeko helburuarekin. Deskribatu zen lehen substratua p53 proteina izan zen (Huibregtse et al., 1991). UBE3A adierazten ez zuten saguetan p53 proteinaren maila altuak atzeman zituzten, eta hori ubikitina bidezko degradazio ezagatik izan zitekeela proposatu zuten (Jiang et al., 1998). Ordutik, UBE3Aren hainbat substratu identifikatu dira; DNAren erreplikazioan parte hartzen duen Mcm proteina (Kühne eta Banks, 1998), Bak proteina proapoptotikoa (Thomas eta Banks, 1998), Blk tirosina kinasa (Oda et al., 1999), proteinen degradazioan eta DNAren konponketan parte hartzen duen HHR23A proteina (Kumar et al., 1999) edota AIB1 (Mani et al., 2006), p27 (Mishra et al., 2009) eta Ring1B proteinak (Zaaroor-Regev et al., 2010). Horrez gain, UBE3A bera ere auto-ubikitinatu egiten da, eta beraz, bere jarduera nola modulatzen den azaltzeko, auto-erregulazio mekanismo bat proposatu da (Greer et al., 2010; Nuber et al., 1998).

XXI. mendean, masa espektrometriaren garapenak UBE3Aren balizko substratu gehiagoren identifikazioa ahalbidetu du; esaterako, Pbl eta ATPα proteinak *Drosophila melanogaster* eulian (Jensen et al., 2013; Reiter et al., 2006), Arc eta Epexina-5 proteinak saguen burmuinetan (Greer et al., 2010; Margolis et al., 2010) eta Anexina A1 giza kartzinoma zeluletan (Shimoji et al., 2009).

Hala ere, gaur gaurkoz, oraindik ez dute frogatu proteina horiek zelulako baldintzetan zuzenean UBE3Aren jardunez ubikitinatzen direnik. Ikerketa batzuk, substratuen mailak UBE3Aren presentzian edo faltan aldatu egiten direla frogatu dute (AIB1, Bak, Blk, Mcm7, p53 edo Pbl-ren kasuan) (Jiang et al., 1998; Kühne eta Banks, 1998; Mani et al., 2006; Margolis et al., 2010; Oda et al., 1999; Reiter et al., 2006). Alabaina, ebidentzia ez-zuzena da, proteina horien ugaritasuna beste faktore batzuen mende egon baitaiteke, esaterako transkripzio-mailako erregulazioa. Beste kasu batzuetan, zuzenean UBE3Arekin elkarrekiten duten substratuak identifikatu dituzte, baina *in vitro* saioak erabiliz (esaterako, Arc, HHR23A, ATPα, p27, Ring1B eta UBE3A)(Greer et al., 2010; Jensen et al., 2013; Kumar et al., 1999; Mishra et al., 2009; Nuber et al., 1998; Zaaroor-Regev et al., 2010). *In vivo* burututako saioak, berriz, afinitate purifikazioetan oinarritu dira, eta

saio horietan proteina kontaminatzaileak aurkitzeko aukera handia dago (Anexina A1 eta Epexina 5) (Margolis et al., 2010; Shimoji et al., 2009). Adibide horiek guztiek agerian uzten dute teknologiaren garapenari esker, aurrera pausu handiak egin direla UBE3Aren substratuen identifikazioan; ez horrenbeste beraien balioztatzean. Hori dela eta, UBE3Aren substratuak *in vivo* balioztatzea erronka nagusia bilakatu da.

UBE3Aren substratuen identifikazio-metodo fidagarrien faltagatik emaitza kontrajarriak azaldu izan dira literaturan. Esaterako, *in vitro* burututako esperimentu batean Arc proteina UBE3Aren substratu dela baieztatu zuten (Greer et al., 2010), baina beste talde batek Arc proteinaren ubikitinazioa ez duela UBE3Ak kontrolatzen erakutsi du (Kuhnle et al., 2013), eta beste E3 ligasa ezberdin bat proposatu du Arc-en erregulatzaile gisa (Mabb et al., 2014). Modu berean, hasiera batean Na^+/K^+ ATPasa UBE3Aren substratu gisa deskribatu zen arren (Jensen et al., 2013), ATPasaren eta E3 ligasaren arteko interakziorik ezin izan da detektatu ASren modelo diren saguen burmuinetan (Kaphzan et al., 2011). Horrek guztiak efektu ez-zuzen bat egon daitekeela pentsarazten digu. Hau da, UBE3Ak zuzeneko substratuak ubikitinatzen ditu, eta horiek, nolabait, deskribatu diren beste proteina horietan dute eragina. Hortaz, efektu ez-zuzen batez eraldatutako proteina horiek ASa duten pazienteetan garrantzitsuak izan daitezkeen arren, horien gainetik dauden substratu zuzenak ezagutzea da interesgarriagoa, berauen erregulazio faltak eragin baitezake ASren patofisiologia (Sell eta Margolis, 2015).

UBE3Aren substratu zuzenak identifikatzeko ahalegin horretan, gure taldeak *Drosophila melanogaster* euliaren neurona fotohartzaileetan burututako ikerketa batean *Ube3a* proteinaren balizko substratuen lista bat lortu du (Ramirez et al., 2018). Zerrenda horretan, besteak beste, *Rngo* anezka-proteina dago, legamietan (*Ddi1*) nahiz gizakietan (DDI1 eta DDI2) kontserbatuta aurkitzen dena.

Legamietako *Ddi1* proteinak proteasoma-anezka gisa jarduten du (Sivá et al., 2016), proteinen birziklapenean parte hartzen du (Sirkis et al., 2006), zenbait t-SNARE proteinekin elkartzen da (Marash eta Gerst, 2003), eta exozitosia edo proteinen sekrezioa erregulatzen ditu (Lustgarten eta Gerst, 1999; Perteguer et al., 2013). Guzti hori dela eta, SNARE-bidezko exozitosia kontrolatuz, transmisio sinaptikoan parte hartzen duen proteina bezala deskribatu da (Gabriely et al., 2008). Aldiz, ornodunetan dituen bi homologoen −DDI1 eta DDI2− funtzio

biologikoa ez da oraindik guztiz argitu (Morawe et al., 2011). Giza DDI2 proteinak proteasa gisa jarduten du (Mótyán et al., 2020; Perteguer et al., 2013); Nrf1 moztu eta aktibatzen du proteasomaren funtzioa kaltetuta dagoenean (Koizumi et al., 2016). Aldiz, ez da oraindik giza DDI1 proteinaren funtzio biologikorik deskribatu. Horrez gain, DDI2 giza gorputzeko ehun guztietan aurkitzen bada ere, DDI1en lokalizazioa barrabil-ehunetara mugatzen da gehienbat (Uhlén et al., 2015).

DDI1/DDI2 proteinen garrantzia biologikoa argitzeke dagoen arren, beraien egiturak ezagunak dira. Legamien Ddi1 (yDdi1), *Drosophila melanogaster*ren Rngo, saguen DDI1/DDI2 (mDDI1/mDDI2) eta gizakion DDI1/DDI2 (hDDI1/hDDI2) proteinek hiru domeinu dituzte, espezie guztien artean kontserbaturik daudenak; ubikitina-bezalako domeinua (*Ubiquitin-Like-Domain*, UBL), helize domeinua (*Helical-Domain*, HDD) eta proteasa domeinua (*Retroviral Protease Domain*, RVP) (Sivá et al., 2016) (15. irudia). Giza eta saguen DDI1 proteinak ezik, gainerakoek ere ubikitina lotzeko domeinua dute karboxilo muturrean, proteasoma-anezketan ohikoa den bezala; UBA domeinua Drosophilan eta legamian, eta UIM motiboa gizakien eta saguen kasuan.

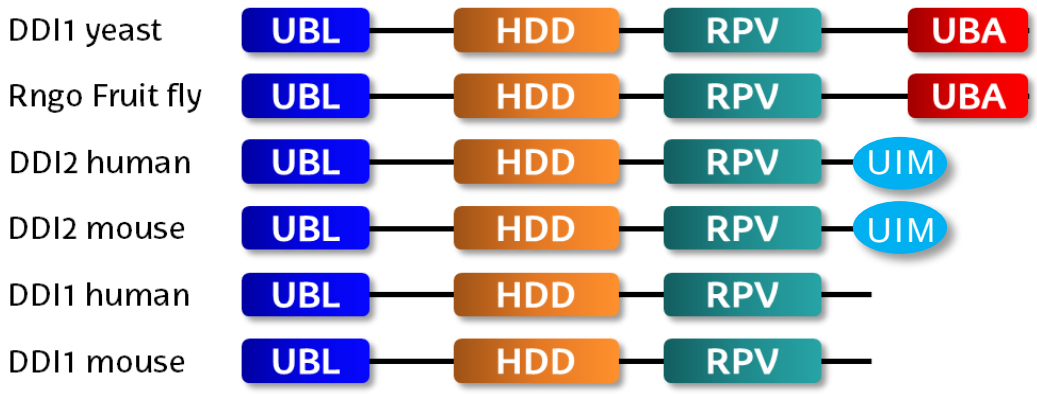

15. irudia. Legamia, Drosophila, sagu eta gizakien DDI1 homologoen egiturak. Legamien *Ddi1* (*yDdi1*), Drosophilaren *Rngo*, giza DDI1 eta DDI2 (hDDI1/hDDI2) eta saguen DDI1/DDI2 (mDDI1/mDDI2) proteinen egituren domeinu ezberdinen adierazpen grafikoa. Urdinez, ubikitina bezalako domeinua (UBL); laranjaz, helize domeinua (HDD); berdez, proteasa domeinua (RPV); gorriz, ubikitinarekin lotzeko domeinua (UBA); urdin argiz, ubikitinarekin elkarrekiteko motiboa (UIM). Guztiek dituzte UBL, HDD eta RPV domeinuak, *yDdi1* eta *Rngo* proteinek UBA domeinua dute, eta giza eta sagu DDI2k UIM motiboa.

Ubikitina bezalako domeinuak (UBL) proteasomarekin elkarrekiten du, proteinen ezagutza eta degradazioa baimentzeko (ikusi *1.1.6. Ubikitina Hartzaileak* atala). Helize domeinuak ongi kontserbatutako eremua dauka, eta legamien beste proteasoma-anezka batzuekin –*Rad23* eta *Dsk2*–, antzekotasun handia dauka (Sivá et al., 2016). Proteasa domeinuan azido aspartiko hondar katalitikoak kontserbaturik daude, eta horrek baimentzen du proteina horiek proteasa funtzioa burutzea (Dirac-Svejstrup et al., 2020; Mótyán et al., 2020).

Legamien eta Drosophila*ren* kasuan, *yDdi1/Rngo* proteinek ubikitinarekin batzeko domeinua (UBA) daukate. Modu horretan, degradatu behar diren proteinen ubikitina kateekin elkarrekin dezakete (Bertolaet et al., 2001; Kaplun et al., 2005; Morawe et al., 2011). Nahiz eta gainerako homologoek UBA domeinurik izan ez, funtzio hori ordezkatzen duten domeinu ezberdinak deskribatu dira; DDI2ren kasuan, gizakion eta saguen homologoek ubikitinarekin elkarrekiteko motiboa (UIM) dute karboxilo muturrean, DDI2k proteasoma-anezka bezala jarduteko aukera zabalduz. Giza eta saguen DDI1en kasuan, ez dute ez UBA, ez UIM domeinurik. Hala ere, amino muturreko UBL domeinuak ubikitina ezagutu dezakeela frogatu da, eta proteasoma-anezken mekanismo berri bat proposatu da (Nowicka et al., 2015).

2.2.2. UBE3A: isoformak, egitura eta lokalizazioa

Drosophila euliek *Ube3a*ren isoforma bakarra daukate (Wu et al., 2008). Aldiz, saguetan eta gizakietan hiru isoforma deskribatu dira (LaSalle et al., 2015; Yamamoto et al., 1997) (16. irudia). Saguen kasuan, I. isoforma transkripto ez-kodetzaile bat da, eta burmuinaren garapenean garrantzitsua dela frogatu den arren (Valluy et al., 2015), gizakietan ez da existitzen. Saguen II. isoforma da luzeena, eta ASren sagu modeloetan dendriten fenotipo osasuntsua berreskuratzeko ahalmena du (Miao et al., 2013). Azkenik, saguen III. isoformari amino muturreko zati bat falta zaio, eta isoforma horren gabeziak arazo elektrofisiologikoak eta jokabide-arazoak dakartza (Avagliano Trezza et al., 2019). Gizakion kasuan, UBE3Aren lehen 8 exoien moztitsasketa alternatiboz sortutako hiru isoforma bereizten dira. Horien arteko ezberdintasun fisiologikoak ez dira guztiz ezagutzen, ezta horietako bakoitzak Angelman sindromean duen garrantzia ere. Frogatu da gizakion I. isoforma (saguen III. isoformaren baliokidea)

dela ugariena ama-zelula enbrionarioetatik eratorritako neuronetan (Sirois et al., 2020). Hala ere, I. isoformaren gabeziak gainerakoek baino sintomotalogia leunagoa dakarrela frogatu dute (Sirois et al., 2020). II. isoforma luzeena da, eta sekuentzia kanonikoa kontsideratzen da. Gizakion III. isoformari dagokionez (saguen II. isoformaren parekoa), beste hainbat organismotan aurkitu dituzten transkriptoen baliokidea da (LaSalle et al., 2015). Isoforma horietako bakoitza amino muturreko sekuentzian desberdintzen da (16. irudia).

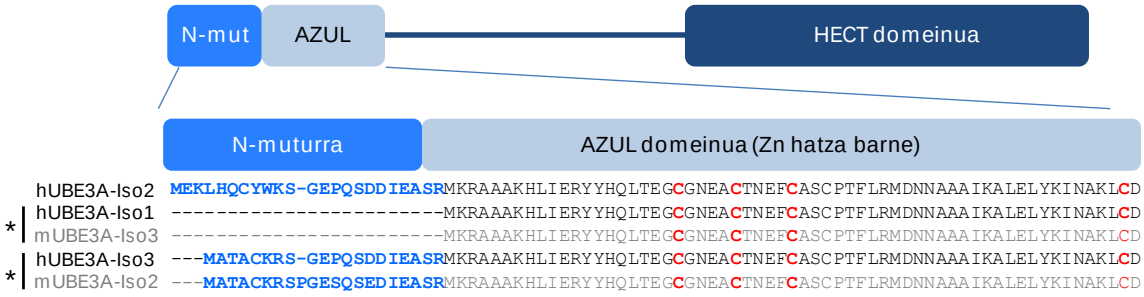

16. irudia. UBE3A proteinaren isoforma ezberdinak sagu eta giza espezieetan. Amino muturra (urdina), AZUL domeinua (urdin argia) eta HECT domeinua (urdin iluna) bereizten dira. Behean, gizakien (hUBE3A, beltzez) eta saguen (mUBE3A, grisez) aurki daitezkeen isoforma ezberdinen proteina-sekuentzien alineazioa azaltzen da. Letra urdinez, amino muturra azpimarratzen da, eta gorriz, AZUL domeinuko zisteinak markatu dira, zink ioia batzen duten hondarrak aurkitzen diren guneak. *Gizakiaren eta saguaren isoforma baliokideak.

UBE3A proteinaren egiturari dagokionez, bi domeinu ezagutzen dira: amino muturreko AZUL (*Amino-terminal Zn-finger of Ube3a Ligase*) domeinua, eta karboxilo muturreko HECT domeinua (17. irudia). Bi domeinu horien artean, HPV16 giza papilomabirusaren E6 proteina batzeko gunea kokatzen da (Khatri eta Man, 2019). Horrez gain, UBE3A proteinak oligomero gisa jarduten duela ere proposatu da (Ronchi et al., 2014).

1999an, UBE3Aren HECT domeinua kristalizatu zuten, bere bikote den UbcH7 E2 entzima-konjugatzailearekin eratutako konplexua aztertuz (Huang et al., 1999). Bertan kokatzen da ubikitina garraiatzeaz arduratzen den zisteina katalitikoa (C833) (17. irudia). HECT domeinua karakterizatze aldera, K-lobulua kristalizatu dute ligasaren katalisi-propietateak aztertzeko (Ries et al.) eta UBE3A-E6-p53 konplexuaren egitura dinamika ere ikertu dute (Sailer et al., 2018). HECT E3 ligasa bakoitzak ubikitina-kateen sintesirako mekanismo ezberdinak ditu, eta beraz, HECT domeinuek baldintzatuko dute zein kate-mota eraikiko dituzten

(French et al., 2017; Lorenz, 2018; Wang eta Pickart, 2005). UBE3Aren kasuan, HECT domeinuaren karakterizazioak UBE3Ak gehienbat K48 motako ubikitina-kateak sortzen dituela erakutsi du (Elu et al., 2019; Kobayashi et al., 2018; Ries et al., 2019).

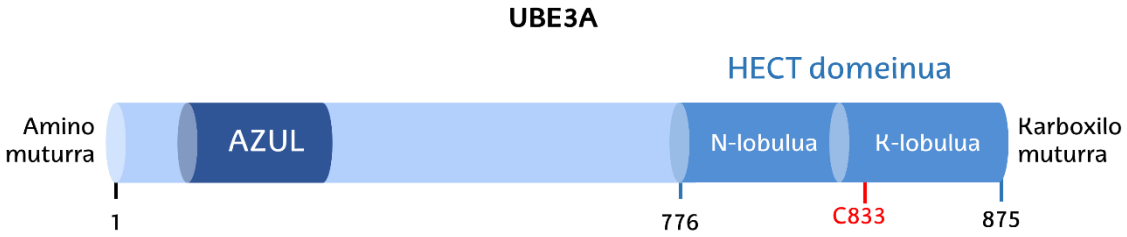

17. irudia. UBE3A E3 ligasaren egitura. Amino muturrean AZUL domeinua eta karboxilo muturrean HECT domeinu katalitikoa bereizten dira. HECT domeinuaren karboxilo muturreko K-lobuluan ubikitinarekin interakzionatzen duen zisteina katalitikoa (C833) aurkitzen da. Giza papilomabirusaren (HPV16) E6 proteina lotzeko gunea HECT domeinuaren aurrean kokatzen da. Khatri eta Man, 2019tik moldatua.

UBE3Aren amino muturra ezezagunagoa bada ere, jakin badakigu bertan kokatzen dela zinkarekin batzen den AZUL (*Amino-terminal Zn-finger of Ube3a Ligase*) domeinua (Lemak et al., 2011) (18. irudia). Domeinu horrek helize-bira-helize konformazioa hartzen du Cys-X_4-Cys-X_4-Cys-X_{28}-Cys motiboa osatuz, non lau zisteina hondarrek Zn^{2+} ioia koordinatzen duten (18. irudia). Lehen hiru zisteinak 23 aminoazidotako biran kokatzen dira, eta bi helizeak egonkortzen dituzte. Laugarren zisteina berriz, domeinu horren karboxilo muturrean kokatzen da. Oraintsu, giza Rpn10 proteasoma-hartzailea (PSMD4) UBE3Aren AZUL domeinuarekin batzen dela, eta domeinu hori UBE3A nukleoan kokatzeko beharrezkoa dela frogatu dute (Avagliano Trezza et al., 2019; Buel et al., 2020).

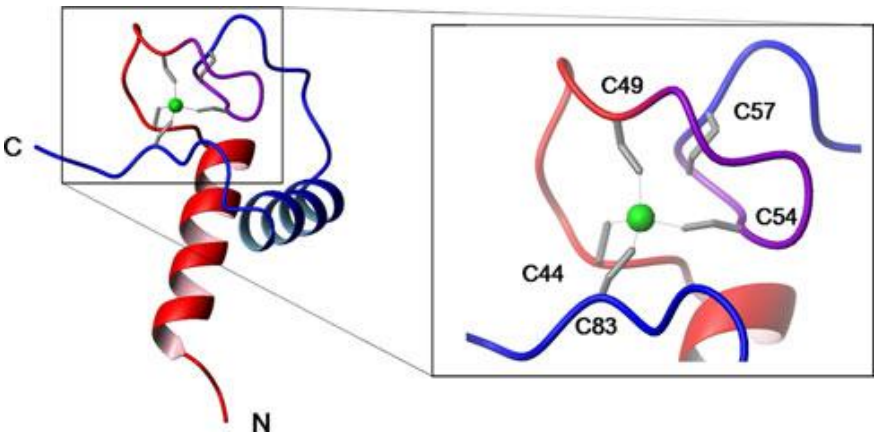

18. irudia. UBE3A E3 ligasaren AZUL domeinuaren egitura. Kristalografia bidez AZUL domeinuak helize-bira-helize itxura duela ebatzi da, non bira osatzen duten zisteina hondarrek zink atomo batekin interakzionatzeko gunea osatzen duten. Lemak et al., 2011tik hartuta.

UBE3A proteinaren lokalizazioa zitoplasmatikoa nahiz nuklearra izan daiteke. PSMD4 proteinak, UBE3Aren edozein isoformaren AZUL domeinura batuz, UBE3A nukleora translokatzen du (Avagliano Trezza et al., 2019). Jarraian, UBE3Aren amino muturreko sekuentziari esker garraio aktiboz zitosoloera bueltatzen da. Saguetan, II. isoformak esportazio-seinale den amino muturra dauka, aldiz, III. isoforman amino muturreko sekuentzia hori falta denez, ezin da zitosolera bueltatu (Avagliano Trezza et al., 2019). Hortaz, saguetan, II. isoforma zitoplasman aurkitzen da, eta III. isoforma, berriz nukleoan (Miao et al., 2013). Gizakien kasuan, isoforma guztiak zitoplasman zein nukleoan koka daitezke (Sirois et al., 2020).

2.3. Angelman sindromeari aurre egiteko estrategiak, terapiak eta tratamendu farmakologikoak

Angelman sindromearen inguruko ikerketek gaixotasuna tratatzeko alternatiba berrien garapenerako ateak ireki dituzte (Bi et al., 2016; Tan eta Bird, 2017). Momentuz, estrategia gehienak UBE3A proteinaren berrezarpenera bideratzen dira. Esaterako, sagu gazteetako neurona GABAergikoetan UBE3A zuzenean berrezarri, eta epileptogenesia gutxitzea lortu dute (Gu et al.). UBE3A berrezartzeko gehien erabiltzen den estrategia inprontapean dagoen aitaren UBE3A aleloa aktibatzea da. Horretarako, UBE3Aren adierazpena blokeatzen duen UBE3A-AS transkriptoaren sintesia saihesten da. Betaina eta azido folikoa bezalako gehigarri dietetikoen bidez, UBE3A-ASren promotorea hipermetilatu, eta ondorioz, bere adierazpena blokeatu dute (Bird et al., 2011; Peters et al., 2010). Zuzenean UBE3A-AS transkriptoarekin batzen diren oligonukleotido espezifikoak, hala nola topoisomerasak eta transkripzio-faktore artifizialak ere erabili dituzte, UBE3A-ASren funtzioa blokeatu edo adierazpena murrizteko (Bailus et al., 2016; Huang et al., 2011; Meng et al., 2015; Milazzo et al., 2021). Horrez gain, badira UBE3A-AS transkriptoa ituratu beharrean, terapia geniko bidez UBE3A saguetan

txertatu duten ikerketak (Daily et al., 2011). Nahiz eta estrategia horiek guztiak klinikoki bideragarriak izan, momentuz behintzat, ez dute gaixotasunaren sintometan onura esanguratsurik erakutsi. Aldiz, saguen enbrioi goiztiarretan UBE3A berrezarriz, lortu da ASren fenotipoa ekiditea (Silva-Santos et al., 2015). Hori dela eta, arestian aipatutako saiakeren porrotaren arrazoietako bat UBE3Ak bereziki garapen prozesuan duen garrantzia izan daiteke. Ildo horretatik, gizakietan ere jaio aurretiko tratamenduak burutzeko estrategiak planteatu dituzte (Zylka, 2020). UBE3Aren gabeziaren ondorioz kaltetutako prozesu zelularrak tratatzea helburu duten estrategiak ere badira. Esaterako, bide dopaminergikoak, kaltzio-kalmodulinaren fosforilazioa, mutur dendritikoen heltzea, zitoeskeletoaren antolakuntza, seinalizazio-sinaptikoa, histonen azetilazioa edo mitokondrioen disfuntzioa (Kumar et al., 2019; Tan eta Bird, 2017; Tonazzini et al., 2019).

Edonola ere, orain arte pazienteengana iritsi diren tratamenduak sintometan zentratzen dira soilik; zehazki, epilepsia eta lo arazoak ekiditeko farmakoak dira (Egan et al., 2020; Hanzlik et al., 2020; McDougle eta Keary, 2020; Tan eta Bird, 2017). Ikerketa fasean dauden Lovastatina eta Cannabidiol farmakoek ASren sagu modeloetan epilepsia eta hiper-kitzikapena murrizten dituztela frogatu dute (Chung et al., 2018; Gu et al., 2019). Ganaxolonak eta garapen bidean dagoen NSI-189 molekulak saguen memorian eta plastikotasun sinaptikoan onurak eragiten dituztela ere frogatu da (Ciarlone et al., 2016; Liu et al., 2019). Horrez gain, Perampanel deritzon AMPA hartzaileen antagonistak ASdun banakoek azaltzen duten mugimendu ez-boluntario mota bat gutxitzen duela frogatu berri dute (Kawano et al., 2020).

2.4. Angelman sindromea ikertzeko animalia modeloak

Edozein gaixotasun ikertzeko, nahiz itu terapeutikoak aurkitu eta saiakera klinikoetara eraman ahal izateko, modelo egokiak aurkitu behar dira. Modelo horiek gaixotasunaren genotipo eta fenotipo antzekoa izateaz gain, jokabidean ere antzekotasunak azaldu behar dituzte (Sonzogni et al., 2018). Angelman

sindromearen ikerkuntzan gehien erabili diren animalia modeloak saguak, arratoiak eta *Drosophila melanogaster* eulia izan dira.

2.4.1. Modelo murinoak

Ikerkuntzan sarritan erabili ohi den organismoa sagua da, gaixotasun askoren ezaugarri fenotipikoak eta genotipikoak azaltzen baitituzte. Angelman sindromearen kasuan ere, sagua gaixotasuna ikertzeko modelo bikaina da. AS pairatzen duten gaixoetan kaltetutako eta saguen 7. kromosomako locusak antzekotasun genetiko handia dute, gene berdinak izateaz gain, gene horien inpronta genetikoa berdina baita.

ASren modelo diren saguak lortzeko hainbat estrategia garatu dira, eta guztiek UBE3A proteinaren adierazpena oztopatzen dute: mutazio puntualak, locusaren delezioak, inpronta-zentruen eraldaketa eta alelo aitatiarraren bikoizketa, besteak beste (Rotaru et al., 2020). Sagu horiek Angelman sindromedun banakoek dituzten mugimendu, adimen, hizkuntza eta loaren arazo berdintsuak dituzte (Rotaru et al., 2020), nahiz eta lerro ezberdinen artean ezberdintasunak egon (Born et al., 2017). Hortaz, bai genetikoki eta bai fenotipikoki, saguak ASa ikertzeko organismo baliagarriak dira.

Sagu modeloei esker, UBE3A neuronen nukleoan kokatzen dela, eta UBE3Aren galerak neuronen aktibitate elektrofisiologikoan aldaketak dakartzala ondorioztatu ahal izan da (Avagliano Trezza et al., 2019). Horrez gain, UBE3Aren adierazpena oztopatuta duten saguak erabiliz, ASren fenotipoak ekiditeko UBE3A garunaren zein garapen fasetan berrezarri beharko litzatekeen jakin ahal izan dute (Silva-Santos et al., 2015). Are gehiago, sagu horiek erabiliz, frogatu dute fase helduan UBE3A berraktibatzeak neuronen aktibitate elektrofisiologiko egokia berrezartzen duela (Rotaru et al., 2018).

ASren oinarria UBE3Aren gabeziak sortzen duen arren, ASren inguruko ikerketa batzuk UBE3A gainadierazten duten saguak erabiltzen dituzte. Sagu horiek autismoarekin erlazionaturiko ezaugarriak izateaz gain, glutamato bidezko transmisio sinaptikoak gutxituta dauzkate (Smith et al., 2011), beraz, ASren ezaugarri batzuk ikertzeko ere oso egokiak dira. Esaterako, gure laborategian,

UBE3A gainadierazten duten saguak erabili ditugu UBE3Aren substratuak aurkitzeko (eskuizkribua berrikuspenean, Lectez et al ,2022).

Ohikoenak saguak diren arren, oraintsu, *Ube3a* gene osoa ezabatuz, ASren modelo gisa erabili daitekeen arratoia garatu dute (Dodge et al., 2020). Arratoi horrek ez du garunean UBE3A adierazten, eta ondorioz, koordinazio motorean, oroimenean eta adimenean arazoak ditu.

2.4.1.1. Portaera ikertzeko teknikak

Modelo murinoetan, mekanismo molekularrak ikertzeaz gain, portaerak ere aztertu daitezke, organismo konplexu bat izanik giza gaixotasunen sintoma asko aurkezten baitituzte. Oraintsu, ASren sagu modelo batekin buruturiko ikerketa batean sagu horiek portaera oldarkorra azaltzen dutela deskribatu dute (Simchi eta Kaphzan, 2021). Angelman sindromeak autismoaren koadro klinikoarekin dituen antzekotasunak direla eta, ohikoena autismoaren ikerketan erabiltzen diren portaera-azterketak burutzea da AS ikertzeko. Taula honetan laburbildu dira frogarik ohikoenak, eta beraz, Tesi honetan egin direnak (2. taula):

2. taula. Saguen portaera aztertzeko frogarik ohikoenak, zein adin-tartetan burutu behar diren eta horien deskribapena.

		Adina	Deskribapena
Portaera soziala	Ultrasoinu bokalizazioak	P0-P2	Saguak amarengandik banatzen dira eta ultrasoinu bezala egiten dituzten bokalizazioak zenbatzen dira.
	Elkarrekintza soziala	P25-P28	Saguek elkarrekiten pasatzen duten denbora zenbatzen da.
	Hiru ganberak	P40-P50	Alboetako bi ganberetan ontzi opako bana jartzen da, bata sagu batekin eta bestea hutsik. Saguak ontzi bakoitza esploratzen pasatzen duen denbora neurtzen da.

Aktibitate lokomotorea	Eremu irekia	P28-P33	Distantzia eta abiadura neurtzen da.
Antsietatea	Ilunpe-argi ganberak	P50-P60	Bi ganbera, bat argitan eta bestea ilunpetan. Saguak ganbera bakoitzean pasatzen duen denbora eta lehen aldiz argitako ganberara irteteko behar duen denbora neurtzen dira.
Portaera errepikakorrak	*Grooming*	P50etik aurrera	Saguak bere burua miazkatzen pasatzen duen denbora neurtzen da.
Bestelakoak	Plaka beroa	P50etik aurrera	Oso bero dagoen zoru baten gainean sagua utzi eta mina sentitzeko zeinuak egiten hasi arteko denbora neurtzen da (gehienez 15 segunduz).

2.4.2 *Drosophila melanogaster* eulia

XX. mendearen hasieran, Williams E. Castle-ek Harvard Unibertsitatean (Cambridge, USA) estreinakoz *Drosophila melanogaster* eulietan hasi zituen ikerketak (Castle, 1906; Roberts, 2006). Ordutik, fruta-eulietan eginiko ikerketek ornogabeetatik gizakietara kontserbatutako oinarrizko prozesu biologiko ugari ulertzen lagundu digute: esaterako, sexuari loturiko herentzia (Morgan, 1910) eta kromosomen bidezko herentzia (Doncaster, 1916; Roberts, 2006), X-izpien aktibitate mutagenikoa (Muller, 1927), garapen enbrionarioa kontrolatzen duten gene esentzialen karakterizazioa (Lewis, 1978; Nüsslein-Volhard eta Wieschaus, 1980), edota inmunitate sistemaren aktibaziorako beharrezkoak diren Toll hartzaileen identifikazioa (Lemaitre et al., 1996).

Drosophila ikerkuntza-modelo gisa arrakastatsua izatearen hiru arrazoi nagusiak ondorengoak lortzeko azkartasuna, zainketa erraza eta mantenu-kostu

baxua dira. Bizi-zikloari dagokionez, lau etapa nagusitan banatzen da morfologian oinarrituz: arrautza, larba, pupa eta euli heldua (19. irudia). Arrautzatik euli heldua izan arte behar duen denbora tenperaturaren eta hezetasunaren araberakoa da. Hori horrela, 25 ºC eta % 60ko hezetasun erlatiboarekin, euliaren bizi-zikloa 10 egunekoa da. Aldiz, tenperatura 20 ºC-koa bada, euliak bizi-zikloa betetzeko 15 egun behar ditu. Euli-enbriogenesiak 24 ordu irauten du. Ondoren, ar itxurako animalia bat jaiotzen da, lehen larba (L1) gisa ezagutzen dena. L1 larba 24 orduz elikatu ostean, bigarren larba handiago batean bihurtzen da (L2), eta modu berean, L2 hori 24 ordu geroago hirugarren larban (L3) bilakatzen da. L1, L2 eta L3 larben ezberdintasun nagusia beraien tamaina da (L1 txikiena eta L3 handiena). 2-3 egun irauten duen L3 larba etaparen ostean pupa etapa hasten da. Pupazio aurretik larbak elikatzeari uzten dio, eta pupaziorako egokia den leku lehor bat bilatzen du. Momentu horretan, larba geldirik geratzen da eta gradualki pupa itxura hartzen du. Hurrengo 4-5 egunetan metamorfosia ematen da, eta larba egitura gehienak eraldatu egiten dira helduen organoen garapena emateko. Aldeak alde, ernalketa gertatzen denetik 10-11 egunera pupatik euli heldua ateratzen da.

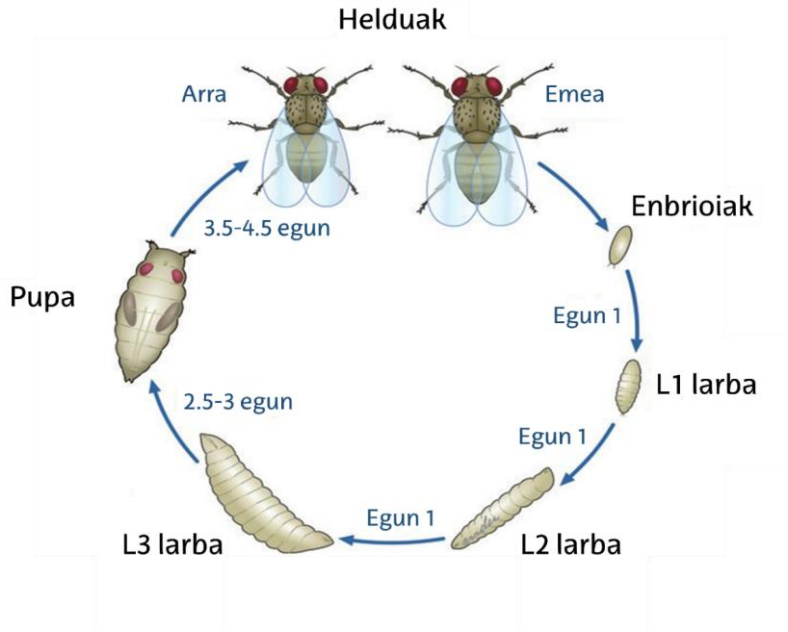

19. irudia. *Drosophila melanogaster* euliaren bizi-zikloa. Ernalketa eman eta enbrioiak jaiotzen direnean, larba bilakatzen dira. Lehen 24 orduetan L1 larba garatzen da. Hurrengo 24 orduetan elikatzen jarraituz L2 larba bihurtzen da, eta 24 ordu geroago tamaina handieneko L3 larba bilakatzen da. 2-3 egun beranduago elikatzeari utzi eta pupa izatera pasatzen da. Orduan metamorfosi fasea hasten den. Beste 3-4 egun pasa ostean, eulia jaiotzen da 11 eguneko zikloari amaiera emanez.

Bizi-ziklo laburra izateaz gain, genoma txikia dutenez, X/Y sexu-kromosoma bikote batez eta hiru autosoma-bikotez osatua (Adams et al., 2000), genetika eta geneen funtzio biologikoak ulertzeko sistema egikia da. Gainera, gaixotasunekin erlazionatutako giza geneen % 75ak eulietan homologoa daukate (Reiter et al., 2001). Beraz, Drosophilak *in vivo* sistema sinple bat eskaintzen du gene horien funtzioa ikertu ahal izateko (Pandey eta Nichols, 2011). Hori dela eta, hainbat giza gaixotasun aztertzeko euli modeloak sortu izan dira (Jackson, 2008; Pandey eta Nichols, 2011; Sang eta Jackson, 2005).

Angelman sindromea ikertzeko ere modelo bikaina da, *D. melanogaster* euliek giza UBE3Aren homologoa den *Ube3a* proteina adierazten baitute, sekuentzia mailan % 63ko antzekotasuna izanik. Eulietan *Ube3a*ren gabeziak aktibitate motorean akatsak eta memoria arazoak sortzen ditu (Gatto eta Broadie, 2011; Wu et al., 2008). Esaterako, euliek geotaxiagatik berezkoa duten gora egiteko ahalmena galtzen dute (Wu et al., 2008). Garapen faseko *Ube3a*ren gehiegizko adierazpenak berriz, morfologia arazoak eta hilkortasuna eragiten ditu (Wu et al., 2008). Euli modeloekin egindako ikerketei esker, *Ube3a*ren hainbat substratu berri ezagutzeaz gain (Ramirez et al., 2018), E3 ligasa sinapsien hazkuntzarekin eta endozitosiarekin erlazionatuta dagoela dakigu (Li et al., 2016a).

Azken mendean, Drosophilarekin lan egiteko tresna eta baliabide ugari garatu dira. Horien artean ezagunena GAL4/UAS sistema binarioa da. Sistema hori 1993an sortu zuten Andrea H. Brand eta Norbert Perrimonek. Euliekin lan egiterakoan erabili ohi den teknika genetikoa da. Sistema honen bidez gene jakin bat *in vivo* adierazi daiteke modu ituratuan, edozein zelula motan eta euliaren garapen prozesuko une konkretu batean. Adierazten den genea euliarena nahiz beste organismo batena izan daiteke. Sistema hori GAL4 proteinak eta UAS (*Upstream Activating Sequence*) sekuentziak osatzen dute (20. irudia).

GAL4 legamiaren proteina da, eta geneen transkripzioa aktibatzen du. Zehazki, galaktosaren katabolismorako beharrezkoak diren geneak aktibatzen ditu (Traven et al., 2006). Horretarako, GAL4 proteinak gene horien UAS sekuentziekin elkarrekin behar du. UAS sekuentziak DNAren eremu zehatzak dira 5′-CGG-N11-CCG-3′ kontsentsu-sekuentziadunak (Marmorstein et al., 1992). GAL4-UAS elkarrekintza oso espezifikoa denez, GAL4 proteinak ezin du UAS sekuentziarik ez daukan gene baten transkripzioa aktibatu. *D. melanogaster*

euliak ez dauka GAL4 proteinaren homologorik, ezta ere UAS sekuentziadun generik. Hortaz, intereseko genea UAS sekuentziaren ostean adierazten duen euli bat, GAL4 proteina adierazten duen euliarekin gurutzatuz gero, ondorengoetan intereseko genearen transkripzioa lortuko da (Fischer et al., 1988)(20. irudia). Horrez gain, GAL4 proteinaren adierazpena intereseko sustatzaile baten mende jartzen da. Hau da, sustatzaile hori ehunekiko edo garapen fasearekiko espezifikoa bada, intereseko proteina leku edo momentu jakin batean besterik ez da adieraziko (Brand eta Perrimon, 1993).

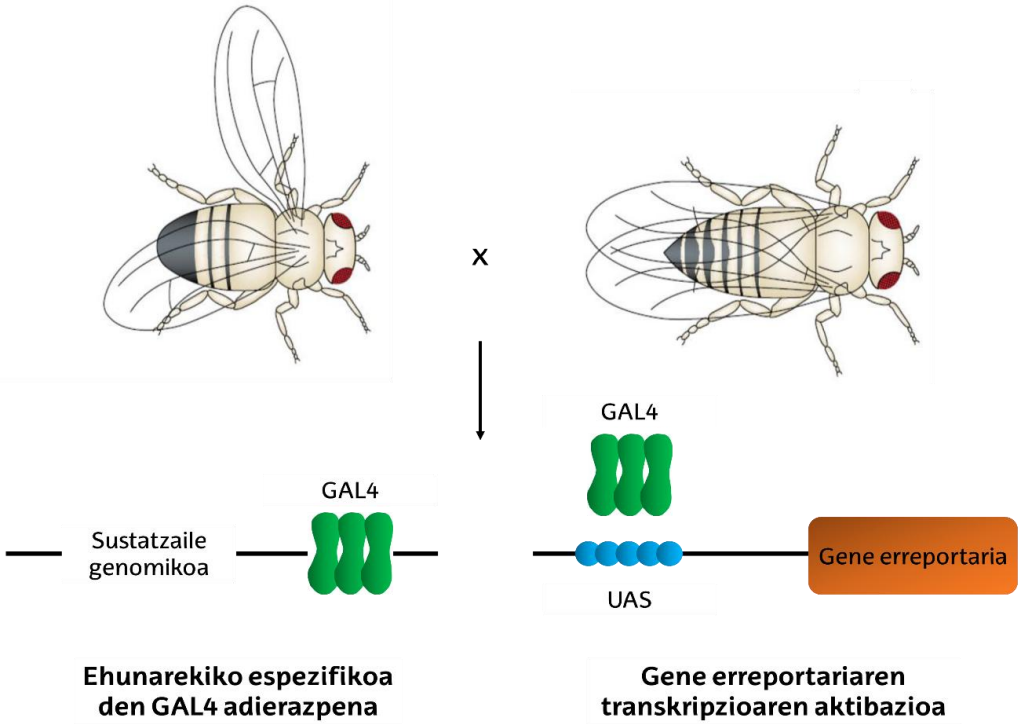

20. irudia. GAL4/UAS sistema binarioa. GAL4/UAS sistema bi elementuz osatzen da: legamiaren GAL4 proteina eta edozein gene erreportaritik ur-gora aurkitzen den UAS sekuentzia aktibatzailea. GAL4 proteina Drosophila eulietan adierazi daiteke ehun espezifiko batean edo denbora jakin batean, horretarako GAL4 proteinaren aurrean sustatzaie genomikoak edo promotore ezagunak jarriz. Bestalde, UAS sekuentzia intereseko genearen alboan gehituz, gene horren adierazpena GAL4ren presentziaren menpekoa izango da. Hortaz, UAS-intereseko genea duten euliak, ehun espezifiko batean GAL4 adierazten duten euliekin gurutzatzean, ondorengo euliek intereseko genea GAL4 proteinaren distribuzio berdinean adieraziko dute. St Johnston, 2002tik moldatuta.

GAL4/UAS sistemaz gain, Drosophilarekin lan egiteko tresna gehiago ere garatu dira. Horien artean aurki ditzakegu, esaterako, balantza-kromosomak. Balantza-kromosomak ingenieritza-genetiko bidez garatutako kromosoma artifizialak dira, hasiera batean mutazio azpirakor hilgarriak ikertzeko erabiliak (Muller, 1918). Eulien-lerro mutante bat egonkortzeko, populazio homozigotoa

lortu behar da, gurutzaketetan ondorengo guztiek ere mutazioa mantentzeko. Alabaina, mutazio azpirakor hilkorren kasuan ondorengo homozigotoak jaio aurretik hiltzen dira. Ondorengo heterozigotoen portzentai batek berriz, genotipo basatia du, eta horiek baztertu ezean, belaunaldiz-belaunaldi populazioan intereseko mutazioa gal daiteke. Arazo horiek ekiditeko balantza-kromosomek hiru ezaugarri nagusi dituzte: batetik, mutazio azpirakor hilkorrak garraiatzen dituzte, bi balantza-kromosoma dituzten indibiduoak saihesteko; bestetik, birkonbinazio genetikoa ekiditzen dute, *de novo* kromosoma basatirik ez sortzeko; eta azkenik, markatzaile genetiko gainhartzaileak garraiatzen dituzte, intereseko genea duten eulien identifikazioa errazteko (Miller et al., 2019).

3. Ubikitinazioa ikertzeko metodologia

Angelman sindromearen eragilea UBE3A E3 ligasa izanik, gaixotasunaren mekanismo molekularrak ulertzeko proteinen ubikitinazioa aztertu behar da, eta horretarako, teknika egokiak, sentikorrak eta fidagarriak eskura izatea ezinbestekoa da. Ubikitinatutako proteinak ehunetatik eta baldintza fisiologikotan isolatzea eta identifikatzea benetako erronka da, besteak beste ubikitinarekin eraldatutako proteinak zeluletan oso maila baxuetan aurkitzen direlako. Halaber, ubikitinarekin konjugatutako proteina batzuk degradazio-zinetika azkarrak dituzte (Choi et al., 2013), deubikitinasen jardueraren ondorioz ubikitinatutako proteinek ubikitina galdu dezakete (Stegmeier et al., 2007), eta hori gutxi balitz, proteinak ondo definitutako denbora-tarte jakinetan soilik diraute ubikitinatuta (Clute eta Pines, 1999). Horrek guztiak asko zailtzen du zelulako proteina ubikitinatuen, alegia, ubikitomaren azterketa. Edonola ere, ubikitinazioak *in vivo* duen funtzioa hobeto ulertzeko beharrezkoa da ehun jakinetan dauden ubikitinatutako proteinak identifikatzea. Azken bi hamarkadetan ubikitinatutako materiala ikertzeko garatutako teknika ezberdinei esker, eta masa espektrometriaren alorrak jasan duen garapenari esker, posible da aldi berean milaka proteina, edo proteinen oso portzentaje txikian dauden itzulpen ondoko aldaketak identifikatzea eta kuantifikatzea.

3.1. Ubikitinatutako materiala aberasteko estrategiak

Arestian aipatu bezala, ubikitinatutako proteinek zeluletan oso estekiometria baxua dute, beraz, edozein detekzio-metodo erabili baino lehen, horiek aberastea ezinbestekoa da (Mayor eta Peng, 2012). Ubikitinatutako materiala aberasteko prozedurarik ohikoena ubikitinatutako proteinak arrantzatzeko antigorputzak erabiltzea da. Antigorputz batzuk zuzenean ubikitina ezagutzen dute (Bennett et al., 2007; Lopitz-Otsoa et al., 2012; Matsumoto et al., 2005; Vasilescu et al., 2005; Xu et al., 2010a). Beste prozedura batzuk etiketa berezi batekin markatutako ubikitina (HIS, HA, FLAG, STREP…) erabiltzen dute, eta etiketa horiek ezagutzen dituzten antigorputzen bidez purifikatzen dituzte

ubikitinatutako proteinak (Greer et al., 2010; Peng et al., 2003; Schmidt eta Skerra, 2007). Amino muturreko etiketek ubikitina-kate-linealen sorrera oztopatzen dutenez, etiketa sekuentziaren erdialdean duen ubikitina eraldatua ere erabiltzen da (Kliza et al., 2017).

Antigorputzak erabiliz ubikitinatutako proteinak ez ezik, ubikitinatutako peptidoak purifikatzea ere posible da. Masa espektrometriarako laginak prestatzeko erabili ohi den tripsinak arginina eta lisina hondarren ostean dagoen lotura peptidikoa mozten du, prolina dagoen kasuetan izan ezik. Hortaz, laginaren prestaketan sortzen diren peptido guztien karboxilo muturrek arginina edo lisina hondarrak dituzte (Olsen et al., 2004). Ubikitinatutako proteinak tripsinarekin tratatzean, tripsina ez da gai ubikitina lotuta duen lisinaren osteko lotura peptidikoa hidrolizatzeko, lisinak karga positiboa galdu duelako, beraz *misscleaveage* bat sortzen da. Ondorioz, ubikitinari dagozkion bi glizina hondar gelditzen dira ubikitinatutako proteinaren lisinara lotuta (21. irudia). Bi glizina horiek, di-Gly sinadura bezala ezagutzen dira, eta sinadura horrekiko espezifikoak diren antigorputzen bidez purifikatu daitezke peptido horiek (Xu et al., 2010a).

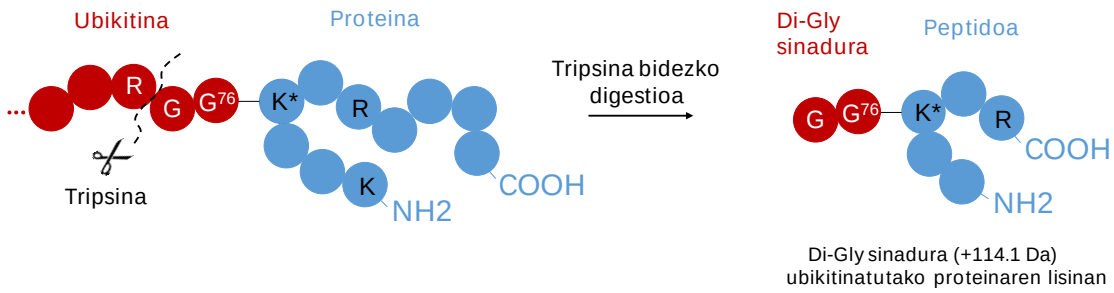

21. irudia. di-Gly sinaduraren sorrera. Tripsina bidezko digestio proteolitikoak ubikitinaren karboxilo muturreko -RGG sekuentzian argininaren atzetik mozten du, beraz ubikitinatutako proteinako lisinan GG dinukleotidoa gelditzen da. Di-Gly sinadura horrek 114.1 Da ditu, eta *misscleaveage* bat sortzen du.

Aipaturiko antigorputzen bidez ubikitinatutako materiala purifikatzeak, hala ere, baditu desabantailak. Di-Gly antigorputzei dagokienez, di-Gly sinadura hori beste ubikitina-bezalako proteinek ere uzten dute, esaterako Nedd8 edo ISG15 proteinek. Baldintza fisiologikoetan, Nedd8 eta ISG15 bidezko eraldaketak ez dira ubikitinazioa bezain arruntak, baina proteasoma blokeatuta dagoenean (oso ohikoa ubikitinoma aztertzerakoan), beraien kontzentrazioa izugarri emendatzen da (Leidecker et al., 2012), beraz ezinezkoa da eraldaketa

ubikitinazioa, nedilazioa (Nedd8) edo ISGazioa (ISG15) den bereiztea. Gainera, di-Gly antigorputzak erabiltzeko proteinak tripsinaz digeritu behar direnez, prozedurak ez du aukerarik ematen ondoren ubikitinatutako proteinak balioztatu eta karakterizatzeko.

Antigorputzak erabiliz baldintza natiboetan gauzatutako purifikazio prozedurek arazo nagusi bat daukate: nahiz eta ubikitinarekin konjugatuta ez egon, ubikitinatutako proteinekin ez-espezifikoki elkarrekiten duten proteina kontaminanteak ere purifikatu egiten dira (Tirard et al., 2012). Horrez gain, baldintza ez-desnaturalizatzailetan proteasak eta deubikitinasak aktibo diraute, eta beraz, purifikatutako ubikitinatutako materiala murritzagoa izan ohi da.

Hain zuzen ere, proteina kontaminanteen presentzia eta proteasen jarduera saiheste aldera, ubikitinatutako proteinak baldintza desnaturalizatzailetan aberasten dituzten estrategien artean ezagunena poli-histidina etiketarekin (HIS) markatutako molekulen nikel bidezko purifikazioa da (Hitchcock et al., 2003; Mayor et al., 2007; Peng et al., 2003; Xu et al., 2009). Hala ere, ugaztunetan histidina hondarretan aberatsak diren proteina endogeno ugari daude, beraz, proteina horiek nikelezko bolatxoetan harrapatzen dira afinitate handiz, eta intereseko proteinen purifikazioa oztopatzen dute.

Ubikitinatutako proteinen azterketarako teknika egoki baten falta somaturik, Ugo Mayor ikertzailearen laborategiak arazo nagusiei konponbidea ematen dion eta baldintza denaturalizatzaileetan burutzen den purifikazio-estrategia bat garatu du, BioUb sistema (Franco et al., 2011). Sistema horrek bi abantaila nagusi ditu. Batetik, proteina kontaminante gehienen presentzia ekiditen du, eta bestetik, identifikatutako proteinak antigorputzen bidez balioztatzeko lagin bera erabili daiteke. Horrez gain, Ugo Mayor ikertzailearen lan taldean proteinen ubikitinazioa monitorizatzeko estrategia bat ere garatu dugu, baldintza denaturalizatzaileetan burututako GFP *pull-down* delakoa. Modu horretan, soilik intereseko proteinaren ubikitinazioa egoera ezberdinetan nola aldatzen den behatu daiteke (Lee et al., 2014).

3.1.1. BioUb sistema

BioUb sistema ubikitinatutako konjugatuak *in vivo* isolatzeko estrategia bat da, biotinilazioan oinarritzen dena (Franco et al., 2011). Ugaztunetan biotinilazioa oso prozesu espezifikoa da, eta *in vivo* oso proteina gutxik pairatzen dute. Horien artean aurkitzen dira biotinaren mendeko karboxilasak (Chandler eta Ballard, 1985). Karboxilasek biotinaren beharra dute gantz-azidoen, aminoazidoen eta karbohidratoen metabolismoan parte hartzeko (Tong, 2013). Biotinilazio erreakzioa biotina-holoentzima sintetasak (BirA E.coliren kasuan) katalizatzen du (Bennett et al., 2007) eta erreakzio oso espezifikoa da, 16 aminoazidotako sekuentzia espezifikoa ezagutzea nahikoa baitu biotina gehitzeko (Beckett et al., 1999).

Ugo Mayorren taldeak BirA proteinaren espezifikotasuna aprobetxatuz, fusio-proteina bat sortu du (Franco et al., 2011). Fusio-proteina hori karboxilo muturrean kokatutako *E.coli*-ren BirA proteinaz, eta amino muturrean jarritako sei ubikitina-kopiaz osatzen da. Ubikitina-kopia bakoitzak biotinilaziorako beharrezkoa den 16 aminoazidotako sekuentzia dauka (22A. irudia). Polipeptido aintzindari hori zelula-lerroetan edo organismoetan *in vivo* adierazi daiteke. Ubikitinaren gene endogenoekin gertatzen den bezala, DUB endogenoek aintzindaria digeritzen dute, eta ondorioz, zeluletan 16 aminoazidotako sekuentziadun ubikitinak, eta bakterioen BirA entzima askatzen dira (Kimura eta Tanaka, 2010) (22B. irudia). BirA-k ubikitinen amino muturreko sekuentzia biotinilagarriak ezagutzen ditu, eta horietara biotina konjokatzen du (22C. irudia). Modu horretan, biotinadun ubikitinak lortzen dira, ubikitina endogenoekin batera proteinetara konjugatzen direnak (22D. irudia). Abidina eta biotinak elkartzeko duten afinitate handiari esker, biotinadun ubikitina lotuta duten proteinak abidina bolatxoetara batuko dira. Beraz, bolatxo horiek ubikitinatutako materiala purifikatzea eta aberastea baimentzen dute (22E. irudia).

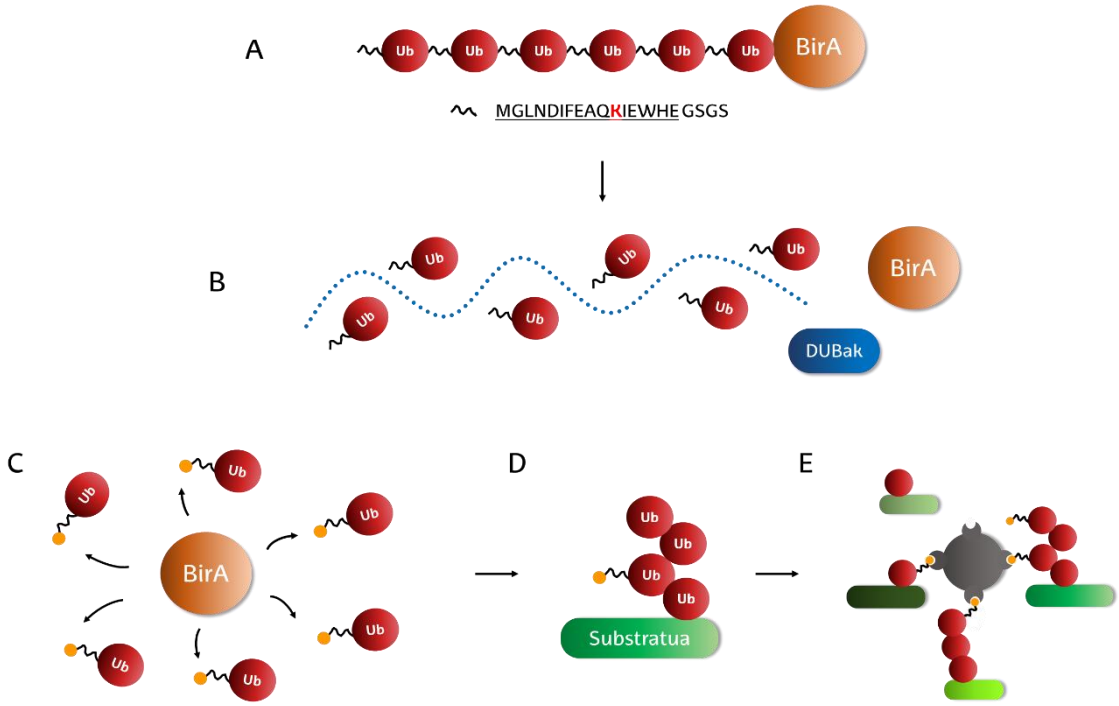

22. irudia. BioUb sistema. A) Ubikitina molekularen sei kopia adierazten dira elkarren segidan, *E.coli*-ren BirA proteinarekin batera. Ubikitina molekulek BirA entzimak ezagutzen duen sekuentzia daramate amino muturrean. B) Fusio-proteina hori adierazten denean, zelularen deubikitinasa endogenoek ubikitina molekula bakoitzaren atzetik mozten dutenez, zelulan ubikitinak eta BirA askatzen dira. C) BirA entzimak ubikitinen amino muturreko sekuentzia ezagutu eta biotina jartzen du, ubikitina biotinilatuak lortuz. D) Proteinei, ubikitina endogenoez gain, biotinilatutako ubikitinak atxikituko zaizkie. E) Biotinaren bidezko markaketari esker, eta biotina-abidina interakzio sendoa aprobetxatuz, abidina bolatxoak erabiltzen dira biotinilizatutako/ubikitinatutako materiala purifikatzeko.

Aurrez aipatutako estrategiekin konparatuz, BioUb sistemarekin proteina ez-espezifikoen purifikazioa saihestu egiten da. Izan ere, garbiketa oso zorrotzak burutu daitezke, abidinak biotinarekiko erakusten duen afinitatea oso altua baita (Franco et al., 2011; Marttila et al., 2000). Beraz, BioUb sistemarekin soilik biotinilatutako ubikitinarekin eraldatutako proteinak, hala nola zelulan berez biotinilatuta dauden karboxilasak purifikatzen dira. Estrategia horrek ubikitina kate linealak eragozteko arriskua badu ere, mota horretako kate linealak identifikatu ditugu ere gure analisietan (publikatu gabeko datuak). Gainera, isolatutako materiala masa espektrometria edo Western-plapaketa bidez aztertu daitekeenez, lagin bera proteinen balioztatze eta karakterizazioa burutzeko ere erabili daiteke (Franco et al., 2011; Lectez et al., 2014; Min et al., 2014; Ramirez et al., 2015, 2018). Estrategia horri esker, ehunka ubikitina-konjugatu purifikatu dira eulietan (Franco et al., 2011; Ramirez et al., 2015, 2018), saguetan (Lectez et al., 2014) eta baita giza zelula lerroetan ere (Min et al., 2014). Horrez gain, E3 ligasen

substratuak identifikatzeko ere erabili da: E3 ligasa gainadierazi osteko zelulen ubikitoman proteina batzuk ugariagoak badira E3 gainadierazi gabeko ubikitomarekin konparatuz, proteina horiek E3 ligasen substratu kontsideratu daitezke (Martinez et al., 2018; Ramirez et al., 2018).

3.1.2. GFP *pull-down* estrategia baldintza denaturalizatzaileetan

Ubikitoma osoa aztertu beharrean, kasu batzuetan proteina indibidualen ubikitinazioa ikertzea bilatzen da. Esaterako, BioUb bidez identifikatutako E3 ligasen substratuak balioztatzeko, edota proteina jakin batzuen ubikitinazio-maila ezagutzeko, indibidualki proteina horien ubikitinazioa aztertu behar da. Horretarako, antigorputzen bidez proteina ubikitinatua detektatzeko gai izan behar gara. Tamalez, antigorputzak ez daude beti eskuragarri, edo ez dute intereseko proteina detektatzen, eta balioztatzea zailtzen dute. Horrez gain, ohiko purifikazio metodoetan proteina-kontaminatzaileak detektatzen direnez, ezinezkoa izaten da ubikitinazioa intereseko proteinarena dela frogatzea. Egoera horrek bultzatuta, Ugo Mayorren laborategiak ko-immunoprezipitaziorako erabiltzen diren GFP agarosa bolatxoei (Chromotek) beste erabilera bat eman die.

Moldatutako GFP *pull-down* estrategia berezi horretan intereseko proteina GFP isatsarekin, eta ubikitina FLAG etiketarekin adierazten dira edozein sistematan (zelulak, euliak...) (23. irudia). Anti-GFP antigorputzaren V_HH fragmentu errekonbinatuz estalitako bolatxoak erabiliz (Chromotek, GFP-Trap), GFP molekula, eta beraz, intereseko proteina purifikatzen dira. Bolatxo horiek GFP molekularekin sortzen duten interakzio bereziki egonkorrari esker, eta ubikitinazioa lotura kobalentez ematen denez, garbiketa zorrotzak burutzen dira gainerako proteina guztiak baztertzeko. Azkenik, GFP eta FLAG etiketen aurkako antigorputzak erabiliz, intereseko proteina eta bere ubikitinazio-patroia detektatzen dira, hurrenez hurren (Elu et al., 2020).

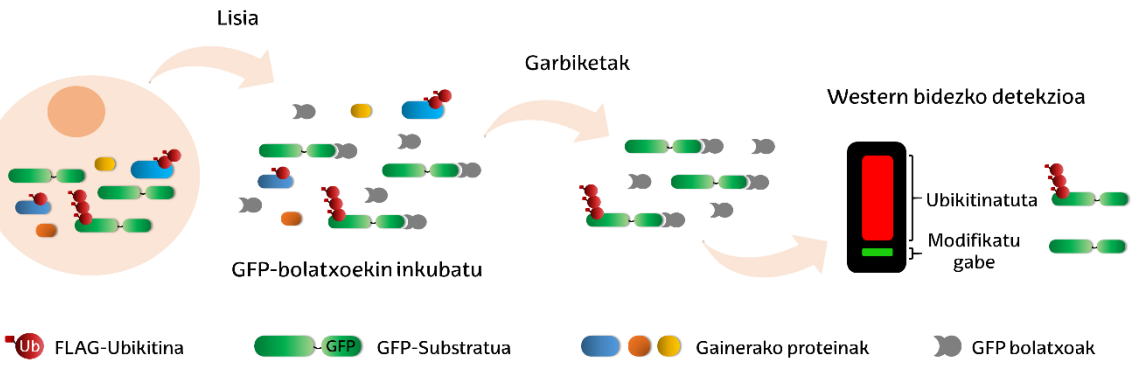

23. irudia. GFP *pull-down* estrategia. Zeluletan GFP isatsa duen intereseko proteina (berdea) eta FLAG isatsa duen ubikitina (gorria) adierazten dira. Zelulak lisatu eta materiala GFP-arekin batzen diren bolatxoekin inkubatzen da (grisak). Bolatxoak GFP isatsa duten proteinekin batuko dira, gainerako proteinak (urdina, laranja eta horia) baztertuz. Purifikatutako materiala bolatxoetatik askatu eta Western blot plapaketa bidez detektatu daiteke. Berdez, modifikatu gabeko intereseko proteinaren banda ikusiko da, eta gorriz, proteina horren ubikitinazio-patroia.

Estrategia horrek hainbat aplikazio ezberdin ditu. Lehenengoz *Drosophila melanogaster* euliaren neuronetan ubikitinazioa monitorizatzeko erabili zen (Lee et al., 2014). Oraintsu, UBE3A E3 ligasaren substratuak balioztatzeko ere erabili da (Ramirez et al., 2018). Tesi honetan, UBE3Aren balizko substratuak balioztatzeko nahiz UBE3Aren aurkako funtzioa duten DUBak identifikatzeko erabili da, DUB ezberdinak isildu eta UBE3Aren substratuaren ubikitinazioa monitorizatuz (Elu et al., 2019). Horrez gain, estrategia horren bidez substratu jakin baten ubikitinazio-guneak ere identifikatu dira (Elu et al., 2019, 2020).

3.2. Proteinen arteko elkarrekintzak ikertzeko estrategiak

Funtzio zelular konplexuak dituzten proteinek, sarritan, beste proteina batzuekin elkartuz burutzen dute beraien funtzioa. Beraz, burutzen duten funtzioa osotasunean ulertzeko, berarekin lotzen diren proteinak ezagutzea beharrezkoa da. Interaktoreak ezagutuz, gaixotasunen mekanismo molekularrak ulertu ez ezik (Sang et al., 2011), proteina bat gaixotasun batekin erlazionatu ahal izan da (Butland et al., 2014). Hortaz, UBE3Aren inguruan jarduten duten proteinak zeintzuk diren jakiteak gaixotasunaren ikuspegi globala eman diezaguke.

Proteinen arteko elkarrekintzak identifikatzeko teknika ugari garatu izan dira. Lehenengotarikoa, 90. hamarkadan deskribatutako Y2H (*Yeast Two Hybrid*) teknika da. Teknika horretan, bi proteinek elkarrekiten badute, transkripzio faktore funtzional bat osatzen da, eta horrek gene erreportari baten adierazpena baimentzen du (Song eta Fields, 1989). Gene horrek bideratzen duen fenotipoari esker, elkarrekintza eman den legamia koloniak bistaratu daitezke, eta proteina horien arteko elkarrekintza eman dela ondorioztatu daiteke. Ohiko beste teknika bat antigorputzen bidezko *pull-down* estrategia da. Hau da, intereseko proteinarekiko antigorputz espezifikoak erabiltzen dira, proteina hori eta berarekin elkarrekiten dutenak batera purifikatzeko. Azken urteotan, proteinen arteko elkarrekintzak ikertzeko, mikroarraien erabilera ere asko garatu da. Mikroarrai horietan hainbat proteina ezberdin inmobilizatzen dira, eta intereseko proteinarekin horietatik zeintzuk elkarrekiten duten jakiteko balio dute (Hall et al., 2007).

Aipaturiko tekniken bidez, hala ere, zaila izan daiteke interaktoreak identifikatzea, batetik, proteinen arteko elkarrekintzak ikertzerakoan garrantzitsua delako ingurune zelular fisiologikoa mantentzea, eta bestetik, proteinen arteko elkarrekintzak momentu labur batekoak izan daitezkeelako. Muga horiei aurre eginez, azken hamarkadan, BioID estrategia arrakastatsua garatu dute (Roux et al., 2012). Teknika hori zeluletan *in vivo* erabili daitekeenez, ingurune fisiologikoa mantentzen da, eta horrez gain, denbora laburreko elkarrekintzak ere ikertu daitezke (Roux et al., 2012).

3.2.1. BioID2 estrategia

BioID estrategia proteinen arteko elkarrekintzak detektatzeko erabiltzen da, intereseko proteinarengandik hurbil dauden proteinak purifikatzea ahalbidetzen baitu. BioUb kasuan bezala, *E.coli*-ko BirA proteinaz baliatzen da, baina kasu honetan BirA proteinaren bertsio promiskuo bat erabiltzen da (Roux et al., 2012). Mutazio puntual baten ondorioz, BirA proteina promiskuo horrek inguruko proteina guztiak biotinilatzen ditu modu ez-espezifikoan. Horrela, BirA promiskuoa intereseko proteinarekin batera adieraziz gero, azken horren interaktoreak edo hurbil dauden proteinak biotinilatuko ditu, eta proteina horiek abidina bolatxoak erabiliz purifikatu ahal izango dira (24. irudia).

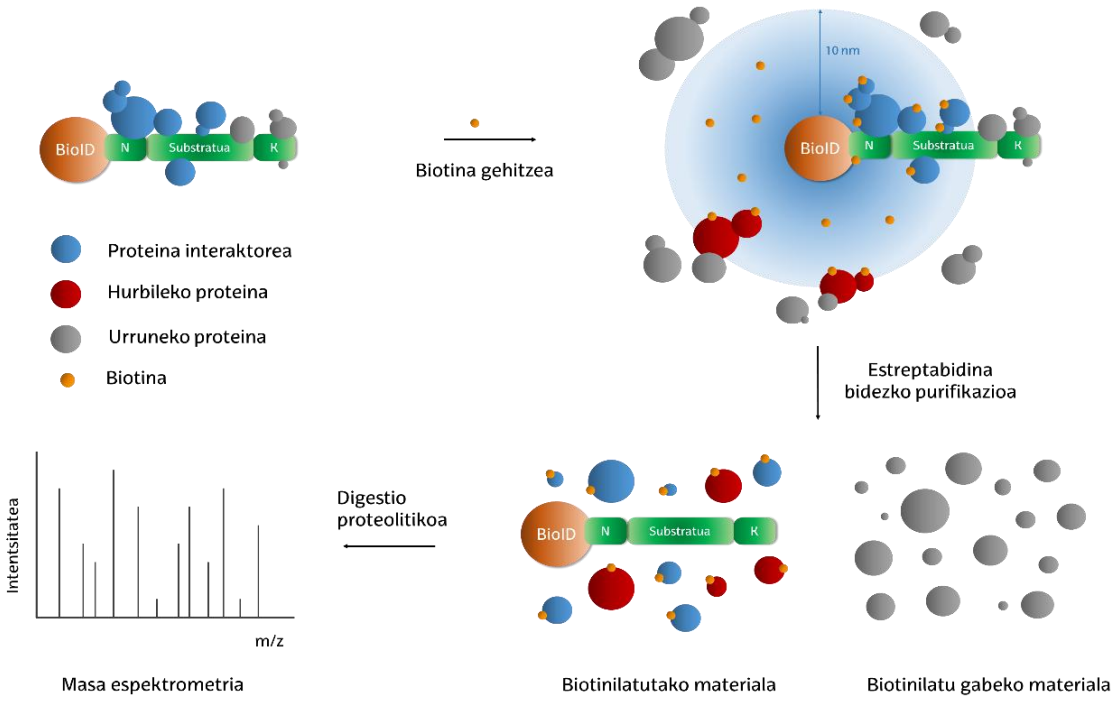

24. irudia. BioID2 estrategia. Intereseko proteina (berdea) BioID proteinarekin batera (laranja) adierazten da. Medioan biotina gehigarria jarriz (horia), BioID proteinak fusionatuta daukan proteinaren interaktoreak (urdinak) eta 10 nm-ko distantziaren barruan aurkitzen diren beste proteina batzuk (gorriak) biotinilatuko ditu. Erradio horretatik kanpo dauden proteinak (grisak) ez dira biotinilatuko. Biotina-abidina interakzio sendoa aprobetxatuz, estreptabidina erabiltzen da biotinilatutako material guztia purifikatzeko. Azkenik, digestio proteolitikoa burutu eta lagina masa espektrometria bidez analizatzen da.

Oraintsu teknika horren aldaera ugari garatu dira. Batzuk hasierako BirA promiskuoarekin konparatuz biotinilazio-ahalmen handiagoa bilatu dute, BioID2 (Kim et al., 2016) edo TurboID (Branon et al., 2018) kasuetan bezala. Split-BioID edo 2C-BioID konstruktoak dimerizazioaren beharra duten interakzioak ikertzeko balio izan dute (Chojnowski et al., 2018; Munter et al., 2017). BioID estrategiaren beste aldaera batek zelulan lokalizazio konkretu bat duten proteinen arteko elkarrekintzak ikertzea ere baimendu du; esaterako, zentrosometan, zelulen lotura guneetan, autofagian, seinaleztapen-bideetan edota mitokondrioetan jarduten duten proteinen interaktoreak ezagutu ahal izan dira (Varnaitė eta MacNeill, 2016).

.

3.3. Masa espektrometria

Ubikitinatutako materiala aberastu ondoren, nahiz proteinen arteko elkarrekintzak aztertzeko purifikazio metodoak erabili ondoren, detekzio metodo sentikor eta fidagarri bat berebizikoa da proteina horiek identifikatu ahal izateko. Masa-espektrometria (*Mass Spectrometry, MS*) proteomika alorrean oso teknika arrunta da, eta azken hamarkadan jasandako garapena dela eta, ubikitomaren ikerketan oso erabilia da; sentikortasun handiari esker, aldi berean E3 ligasen nahiz DUBen milaka substratu nahiz interaktore identifikatzeko aukera ematen du.

Laburki, MS bidez proteinak identifikatu eta kuantifikatzen dira, proteinetatik eratorritako peptidoak ionizatu, eta beren masa/karga ratioa (m/z) neurtuz (Steen eta Mann, 2004). Ubikitinatutako proteinen kasuan, zelulan duten estekiometria baxua dela eta, MS bidez aztertu baino lehen lagina aberastu egiten da (Mayor eta Peng, 2012). Arestian aipatutako di-Gly sinadurari esker, ubikitinatutako peptidoek 114 Da gehiagoko pisu molekularra izango dute ubikitinatu gabeko peptidoekin konparatuz, beraz, MS bidez ubikitinatutako proteinak, ubikitinazio-guneak eta abar identifikatu daitezke (Kim et al., 2011; Na et al., 2012; Sarraf et al., 2013; Wagner et al., 2011, 2012; Xu et al., 2010a).

Masa-espektrometrian oinarritutako proteomikako ohiko esperimentu batean, lehenbizi, ehun edo zeluletatik erauzitako proteinak proteasa batekin, tipikoki tripsinarekin, digeritzen dira (25A. irudia). Jarraian, sortutako peptidoak kromatografia bidez banatzen dira masa espektrometrora sartu aurretik laginaren konplexutasuna murrizteko; peptido bakoitzak erretentzio-denbora jakin bat duenez, sekuentzialki ateratzen dira kromatografia-zutabetik. Peptido horiek zutabetik atera ahala, ionizatu eta masa espektrometroan kargatzen dira. Masa espektrometroan, ionizatutako peptidoen m/z ratioa, hala nola beren intentsitatea neurtzen da. Bi neurketa horiekin MS1 espektroa eraikitzen da. Normalean, tandem masa espektrometria (MS/MS edo MS2) deritzon estrategia jarraitzen da, eta ondorioz, peptido horiek kolisio energia bidez are gehiago txikitzen dira. Fragmentu horien m/z eta intentsitatea ere neurtzen da, eta neurketa horiekin MS2 espektroak sortzen dira. MS bidezko analisi batean lortutako datu guztiak (bereziki, peptido eta fragmentuen m/z) datu-base bateko

proteina guztien digestio teorikotik ondorioztatutako datuekin alderatzen dira (25B. irudia). Software bereziekin gauzatzen den analisi bioinformatiko horretatik ondorioztatzen da zeintzuk diren lagin biologikoan dauden peptidoak, eta horrenbestez, proteinak. Gainera, proteinen kuantifikazio erlatiboa egitea ahalbidetzen duten kuantifikazio metodo ezberdinak existitzen dira (LFQ, SILAC, iTRAQ, ^{18}O markaketa ...) (Matthiesen eta Bunkenborg, 2020).

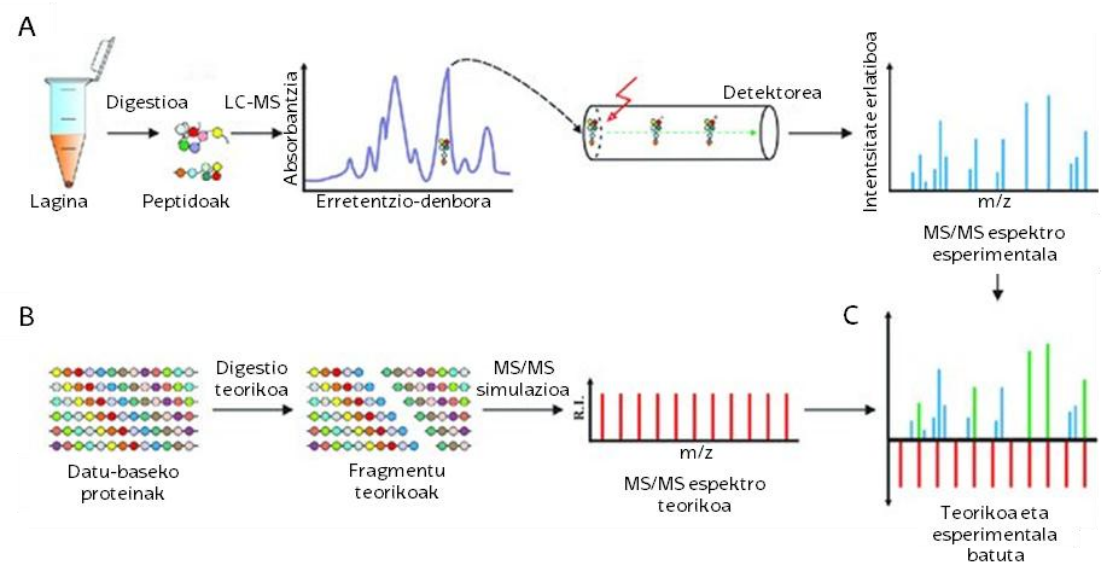

25. irudia. Proteinen identifikazioa masa-espektrometria bidez. A) Proteinen nahastura konplexua proteolitikoki digeritzen da peptidoak lortzeko. Peptido horiek likido kromatografiaz banatzen dira, eta erretentzio-denboraren arabera zutabetik atera ahala, ionizatu eta masa espektrometrora sartzen dira. Bertan peptidoen m/z neurtu eta fragmentatu egiten dira. Fragmentuen m/z neurtuz, MS/MS fragmentazio-espektrua (urdina) lortzen da. B) Proteinen datu-base batean digestio teorikoak egiten dira eta fragmentuen m/z teorikoak lortzen dira (gorria). C) Tresna informatikoekin MS/MS espektru esperimentala teorikoarekin konparatzen da eta hasierako lagineko proteinak identifikatzen dira. Chugunova et al., 2018tik moldatuta.

Oro har, masa espektrometro batek 3 osagai nagusi ditu: ionizazio-iturria, masa-analizatzailea eta datuen prozesamendurako elektronika (26. irudia) (Yates et al., 2009). Ionizazio-iturriari esker, analizatu behar diren molekulak, peptidoak kasu honetan, kargadun ioi bilakatzen ditu. Proteomikan gehien erabiltzen diren ionizazio teknikak ESI (*Electrospray Ionization*) eta MALDI (*Matrix Assisted Laser Desorption/ Ionization*) dira (Fenn et al., 1989; Karas eta Hillenkamp, 1988). ESI metodoa soluzioan dauden molekulak ionizatzeko erabiltzen da. Peptidoak kromatografotik ateratzen diren heinean, elektroesprayari esker ionizatu egiten dira, eta zuzenean MSra sartzen dira. Aldiz, MALDIren kasuan, lagina euskarri solido batean jartzen da, hau da, ko-kristalizatu egiten da matrize organiko

batean. Ondoren, laser pultsuen bidez lagina erradiatu, eta bertako molekulak gas faseko ioi bilakatzen dira (Yates et al., 2009).

Behin peptidoak ionizatuta MSra sartzen dira, zehazki masa-analizatzailera. Masa-analizatzaileak eremu elektriko edo magnetiko bat ezarriz ioiak beren m/z ratioaren arabera banatu, eta detektorera bideratzen ditu. Proteomikan erabiltzen diren masa analizatzaile ohikoenak lau dira: kuadrupoloa, ioi-tranpak, TOF (*Time of Flight*) eta Orbitrap-a (Yates et al., 2009). Bakoitzak oinarri fisiko eta errendimendu analitiko espezifikoa dauka. Esaterako, TOF analizatzaileetan ioiak distantzia konkretu bat hegan egiteko behar duten denbora neurtzen da. Aldiz, kuadrupolo eta ioi-tranpek, tentsio ezberdinak aplikatuz, soilik m/z jakin bat duten ioiak uzten dituzte pasatzen analizatzailean zehar. Oro har, analizatzaile ezberdinek sentikortasun, erresoluzio eta eskaneatze-ahalmen ezberdinak dauzkate, beraz, baldintzen eta ikertzailearen beharren arabera, analizatzaile konbinazio ezberdinak erabiltzen dira (Domon eta Aebersold, 2006; Yates et al., 2009).

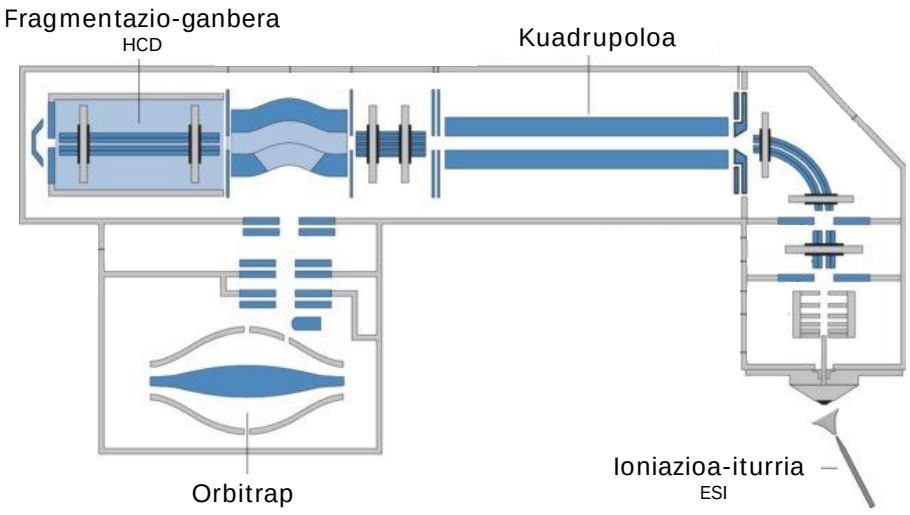

26. irudia. *Thermo Scientific*-en Q-Exactive masa espektrometroaren eskema. Tesi honetan erabili den Q-Exactive masa espektrometroa hibridoa da, eta bi masa analizatzaile ditu: Orbitrapa eta kuadrupoloa. Orbitrapak peptido eta fragmentuen masa aztertzen du, eta kuadrupoloak intereseko tamainadun peptidoak aukeratzeko balio du. Lehenik eta behin, kuadrupoloak ionizatutako peptido guztiak Orbitrap-era bideratzen ditu, baina ondoren, soilik intentsoenak aukeratzen ditu fragmentazio-ganberan fragmentatuak izan daitezen. Azkenik, Orbitrap-ak aztertuko ditu fragmentu horien masak. Horrez gain, Q-Exactive-ak ESI ionizazio-iturria, eta arestian aipatutako HCD (*High Collision Disociation*) bidezko fragmentazio-ganbera ditu.

Arestian aipatu bezala, ioi analizatzaileak peptidoak m/z-ren arabera banandu, eta ioi-detektorera bideratzen ditu, eta bertan peptidoen m/z neurtzen

da. Tipikoki, ioirik ugarienak fragmentazio-ganbera batean sartzen dira fragmentatuak izan daitezen. Beste behin ere, ioi-detektorea da sortutako fragmentu bakoitzaren m/z neurtzen duena. Peptido eta fragmentuen m/z ratioak neurtuz eraikitako MS1 eta MS2 espektroak, hurrenez hurren, datu-base bateko proteinen digestio teorikotik lortutako emaitzekin konparatzen dira software espezifiko bat erabiliz (Steen eta Mann, 2004). Horrela, aztertutako laginean ze peptido, eta ondorioz ze proteina dauden ondorioztatu daiteke.

Ioi detektoreak m/z jakin bakoitzeko ioi-kopurua ere erregistratzen du, neurtu daitekeen korronte elektriko bilakatuz (Finehout eta Lee, 2004; Steen eta Mann, 2004; Yates et al., 2009). Balio hori, intentsitate gisa definitua, peptidoen ugaritasunarekin bat dator, eta beraz, peptidoak kuantifikatzeko erabil daiteke. Hain zuzen, proteinak kuantifikatzeko peptidoen intentsitatetan oinarritzen den estrategiari LFQ (*Label Free Quantification*) edo markaketarik gabeko peptidoen kuantifikazioa deritzo.

Peptidoen kuantifikaziorako LFQ nahiz markaketa bidezko estrategiak erabili daitezke. Markaketa bidezko estrategietan (SILAC, iTRAQ/TMT, ^{18}O…) lagineko proteina, peptido nahiz molekulen bertsio astunak lortzen dira isotopo egonkorrekin markatuz. Peptido normalak eta isotopikoki markatutakoak masan soilik ezberdintzen dira. Hortaz, kromatografia zutabetik batera ateratzen dira, baina masa diferentzia dela eta, masa espektrometroan erraz bereizten dira. Azkenik, peptido beraren bertsio arinaren eta astunaren arteko intentsitate diferentziak, peptido horren kuantifikazio erlatiboaren berri ematen du.

Tesi honetako espektrometria-esperimentuetan LFQ kuantifikazioa erabili da. Markaketa bidezko metodoekin alderatuz, markaketarik gabeko peptidoen kuantifikazioak baditu hainbat abantaila. Edozein lagin biologikotik (zelula-lerro, ehun..) eratorritako peptidoak aztertu daitezke; laginak software mailan konparatzen direnez, nahi beste lagin konpara daitezke; printzipioz, detektatzen den edozein peptido erabil daiteke kuantifikatzeko; eta inolako erreaktibo berezik behar ez denez, merkea da. Alabaina, lagin bakoitza bere aldetik aztertzen denez, errepikakortasunak berebiziko garrantzia dauka. Laginaren prestaketa prozedura oso estandarizatuta egotea komeni izaten da, eta MS analisi ezberdinetako laginak konparatu ahal izateko, ezinbestekoa da m/z eta peptidoen erretentzio denborek zehaztasun handia izatea.

VI.

HIPOTESIAK ETA HELBURUAK

Tesi honetan Angelman sindromearen sorrerarekin erlazionatutako mekanismo molekularrak zeintzuk diren argitzea izan da helburu nagusia. Gure laborategiak urteetan zehar ubikitinazioaren ingurukoak ikertzeko hainbat estrategia garatu ditu, eta Tesi honen aurretik ikerketa taldeak burututako lanak estrategia horiek *in vivo* baliagarriak direla egiaztatu du. Hortik abiatuta, metodologia ezberdinak aplikatu nahi izan dira gaixotasunaren garapenean UBE3A proteinak duen rola hobeto ulertzeko. Gure hipotesiaren arabera, UBE3A proteina osotasunean ezagutzeak –egitura ebazteak, edota substratuak, interaktoreak eta aurkako funtzioa duten deubikitinasak identifikatzeak–, gaixotasunaren mekanismo molekularra ulertzen lagunduko digu, eta mekanismo hori deskribatuz gero, etorkizunean tratamendurako bidea egiten lagunduko luke.

Bide horretan lehen urratsak emateko asmoz, bost izan dira Tesi honetako helburu nagusiak:

1. UBE3A proteinaren substratuak giza zeluletan *in vivo* balioztatu eta karakterizatzea.

2. UBE3Aren aurkako funtzioa burutzen duten deubikitinasa proteinak identifikatzea, balioztatzea eta horien aurkako farmakoak Angelman sindromedun banakoetan erabilgarriak izan daitezkeen ikertzea.

3. UBE3Ak zelulan izan ditzakeen interaktore ezberdinak identifikatzea, eta interaktore horiek UBE3Aren amino edo karboxilo muturrarekin, edo proteina osoarekin elkarrekiten duten zehaztea.

4. UBE3Aren kristalografia bidezko egitura osoa ebaztea.

5. UBE3A gainadierazten duten saguen portaera karakterizatzea.

VII.

MATERIAL ETA METODOAK

1. Biologia molekularra

1.1. Plasmidoak

Tesi honetan erabilitako plasmido guztiak beste laborategietatik lortu dira, konpainia ezberdinetan erosi dira, edo laborategian bertan klonatu dira. Erabilitako plasmido guztiak honako taulan bildu dira (3. taula).

3. taula. Tesian zehar erabilitako plasmidoak.

Plasmidoa	Bektorea	Nork emana	Erres.	Abiaraz.
Substratuen balioztatzea eta karakterizazioa				
FLAG-UBE3A^{WT}	pCMV	Dr. Tomaic	AMP	-
FLAG-UBE3A^{LD}	pCMV	Dr. Tomaic	AMP	-
FLAG-Ub	pCDNA3.1	Dr. Rodriguez	AMP	-
DDI1-GFP	pEGFP-N1*	Clontech	KAN	1,2
GFP-DDI1	PM-GFP-C1*	Dr Abankwa	KAN	1,2
DDI1^{K77R}-GFP	pEGFP-N1*	Clontech	KAN	5,6
DDI1^{K133R}-GFP	pEGFP-N1*	Clontech	KAN	3,4
DDI1^{K161R}-GFP	pEGFP-N1*	Clontech	KAN	7,8
DDI1$^{K77R+K133R}$-GFP	pEGFP-N1*	Clontech	KAN	5, 6
DDI1$^{K77R+K161R}$-GFP	pEGFP-N1*	Clontech	KAN	5, 6
DDI1$^{K133R+K161R}$-GFP	pEGFP-N1*	Clontech	KAN	7,8
DDI1$^{K77R+K133R+K161R}$-GFP	pEGFP-N1*	Clontech	KAN	5,6
DDI2-GFP	pEGFP-N1	Clontech	KAN	-
EMPTY	pCDNA3.1	Invitrogen	AMP	-
GFP-TAX1BP1	pCMV3-N-GFPSpark	Sino Biologicals	KAN	-
GFP-BLMH	pCMV3-N-GFPSpark	Sino Biologicals	KAN	-
UBE2L3-GFP	pCMV3-C-GFPSpark	Sino Biologicals	KAN	-
PSMA5-GFP	pCMV3-C-GFPSpark	Sino Biologicals	KAN	-
MINDY2-GFP	pcDNA5 FRT/TO	Dr. Kulathu	AMP	-

UBE3Aren interaktoreen identifikazioa

BioID2			AMP	-
BioID2-UBE3A^{FL}	pCAG*		AMP	-
BioID2-UBE3A^{Cter}	pCAG*		AMP	11,12
UBE3A^{Nter}-BioID2	pCAG*		AMP	13,14

UBE3Aren egitura ebaztea

hUBE3A-HisP2	His-Parallel2*	Dr. Rojas	AMP	11, 13
hUBE3A-GSTP2	GST-Parallel2*	Dr. Rojas	AMP	15, 17
hUBE3A-SUMO	pET-28M-SUMO3-GFP*	Dr. Rojas	KAN	16, 17

*laborategian burututako klonazioa adierazten du. Erres.= erresistentzia, Abiaraz. = abiarazleak (ikusi 4. taula), AMP= Anpizilina, KAN = Kanamizina.

1.2. Oligonukleotidoak

Laborategian klonatutako plasmidoak lortzeko abiarazleak 18-30 nukleotido bitartean izateko eta moldearekiko osagarriak izateko diseinatu ditugu. Horrez gain, 3′ muturra G edo C nukleotidoekin amaitzea nahi izan dugu, abiarazlearen eta moldearen arteko elkarrekintza errazteko. 5′ muturrean murrizketa endonukleasek mozteko guneak, hots, murriztegune berriak gehitu ditugu (4. taula, gorriz), eta baita digestioa egoki ematen dela ziurtatzeko nukleotido batzuk ere (4. taula, berdez). Kasu batzuetan, irakurtaraua mantentzeko, nukleotido bat edo bi gehitu behar izan ditugu (4. taula, laranjaz). Abiarazle bati *FLAG* isatsa ere gehitu diogu (4. taula, urdinez). Mutazio bakanak, bikoitzak eta hirukoitzak sortzeko abiarazleak 25-45 nukleotido inguru izateko diseinatu ditugu. Tm ≥ 78 ºC eta mutazioa sekuentziaren erdian izateko diseinatu ditugu, konpainiaren gomendioei jarraituz (Invitrogen). Tesi honetan erabilitako abiarazle guztiak Invitrogen konpainiak sintetizatu ditu, eta taula honetan bildu ditugu (4. taula).

4. taula. Tesian zehar erabilitako abiarazleak.

DDI1en klonazioa		
1	DDI1 Fw KpnI	TATAGGTACCATGCTGATCACCGTG
2	DDI1 Rv AgeI	TATAACCGGTCCATGCTCTTTTCGTCC
3	DDI1 K133R Fw	CTTGGCGTCAGGAGAGAGGGTGGCCGG
4	DDI1 K133R Rv	CCGGCCACCCTCTCTCCTGACGCCAAG
5	DDI1 K77R Fw	TATCGTGGTTTTACTGCAGAGGGACAATGTGGGAC
6	DDI1 K77R Rv	GTCCCACATTGTCCCTCTGCAGTAAAACCACGATA
7	DDI1 K161R Fw	GATCTGTCCCTGCTCAGGGAACGCAACCCT
8	DDI1 K161R Rv	AGGGTTGCGTTCCCTGAGCAGGGACAGATC
9	HA-DDI1 Fw NheI	TATGCTAGCATGTACCCATACGATGTTCCAGATTACGC TATGCTGATCACCGTGTAC
10	DDI1 Rv XbaI	GCGTCTAGATCAATGCTCTTTTCGTCCTGAATCCATGA CTGAATGTGTAATTTCC
UBE3Aren interaktoreen identifikazioa		
11	Fw C-ter UBE3A	AAAGCGGCCGCATCTTTTATGACATGTCCC
12	Rv C-ter UBE3A	GGCATCGATTTACAGCATGCCAAATCC
13	Fw N-ter UBE3A	GAGACCGGTATGGAGAAGCTGCAC
14	Rv N-ter UBE3A	TATGCGGCCGCAGCGAATTCTATTGTC
UBE3Aren egituraren ebazpena		
15	hUBE3A SalI Fw	TATAGTCGACAATGGAGAAGCTGCACCAG
16	hUBE3A AgeI Fw	TATAACCGGTGGAATGGAGAAGCTGCACCAG
17	hUBE3A NotI Rv	TATAGCGGCCGCTTACAGCATGCCAAA

Berdea= nukleotido gehigarriak digestioa errazteko

Gorria= murriztegunea

Laranja= irakurtaraua mantentzeko nukleotido gehigarriak

Urdina= *FLAG* isatsa

1.3. Klonazio prozedura

Klonazio prozedura guztietan lehendabizi intereseko genea anplifikatu dugu, dagozkion zuzeneko eta alderantzizko abiarazleak erabiliz (3. Taula)(Thermo Scientific). PCR erreakzioak termozikladorean burutu ditugu (C1000 Touch Thermal Cycle BIO-RAD), honako konposatu hauek nahastuz: 10 ng DNA molde, 200 mM dNTP, 1.5 mM $MgCl_2$, 0.5 M abiarazle eta 0.02 U/L DNA polimerasa (*Phusion High-Fidelity* DNA polimerasa entzima, 1X *Phusion HF* disoluzio indargetzailean nahastuta). Erreaktibo guztiak Thermo Scientific konpainiatik eskuratu ditugu. PCR erreakzioek honako programa jarraitu dute: hasierako desnaturalizazioa 30 segunduz 98 ºC-tan, ondoren 30 ziklo ((i)10 segundu 98 ºC-tan, (ii) 20 segundu abiarazlea moldera elkartzeko beharrezko tenperaturan eta anplikoiaren tamainaren arabera, (iii) 20 segundu kilobase bakoitzeko 72 ºC-tan), eta azkenik, 5 minutuko hedapena 72 ºC-tan. Abiarazlea eta moldea elkartzeko beharrezko tenperatura (Tm, *melting temperature*) Thermo Fisher Scientific konpainiaren *Tm calculator* tresna erabiliz kalkulatu dugu. Tenperatura hori 72ºC baino altuagoa den kasuetan, 2 pausuko PCR erreakzioa burutu dugu abiarazle-molde elkarketa eta hedapena pausu bakarrean burutuz (72 ºC-tan). Mutazio puntualak egiteko mutagenesis kit komertziala erabili dugu, konpainiaren gomendioak jarraituz (Agilent technologies).

PCR erreakzioen ostean, produktuen tamaina egokiak agarosa gel batean egiaztatu ditugu, eta jarraian, *E.Z.N.A. Gel Extraction* (Omega Bio-tek) kita erabiliz DNA berreskuratu eta kontzentrazioa neurtu dugu nano-espektrofotometro batean (Biodrop). 200ng PCR produktu (insertoa) eta 500ng intereseko bektorea murrizketa endonukleasekin digeritu ditugu 2 orduz 37 ºC-tan, entzima bakoitzari dagokion indargetzaile-tanpoia erabiliz (Thermo-Scientific). Inkubazioa bukatzean, murrizketa endonukleasak inaktibatu ditugu 20 minutuz 80 ºC-tan. Ondoren, bektorea digeritzeko eta bir-ligazioa ekiditeko, digestio produktua ordu batez inkubatu dugu 37 ºC-tan Fosfatasa Alkalino entzimarekin (AP, Roche).

Bektorea eta insertoaren arteko lotura emateko, digestio produktua T4 ligasa entzimarekin (New England Biolabs) inkubatu dugu gau osoz 18 ºC-tan. Bektore:inserto ratio ezberdinak erabili ditugu (1/5, 1/10, 1/20) ligaziorako aukera gehiago izateko.

Ligazioaren ostean, produkturaren 5-10 µL, 25 µL DH5α bakteriorekin (NZYTech) inkubatu dugu. Transformazioa burutzeko txoke termikoa erabili dugu: ligazio-produktua bakterioekin 30 minutuz izotzetan inkubatu ostean, bakterioak 45 segunduz 42 ºC-tan, eta ondoren berriz izotzetan jarri ditugu 2 minutuz. Bakterioak gau osoz 37 º C-tan utzi ditugu hazten LB agar plaketan (Condalab), plasmido bakoitzari dagokion antibiotikoa erabiliz, anpizilina edo kanamizina (Sigma).

Inkubazioaren ostean, bakterioa transformatu den egiaztatzeko, kolonia ezberdinak testatu ditugu PCR erreakzio bidez. Kolonia positiboak gau osoz hazten utzi ditugu LB mediotan (Condalab) 37 ºC-tan. Ondoren, *E.Z.N.A. plasmid mini kits* (Omega Bio-tek) purifikazio kita erabiliz, plasmidoa purifikatu dugu. Azkenik, purifikatutako plasmidoen sekuentzia egokia dela egiaztatu dugu Eurofins GATC Biotech konpainiaren bidez sekuentziatuz (Köln, Germany).

2. Zelulen kultiboak eta transfekzioak

Giza enbrioien giltzurruneko zelulak (*Human Embryonic Kidney cells*, HEK293T) eta giza neuroblastoma zelulak (SH-SY5Y) ohiko baldintzatan mantendu ditugu (37 °C, %5 CO2), DMEM/F-12 medioarekin (*Dulbecco's modified Eagle medium/nutrient mixture F-12 with GlutaMAX*, Gibco, Thermo Scientific), kultibo medioari honako osagaiak gehituz: % 10 behi-fetu seruma (Thermo Scientific), 100 U/ml penizilina (Invitrogen) eta 100 mg estreptomizina (Invitrogen). Zelulen paseak astean hiru aldiz burutu ditugu. Horretarako, zelulak 5 minutuz 364 xg-ko (1250 rpm) abiaduran zentrifugatu ditugu, Allegra X-12R zentrifugan (Beckman Coulter). Jarraian, aurrez aipatutako DMEM kultibo-medioan birsuspentsatu ditugu, eta 100 mm-ko plaketan (NeoLab line) hazi ditugu. Tesi osoan zehar 20 pase baino gutxiagoko zelulak erabili ditugu.

Transfekzio esperimentuak burutzeko, HEK293T ($6{\cdot}10^5$ zelula) eta SH-SY5Y zelulak ($3{\cdot}10^5$ zelula) sei putzuko plaketan (NeoLab line) hazi ditugu. SH-SY5Y zelulen kasuan, DMEM medioa kendu eta serum gabeko OptiMEM medioan (Gibco, Thermo Scientific) jarri ditugu zelulak gau osoz transfekzioa burutu baino egun bat lehenago transfekzio-efientzia handitzeko asmoz. Hurrengo egunean,

SH-SY5Y zelulak berriz DMEM kultibo medioan jarri ditugu, (Gibco, Thermo Scientific). HEK293T eta SH-SY5Y zelulak 3 µg DNA totalarekin ko-transfektatu ditugu, eta 72 orduz utzi ditugu inkubatzen. Transfekzioak burutzeko *Lipofectamine 3000* (Invitrogen) edo *Jetprime* (Polyplus transfection) erreaktiboak erabili ditugu, konpainien gomendioak jarrituz.

Masa espektrometria bidez ubikitinazio-guneak eta ubikitina kate-motak identifikatzeko esperimentuetan, HEK293T zelulak hazteko 100 mm-ko plakak erabili ditugu ($2{\cdot}10^6$ zelula). Zelulak plakeatu eta 24 ordu geroago, guztira 25 µg DNArekin transfektatu ditugu, horretarako *Lipofectamine 3000* erreaktiboa (Invitrogen) erabiliz fabrikatzailearen gomendioei jarraituz.

DUBen isilpen esperimentuak burutzeko, HEK293T zelulak 6 putzuko plaketan ($6{\cdot}10^5$ zelula) hazten jarri ditugu transfekzioaren aurreko egunean. Putzu bakoitzari DUB jakin baten aurkako 10 nM siRNA (Ambion; life technologies) gehitu dizkiogu. Horretarako *Lipofectamine RNAiMAX* (Thermo Fischer) transfekzio erreaktiboa erabili dugu fabrikatzailearen gomendioei jarraituz. 24 orduz inkubatzen utzi ostean, guztira 3 µg DNA transfektatu ditugu putzu bakoitzean, eta beste 48 orduz inkubatzen utzi ditugu zelulak. Transfekziorako *Lipofectamine 3000* (Invitrogen) transfekzio erreaktiboa erabili dugu. Esperimentu guzti horietan zelulak bi aldiz garbitu ditugu PBS tanpoiarekin, eta -20ºC-tan gorde ditugu behar izan arte.

2.1. UBE3A substratuen balioztatzea

$6x10^5$ HEK293T zelula hazi ditugu sei putzuko plakako (NeoLab line) putzu bakoitzean, 2 mL DMEM+FBS+penizilina/estreptomizina kultibo mediotan. SH-SY5Y zelulen kasuan, $7x10^5$ zelula hazi ditugu 6 putzuko plaketako putzu bakoitzean, 2 mL OPTIMEM (Gibco, Thermo Scientific) erabiliz. 24 ordu geroago, zelulak ko-transfektatu ditugu *Jetprime* (Polyplus transfection) erreaktiboa erabiliz. Putzu bakoitzean guztira 3 µg DNA jarri ditugu (1 µg $UBE3A^{WT}$ edo $UBE3A^{LD}$, 1 µg FLAG-ubikitina eta 1 µg GFP- substratua) 200 µL *Jetprime* tanpoitan eta 6 µL *Jetprime* erreaktibotan diluituta. Zelulak 48 orduz inkubatu ditugu, eta jaso aurretik, GFP proteinaren adierazpena ziurtatu dugu fluoreszentziazko

mikroskopioa erabiliz (Nikon Eclipse TS2). Zelulak bi aldiz garbitu ditugu PBS tanpoiarekin, eta -20ºC-tan gorde ditugu erabili arte.

2.2. Ubikitinazio-guneak eta ubikitina kate-motak

Masa espektrometria bidez DDI1 eta DDI2 proteinen ubikitinazio-guneak eta ubikitina kate-motak identifikatzeko, HEK293T zelulak 100 mm plaketan hazi ditugu ($2x10^6$ zelula). 24 ordu geroago, zelulak *Lipofectamine 3000* (Invitrogen) transfekzio erreaktiboarekin transfektatu ditugu. Alde batetik, 1mL OPTIMEM 45 µL *Lipofectamine 3000* erreaktiboarekin nahastu dugu (A nahasketa). Bestetik, guztira 25 µg DNA (12,5 µg DDI1-GFP edo DDI2-GFP eta 12,5 µg $UBE3A^{WT}$ edo $UBE3A^{LD}$) 1mL OPTIMEM medioarekin eta 45 µL *Lipofectamine P3000* erreaktiboarekin nahastu dugu (B nahasketa). A eta B nahasketak batu ditugu, eta 5 minutu inkubatu ostean, zelulei gehitu diegu. Nahasketa erreplika guztientzako prestatu dugu, transfekzio-efientzia ezberdintasunak ekiditeko. Zelulak 74 orduz inkubatu ditugu, eta azkenik, bi aldiz PBS tanpoiarekin garbitu eta -20ºC-tan gorde ditugu erabili arte.

2.3. Giza DUBen baheketa

HEK293T zelulak transfekzio aurreko egunean sei putzuko plaketan hazi ditugu ($6x10^5$ zelula). Putzu bakoitza DUB jakin baten aurkako 10 nM siRNA-rekin (Ambion; life technologies) inkubatu dugu. Horretarako, *Lipofectamine RNAiMAX* (Thermo Fischer) transfekzio erreaktiboa erabili dugu. 2 mL DMEM mediotan dauden zelulen putzu bakoitzera 500 µL OPTIMEM medio, 3 µL siRNA eta 2 µL siRNA erreaktibo (Thermo Fischer) gehitu ditugu. 24 orduz inkubatzen utzi ostean, 1,5 µg DDI1-GFP eta 1,5 µg FLAG-Ub gehitu ditugu putzu bakoitzera, transfekziorako *Lipofectamine 3000* (Invitrogen) erabiliz: DNA 6 µL *Lipofectamine P3000* erreaktiboarekin nahastu dugu, eta jarraian, 6 µL *Lipofectamine* eta 250 µL OPTIMEM nahasketarekin batu dugu. Beste 48 orduz inkubatu ostean, zelulak bi aldiz PBS tanpoiarekin garbitu eta -20ºC-tan gorde ditugu berriz erabili arte.

3. GFP *pull-down* protokoloa

3.1. Protokolo zorrotza ubikitinazioa ikertzeko

HEK293T eta SH-SY5Y zelulen putzu bakoitzari 500 µL (6-putzuko plaketan) eta 2 mL (100 mm plaketan) liseriketa tanpoi gehitu dizkiogu (50 mM Tris-HCl pH 7.5, 150 mM NaCl, 1 mM EDTA, % 0.5 Tritoi, 1x proteasa-inhibitzaile nahasketa (Roche Applied Science) eta 50 mM N-etilmaleimida (Sigma)). 30 minutuz liseritu ostean, materiala 14.000 xg-ko abiaduran zentrifugatu dugu 10 minutuz. Gainjalkina *GFPTrap-A* agarosa bolatxoekin (Chromotek GmbH) nahastu dugu. 25 µL (6-putzuko plakak) eta 50 µL (100 mm-ko plakak) agarosa bolatxo erabili ditugu putzu/plaka bakoitzeko. Agarosa bolatxoak aurretiaz bi aldiz garbitu ditugu diluzio tanpoiarekin (10 mM Tris–HCl pH 7.5, 150 mM NaCl, 0.5 mM EDTA, 1x proteasa-inhibitzaile nahasketa eta 50 mM N-etilmaleimida). Jarraian, lisatua bolatxoekin nahastuta, hiru orduz inkubatzen utzi dugu giro tenperaturan emeki biratuz. Inkubazioaren ostean, laginak 2700 xg-ko abiaduran zentrifugatu ditugu bi minutuz, GFP agarosa bolatxoak elkartu gabeko materialetik banatzeko. Jarraian, bolatxoak hiru aldiz garbitu ditugu; behin diluzio tanpoiarekin, hiru aldiz garbiketa tanpoiarekin (8 M urea, % 1 SDS PBS-tan) eta behin PBS-tan diluitutako % 1 SDS tanpoiarekin. GFP isatsa duten proteinak agarosa bolatxoetatik askatzeko laginak 95 °C-tan irakin ditugu 10 minutuz 25 µL eluzio tanpoirekin (250 mM Tris-HCl pH 7.5, % 40 glizerola, % 4 SDS, % 0.2 bromofenol urdina eta 100 mM DTT). Behin eluituta, laginak -20ºC-tan gorde ditugu erabili arte.

3.2. Protokolo leuna interaktoreak identifikatzeko

HEK293T zelulak 200 µL lisi-tanpoirekin (10 mM Tris/Cl pH 7.5, 150 mM NaCl, 0.5 mM EDTA, % 0.5 NP-40, 1x proteasa-inhibitzaile nahasketa (Roche Applied Science) eta 50 mM N-etilmaleimida (Sigma)) liseritu ditugu. 30 minutuz izotzetan inkubatu ostean, lisatutako zelulak 14.000 xg-tara zentrifugatu ditugu 10 minutuz 4ºC-tan. Gainjalkinak *eppendorf* hodi berrietara pasatu eta 300 µL diluzio-tanpoirekin diluitu ditugu (10 mM Tris/Cl pH 7.5, 150 mM NaCl eta 0.5 mM EDTA). Diluitutako lagin bakoitza aurretiaz diluzio-tanpoiarekin garbitutako 25 µl *GFPTrap-A* agarosa bolatxoekin (Chromotek GmbH) inkubatzen utzi dugu. Ordu

batez 4 ºC-tan biratzen utzi ostean, laginak 2500 xg-ko abiaduran zentrifugatu ditugu. Gainjalkina baztertu dugu, eta bolatxoak bi aldiz 500 µL diluzio-tanpoirekin garbitu ditugu. Azkenik, 2500 xg -ko abiaduran 4 ºC-tara 2 minutuz zentrifugatu ostean, bolatxoak 100 µL eluzio-tanpoirekin (120 mM Tris-HCl pH 6.8, % 20 glizerol; % 4 SDS, % 0.04 bromofenol urdina; % 10 β-merkaptoetanol) nahastu ditugu, eta 95 ºC-tan irakin ditugu 10 minutuz, GFP-proteina eta bere interaktoreak bolatxoetatik askatzeko. Eluitutako laginak -20 ºC-tan gorde ditugu erabili arte.

4. BioID2 *pull-down* protokoloa

HEK293T zelulak 200 µL lisi tanpoirekin (10 mM Tris/Cl pH 7.5, 150 mM NaCl, 0.5 mM EDTA, % 0.5 NP-40, 1x proteasa-inhibitzaile nahasketa (Roche Applied Science) eta 50 mM N-etilmaleimida (Sigma)) liseritu ditugu. Zelulen lisatuak 5 minutuz zentrifugatu ditugu abiadura maximoan (16100 xg), 4 ºC-tan, 5415-R zentrifugan (Eppendorf). Gainjalkinak PD10 zutabeetatik (GE Healthcare) pasatu ditugu gatzak baztertzeko. Zutabe horiek aurretiaz orekatu ditugu 3 M Urea (Sigma), 1 M NaCl (Sigma), % 0.25 SDS (Sigma) eta 50 mM NEM (Sigma) PBS-tan diluituta dituen tanpoia erabiliz. Jarraian, eluitutakotik 50 µL gorde ditugu *input* bezala, SDS-PAGE bidez monitorizatzeko. Gainerako guztia biratzaile (Stuart) batean inkubatu dugu 150 µL of *NeutrAvidin* agarosa bolatxorekin (Thermo Scientific), ordu batez giro tenperaturan, eta beste bi orduz 4 ºC-tan. Bolatxoak Allegra X-12R zentrifugan (Beckman Coulter), 233 xg-tan 2 minutuz zentrifugatu ditugu, eta bolatxoei lotu ez den materiala (*Flow through*, FT) gorde dugu. Jarraian, bolatxoak tentuz garbitu ditugu, sei garbiketa-tanpoi ezberdin erabiliz (*Whasing Buffer, WB).* Honakoak dira erabilitako garbiketa tanpoi eta baldintzak: bi aldiz WB1 (8 M Urea, % 0.25 SDS), hiru aldiz WB2 (6 M Guanidinio-HCl), behin WB3 (6.4 M Urea, 1 M NaCl, % 0.2 SDS), hiru aldiz WB4 (4 M Urea, 1 M NaCl, % 10 isopropanol, 10 % etanol, 0.2 % SDS), behin WB1, behin WB5 (8 M Urea, % 1 SDS) eta hiru aldiz WB6 (% 2 SDS). Tanpoi guztiak PBS-tan prestatu ditugu (Fisher Scientific). Guanidinio-HCl, isopropanola eta etanola, Sigma, Panreac and Merck konpainietatik lortu ditugu, hurrenez hurren. Garbiketa bakoitzean bost minutu mantendu ditugu laginak biratzailean (Stuart) eta jarraian bi minutuz zentrifugatu

ditugu 233 xg-tara Allegra X-12R zentrifugan (Beckman Coulter). Bolatxoei atxikitutako materiala eluitzeko, laginak 95 ºC-tan irakin ditugu 30 µL 4X Laemmli tanpoiarekin (250 mM Tris-HCl pH 7.5, % 40 glizerola, % 4 SDS, % 0.2 Bromofenol urdina) eta 100 mM DTTrekin. Iraikindako laginak 0.8 µm-ko porodun filtroak dituzten zutabetara (Sartorius) gehitu ditugu, eta 2 minutuz zentrifugatu ditugu abiadura maximoan (16160 xg) Microfuge-16 zentrifugan (Beckman Coulter). Modu horretan, eluitutako materiala bolatxoetatik banandu dugu, Western plapaketa bidez edo masa espektrometria bidez aztertu ahal izateko.

5. Western plapaketa eta zilar tindaketa

5.1. Antigorputzak

Honako antigorputz primarioak 1/1000 kontzentrazioan erabili ditugu: sagu-anti-GFP antigorputz monoklonala (Roche Applied Science; katalogo zenbakia 11814460001); sagu-anti-FLAG M2-HRP antigorputz monoklonala (Sigma; katalogo zenbakia A8592); sagu-anti-UBE3A antigorputz monoklonala (E6AP-300 klona) (Sigma; katalogo zenbakia E8655), untxi-anti-UCHL-5 antigorputz poliklonala (Abcam, ab124931), untxi-anti-USP9X antigorputz poliklonala (Proteintech, 55054-1-AP), sagu-anti-USP7 (Dr. Emilio Leconak emana), untxi-anti-USP42 antigorputz poliklonala (Sigma, HPA006752), oilo-anti-bioID2 antigorputz poliklonala (BioFront Technologies) eta HRP konjugatutako ahuntz-anti-biotina antigorputza (Cell Signaling Technology). Jarraian azaltzen diren antigorputz sekundarioak 1/4000 kontzentrazioan erabili ditugu: ahuntz-anti-sagu-HRP antigorputza (Thermo Scientific; katalogo zenbakia 62-6520) eta ahuntz-anti-untxi-HRP antigorputza (Cell Signalling; katalogo zenbakia 7074). Antigorputz sekundario fluoreszenteak 1/8000 kontzentrazioan erabili ditugu: IRDye800CW eta IRDye600CW (Li-COR).

5.2. Western plapaketa

SDS-PAGE elektroforesirako, % 4–12 *Bolt Bis-Tris Plus pre-cast* (Invitrogen) gelak erabili ditugu. Jarraian, proteinak PVDF mintzetara transferitu ditugu iBlot

sistema erabiliz (Invitrogen). Mintzak blokeatzeko % 5 esne-hautsa, % 0.05 Tween duen PBS (PBS-T) tanpoian bersuspentsatuta erabili dugu. Antigorputz primarioak gau osoz 4 ºC-tan inkubatu ditugu, eta sekundarioak ordu batez inkubatu ditugu giro tenperaturan. Jarraian, mintzak errebelatzeko *ECL* kit-a (Biorad Clarity) erabili dugu, eta *ChemiDoc Imaging System* (BioRad) aparatuan ikustarazi dugu. Bi koloretako irudiak lortzeko, HRP eta fluoreszentziazko antigorputz sekundarioak konbinatu ditugu, eta kanal independenteetan ikustarazi ditugu. Western plapaketetarako, kasuan kasu, lagin guztiaren %15-%50 bitartean erabili dugu.

5.3. Zilar tindaketa

Masa espektrometria bidezko analisia baino lehen, GFP *pull-down* protokoloaren efizientzia testatu dugu zilar tindaketa bidez. Lagin netoaren % 10arekin SDS-PAGE (% 4-12 *Bolt Bis-Tris Plus precast* gelak, Invitrogen) bat burutu dugu. Jarraian, zilar tindaketa burutzeko eta bandak ikustarazteko *SilverQuest* (Invitrogen) kit-a erabili dugu, fabrikatzailearen gomendioak jarraituz. Laburki, gela % 40 etanol eta % 10 azido azetikorekin fixatu dugu ordu batez giro tenperaturan inkubatuz. Jarraian, sentikortze tanpoiarekin inkubatu dugu gela, proteinen tindaketa indartzeko. Tanpoi hori H_2O destilatua erabiliz garbitu dugu, eta azken, tindaketa tanpoiarekin inkubatu dugu 5 minutuz. Bandak intentsitate egokiz ikusi ditugun momentuan erreakzioa gelditu dugu gelditze-tanpoiarekin (Invitrogen). Azkenik, gelak H_2O destilatutan utzi ditugu eskaneatu bitartean.

6. Masa espektrometria: laginen prestaketa, datuen bilketa eta analisia

6.1. *In-gel* tripsina bidezko digestioa eta peptidoen erauzketa

GFP *pull-down* protokoloa aplikatuz aberastutako proteinen % 90arekin SDS-PAGEa burutu dugu (% 4-12 *Bolt Bis-Tris Plus precast* gelak erabiliz, Invitrogen) eta gela *Colloidal Blue* (Invitrogen) erreaktiboarekin tindatu dugu fabrikatzailearen gomendioak jarraituz. Ondoren, baldintza bakoitzari dagokion gel kalea bi zatitan moztu dugu, mono- eta poli-ubikitinatutako DDI1 proteina

isolatzeko asmoz (>75 KDa). Jarraian, gel zati horietako bakoitza txikitu dugu, eta proteinak *in-gel* digestio protokoloarekin digeritu ditugu (Osinalde et al., 2015). Hasteko, gel zatitxoak azetonitriloarekin (AZN) deshidratatu ditugu. Jarraian, bertako proteinak 10 mM DTT-rekin (ditiotreitol) erreduzitu, 55 mM kloroazetamidarekin alkilatu eta 12.5 ng/mL tripsinarekin gau osoz inkubatzen utzi ditugu 37 ºC-tan. Hurrengo egunean, peptido triptiko horiek geletik atera ditugu % 100 AZNrekin eta % 30 AZN-tan diluitutako % 1 azido trifluoroazetikorekin inkubazio ezberdinak burutuz. Azkenik, masa espektrometria bidez analizatu baino lehen, peptidoen soluzioak lehortu egin ditugu SpeedVac zentrifuga erabiliz (Thermo Scientific).

6.2. LC-MS/MS analisia

Masa espektrometriako analisiak *EASY-nLC 1200* likido kromatografiari akoplatutako *Q Exactive HF-X* masa espektrometroan burutu ditugu (Thermo Scientific), horretarako ioi-iturri gisa *nanospray*-a erabiliz. Lehortutako peptidoak % 0.1 azido formikotan disolbatu, eta *Acclaim PepMap RSLC C18* (75 m x 25 cm, Thermo Scientific) zutabe analitikora lotutako *Acclaim PepMap100* aurre-zutabean kargatu ditugu (75 m x 2 cm, Thermo Scientific). Peptidoak zutabetik eluitu ditugu honako azetonitrilo gradientea erabiliz (% 0.1 azido formikotan): 18 minutu % 2.4tik % 24ra, 2 minutu % 24tik % 32ra eta 12 minutu % 80ra, jario-tasa 300 $nL \cdot min^{-1}$ izanik. Masa espektrometroak ioi-modu positiboan funtzionatu du.

MS datuak m/z 375etik 1800ra jaso ditugu, 120.000ko bereizmena erabiliz m/z 200ean. 10 ioi intentsoenak fragmentatu ditugu energia altuko *C-trap* disoziazioz, horretarako 28 eV-ko kolisio-energia normalizatua erabiliz. MS/MS espektroak 15.000ko bereizmenaz erregistratu dira m/z 200an. Ioi-injekzio denbora maximoa 100 ms eta 120 ms izan dira, aldiz, AGC balioak 3 x 106 eta 5 x 105 izan dira, MS eta MS/MS bilketan, hurrenez hurren. Peptido beraren sekuentziazioa ekiditeko, 12 segunduz fragmentatutako prekurtsore bat ez hautatzeko hautua egin dugu (baztertze-dinamikoa). Karga bakarreko ioiak edo karga-egoerarik definitu gabeko ioiak baztertu egin ditugu MS/MSetik. Datuak XCalibur softwarea (Thermo Scientific) erabiliz bildu dira.

6.3. Datuen prozesamendua eta analisi bioinformatikoa

Eskuratutako datu gordinen fitxeroak MaxQuant softwarearekin (Cox and Mann, 2008) prozesatu ditugu (1.5.3.17 bertsioa), Andromeda (Cox et al., 2011) barne bilatzailea erabiliz, eta bilaketa UniProt datubaseko *Homo sapiens* sarrerekiko burutuz (2017_03; 42165 sarrera). Horrez gain, bilaketa horretarako datubasean FLAG_UBIQUITIN eta DDI1_GFP proteinen sekuentziak eskuz gehitu ditugu. DDI1 proteinan aurkitzen diren ubikitina kate-motak aztertzeko, soilik poli-ubikitinatutako DDI1en laginari dagozkion fitxero gordinak erabili ditugu. Aldiz, DDI1en ubikitinazio guneak ikertzeko, bai mono-, bai poli-ubikitinatutako fitxero gordinak batera analizatu ditugu. Karbamidometilazioa (C) eraldaketa egonkor bezala ezarri dugu, aldiz, Met oxidazioa, N-muturreko azetilazioa eta Lys GlyGly (ez karboxilo-muturrekoa) eraldaketa aldakor bezala jarri ditugu. Masa tolerantzia 8 eta 20 ppm-tan ezarri dugu MS eta MS/MS mailatan, hurrenez hurren. Entzimaren espezifikotasunean tripsina ezarri dugu, eta gehienez 3 *missed cleavage* onartu ditugu. *Match between runs* aukera aktibatu dugu, 1,5 minutuko kointzidentzia-leiho batekin eta 20 minutuko lerrokatze-leiho batekin, laginen arteko identifikazioa lortzeko asmoz. Peptidoaren gutxieneko luzera minimoa zazpi aminoazidotan ezarri dugu, eta peptido zein proteinentzako aurkikuntza faltsuaren tasa (*False Discovery Rate* (FDR)) % 1ean. Ubikitinazio-guneak ikertzerakoan, gutxieneko lokalizazio-probabilitatea 0,75ekoa izatea erabaki dugu. LFQ (*Label Free Quantification*) intentsitate normalizatuak MaxLFQ algoritmoa erabiliz kalkulatu ditugu.

7. *Drosophila melanogaster* eulien igotze-abiaduraren testa

Bi eguneko adina duten 4 genotipo ezberdineko euliak erabili ditugu beraien igotze-abiadura testatzeko: jatorrizkoa (*wild-type, WT*), *Ube3a* mutante homozigotoa (15B), *Ube3a* mutante heterozigotoa (15B/TM6) eta *faf* mutantea (faf-RNAi).

Euliak DMSO edo WP1130 farmakoarekin tratatu ditugu. Horretarako, tratamendua baino bost ordu lehenago euliak janaririk gabeko hodi huts batera pasatu ditugu. Jarraian, hodi berriak prestatu ditugu, eta janariari gainera DMSO

edo 0.7 mM WP1130 gehitu diogu. Bost orduko baraualdiaren ondoren, eta janaria lehorra dagoela egiaztatu ondoren, euliak hodi berri horietara pasatu ditugu. Azkenik, igotze-testa burutu dugu 24h, 48h eta 72h geroago.

Igotze-abiaduraren testa burutzeko, fenotipo bakoitzerako hodi huts bat prestatu dugu, eta 5 ar eta 5 eme sartu ditugu bertan (n=10). Minutu batez egokitzen utzi ostean, kolpe batekin euli guztiak hodiaren hondora mugiarazi ditugu, eta aldi berean, kronometroa martxan jarri dugu. Lehenengo euliak 4 zentimetrotara markatu dugun lerroa gurutzatzen duenean kronometroa gelditu dugu, eta denbora hori aputatu dugu. Genotipo bakoitzarekin bost aldiz egin dugu testa, eta neurketa bakoitzaren artean euliei 2 minutuko atsedena eman zaie, errekuperatu daitezen. Igotze-abiaduraren test hori hiru aldiz errepikatu dugu, euli-belaunaldi ezberdinekin.

8. UBE3Aren purifikazioa eta kristalizazioa

8.1. Bakterioen transformazioa eta proteinaren adierazpena

Escherichia coli BL21 (DE3 eta TR1 anduiak)(Stratagene) His-P2-hUBE3A, GST-P2-hUBE3A eta His-SUMO-hUBE3A plasmidoekin transformatu ditugu. Kolonia bakar bat hartu eta 10 mL LB (*Luria Broth*) mediotan pre-inokulatu dugu. 24 ordu geroago, pre-inokulo hori 2 L LB mediotan inokulatu dugu, eta bakterioak 37 ºC-tan hazi ditugu dagozkien antibiotikoekin (kanamizina edo anpizilina). Dentsitate-optikoa (OD_{600}) 0.7 denean, proteinen adierazpena induzitu dugu 1M IPTG (isopropil 1-tio-β-D-galaktopiranosido) erabiliz. 12 orduz 20 ºC-tan inkubatu ostean, bakterioak zentrifugatu ditugu (30 minutuz, 4500 rpm-tan) (Beckman Coulter, JLA 8.100), eta jalkina TBS tanpoian berresegi dugu (200 mM NaCl, 25 mM Tris-HCl, pH 7.4, eta 10 mM imidazol (HIS konstruktoarentzako) edo 1 mM DTT (GST konstruktoarentzako) eta DNAsa (100 µl, 2,5 mg/mL). Zelulak sonikatu egin ditugu 4°C-tan 30 minutuz (10 segundu piztuta, minutu bat itzalita, %60ko anplitudearekin), eta jarraian 0.1 mM PMSF (fenilmetilsulfonil fluoruroa) eta 1 mg/mL lisozima gehitu ditugu. Azkenik, lisatutako materiala ultrazentrifugatu dugu (1h, 20.000 rpm) eta gainjalkina erabili dugu UBE3A proteinaren purifikaziorako.

8.2. Afinitate purifikazioa eta mozketa

Lehenik eta behin afinitate kromatografia burutu dugu gainjalkinetik abiatuta giza UBE3A protein purifikatzeko. Horretarako 3 mL Ni-NTA (QIAGEN) edo Glutation Sefarosa bolatxoak (GE Healthcare) paketatu ditugu zutabe ezberdinetan. Grabitate bidez, zutabeak garbitu ditugu garbiketa tanpoiarekin (200 mM NaCl, 25 mM Tris-HCl, pH 7.4) eta jarraian, proteinak eluitu ditugu 250 mM imidazol (HIS-isatsaren kasuan) edo 20 mM Glutation (GST isatsaren kasuan) erabiliz. Eluitutako materiala dialisi poltsan sartu, eta gau osoz dialisi tanpoian sartuta utzi dugu (100 mM NaCl, 1 mM DTT eta 25 mM Tris-HCl pH 7.4). Horrez gain, *Tobacco etch virus* (TEV) edo *SUMO Specific Peptidase 2* (SENP2) proteasa entzimak gehitu dizkiegu, GST eta SUMO laginen kasuan, hurrenez hurren. 1/20 proteasa/proteina ratioa mantendu dugu, gauean zehar dialisiaz gain GST eta SUMO isatsak mozteko. Mozketaren ostean laginak berriz ere aurretiaz erabilitako zutabera berdinera gehitu ditugu GST eta SUMO isatsak baztertzeko.

8.3. Ioi-kromatografia

Afinitate kromatografiaren ostean, moztutako eta eluitutako laginak anioi-trukeko kromatografia zutabean (HiTrap Q HP; 5 ml; GE Healthcare) kargatu ditugu. Zutabea lehendabizi A tanpoiarekin garbitu dugu (25 mM Tris-HCl pH 7.4, 1 mM DTT), zutabearen bolumena 3 aldiz pasatuz. Jarraian, B tanpoiaren (25 mM Tris-HCl pH 7.4, 1 mM DTT and 1M NaCl) hiru zutabe-bolumen, eta berriz ere A tanpoia pasatu ditugu. Azkenik, laginak zutabetik eluitzeko gatz-gradientea erabili dugu: hasierako tanpoia 25 mM Tris-HCl, pH 7.4 da, eta gradientea 0-1 M NaCl bitartean burutu da. Jario-tasa 2.0 ml/min izan da, eta 2 mL-tako frakzioak batu ditugu.

8.4. Gel-iragazpeneko kromatografia

SDS-PAGE elektroforesi bidez giza UBE3A duten laginak identifikatu ostean, lagin horiek bateratu, kontzentratu eta TBS tanpoitan garbitu ditugu (25 mM Tris-HCl pH 7.4, 200 mM NaCl eta 1 mM DTT). Jarraian, laginak *HiLoad 10/30 Superdex 200* gel-iragazpen zutabera gehitu ditugu (GE Healthcare), zutabe hori

aurretiaz TBS tanpoiarekin garbitu ostean. UBE3A proteina puruenak dituzten frakzioak bateratu ditugu, eta 2 mg/mL-ra kontzentratu ditugu Amicon zentrifugazio-kontzentradoreak erabiliz (Millipore). Azkenik, purifikatutako proteinaren kontzentrazioa neurtu dugu. Horretarako 280 nm-tako absorbantzia neurtu dugu, eta extintzio-koefizientea erabiliz (*Protparam* programaren arabera, UBE3Aren kasuan 0,79 m^{-1} cm^{-1}), UBE3Aren kontzentrazioa kalkulatu dugu.

8.5. Aurre-kristalizazio testa

Aurre-kristalizazio testa burutzeko *Hamptom Research* gidan azaltzen den *Pre-crystallization Test* (PCT) kit-a erabili dugu, zintzilikatutako tantaren lurrun-difusioa deritzon teknika aplikatuz. 1 µL purifikatutako hUBE3A (2 mg/mL) eta 1 µL prezipitatzaile-tanpoi nahastu ditugu 18 °C-tan. Erabilitako prezipitatzaile tanpoi ezberdinak honakoak dira: A1 (0.1 M TRIS-HCl pH 8.5, 2.0 M Amonio sulfatoa), A2 (0.1 M TRIS-HCl pH 8.5, 0.2 M Magnesio kloruroa, 30% w/v Polietilenglikola 4,000), B1 (0.1 M TRIS-HCl pH 8.5, 1.0 M Amonio sulfatoa) eta B2 (0.1 M TRIS-HCl pH 8.5, 0.2 M Magnesio kloruroa, 15% w/v Polietilenglikola 4,000). Laginak 30 minutuz inkubatu ditugu, eta tantak argi mikroskopioz aztertu ditugu.

8.6. Kristalizazioa

hUBE3A proteinaren kristalak lortzeko, berriz ere zintzilikatutako tantaren lurrun-difusioa deritzon teknika aplikatu dugu. Kristalizazio tantak 1 µL proteina (2 mg/mL) eta 1 µL tanpoi ditu. Baheketa burutu dugu 96-putzuko plaketan kristalizaziorako tanpoi ezberdinak jarriz, kristalizazio-baldintza egokienak aurkitzeko. Erabilitako baheketa kitak honakoak dira: Morpheus (Molecular Dimensions, MD1-124), PACT (Qiagen), Proplex (Molecular Dimesions, MD1-38) eta Amonium sulfate (Hampton Research, HR2-211). 96-putzuko plaketan, putzu bakoitzaren baldintzak 1. Dokumentu Osagarrian aurkitu daitezke.

9. Saguen portaera

UBE3A gainadierazten duten saguak (UBE3A-OE$^{+/+}$) eta adin bereko kontrol saguak (C57BL/6) erabili ditugu portaera esperimentuetarako. Kutxa bakoitzean 4-5 sagu jarri ditugu, eta 12-12h argi/ilun zikloak, 21-23 ºC eta % 65-70eko hezetasuna mantendu ditugu. Janaria eta ura *ad libitum* eman dizkiegu. Animalien mantenua eta esperimentazio prozedurak Europako 2010/63/EU eta Espainiako 53/2013 errege dekretuetan ezarritako oinarrien arabera burutu ditugu. Horrez gain, prozedura guztiak EHUko etika batzordeak (CEEA) onartu ditu. Autismoarekin erlazionatutako honako portaera test ezberdinak burutu ditugu, Silverman et al. (2010) taldeak deskribatu bezala.

9.1 Ultrasoinu-bokalizazioak(UsV)

P7 adineko saguak kutxatik atera ditugu, eta soinu-gabeko ganbera batean sartu ditugu. Ganbera horretan dauden bitartean, 5 minutuz, ultrasoinu-bokalizazioak grabatu ditugu. Azkenik, fitxategi horiek laborategiko animalientzako garatutako Avisoftsound programaren bidez analizatu ditugu.

9.2 *Elkarganako elkarrekintza sozialaren* testa

P21-28 adineko saguak aurretiaz ezaguna duten kutxa batean sartu ditugu. Kutxa horretan ezagutzen ez duten eta familiakoa ez den adin, sexu eta genotipo bereko sagu bat jarri dugu, eta elkarrekiten utzi ditugu 10 minutuz. Elkarrekintza soziala zenbat denboraz eman den neurtu dugu pare bakoitzean. Elkarrekintza kontsideratu dugu bi saguen sudurrak elkarren aurka jarri eta usaintzen, sudurrarekin uzkia usaintzen, elkarri segika, edota elkarren gainean edo azpian pasatu duten denbora. Neurketa horiek bi esperimentu independentetan burutu ditugu.

9.3 *Eremu irekiaren* testa

P30 adineko saguak Plexiglas kutxa batean sartu ditugu 20 minutuz, eta bideo bidezko grabaketen bidez, aktibitate lokomotorea neurtu dugu. Bideo horietan zenbateko distantzia bidaiatu duten eta zein abiadurarekin neurtu dugu, horretarako ANY-maze portaera ikertzeko software-a erabiliz.

9.4 *Grooming-a*

Grooming portaera saguek beraien burua txukun mantentzeko ahaleginean edo garbitzean burutzen duten mugimendu errepikakorra da. P30 adineko saguak erabili ditugu test hori burutzeko, eta *grooming* egiten pasatzen duten denbora eskuz neurtu dugu. Horretarako saguei 10 minutuko jarraipena egin diegu ohiko kutxetan isolatuz.

9.5 *Hiru ganberen* testa

Hiru ganberen testa saguen alderdi soziala aztertzeko burutzen da. Test hau P35-42 adineko saguekin burutu dugu. Lehenik eta behin, egokitzapen gisa, saguari 10 minutuz hiru ganberako Plexiglas kutxa aztertzen utzi diogu. Behin egokitzapena bukatuta, sagua kutxaren erdian kokatu dugu. Hiru ganberak konektatuta daudela kontuan izanda, saguak hiru eremuetako edozein aukeratzeko askatasuna dauka. Ganbera batean ontzi huts bat jarri dugu, eta beste ganberako ontzian berriz, ezaguna ez den baina adin, sexu eta genotipo berdina duen sagu bat jarri dugu. Modu horretan, testatzen ari garen saguek ontzi bakoitzarekin elkarrekintzan pasatzen duten denbora neurtu dugu, bi esperimentu independentetan.

9.6 *Argi-ilunpe* testa

P45 adineko saguak bi ganbera ezberdin dituen kutxa batean jarri ditugu 10 minutuz. Ganbera horietako bat ilunpetan dago, saguak seguru sentitzeko, eta bestea aldiz, argiztatuta dago, eta horrek saguei antsietatea eragiten die. Test

horretan, saguek ganbera bakoitzean pasatzen duten denbora, eta ganbera ilunetik argira ateratzeko behar duten denbora neurtu ditugu, antsietate-mailaren indikatzaile gisa.

9.7. *Plaka beroaren* testa

P45 edo nagusiagoak diren saguak erabili ditugu plaka beroaren testa burutzeko. Horretarako, saguak 52 ºC-tara dagoen zoru bero baten gainean jarri ditugu, eta minaren adierazle den lehen sintoma agertu arteko denbora neurtu dugu. Sintoma horiek oinak altxatzea, edo aurreko hankekin aurpegia garbitzea izan daitezke. Test hori gehienez 15 segunduz luzatu dugu.

VIII.
RESULTS

Chapter 1

Validation and characterization of candidate UBE3A substrates

1. Validation of previously identified UBE3A substrates

The identification of human UBE3A substrates is crucial for the deep understanding of the molecular mechanisms by which Angelman syndrome is developed, and could explain how the lack of a single protein –UBE3A– can end up in such severe symptoms. We therefore decided to validate in human cell lines potential UBE3A substrates previously identified in our lab in Drosophila and mice experiments (Ramirez et al., 2018; data not published). We aim to confirm that UBE3A mediated ubiquitination of those proteins is conserved within species. For that purpose, we applied a modified GFP pull-down approach based on high-affinity anti-GFP antibody-coated beads (Chromotek-GmbH). Those beads are routinely used in non-denaturing conditions to preserve interactions in co-immunoprecipitation experiments, but our lab has found that they also withstand very stringent washing conditions. As the isopeptide bond of ubiquitin with its substrates is kept intact on denaturing environments, GFP-tagged proteins can be successfully isolated in order to further study their ubiquitination (Lee et al., 2014; Min et al., 2013; Ramirez et al., 2015).

To apply the modified GFP pull-down strategy for the validation of putative UBE3A substrates, we co-transfected the cells with a FLAG tagged version of ubiquitin (FLAG-Ub) together with a GFP tagged candidate protein (X-GFP), in two conditions: overexpressing wild-type ($UBE3A^{WT}$) and ligase-dead ($UBE3A^{LD}$) UBE3A (Figure 27). $UBE3A^{LD}$ is a catalytically inactive version of the UBE3A protein; mutation in C843A allows ubiquitin binding but not its transfer to the substrates (Brimer and Lyons, 2007). After pull-down, immunoblotting detected simultaneously the GFP tagged protein and the FLAG tagged ubiquitin: a secondary fluorescent antibody detected the primary anti-GFP antibody that binds to the non-modified form of the protein of interest (Figure 27, green channel), while the chemiluminescent anti-FLAG antibody directly bound to the ubiquitin's FLAG tag, monitoring the ubiquitination pattern of the protein (Figure 27, red channel). We employed this strategy in HEK293T cell line, due to their easy-of-use and high-transfection efficiency, essential for ubiquitome studies. However, since Angelman syndrome is a neurological disease and HEK293T cells lack the typical characteristics of neuronal cells (dendrites…) we also employed a

neuroblastoma cell line (SH-SY5Y) aiming to validate candidate UBE3A substrates in a cell line closer to their real physiological context.

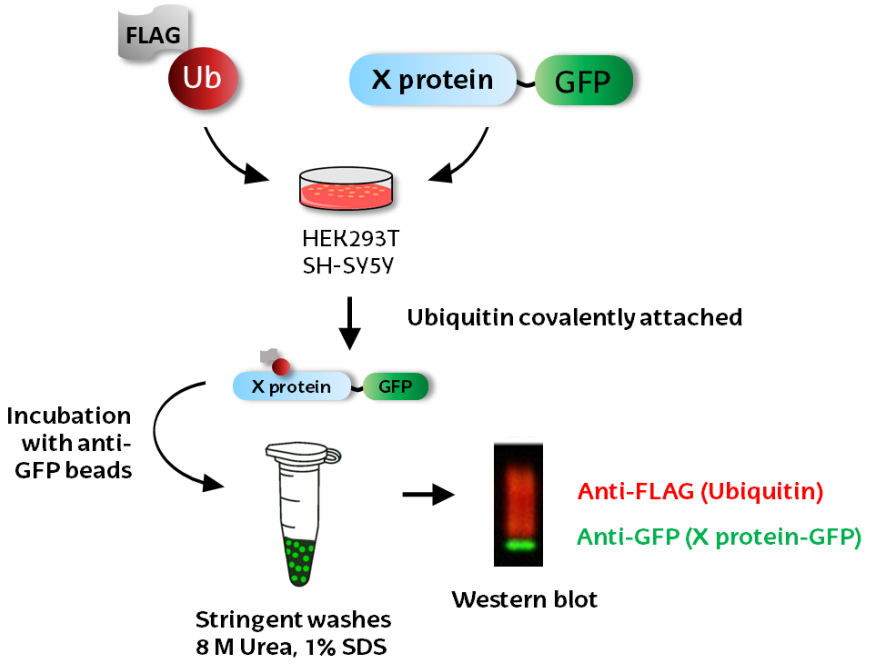

Figure 27. Modified GFP pull-down protocol allows the detection of the protein of interest and its ubiquitination pattern. FLAG-tagged ubiquitin and a GFP-tagged protein are co-transfected in HEK293 and SH-SY5Y cells. Ubiquitin is then covalently attached to the proteins. Cell lysate is incubated with beads that bind GFP. After stringent washes with 8M urea and 1% SDS all contaminants are removed and the protein of interest together with its ubiquitinated fraction can be purified. Immunoblotting with anti-GFP antibody and anti-FLAG antibody detect the protein of interest (in green) and its ubiquitinated fraction (in red), respectively.

Aforementioned experiments in photoreceptor neurons of *Drosophila melanogaster* (Ramirez et al., 2018) as well as mice brain (data not published) identified a high amount of proteasome integral or regulatory subunits as potential UBE3A substrates (Table 5). In this report we aim to validate the following putative candidates as real UBE3A substrates using the GFP pull-down assay described above.

Table 5. List of putative UBE3A substrates to validate.

Protein	Human homolog	Molecular function	Celullar function	References
Rngo	DDI1 *Ddi1 homolog 1*	?	?	(Sivá et al., 2016)
	DDI2 *Ddi1 homolog 2*	Proteasomal shuttle, protease	Protein degradation, neural homeostasis	(Koizumi et al., 2016; Sivá et al., 2016)
PSMA5	PSMA5 *Proteasome subunit alpha type-5*	Proteasome subunit	Protein degradation	(Finley et al., 2016)
MINDY2/ FAM63B	MINDY2 *Ubiquitin carboxyl-terminal hydrolase MINDY-2*	Deubiquitinase	Protein recycling	(Abdul Rehman et al., 2016; Maurer and Wertz, 2016)
UBE2L3/ UbcH7	UBE2L3 *Ubiquitin-conjugating enzyme E2 L3*	E2 conjugating enzyme	Mitophagy	(Nuber et al., 1996)
BLHM	BLHM *Bleomycin hydrolase*	Peptidase	Neurodegeneration	(Suszynska-Zajczyk et al., 2014)
TAX1BP1/ T6BP	TAX1BP1 *Tax1-binding protein 1* T6BP *TRAF6-binding protein*	Protein-binding	Autophagy, signalling	(Ling and Goeddel, 2000; Sarraf et al., 2020; Xiao et al., 2018)

1.1. DDI1 and DDI2

The most confidant Ube3a candidate substrate in the study in Drosophila was Rngo (*Ring lost*). Label-free quantification by mass-spectrometry and immunoblotting verified that Rngo was more ubiquitinated when overexpressing *Ube3a*, which resulted in the first *Ube3a* substrate to be validated *in vivo* in the context of a whole organism (Ramirez et al., 2018). Moreover, this protein was previously observed on a neuronal ubiquitome study performed by our lab (Franco et al., 2011). Such promising results entailed with the succeeding study to confirm if human UBE3A mediates ubiquitination of Rngo's human homologs: DDI1 (Ddi1 Homolog 1) and DDI2 (Ddi1 Homolog 2). *Saccharomyces cerevisiae Ddi1* has been described to function as a proteasomal shuttle protein as well as a ubiquitin-dependent protease, which cleaves substrate proteins only when they are tagged with long ubiquitin chains (Serbyn et al., 2020; Yip et al., 2020; Zientara-Rytter and Subramani, 2019). Human DDI2 has been described to be an ubiquitin-

directed endoprotease (Dirac-Svejstrup et al., 2020) and the identification of an ubiquitin-interacting-motif (UIM) that could work as an UBA domain, indicated also the possibility to work as a proteasomal shuttler (Sivá et al., 2016). Human DDI1 appeared through a retrotransposition event in hDDI2 and its function remains to be elucidated. In this context, we aimed to validate human DDI1 and DDI2 proteins as UBE3A substrates to later characterize their cellular function.

Prior to the validation of candidate substrates, we decided to test if the addition of a GFP tag to the substrate could difficult their ubiquitination. To test the suitability of the GFP tag for proper DDI1 ubiquitination, we tagged DDI1 either N-terminally (GFP-DDI1) and C-terminally (DDI1-GFP). After GFP pull-down, as shown in the Western blot, the detection of their ubiquitinated fraction displayed the same ubiquitination pattern for both constructs. The expression levels were high enough in both conditions for optimal GFP pull-down experiments, although the levels with the N-terminal tag (GFP-DDI1) were slightly higher (Figure 28).

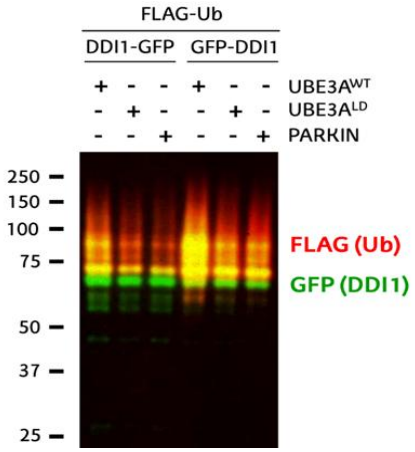

Figure 28. GFP tag does not disrupt DDI1 ubiquitination. Immunoblotting of DDI1-GFP (C-ter tag) and GFP-DDI1 (N-ter tag) after GFP pull-down was performed in three different conditions (overexpression of UBE3A^{WT}, UBE3A^{LD} and PARKIN).

HEK293T cells were then co-transfected with N-terminally tagged DDI1 (GFP-DDI1) together with FLAG-tagged ubiquitin and they were expressed upon UBE3A^{WT} and UBE3A^{LD}. In this first validation we included two more conditions as controls; we co-expressed GFP-DDI1 with an empty vector (pCDNA3.1) and another E3 ligase (PARKIN), in order to test the correct expression of both UBE3A plasmids and to prove that the effect is specific to UBE3A E3 ligase. A clear

increase in GFP-DDI1 ubiquitination could be observed and quantified upon UBE3A^{WT} overexpression (Figure 29). Mono-ubiquitination band and poly-ubiquitination smear could be also clearly discriminated. In contrast, UBE3A^{LD}, PARKIN and pCDNA3.1 control samples showed the same ubiquitination levels and no changes in total protein levels were observed; total GFP-tagged DDI1 levels were equivalent in all samples. Since differences in ubiquitin availability within the samples or a deficient UBE3A expression could affect the resultant DDI1 ubiquitination, we analysed input samples of the cell lysates as quality control. Equivalent ubiquitin levels were obtained in all samples and the correct expression of UBE3A was ensured (Figure 29). The increase in DDI1 ubiquitination in presence of UBE3A^{WT} validates DDI1 as a UBE3A substrate in HEK293T cells.

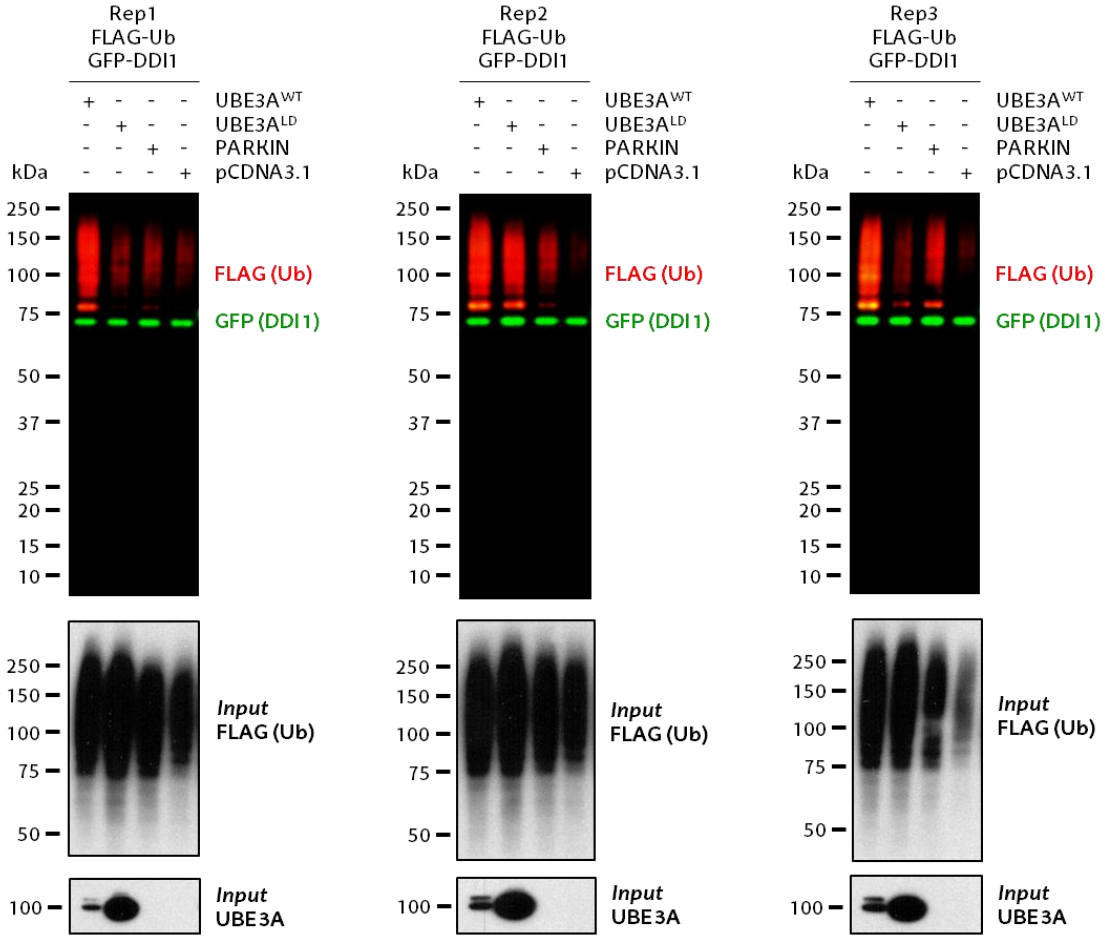

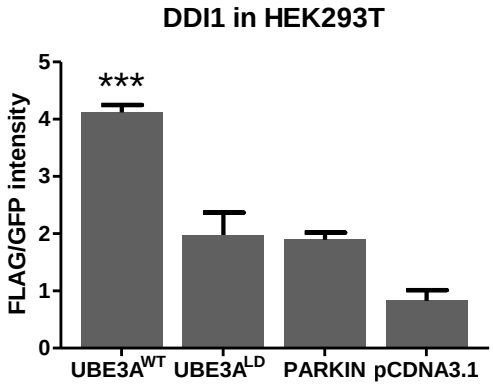

Figure 29. DDI1 is a UBE3A substrate in HEK293T cells. DDI1 ubiquitination was detected by Western blot upon overexpression of wild-type UBE3A ($UBE3A^{WT}$), ligase dead UBE3A ($UBE3A^{LD}$), Parkin E3 ligase (PARKIN) and control vector (pCDNA3.1) in HEK293T cells. Anti-FLAG antibody (red) was used to detect the ectopically expressed ubiquitin, whereas the non-modified GFP-tagged DDI1 was detected by anti-GFP antibody (green). UBE3A overexpression was confirmed in whole cell lysates using anti-UBE3A antibody (Input UBE3A) while the FLAG signal in the inputs corroborated equivalent transfections in all samples [Input FLAG-(Ub)]. Quantification of Western blots was performed with ImageLab, by normalizing the FLAG intensities to the GFP signal. The analysis showed a statistically significant increase of GFP-DDI1 ubiquitination upon $UBE3A^{WT}$ overexpression in comparison to overexpression of $UBE3A^{LD}$ [one-way ANOVA, ***p-value < 0.0001, (mean ± S.E.M.,n = 3)].

Similar results were obtained in SH-SY5Y neuroblastoma cells. Western blot analysis after GFP pull-down of cell lysates overexpressing GFP-DDI1 and FLAG-Ub in presence of $UBE3A^{WT}$, $UBE3A^{LD}$ or control pCDNA3.1 showed a significant increase in DDI1 ubiquitination upon $UBE3A^{WT}$ overexpression (Figure 30). In accordance to the results obtained in HEK293T cells, total ubiquitination levels were equivalent in all samples. The ubiquitination of UBE3A is thought to be a degradation signal, but no decrease in protein levels of DDI1 upon UBE3A expression suggested rather a non-degradative role.

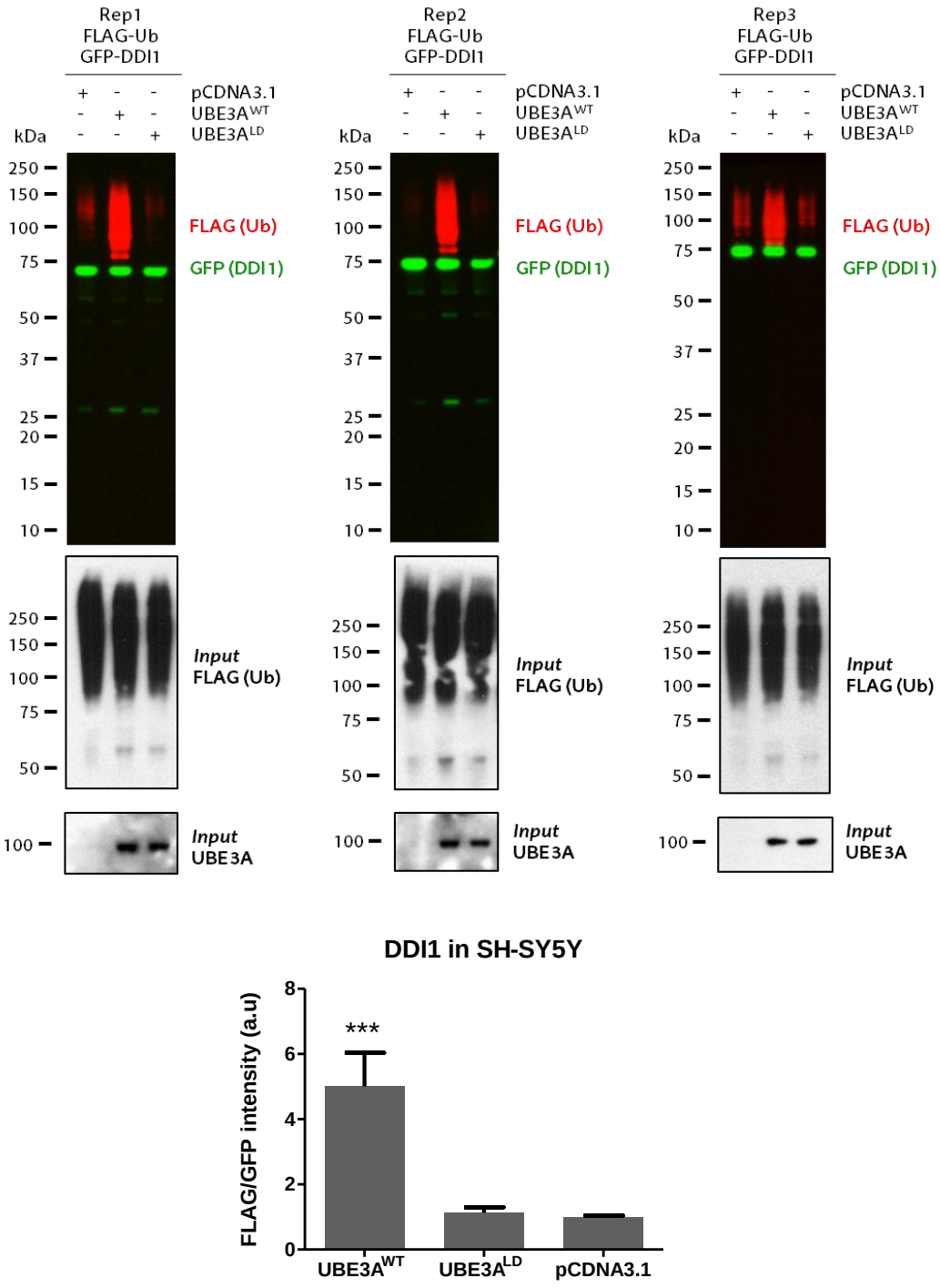

Figure 30. DDI1 is a UBE3A substrate in SH-SY5Y cells. DDI1 ubiquitination was detected by Western blot upon overexpression of wild-type UBE3A (UBE3A^{WT}), ligase dead UBE3A (UBE3A^{LD}) and control vector (pCDNA3.1) in SH-SY5Y cells. Anti-FLAG antibody (red) was used to detect the ectopically expressed ubiquitin, whereas the non-modified GFP-tagged DDI1 was detected by anti-GFP antibody (green). UBE3A overexpression was confirmed in whole cell lysates using anti-UBE3A antibody (Input UBE3A) while the FLAG signal in the inputs corroborated equivalent transfections in all samples [Input FLAG-(Ub)]. Quantification of Western blots was performed with ImageLab, by normalizing the FLAG intensities to the GFP signal. The analysis showed a statistically significant increase [one-way ANOVA, ***p-value < 0.0001, (mean ± S.E.M.,n = 3)] of GFP-DDI1 ubiquitination upon UBE3A^{WT} overexpression in comparison to overexpression of UBE3A^{LD}.

We next studied if the other human homolog of *Rngo*, DDI2, is also a UBE3A substrate. We co-transfected HEK293T and SH-SY5Y cells with FLAG-ubiquitin and a C-terminally tagged DDI2 (DDI2-GFP), in presence of UBE3A^{WT} or UBE3A^{LD}. In SH-SY5Y cells no sufficient ubiquitinated material could be detected to quantify the differences in ubiquitination in both conditions. It is likely that due to lower transfection efficiencies in SH-SY5Y neuroblastoma cells the expression of DDI2 is so low that scapes Western Blot detection. In parallel, GFP pull-down of HEK293T cell lysates and their Western blotting confirmed that the ubiquitination of DDI2 was UBE3A dependent, since its ubiquitination pattern was enhanced in presence of UBE3A^{WT} compared to the UBE3A^{LD} sample (Figure 31). Similar to DDI1, DDI2-GFP levels remained constant within the samples. We also confirmed the same transfection efficiencies in all samples and the correct expression of UBE3A. Since both UBE3A constructs are FLAG tagged, we checked if UBE3A could be detected simultaneously with the ubiquitination smear using anti-FLAG antibody, due to its easy-of-use and the low efficiency of the anti-UBE3A antibody. The UBE3A band at 100 kDa could be discriminated from the ubiquitination smear, therefore, anti-FLAG antibody was favoured to detected UBE3A in future experiments. Altogether confirmed that DDI2 is a real UBE3A substrate in HEK293T cells and proved that DDI2 UBE3A-mediated ubiquitination does not lead to its degradation.

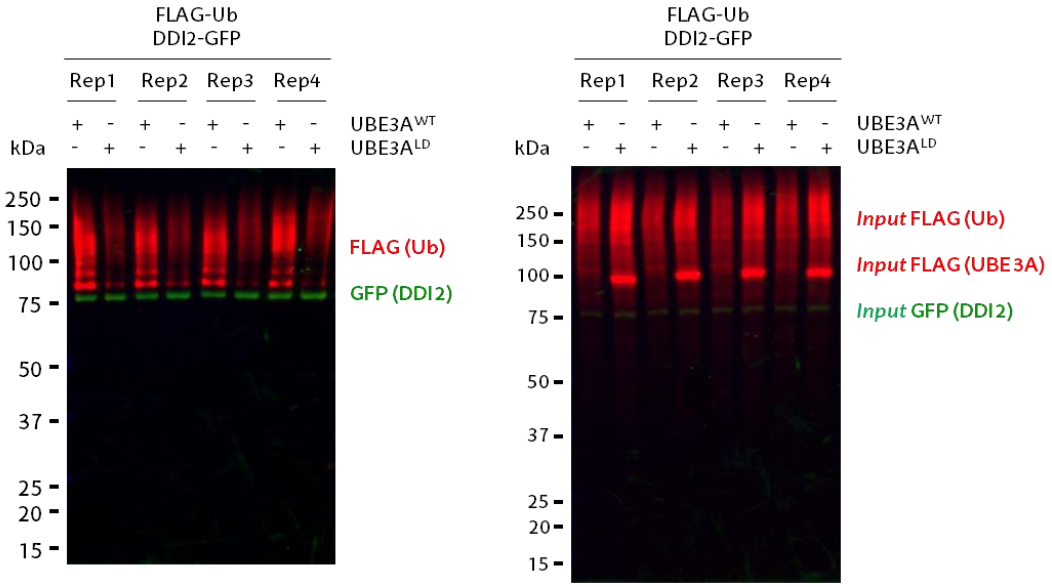

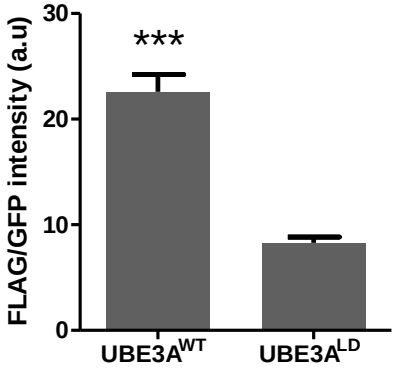

Figure 31. DDI2 is a UBE3A substrate in HEK293T cells. DDI2 ubiquitination was detected by Western blot upon overexpression of wild-type UBE3A (UBE3A^{WT}) and ligase dead UBE3A (UBE3A^{LD}) in HEK293T cells. Anti-FLAG antibody (red) was used to detect the ectopically expressed ubiquitin [FLAG-(Ub)], whereas the non-modified GFP-tagged DDI2 was detected by anti-GFP antibody (green) [GFP-(DDI2)]. UBE3A overexpression [Input FLAG-(UBE3A)] and equivalent transfections [Input FLAG-(Ub)] were confirmed in whole cell lysates using anti-FLAG antibody, while DDI2 transfection was corroborated by anti-GFP antibody [Input GFP-(DDI2)]. Quantification of Western blots was performed with ImageLab, by normalizing the FLAG intensities to the GFP signal. The analysis showed a statistically significant increase of DDI2-GFP ubiquitination upon UBE3A^{WT} overexpression in comparison to overexpression of UBE3A^{LD} [*t*-test, ***p-value < 0.0002, (mean ± S.E.M., n = 4)].

1.2. PSMA5

PSMA5, Proteasome subunit alpha type-5, was described as a putative UBE3A candidate substrate in our lab on a preceding experiment performed in mice. It is a component of the 20S core proteasome complex that is involved in the proteolytic degradation of most intracellular proteins (Finley et al., 2016). It has been related to cell proliferation, migration and invasion (Fu et al., 2019) and it shows high expression in several types of cancer (Li et al., 2016b).

The PSMA5 gene was amplified from a vector kindly provided by Dr. Ebstein and introduced into a vector carrying either an N-terminally or C-terminally GFP tag. None of the constructs displayed the minimum protein expression require for the study of ubiquitination. We therefore opted for a commercial PSMA5-GFP plasmid (Sino biological) which showed high expression levels in comparison to our previous cloning constructs.

PSMA5-GFP construct and FLAG-tagged ubiquitin were co-transfected into HEK293T cells together with UBE3A^{WT} or UBE3A^{LD}. Immunoblotting of the eluted fraction after GFP pull-down detected a clear mono-ubiquitination band and a

less intense ubiquitination smear, so differences in both type of ubiquitination were quantified separately and normalized to GFP expression levels. Analysis showed that PSMA5 total ubiquitination significantly increased upon UBE3A^{WT} overexpression, but no significant increase was observed for the mono-ubiquitination band (Figure 32). Analysis of the inputs showed equivalent transfection of ubiquitin and PSMA5-GFP in all the samples, as well as correct UBE3A overexpression (Figure 32). In conclusion, we could prove that UBE3A mediates PSMA5 ubiquitination in HEK293T cells.

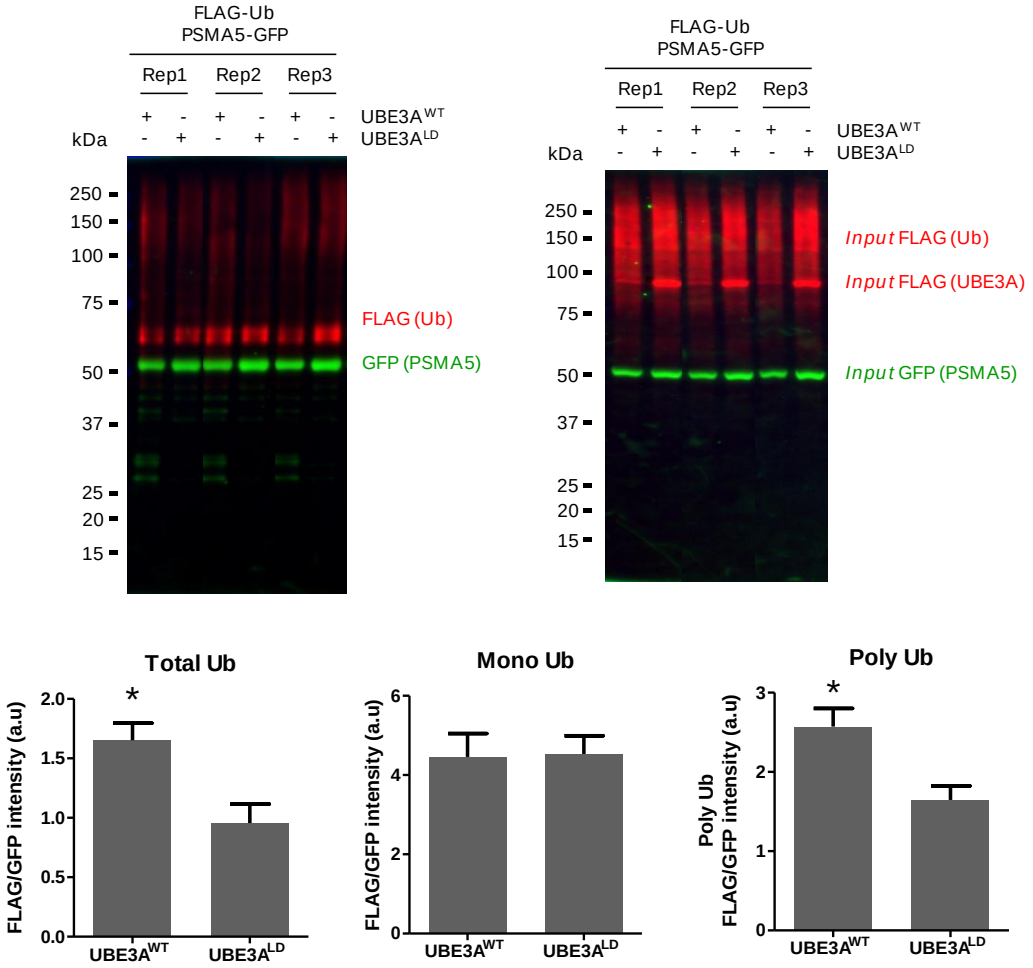

Figure 32. PSMA5 is a UBE3A substrate in HEK293T cells. PSMA5 ubiquitination was analysed by Western blot in presence of wild-type UBE3A (UBE3A^{WT}) and ligase dead UBE3A (UBE3A^{LD}). Anti-FLAG antibody (red) was used to detect the ectopically expressed ubiquitin [FLAG-(Ub)] and the non-modified GFP-tagged PSMA5 was detected by anti-GFP antibody (green) [GFP-(PSMA5)]. UBE3A overexpression [Input FLAG-(UBE3A)] and equivalent transfections [Input FLAG-(Ub)] were confirmed in whole cell lysates using anti-FLAG antibody, while anti-GFP antibody was used to check PSMA5 transfection [Input GFP-(PSMA5)]. Quantification of Western blots was performed with ImageLab, by normalizing the FLAG intensities to the GFP signal. The analysis showed a statistically significant increase of PSMA5-GFP total and poly ubiquitination upon UBE3A^{WT} overexpression (Total Ub and Poly Ub) in comparison to overexpression of UBE3A^{LD} [*t*-test, *p-value < 0.05, (mean ± S.E.M.,n = 3)]. In contrast, no significant differences were observed in the mono-ubiquitination band (Mono Ub).

Regarding the validation in SH-SY5Y cells, immunoblotting of the eluted fraction after GFP pull-down detected changes in the mono-ubiquitination band that do not correlate with a less intense ubiquitination smear (Figure 33). Separate quantification of the mono-ubiquitination band revealed a significant increase upon UBE3A^{WT} overexpression, while not statistically significant changes were observed in the total ubiquitination levels of PSMA5 (Figure 33). Moreover, cell lysate analysis indicated similar ubiquitinated material as well as similar PSMA5 total levels. Those results confirm that UBE3A mediates PSMA5 ubiquitination mainly through its poly-ubiquitination in SH-SY5Y, and that this modification does not affect the abundance of PSMA5 in the cell, suggesting rather non-degradative roles.

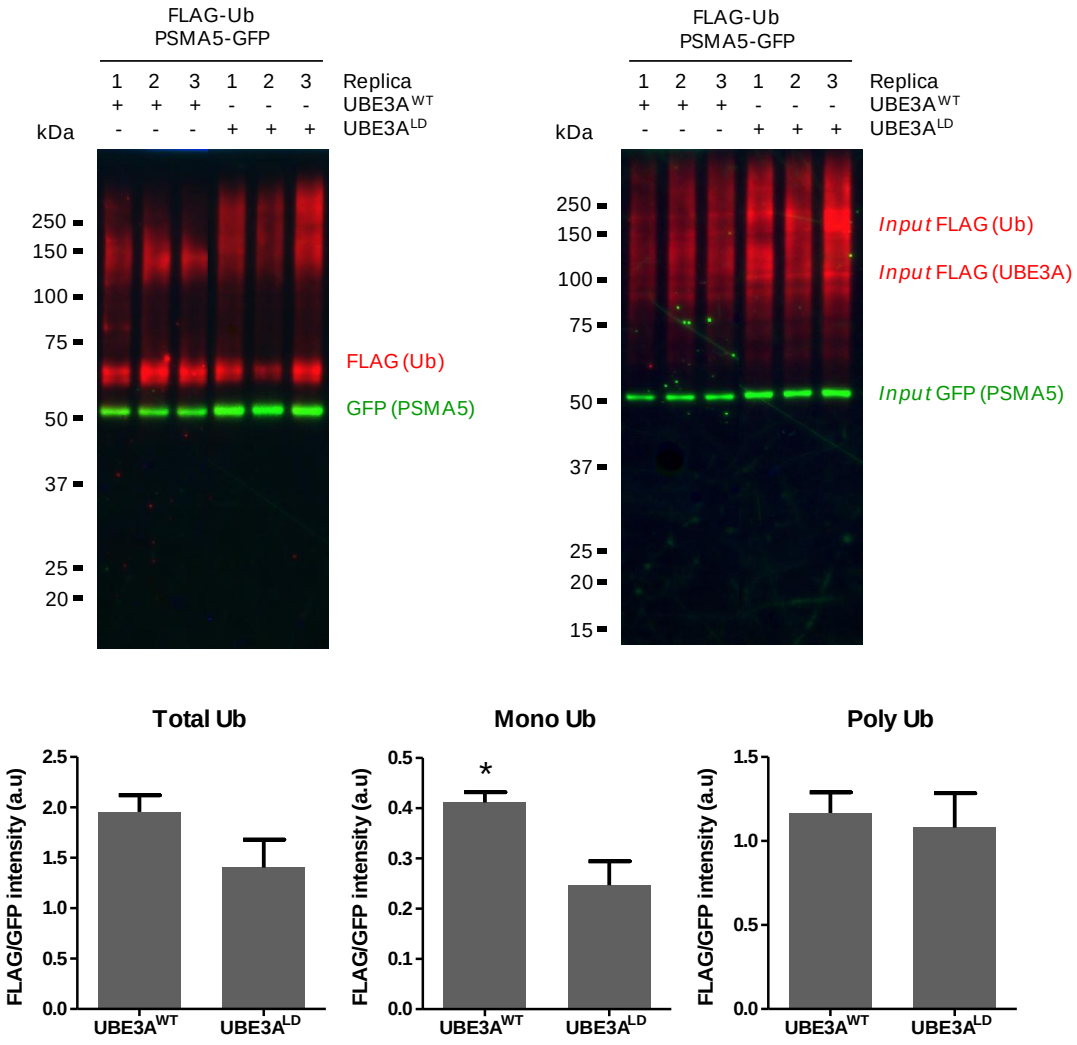

Figure 33. PSMA5 is a UBE3A substrate in SH-SY5Y cells. PSMA5 ubiquitination was analysed by Western blot in presence of wild-type UBE3A (UBE3A^{WT}) and ligase dead UBE3A (UBE3A^{LD}). Ectopically expressed ubiquitin [FLAG-(Ub)] was detected using anti-FLAG antibody (red), while the non-modified GFP-tagged PSMA5 was detected by anti-

GFP antibody (green) [GFP-(PSMA5)]. UBE3A overexpression [Input FLAG-(UBE3A)] and equivalent transfections [Input FLAG-(Ub)] were confirmed in whole cell lysates using anti-FLAG antibody, while anti-GFP antibody was used to check PSMA5 transfection [Input GFP-(PSMA5)]. Quantification of Western blots was performed with ImageLab, by normalizing the FLAG intensities to the GFP signal. The analysis showed a statistically significant increase of the mono-ubiquitination band in PSMA5-GFP upon $UBE3A^{WT}$ overexpression in comparison to overexpression of $UBE3A^{LD}$ [*t*-test, *p-value < 0.05, (mean ± S.E.M., n = 4)]. In contrast, no changes were observed in total or poly-ubiquitinated PSMA5 levels.

1.3. MINDY2

MINDY2, also called FAM63B, is a member of the recently discovered Motif Interacting with Ub-containing Novel DUB family (MINDY). It has been shown that MINDY2 cleaves poly-ubiquitin chains and that is highly selective at hydrolyzing K48-linked polyUb chains (Abdul Rehman et al., 2016). Protein modification with K48 poly-ubiquitin chains has been historically linked to proteasomal degradation, so any kind of regulation of this protein through UBE3A could be crucial for the proper function of the cell. Moreover, hypomethylation of this protein has been associated to bipolar disorder (Starnawska et al., 2016) and cognitive impairment in schizophrenia (Kondratiev et al., 2017).

MINDY2 was identified as a candidate UBE3A substrate on the aforementioned experiment in mice (data not published). In order to assess the effect of UBE3A on MINDY2 ubiquitination, we used the MINDY2-GFP plasmid kindly provided by Dr. Yogesh Kulatu (University of Dundee, UK), which showed a good expression level either in HEK293T and SH-SY5Y cells. First, HEK293T cells were co-transfected with MINDY2-GFP and FLAG-ubiquitin together with WT or LD UBE3A. Immunobloting after GFP pull-down displayed a clear mono-ubiquitination band that is enhanced in presence of $UBE3A^{WT}$ (Figure 34). Meanwhile, GFP levels are visibly lower in those samples. To discard different transfection efficiencies as the cause of the drop, we analysed the whole cell lysates. While ubiquitin levels were constant within the samples, MINDY2-GFP levels were lower in $UBE3A^{WT}$ sample, as it happens in the elutions. Those findings, together with the many breakdown products detected, suggest that UBE3A mediates MINDY2 mono-ubiquitination, probably driving it to degradation.

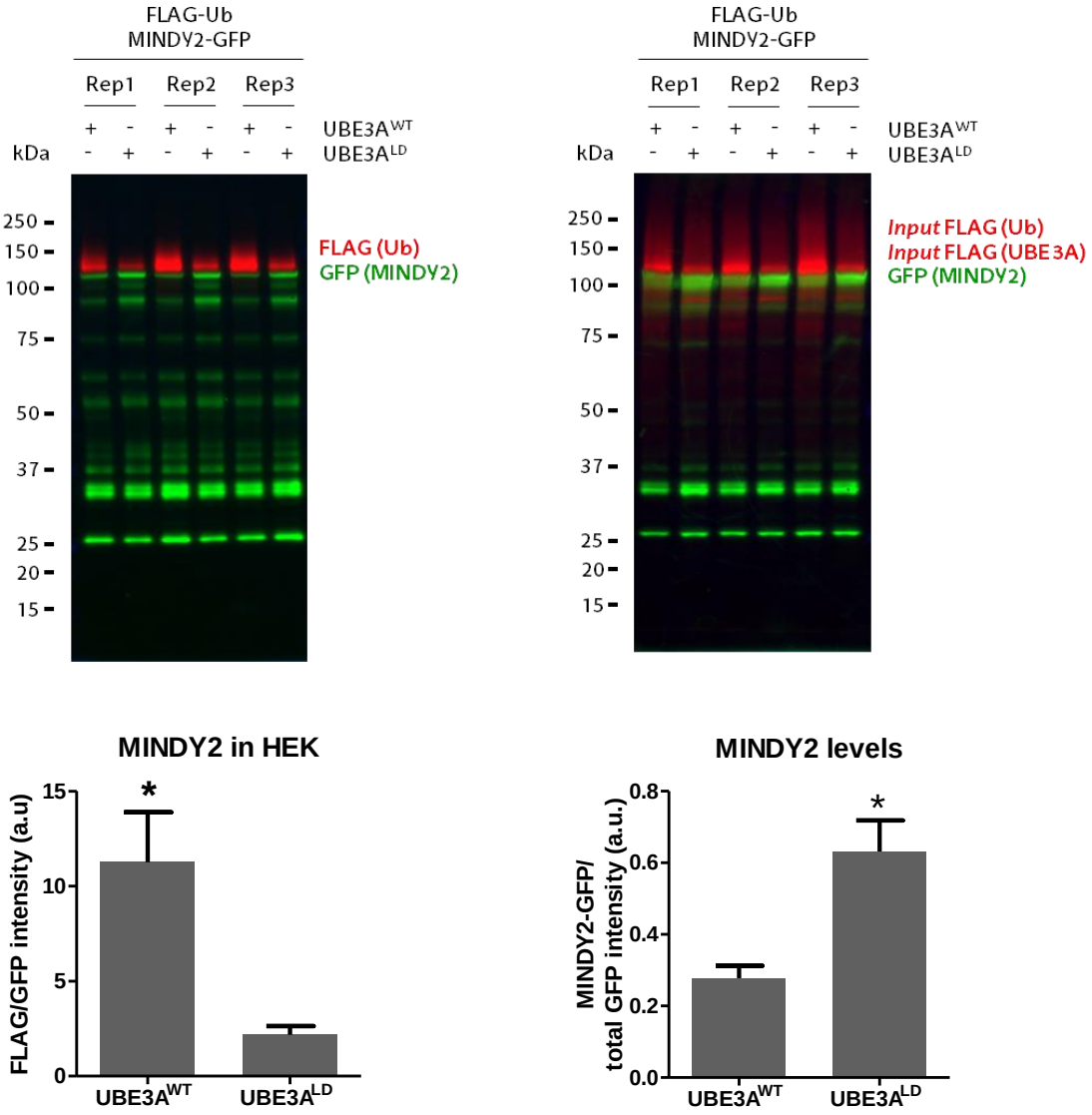

Figure 34. MINDY2 is a UBE3A substrate in HEK293T cells. MINDY2 ubiquitination was analysed by Western blot in presence of wild-type UBE3A (UBE3A^{WT}) and ligase dead UBE3A (UBE3A^{LD}). Anti-FLAG antibody (red) was used to detect the ectopically expressed ubiquitin [FLAG-(Ub)] and the non-modified GFP-tagged MINDY2 was detected by anti-GFP antibody (green) [GFP-(MINDY2)]. UBE3A overexpression [Input FLAG-(UBE3A)] and equivalent transfections [Input FLAG-(Ub)] were confirmed in whole cell lysates using anti-FLAG antibody, while anti-GFP antibody was used to check MINDY transfection [Input GFP-(MINDY)]. Quantification of Western blots was performed with ImageLab, by normalizing the FLAG intensities to the GFP signal. The analysis showed a statistically significant increase of MINDY-GFP ubiquitination upon UBE3A^{WT} overexpression in comparison to overexpression of UBE3A^{LD} [*t*-test, *p-value < 0.05, (mean ± S.E.M., n = 3)]. MINDY2-GFP levels were also normalized to the constant free GFP signal (25 kDa). Significant decrease in MINDY2 levels was observed upon UBE3A^{WT} overexpression [*t*-test, *p-value < 0.05, (mean ± S.E.M., n = 3)].

As for the validation of MINDY2 in SH-SY5Y cells, Western blot after GFP pull-down detected a mono-ubiquitination band that is enhanced upon UBE3A^{WT} overexpression (Figure 35). However, in contrast to the results obtained in

HEK293T cells, no significant changes were observed in MINDY2 protein levels and few breakdown products were detected. Although a lower transfection efficiency in this cell line could explain the aforementioned results, specific roles of MINDY2 in neuronal cells should not be discarded.

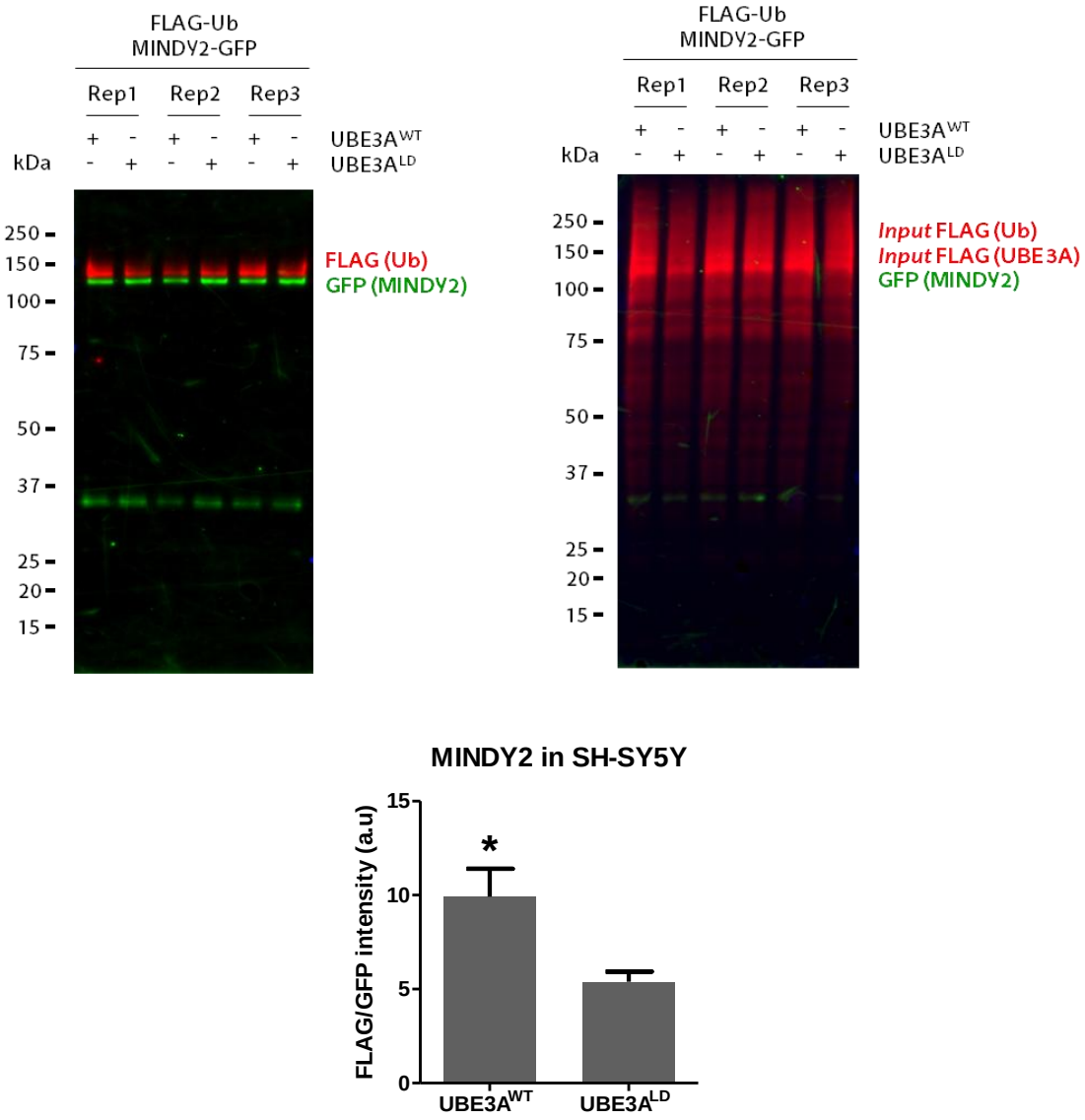

Figure 35. MINDY2 is a UBE3A substrate in SH-SY5Y cells. MINDY2 ubiquitination was analysed by Western blot in presence of wild-type UBE3A (UBE3A^{WT}) and ligase dead UBE3A (UBE3A^{LD}). Anti-FLAG antibody (red) was used to detect the ectopically expressed ubiquitin [FLAG-(Ub)] and the non-modified GFP-tagged MINDY2 was detected by anti-GFP antibody (green) [GFP-(MINDY2)]. UBE3A overexpression [Input FLAG-(UBE3A)] and equivalent transfections [Input FLAG-(Ub)] were confirmed in whole cell lysates using anti-FLAG antibody, while anti-GFP antibody was used to check MINDY transfection [Input GFP-(MINDY)]. Quantification of Western blots was performed with ImageLab, by normalizing the FLAG intensities to the GFP signal. The analysis showed a statistically significant increase of MINDY-GFP ubiquitination upon UBE3A^{WT} overexpression in comparison to overexpression of UBE3A^{LD} [*t*-test, *p-value < 0.05, (mean ± S.E.M., n = 3)].

1.4. UBE2L3

UBE2L3 is an E2 conjugating enzyme that has been previously described to interact with UBE3A, forming an E2/E3 pair in the ubiquitination process (Huang et al., 1999; Purbeck et al., 2010). It has also been assigned an important role in cell cycle, protecting the CDK inhibitor $p27^{Kip1}$ from degradation (Whitcomb et al., 2019). Problems in the regulation of UBE2L3 could lead to problems in ubiquitination of its substrates and could led to a strong dysregulation of protein recycling and cell cycle control. Proteomics data on UBE3A overexpressing mice (manuscript under review, Lectez et al., 2022) reveal that ubiquitin conjugated UBE2L3 is less abundant upon UBE3A overexpression.

To assess whether UBE2L3 ubiquitination is modified by UBE3A, we used a commercial UBE2L3-GFP (Sino biological) plasmid. We transfected HEK293T and SH-SY5Y cells with UBE2L3-GFP, FLAG-ubiquitin and wild-type or ligase-dead UBE3A. In both cases immunoblotting of GFP pull-down purification showed a clear mono-ubiquitination band accompanied by strong UBE2L3-GFP levels (Figure 36). No significant changes were observed for the mono-ubiquitination band of UBE2L3, but due to the reducing conditions of the protocol, this band would correspond to a lysine conjugated form of the enzyme, and not to its active carrier form with a thioester ubiquitin conjugated on its active site. Total ubiquitin and UBE2L3-GFP levels in HEK293T cells remained constant within the samples and both UBE3A proteins were properly expressed.

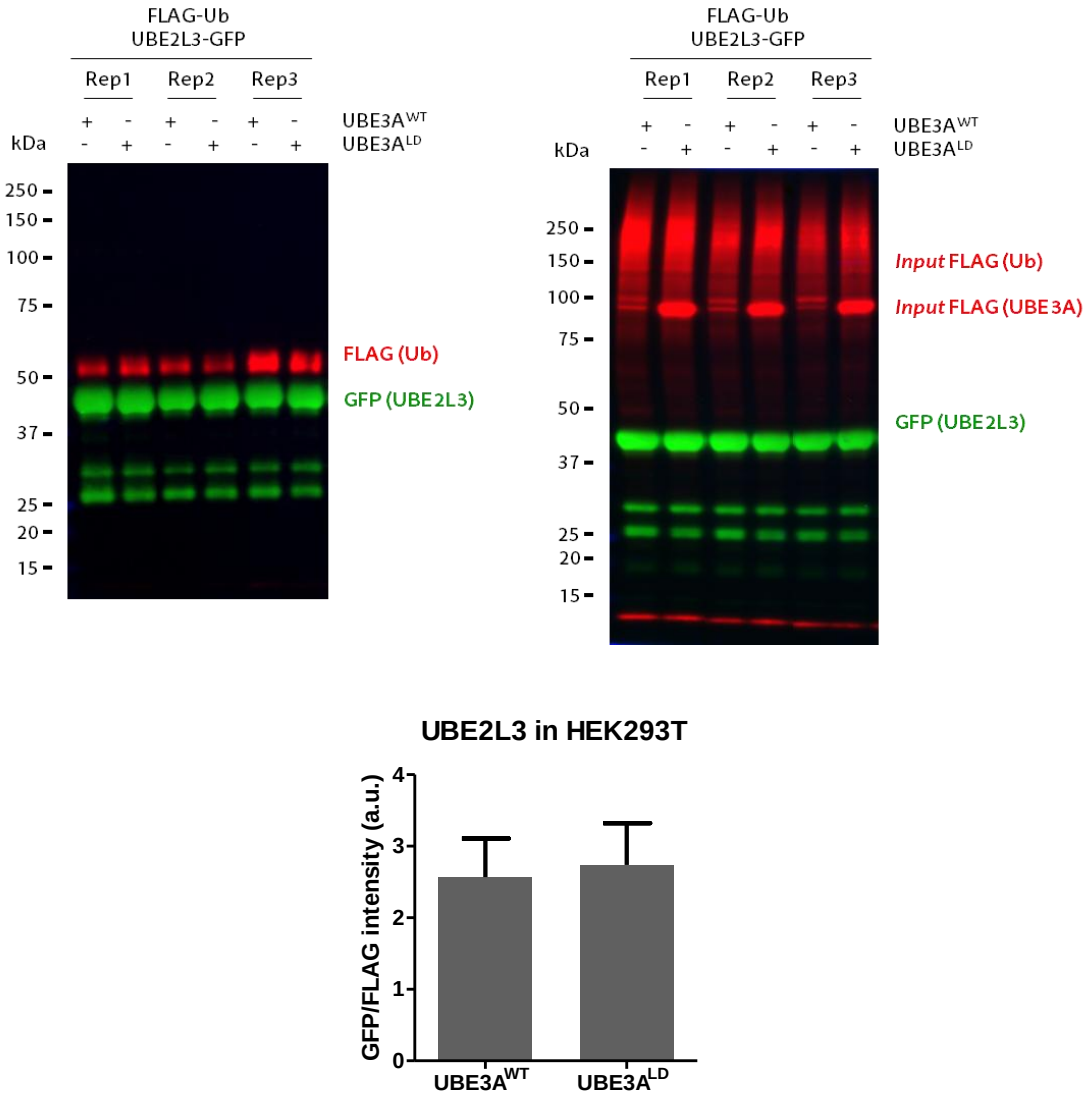

Figure 36. UBE2L3 is not a UBE3A substrate in HEK293T cells. UBE2L3 ubiquitination was analysed by Western blot in presence of wild-type UBE3A (UBE3A^{WT}) and ligase dead UBE3A (UBE3A^{LD}). Anti-FLAG antibody (red) was used to detect the ectopically expressed ubiquitin [FLAG-(Ub)] and the non-modified GFP-tagged UBE2L3 was detected by anti-GFP antibody (green) [GFP-(UBE2L3)]. UBE3A overexpression [Input FLAG-(UBE3A)] and equivalent transfections [Input FLAG-(Ub)] were confirmed in whole cell lysates using anti-FLAG antibody, while anti-GFP antibody was used to check UBE2L3 transfection [Input GFP-(UBE2L3)]. Quantification of Western blots was performed with ImageLab, by normalizing the FLAG intensities to the GFP signal. The analysis did not show a statistically significant difference on UB2L3-GFP ubiquitination in different conditions [*t*-test, p-value > 0.05, (mean ± S.E.M., n = 3)]

In contrast, SH-SY5Y cell UBE3A expression levels were lower and the overall ubiquitinated material decreased in presence of UBE3A^{WT} (Figure 37). Both cell lines presented a slight decrease on UBE2L3 ubiquitination upon UBE3A^{WT} overexpression. UBE2L3 and UBE3A form a E2-E3 pair, but rather than a direct effect, the results may be altered due to differences in the overall ubiquitination

levels, since less total ubiquitination can be observed upon UBE3A^{WT} overexpression.

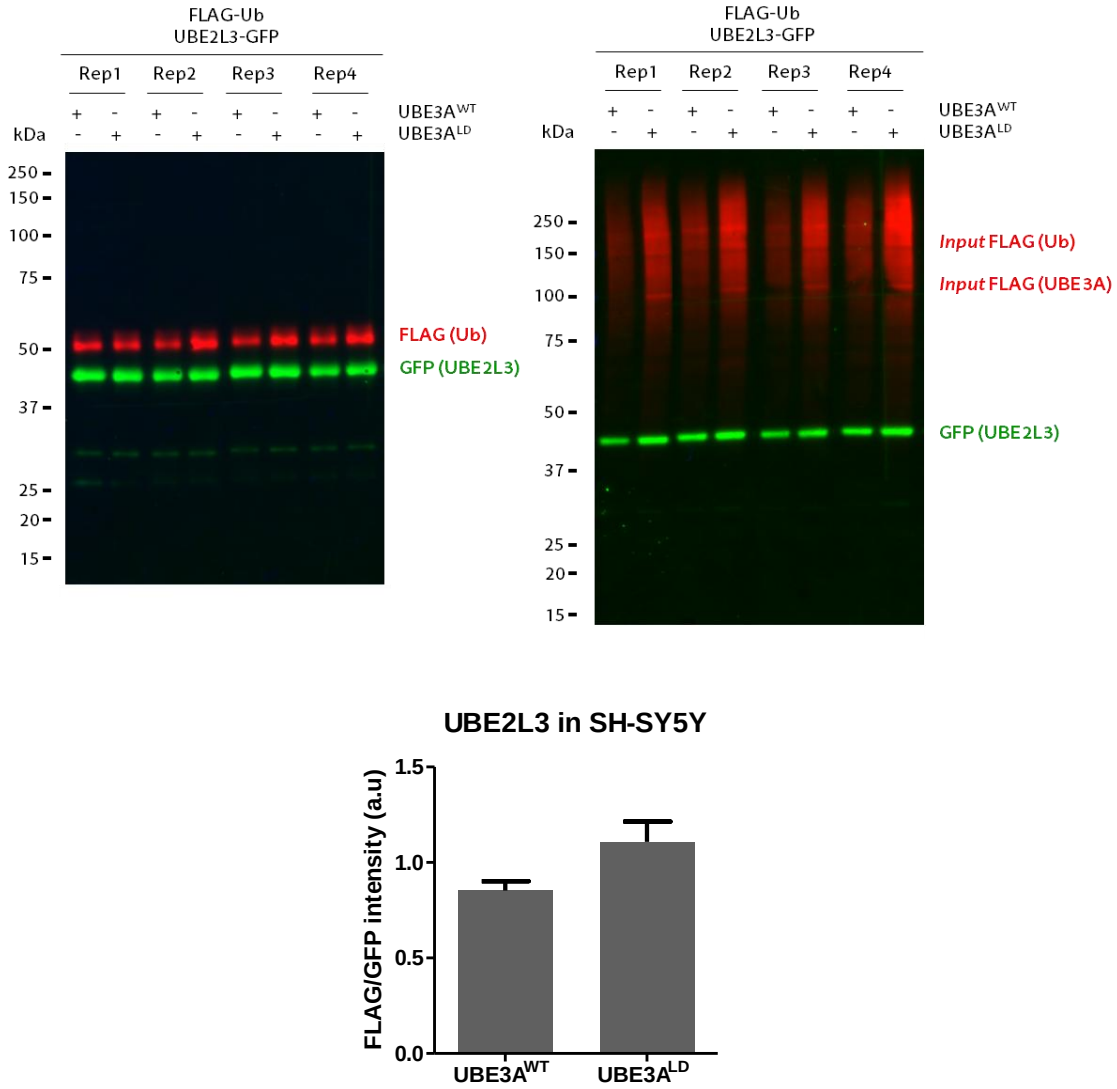

Figure 37. UBE2L3 is not a UBE3A substrate in SH-SY5Y cells. UBE2L3 ubiquitination was analysed by Western blot in presence of wild-type UBE3A (UBE3A^{WT}) and ligase dead UBE3A (UBE3A^{LD}). Anti-FLAG antibody (red) was used to detect the ectopically expressed ubiquitin [FLAG-(Ub)] and the non-modified GFP-tagged UBE2L3 was detected by anti-GFP antibody (green) [GFP-(UBE2L3)]. UBE3A overexpression [Input FLAG-(UBE3A)] and equivalent transfections [Input FLAG-(Ub)] were confirmed in whole cell lysates using anti-FLAG antibody, while anti-GFP antibody was used to check UBE2L3 transfection [Input GFP-(UBE2L3)]. Quantification of Western blots was performed with ImageLab, by normalizing the FLAG intensities to the GFP signal. The analysis did not show a statistically significant difference on UB2L3-GFP ubiquitination in different conditions [*t*-test, p-value > 0.05, (mean ± S.E.M., n = 3)]

1.5. BLMH

Another putative UBE3A substrate identified in mice is bleomycin hydrolase (BLMH). Studies have reported its involvement in antigen-processing for MHC class I molecules, protection against homocysteine thiolactone toxicity and inflammation (Riise et al., 2019; Stoltze et al., 2000; Zimny et al., 2006). More interestingly, BLMH has been described to regulate proteins involved in neurodegeneration (Suszynska-Zajczyk et al., 2014). UBE3A mediated ubiquitination of BLMH could potentially affect the expression of several neurological proteins, which could help to decipher the link between molecular basis and symptoms of Angelman syndrome patients.

For BLMH validation we used a commercial GFP-BLMH (Sino Biological) plasmid. We transfected it into HEK293T and SH-SY5Y cells together with FLAG-ubiquitin and $UBE3A^{WT}$ or $UBE3A^{LD}$. In HEK293T cells, immunoblotting of the eluted samples after GFP pull-down showed an intense mono-ubiquitination band, a more attenuated ubiquitination smear and constant GFP-BMLH protein levels within both conditions (Figure 38). No changes were observed in GFP-BLMH ubiquitination upon $UBE3A^{WT}$ overexpression in comparison to $UBE3A^{LD}$ sample. Quality control of the lysate showed equivalent ubiquitin levels within the samples and correct UBE3A overexpression levels in all conditions. As for the validation in SH-SY5Y cells, we could not detect enough ubiquitinated material for quantification, so comparison between different conditions was not possible. Therefore, we conclude that BLMH ubiquitination is not mediated through human UBE3A E3 ligase.

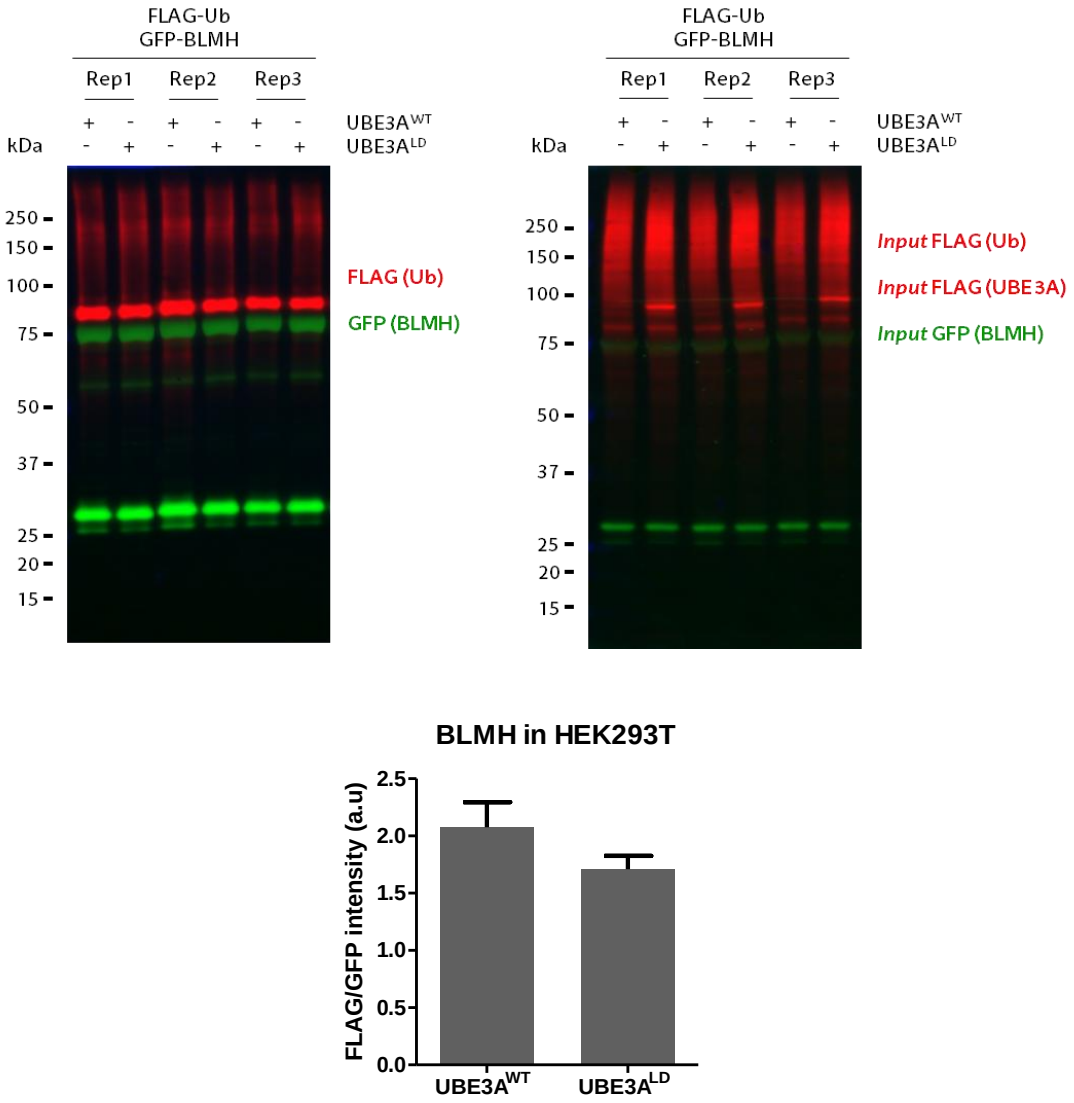

Figure 38. BLMH is not a UBE3A substrate in HEK293T cells. BLMH ubiquitination was analysed by Western blot in presence of wild-type UBE3A (UBE3A^{WT}) and ligase dead UBE3A (UBE3A^{LD}). Anti-FLAG antibody (red) was used to detect the ectopically expressed ubiquitin [FLAG-(Ub)] and the non-modified GFP-tagged BLMH was detected by anti-GFP antibody (green) [GFP-(BLMH)]. UBE3A overexpression [Input FLAG-(UBE3A)] and equivalent transfections [Input FLAG-(Ub)] were confirmed in whole cell lysates using anti-FLAG antibody, while anti-GFP antibody was used to check BLMH transfection [Input GFP-(BLMH)]. Quantification of Western blots was performed with ImageLab, by normalizing the FLAG intensities to the GFP signal. The analysis did not show a statistically significant difference on GFP-BLMH ubiquitination in different conditions [*t*-test, p-value > 0.05, (mean ± S.E.M., n = 3)]

1.6. TAX1BP1

TAX1BP1 was detected on our study in mice (data not published). This protein is involved in IL-1 signaling (Ling and Goeddel, 2000). More interestingly, it is required for the clearance of stress-induced aggregates through autophagy

(Sarraf et al., 2020; Xiao et al., 2018). Loss of TAX1BP1-directed autophagy results in protein aggregate accumulation in the brain (Sarraf et al., 2020).

A commercial GFP-TAX1BP1 (Sino Biological) was used in the validation, which was expressed together with FLAG-ubiquitin and wild-type or ligase dead UBE3A. Expression levels of GFP-TAX1BP1 were high, but after cell lysis for GFP pull-down most of the protein was located on the non-soluble membrane debris fraction. The impossibility to solubilize the sample resulted in low protein levels for GFP pull-down. In consequence, immunoblotting after GFP pull-down showed low levels of GFP in the eluted sample (Figure 39). However, in HEK293T cells an intense ubiquitination smear could be observed and quantified; although a tendency could be observed, there was no statistically significant difference within UBE3A^{WT} and UBE3A^{LD} samples. Moreover, similar ubiquitinated material was detected in the cell lysate and proper UBE3A expression was ensured. Similarly, a very low amount of GFP-TAX1BP1 protein was obtained from the lysis in SH-SY5Y cells, resulting in unquantifiable ubiquitination signal after GFP pull-down.

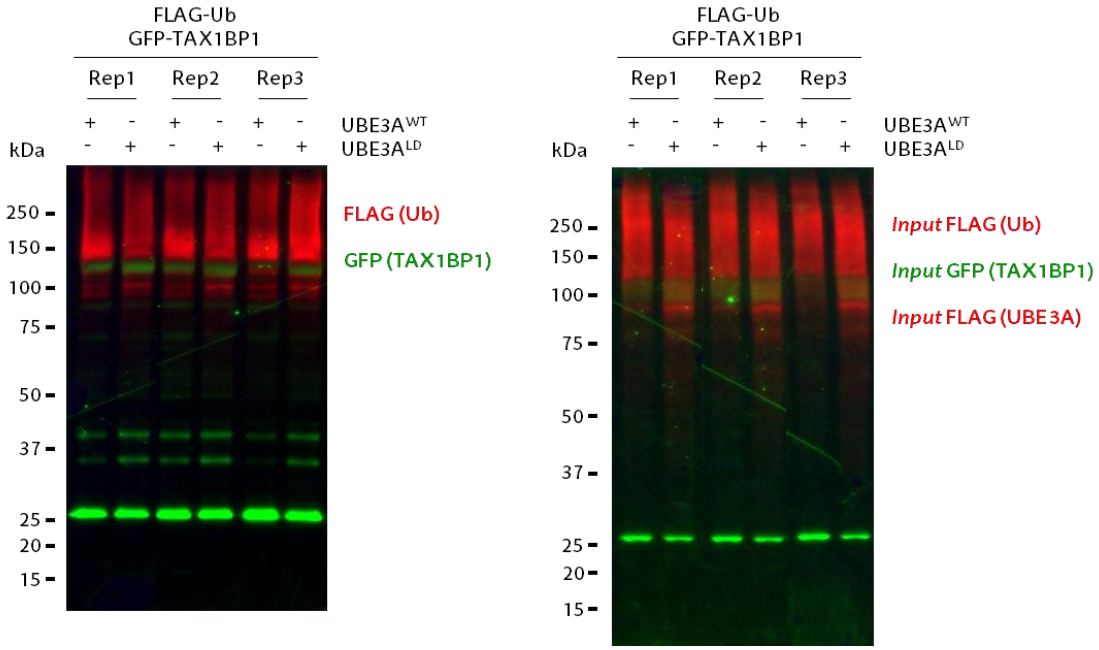

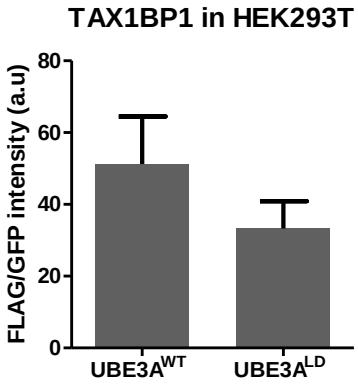

Figure 39. TAX1BP1 is not a UBE3A substrate in HEK293T cells. TAX1BP1 ubiquitination was analysed by Western blot in presence of wild-type UBE3A ($UBE3A^{WT}$) and ligase dead UBE3A ($UBE3A^{LD}$). Anti-FLAG antibody (red) was used to detect the ectopically expressed ubiquitin [FLAG-(Ub)] and the non-modified GFP-tagged TAX1BP1 was detected by anti-GFP antibody (green) [GFP-(TAX1BP1)]. UBE3A overexpression [Input FLAG-(UBE3A)] and equivalent transfections [Input FLAG-(Ub)] were confirmed in whole cell lysates using anti-FLAG antibody, while anti-GFP antibody was used to check TAX1BP1 transfection [Input GFP-(TAX1BP1)]. Quantification of Western blots was performed with ImageLab, by normalizing the FLAG intensities to the GFP signal. The analysis did not show a statistically significant difference on GFP-TAX1BP1 ubiquitination in different conditions [*t*-test, p-value > 0.05, (mean ± S.E.M., n = 3)]

1.7. Substrate expression and cellular localization

Interaction between UBE3A and its substrates requires both proteins to have the same localization. In order to demonstrate the possibility of UBE3A and validated substrates (DDI1, DDI2, PSMA5, MINDY2) interacting in the cell, we next aimed to describe their localization. Due to the low efficiency of UBE3A antibody, UBE3A could not be detected. Therefore, we considered human UBE3A to be expressed both in the nucleus and in the cytoplasm as previously reported (Sirois et al., 2020), in line also with the localization of our mice UBE3A protein used in previous studies (Ramirez et al., 2018).

As for human DDI1, little is known about its localization. Yeast Ddi1 has been described as a membrane associated protein that localizes either at the plasma membrane and the cytosol (Lustgarten and Gerst, 1999). Currently there is no antibody available and its expression in the majority of cell types seems to be very low (The Human Protein Atlas, FLJ36017). Human DDI2 is located in the nucleoplasm and the cytosol (Koizumi et al., 2016). PSMA5 have been mainly described to be located on the cytosol (The Human Protein Atlas, ZETA). Moreover, proteasomal 19S and 20S components, have been described to be enriched on a subtype of nuclear bodies named clastosomes, so PSMA5 could also

be detected in the nucleus (Lafarga et al., 2002). It has been described that DUBs are predominantly cytosolic or nuclear (Clague et al., 2019).

In order to monitor the localization without using antibodies and to achieve a detectable amount of substrate in the cell, we transfected HEK293T and SH-SY5Y cells with GFP-tagged substrates. Afterwards, we checked their localization by microscope (Figure 40). In both cell types, DDI1 appeared to localize in little clusters within the whole cell that could not be further characterized. In contrast, human DDI2 was widely expressed in the cell. PSMA5 was detected widely in the cytoplasm as well as in little cluster in the nucleus, probably in clastosomes as above described (Lafarga et al., 2002). Having confirmed that UBE3A could be located in the cytoplasm, these results confirm the possibility of UBE3A and validated substrates interacting in the cell.

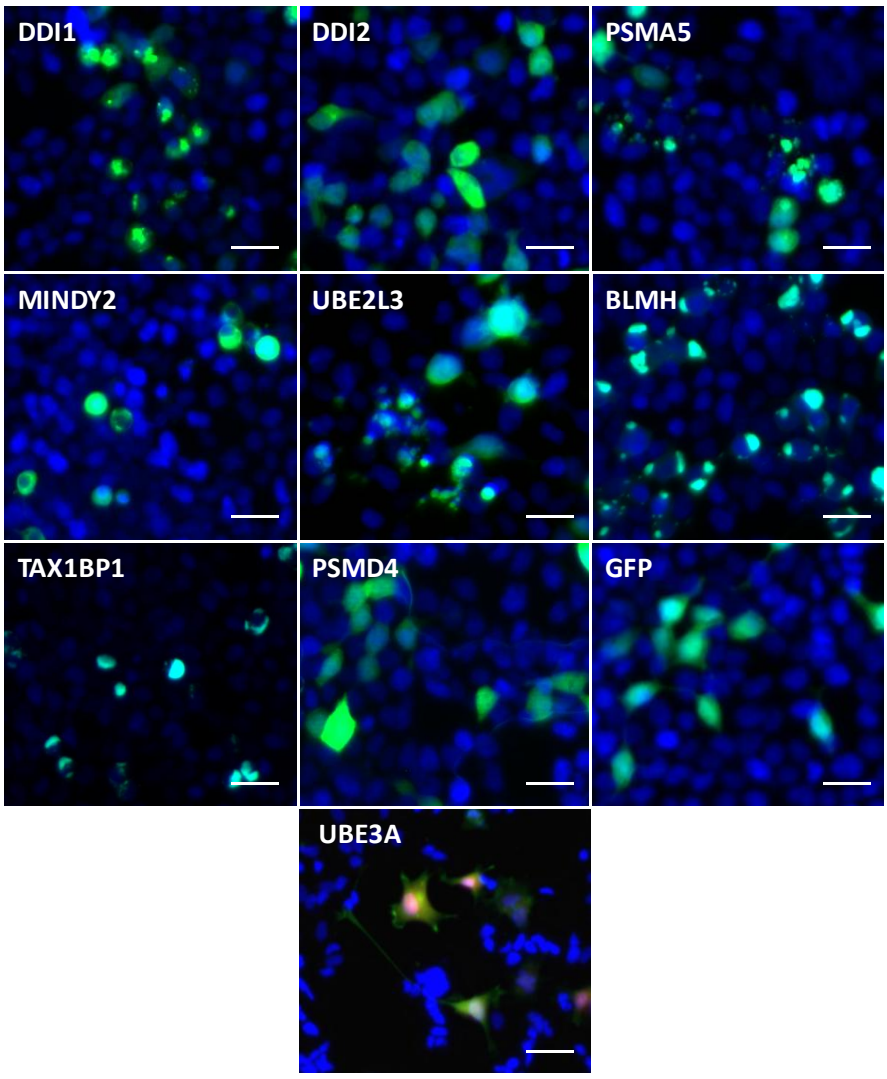

Figure 40. Cellular localization of UBE3A and its validated substrates. DDI1 localized in the cytoplasm forming small clusters that could not be further characterized. DDI2 was widely and uniformly expressed through the cell. PSMA5 was detected either widely through the cytoplasm and forming clusters in the nucleus. MINDY2 was detected only in the cytoplasm. GFP protein alone was used as a control, which showed that it could be expressed widely in the cell. UBE3A was mainly expressed in the cytoplasm, although it could also be observed in the nucleus. Scale bar: 50 μm. UBE3A image was modified from Ramirez et al., 2018.

1.8. Interaction between UBE3A and validated substrates

Identified substrates were further tested by performing a co-immunoprecipitation experiment to confirm if they could physically interact with human UBE3A. For that purpose, a mild GFP pull-down strategy was applied (Chromotek-GmbH). Cells were co-transfected with FLAG-UBE3A and a GFP-tagged substrate (MINDY-2, PSMA5, BMLH, DDI1, DDI2 or UBE2L3). Western blot analysis using anti-GFP and anti-FLAG antibodies confirmed equivalent UBE3A levels in whole cell extracts (Figure 41A). Previously validated substrates –MINDY-2, PSMA5, DDI1 and DDI2– pulled down UBE3A, while non validated substrates –BMLH and UBE2L3 –, did not show any stable interaction (Figure 41B). Moreover, cells co-transfected with GFP alone and pCDNA3.1 control plasmids excluded the possibility of non-specific interactions between UBE3A and GFP, as well as other unspecific binding (Figure 41C). This demonstrated that previosly validated substrates physically interact with UBE3A.

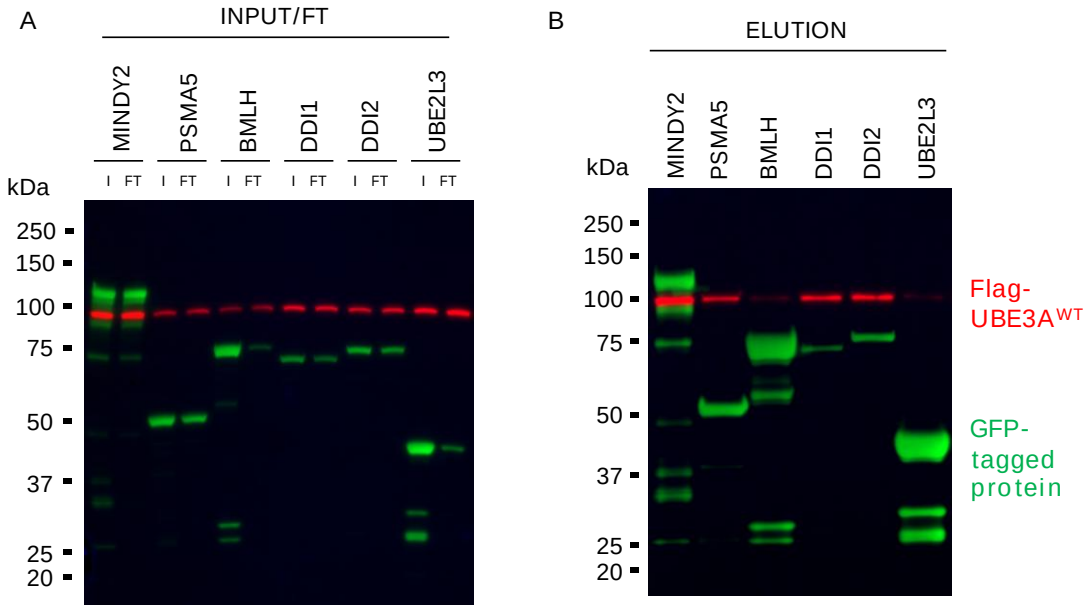

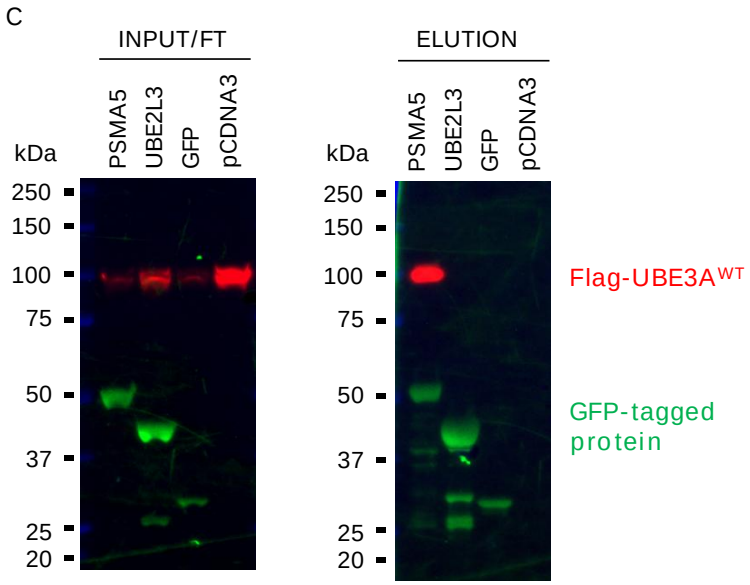

Figure 41. Co-immunoprecipitation of UBE3A and its putative substrates. FLAG-UBE3A and a GFP-tagged substrates (MINDY-2, PSMA5, BMLH, DDI1, DDI2 or UBE2L3) were co-transfected in HEK293T cells. A) Whole cells lysates were analysed by immunobloting with anti-FLAG (red) and anti-GFP (green) antibodies, to confirm equivalent transfection efficiencies (input, I). Non-bound fraction during co-ip was also immunoblotted (flowthrough, FT). B) Co-immunoprecipitation of UBE3A candidate substrates was performed using GFP beads, and eluted samples were immunobloted against anti-GFP, to check substrates, and anti-FLAG to check for UBE3A. MINDY2, PSMA5, DDI1 and DDI2 pulled-down UBE3A, in contrary to BMLH and UBE2L3. C) Cells were co-transfected with FLAG-UBE3A and UBE2L3, GFP or pcDNA3 as negative control, and PSMA5 as positive control. Left panel shows whole cell extracts, while rigth panel corresponds to eluted samples, both immunoblotted against anti-GFP (green) and anti-FLAG (red) antibodies. No UBE3A was pulled down in negative control samples (UBE2L3, GFP and pCDNA3).

2. Characterization of human DDI1 and DDI2 ubiquitination

Identification of neuronal UBE3A substrates is vital for the understanding of the molecular mechanisms by which Angelman syndrome is developed. In addition, the characterization of those substrates (ubiquitination sites, type of linkages…) could decipher their biological role, and could explain how the lack of their ubiquitination entails with the characteristic alterations of the disease, and in consequence, open new therapeutic strategies. In this context, the significance of UBE3A mediated substrate ubiquitination needs to be further analysed.

In previous experiments, human DDI1 and DDI2 (hDDI1, hDDI2) were validated as UBE3A substrates, and no ubiquitination-dependent degradation could be observed (*see 1.1. DDI1 and DDI2*). These results suggested that UBE3A

mediated ubiquitination could have a non-degradative role in hDDI1 and hDDI2. Based on the distintc structural and functional analyses, human DDI1 and DDI2 are likely to play a pivotal role as shuttlers or proteases in neurons. Consequently, misregulation of either DDI1 or DDI2 may affect the whole proteasomal recycling and cell homeostasis, which could in part explain the neurological problems associated to the Angelman syndrome (Morawe et al., 2011; Mótyán et al., 2020). It could be postulated that ubiquitination of residues in certain functional domains, and the formation of specific ubiquitin chain-types, may regulate the function of DDI1/DD2. Therefore, we aimed to identify the ubiquitination sites mediated by UBE3A in hDDI1/hDDI2, locate them within the protein sequence and identify the type of ubiquitin chains formed.

In order to identify ubiquitination sites on hDDI1 and hDDI2 that are modified by UBE3A, we followed an approach that optimized the GFP pull-down protocol (Ramirez et al., 2016) for mass spectrometry (MS)-based detection (Elu et al., 2020). We performed two parallel experiments –one for hDDI1 and one for hDDI2– and each experimental set was performed in triplicate. First, GFP-tagged hDDI1/hDDI2 was transfected on HEK293T cells together with human wild type or, as control, ligase dead UBE3A (hUBE3A^{WT} and hUBE3A^{LD}, respectively). No ubiquitin overexpression construct was used, in order to rely uniquely on the endogenous ubiquitin molecules. hDDI1 and hDDI2 were then isolated from both experimental conditions using the optimized GFP pull-down procedure (Elu et al., 2020). After GFP pull-down, 10% of the eluted samples were resolved by SDS–PAGE and silver stained to check the quality of the purified material (Figure 42A). The remaining 90% of the elutions were also resolved by SDS-PAGE but stained with Coomassie to detect the band corresponding to GFP-tagged hDDI1 (Figure 42B). To focus on the ubiquitinated fraction of hDDI1, we excised a slice of the gel directly above the 75 kDa band (Figure 42B), as we had earlier identified by WB (*see Figure 29*) where the ubiquitinated fraction of DDI1 runs on the gel. Aiming to separate mono- and poly-ubiquitinated hDDI1, this gel piece was further divided into two subsequent slices based on previous immunoblotting results and the observations by silver staining (Figure 42A): a tight band just above the non-modified hDDI1 should correspond to mono-ubiquitinated hDDI1-GFP (Figure 42B, black dotted box), whereas a bigger slice above this one, should contain the smear of poly-ubiquitinated hDDI1 observed by immunoblotting (Figure 42B, orange dotted box). As for hDDI2, silver staining showed similar purified material

within replicas (Figure 42A), and Coomassie staining showed a band at the proper size (~75 kDa) (Figure 42B). Little ubiquitinated hDDI2 was detected in either silver or coomasie staining, so in contrast to hDDI1, a single slice corresponding to the whole ubiquitinated fraction of hDDI2 was cut (Figure 42B, black dotted box).

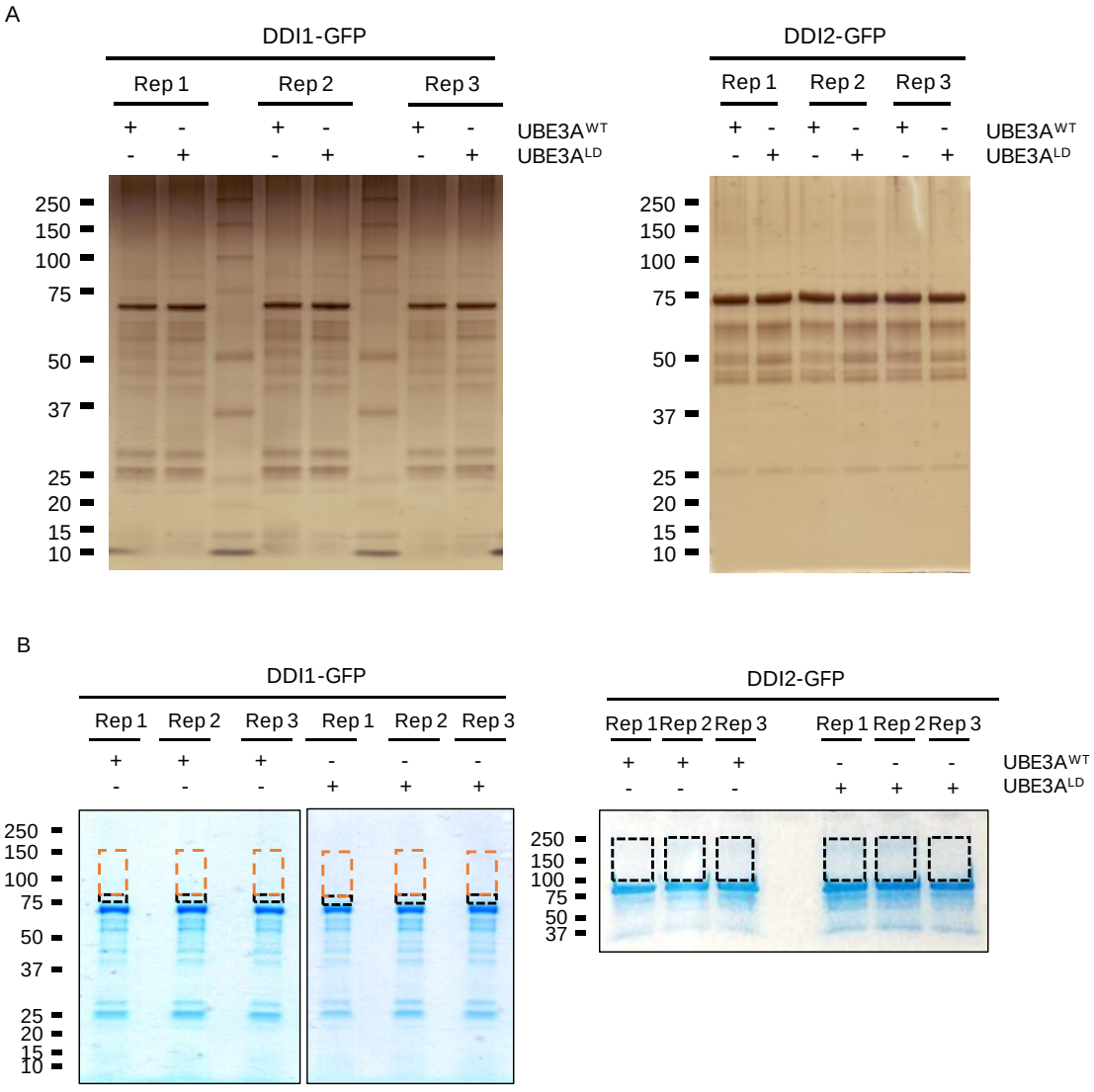

Figure 42. Silver and Coomassie staining of DDI1-GFP pull-down elutions. A) The efficiency of GFP pull-downs was evaluated by silver staining after resolving by SDS-PAGE the 10% of each neat elution. Gel bands visualized by SilverQuest kit showed similar amount of material among different samples (UBE3A^{WT} and UBE3A^{LD}) or among different replicas of each experimental set. Left panel shows results for hDDI1, and right panel for hDDI2. B) The neat elutions were resolved by SDS-PAGE, where clear bands could be observed around 75 kDa corresponding to DDI1-GFP or DDI2-GFP. Although ubiquitination bands could not be visualized, gel slices were cut based on the information obtained by silver stainings and previous inmunoblottings: for DDI1, a band above 75 kDa corresponding to mono-ubiquitinated DDI1 was cut (black dotted-box), as well as a second slice (orange dotted-box) corresponding to the poly-ubiquitination smear. For DDI2, a unique band comprising the whole ubiquitination smear was cut.

Gel slices obtained from each experimental set were subjected to trypsin digestion, resulting peptides were extracted from the gel, and finally, tryptic peptides were analyzed by LC-MS/MS (Figure 43).

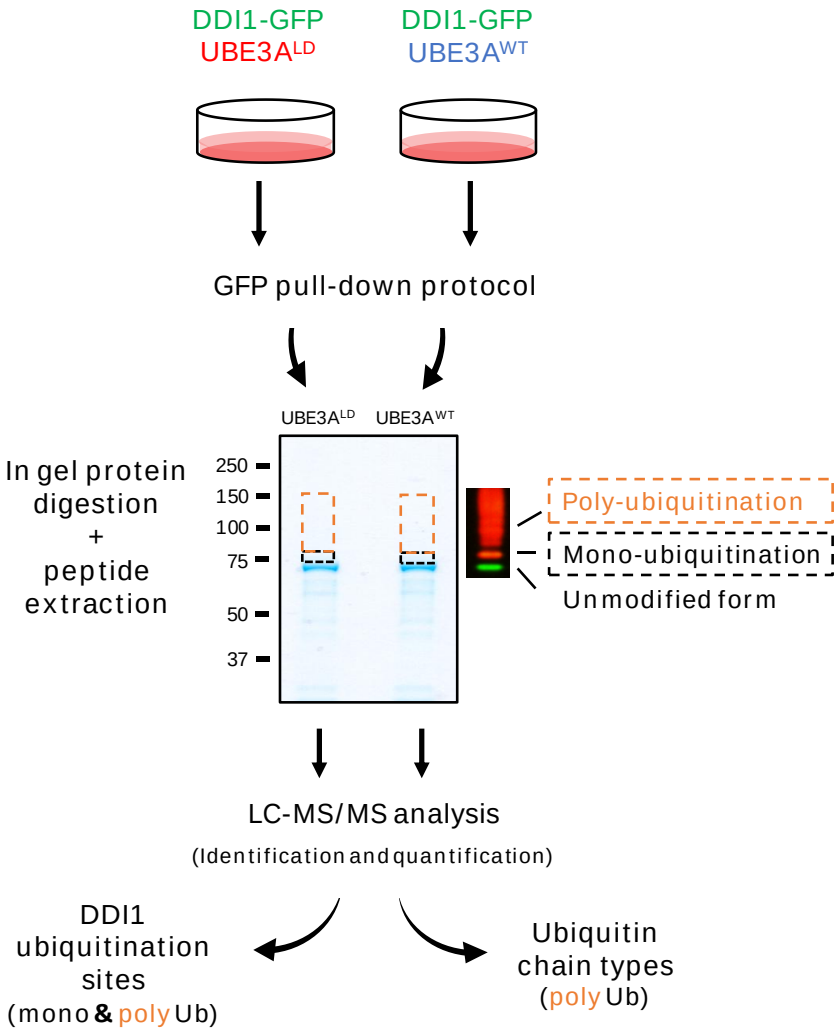

Figure 43. Schematic diagram of the MS-based procedure used to study ubiquitination sites and ubiquitin chain-types. HEK293T cells were co-transfected with hDDI1-GFP or hDDI2-GFP and wild type UBE3A (hUBE3A^{WT}) or ligase dead UBE3A (hUBE3A^{LD}). Unmodified DDI1-GFP/DDI2-GFP as well as their ubiquitinated forms were isolated by GFP pull-down, and separated by SDS–PAGE. The gel slices corresponding to ubiquitinated DDI1-GFP were excised and divided into two; a lower band corresponding for mono-ubiquitinated DDI1-GFP (black), and a band above it corresponding to poly-ubiquitinated DDI1-GFP (orange). In the case of DDI2-GFP, a single slice was cut for the whole ubiquitination smear. Gel slices were digested with trypsin, and resulting peptides were extracted from the gel to further identify and quantify them by LC-MS/MS. Bands were analyzed to infer ubiquitination sites and to detect the nature of the ubiquitin chain types formed on DDI1 and DDI2.

To infer hDDI1 and hDDI2 ubiquitination sites and ubiquitin chain-types, MS-derived raw files were analyzed using MaxQuant software. Based both on

MS/MS counts and LFQ intensity values, GFP-tagged hDDI1 and hDDI2, were, as expected, the most abundant proteins detected by mass spectrometry (Figure 44, Supplementary Table 1). The second most abundant protein in both experimental sets was ubiquitin (Figure 44), despite the lack of ectopic ubiquitin expression.

Regarding DDI1 samples, while DDI1 levels remained practically the same independently of UBE3A activity, Ub levels were significantly increased upon UBE3A^{WT}overexpression (Figure 44A). Similar results were obtained for hDDI2; while equivalent hDDI2 levels were detected in both conditions (UBE3A^{WT} and UBE3A^{LD}), a clear but statistically no significant increase was observed in Ub levels in presence of UBE3A^{WT} (Figure 44B).

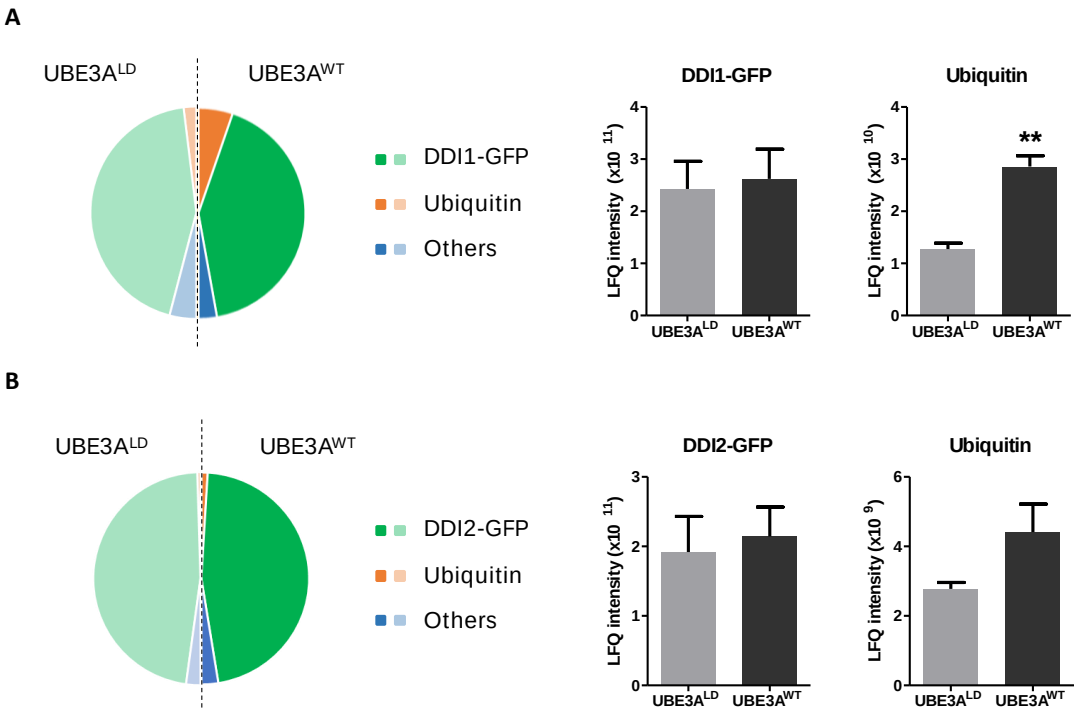

Figure 44. Identification of ubiquitinated proteins. A) Relative LFQ intensity of all the proteins detected by MS demonstrate that DDI1-GFP is the most abundant protein (green) in the GFP pull-down samples, followed by ubiquitin (orange). 287 more proteins (blue) were identified with marginal intensities. Comparison of the intensities recorded for the two most abundant proteins in UBE3A^{WT} and UBE3A^{LD} reveal that whereas the levels of DDI1 detected are similar in both conditions, more ubiquitin was detected in the presence of UBE3A^{WT} overexpression [t-test, **p-value < 0.05, (mean ± S.E.M., n = 3)]. B) Similarly, LFQ intensity of all the proteins purified in the DDI2-GFP pull-down sample showed that DDI2-GFP is the most abundant protein (green). In addition, intensities of DDI2-GFP in both conditions remained similar, while ubiquitin showed a slight statistically no significant increase upon UBE3A^{WT} overexpression [t-test, p-value > 0.05, (mean ± S.E.M., n = 3)].

2.1.1. Ubiquitination sites on hDDI1

Data analysis of LC-MS/MS experiment showed many peptides identified that covered 76% of the hDDI1-GFP sequence (Figure 45, Supplementary Table 1); peptides for 69% of the hDDI1 sequence and 88% of the GFP sequence were detected. Analysis of the non-detected region sequence of hDDI1 revealed no lysine or arginine residues, resulting in long peptides that are harder to identify by mass spectrometry.

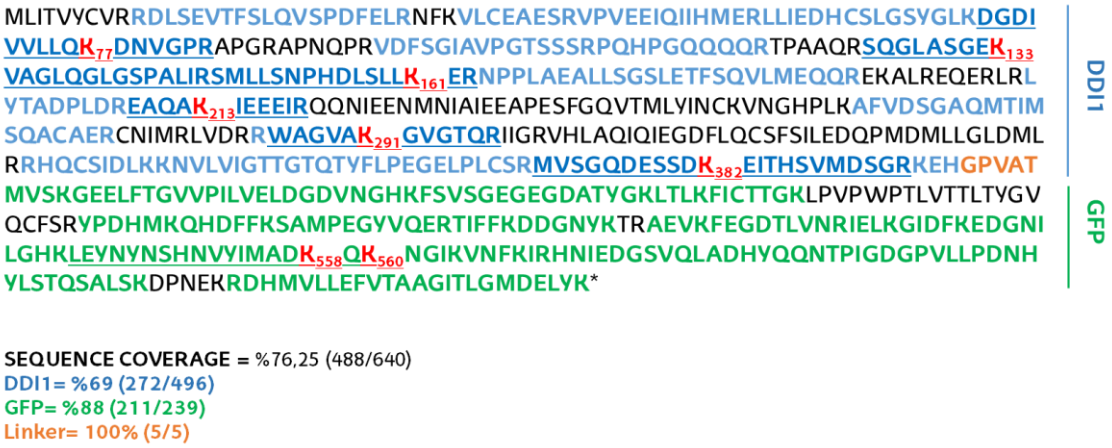

Figure 45. Sequence coverage of hDDI1-GFP sequence. Sequence coverage for hDDI1-GFP is shown, where peptides identified for hDDI1 are highlighted in blue, and peptides identified for GFP in green. Underlined peptides correspond to ubiquitinated or diGly-modified peptides. In each case, the exact lysine that is modified is highlighted in red, and its position within the sequence is indicated. At the bottom, the percentage of sequence coverage obtained for hDDI1-GFP, hDDI1 and GFP are shown.

More interestingly, six diGly-modified peptides were identified across the whole sequence of hDDI1 and one on the C-terminally fused GFP protein. A representative annotated MS/MS spectra obtained in the mass spectrometry analysis shows the sequence of one of the hDDI1 diGly peptides (Figure 46).

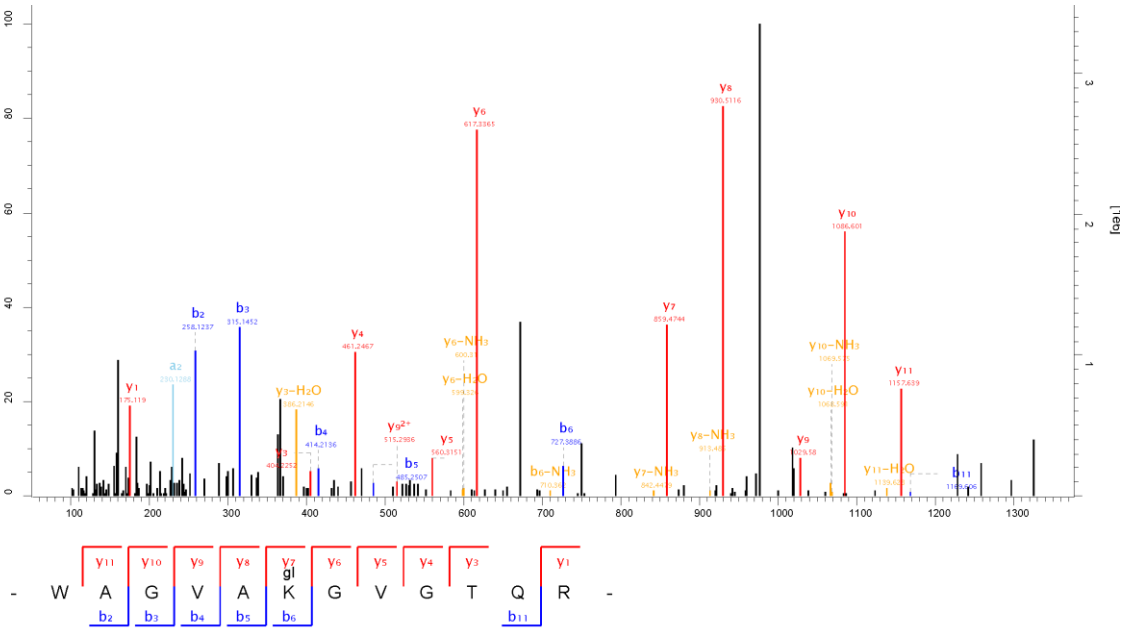

Figure 46. Representative annotated spectra for K133 hDDI1 diGly modified peptide. Anotated spectra for the ubiquitinated WAGVAKGVGTQR peptide identified in hDDI1.

Ubiquitin was conjugated to the following residues on hDDI1: K77, which localizes in the N-terminal ubiquitin-like (UBL) domain; K133, K161 and K213 within the helical domain (HDD); K291, that resides in the aspartyl protease-like RVP domain; and K382, on the C-terminal end of the protein (Figure 47, Supplementary Table 2). It is remarkable that besides K291 ubiquitination, whose homolog lysine had been previously reported to be ubiquitinated on experiments performed in rat brain (Na et al., 2012), the remaining five lysines detected in the present study (K77, K133, K161, K213, and K382) are novel ubiquitination sites of hDDI1.

Aiming to evaluate the effect of UBE3A on hDDI1 ubiquitination, we compared the intensity of the diGly peptides between UBE3A^{WT} and UBE3A^{LD} overexpressing cells. The intensities of the hDDI1 diGly peptides bearing ubiquitination sites K213-, K291-, and K382- were similar in both experimental conditions, indicating that UBE3A is not involved in modifying such residues (Figure 47). On the contrary, the intensity of diGly peptides containing ubiquitinated K133 and K161 was induced 5- and 2- fold, respectively, in the UBE3A^{WT} overexpressing condition (Figure 47). Similarly, ubiquitination on K77

also appeared to be enhanced upon UBE3A^{WT} overexpression, although this increase did not appear to be statistically significant.

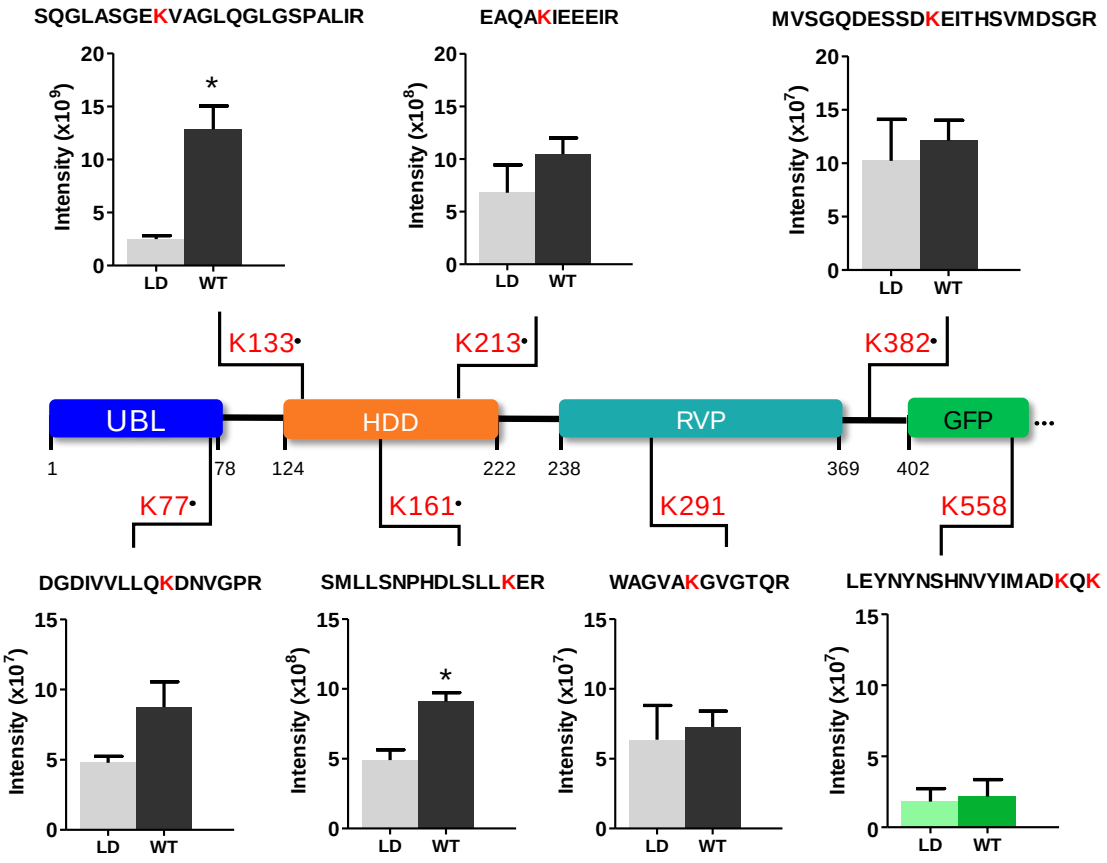

Figure 47. UBE3A ubiquitinates hDDI1 on K133. Schematic illustration of DDI1-GFP sequence, its domains (blue, UBL, ubiquitin-like domain; orange, HDD, helical-double domain; red, RVP, retroviral protease domain; green, GFP, GFP-tag of DDI1 protein) and the localization of the ubiquitination sites detected by mass spectrometry. Additionally, the diGly-modified peptides identified, within the ubiquitinated lysine marked in red, and the intensity values measured in each condition (WT, UBE3A^{WT} and LD, UBE3A^{LD}) are also indicated. "*" indicates that the ubiquitination site is not reported in PhosphoSitePlus database. DiGly peptides encompassing K133 and K161 were statistically more abundant upon UBE3A^{WT} overexpression [t-test, *p-value < 0.05, (mean±S.E.M., n = 3)].

Overall, the data suggested that UBE3A may be involved in the ubiquitination of three (K77, K133, and K161) out of the six ubiquitination sites detected on hDDI1. To confirm that indeed UBE3A is responsible for ubiquitinating hDDI1 on those residues, three hDDI1 point mutations as well as double and triple mutants were generated, each with one or multiple of the above-mentioned lysines replaced by arginines. Following the same GFP pull-down procedure used for UBE3A substrate validations (*see Figure 27*), we isolated the hDDI1-GFP mutants and monitored their ubiquitination by immunoblotting

(Figure 48). We normalized ubiquitin intensities to their respective GFP levels. Afterwards, each experimental set was normalized to its control sample overexpressing hDDI1^{WT} together with UBE3A^{LD}. As shown in Figure 48, ubiquitination of hDDI1 remains virtually unaffected in K77R, K161R and K77R+K161R mutants. By contrast, UBE3A-dependent hDDI1 ubiquitination was significantly reduced in all the mutants containing K133R, but more dramatically in the K133R+K161R double mutant (just one control UBE3A^{LD} sample of the first experimental set is plotted in the graph, Figure 48B).

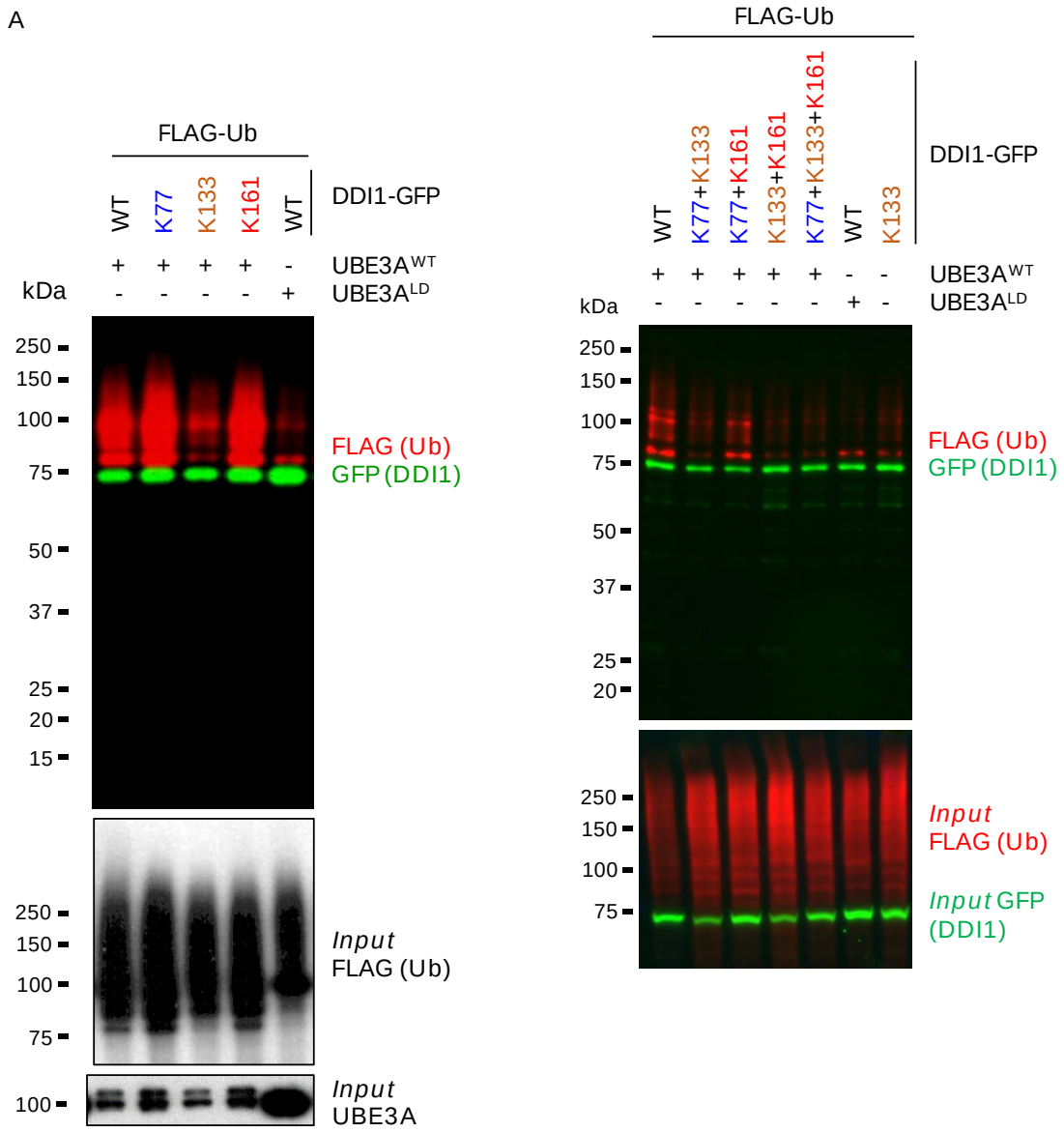

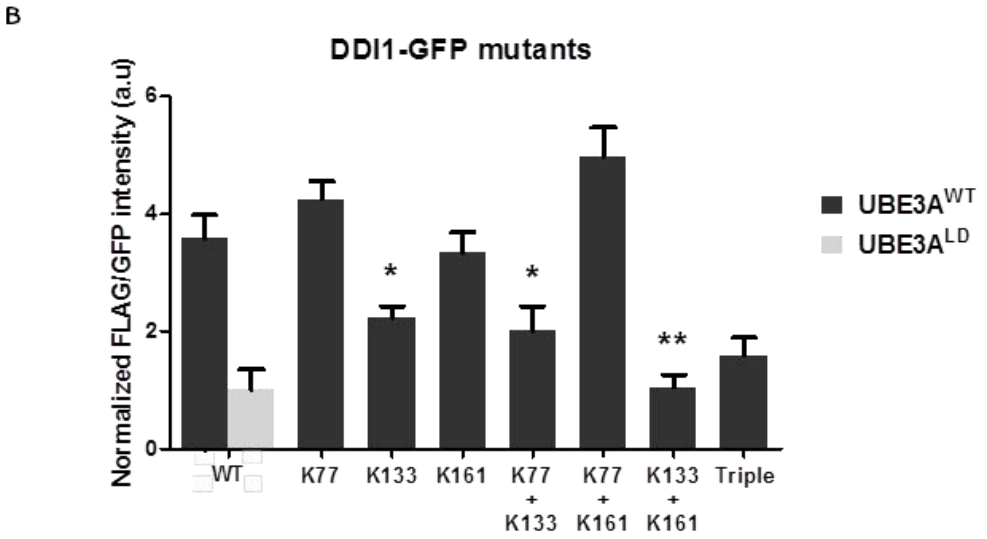

Figure 48. UBE3A-dependent ubiquitination of hDDI1-GFP mutants. A) Single (K77R, K133R, or K161R), double (K77R+K133R, K133R+K161R, K77R+K161R) and triple (K77R+K133R+K161R) DDI1-GFP mutants were monitored by Western blot after isolating by GFP-pull-down. Anti-FLAG antibody (red) was used to detect ubiquitination pattern of DDI1, while anti-GFP antibody (green) detected the unmodified version of DDI1-GFP. In the whole cell extract UBE3A overexpression was corroborated by anti-UBE3A antibody (Input UBE3A), and FLAG-ubiquitin and GFP-DDI1 were measured as loading controls (Input FLAG (Ub) and Input GFP (DDI1)). B) Quantification and statistical analysis of the ubiquitination was performed with ImageLab after normalizing FLAG intensities to GFP levels. Mutation on DDI1 lysine 133 significantly [t-test, *p-value < 0.05, **p-value < 0.01, (mean±S.E.M., n = 3)] abolishes its ubiquitination by UBE3A^{WT}.

These results indicate that UBE3A is responsible for ubiquitinating hDDI1 mainly on K133 and that the presence of this lysine 133 is necessary for UBE3A-mediated ubiquitination of hDDI1.

2.1.2. Ubiquitin chain-types on hDDI1

Next, we aimed to study the types of ubiquitin linkage formed on poly-ubiquitinated hDDI1. For that purpose, we focused on the diGly peptides corresponding to ubiquitin detected the in sample containing poly-ubiquitinated hDDI1-GFP (Figure 42B, Supplementary Table 1).

MaxQuant analysis of the poly-ubiquitinated hDDI1 slice confidently detected four ubiquitination sites within ubiquitin: K11, K29, K48, and K63. Ubiquitin as well as ubiquitin diGly peptide intensity ratios between UBE3A^{WT} and

UBE3A^{LD} were calculated and plotted (Figure 49). The levels of K63 chains remained unaffected upon overexpression of UBE3A^{WT}. K29 ubiquitin linkages were not detected in the UBE3A^{LD} sample, so appeared to be increased in the presence of UBE3A^{WT}, in line with some earlier reports for UBE3A and other HECT E3 ligases (Chastagner et al., 2006; Xu et al., 2018). More convincingly, a clear increase of approximately two fold could be observed for K48 and K11 chains in UBE3A^{WT} over-expressing cells with respect to the control sample (Figure 49). It is worth noting that the intensity fold change measured for K48 and K11 diGly peptides were similar to the global foldchange observed for ubiquitin itself. Based on this data, and in partial agreement with earlier reports (Kim and Huibregtse, 2009), it could be concluded that UBE3A^{WT} overexpression indeed induces both K48 and K11 ubiquitin chains on hDDI1. However, as indicated earlier on (Figure 29-30) this does not lead to degradation of DDI1.

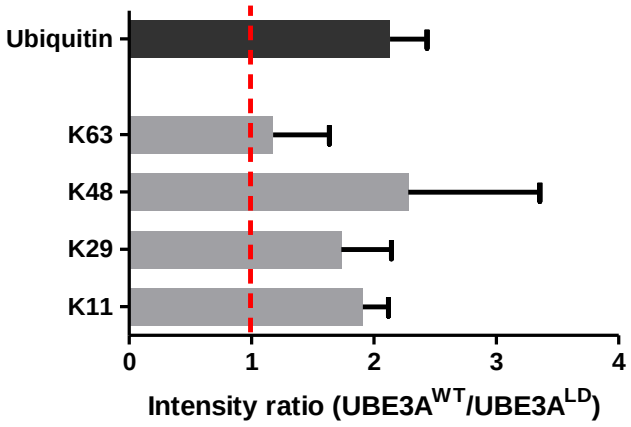

Figure 49. UBE3A forms K48 ubiquitin chains on hDDI1. Four ubiquitination sites on ubiquitin were identified and quantified by mass spectrometry. The intensity ratios for each ubiquitin chain type are given as the ratio of the UBE3A^{WT} overexpressing condition over the intensity recorded for the UBE3A^{LD} sample. The intensity ratio for ubiquitin is also indicated [Anova test, p-value > 0.05, (mean ± S.E.M., n = 3)].

2.1.3. Ubiquitination sites on hDDI2

Similar to hDDI1, LC-MS/MS analysis of hDDI2-GFP enriched samples resulted in the detection of many peptides that covered 70% of the hDDI2-GFP sequence. As shown in Figure 50, a sequence coverage of 65% and 76% was obtained for hDDI2 and GFP, respectively.

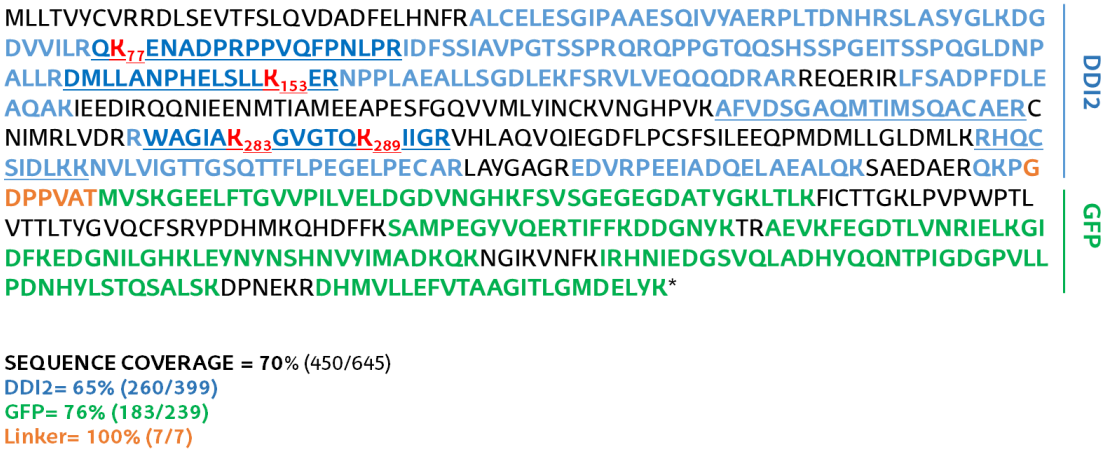

SEQUENCE COVERAGE = 70% (450/645)
DDI2= 65% (260/399)
GFP= 76% (183/239)
Linker= 100% (7/7)

Figure 50. Sequence coverage for hDDI2. Sequence coverage for hDDI2-GFP is shown, where peptides identified for hDDI2 are highlighted in blue, and peptides identified for GFP in green. Underlined peptides correspond to ubiquitinated or diGly-modified peptides. In each case, the exact lysine that is modified is highlighted in red, and its position within the sequence is indicated. At the bottom, the percentage of sequence coverage obtained for hDDI2-GFP, hDDI2 and GFP are shown.

LC-MS/MS analysis resulted in the identification of four diGly-modified peptides across the whole sequence of hDDI2 (Figure 51, Supplementary Table 2) More precisely, ubiquitin was conjugated to residues distributed within the whole hDDI2 sequence: K77, which localizes in the N-terminal ubiquitin-like (UBL) domain; K153 within the helical domain (HDD); and K283 and K289, that reside in the aspartyl protease-like RVP domain (Figure 52). In contrast to hDDI1, no novel ubiquitination sites were detected on hDDI2, since they all had been previously reported (Wagner, 2011).

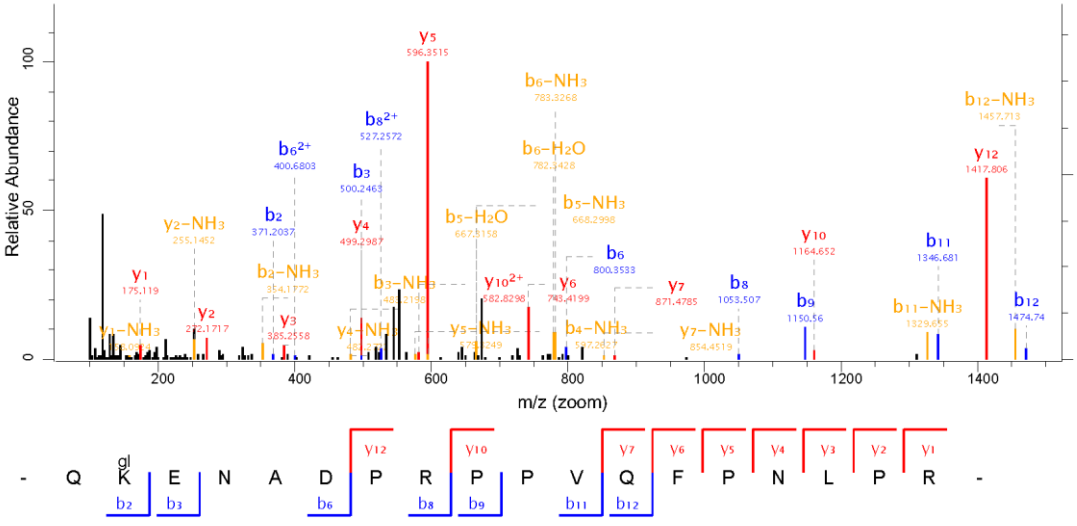

Figure 51. Representative annotated spectra for K77 hDDI2 diGly modified peptide.. Anotated spectra for the ubiquitinated QKENADPRPPVQFPNLPR peptide identified in hDDI2.

To evaluate the effect of UBE3A on hDDI2 ubiquitination, we compared the intensity of the diGly peptides between UBE3A^{WT} and UBE3A^{LD} overexpressing cells. The intensities of hDDI2 ubiquitination sites K283- and K289- containing diGly peptides were similar in both experimental conditions, indicating that UBE3A is not involved in modifying such resides (Figure 52). On the contrary, the intensity of K77-bearing diGly peptide was induced 3-fold in the UBE3A^{WT} overexpressing condition (Figure 52), while total hDDI1 levels remained constant (Figure 44B). Similarly, ubiquitination on lysine 153 also appeared to be enhanced upon UBE3A^{WT} overexpression, although this increase was not statistically significant. Overall, it could be postulated that UBE3A is involved in the ubiquitination of one –K77–, out of the four ubiquitination sites detected on hDDI2.

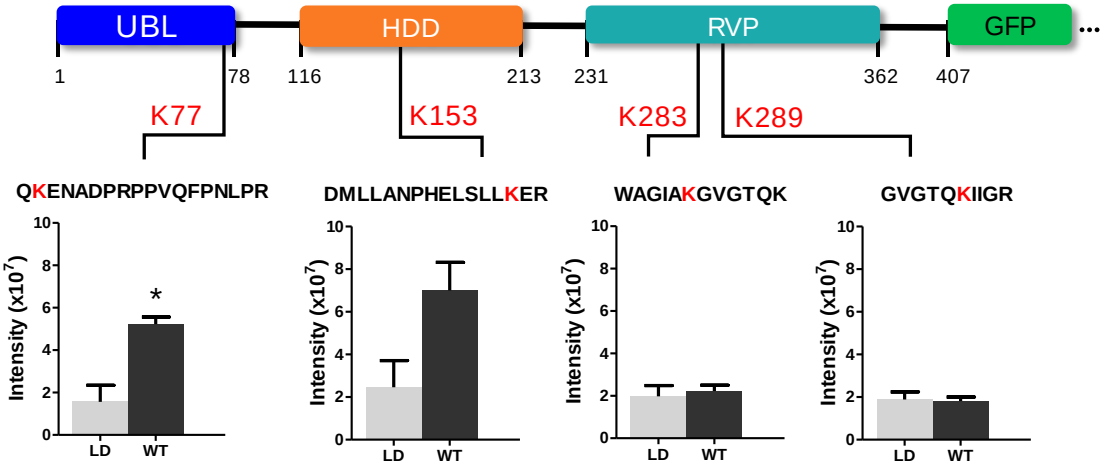

Figure 52. UBE3A ubiquitinates hDDI2 on K77. Schematic illustration of hDDI2-GFP sequence, its domains (blue, UBL, ubiquitin-like domain; orange, HDD, helical-double domain; red, RVP, retroviral protease domain; green, GFP, GFP-tag of DDI1 protein) and the localization of the ubiquitination sites detected by mass spectrometry. Additionally, the diGly-modified peptides identified, within the ubiquitinated lysine marked in red, and the intensity values measured in each condition (WT, UBE3A^{WT} and LD, UBE3A^{LD}) are also indicated. DiGly peptide encompassing K77 was statistically more abundant upon UBE3A^{WT} overexpression [t-test, *p-value < 0.05, (mean±S.E.M., n = 3)].

To confirm that UBE3A is ubiquitinating hDDI2 mostly in residues K77 and K153, we generated three hDDI2 mutants, replacing the above mentioned lysines by arginines: K77R, K153R and K283R. Following the GFP pull-down strategy, we isolated wild-type and mutants hDDI2-GFP, and monitored their ubiquitination by immunoblotting upon UBE3A wild-type overexpression (Figure 53). We normalized ubiquitin intensities to their respective GFP levels. As shown in Figure

53, ubiquitination of hDDI2 is not abolished in none of the mutants. On the contrary, overall ubiquitination of hDDI2 upon UBE3A^{WT} overexpression is higher in mutants compared to wild-type hDDI2, although not in a statistically significant manner.

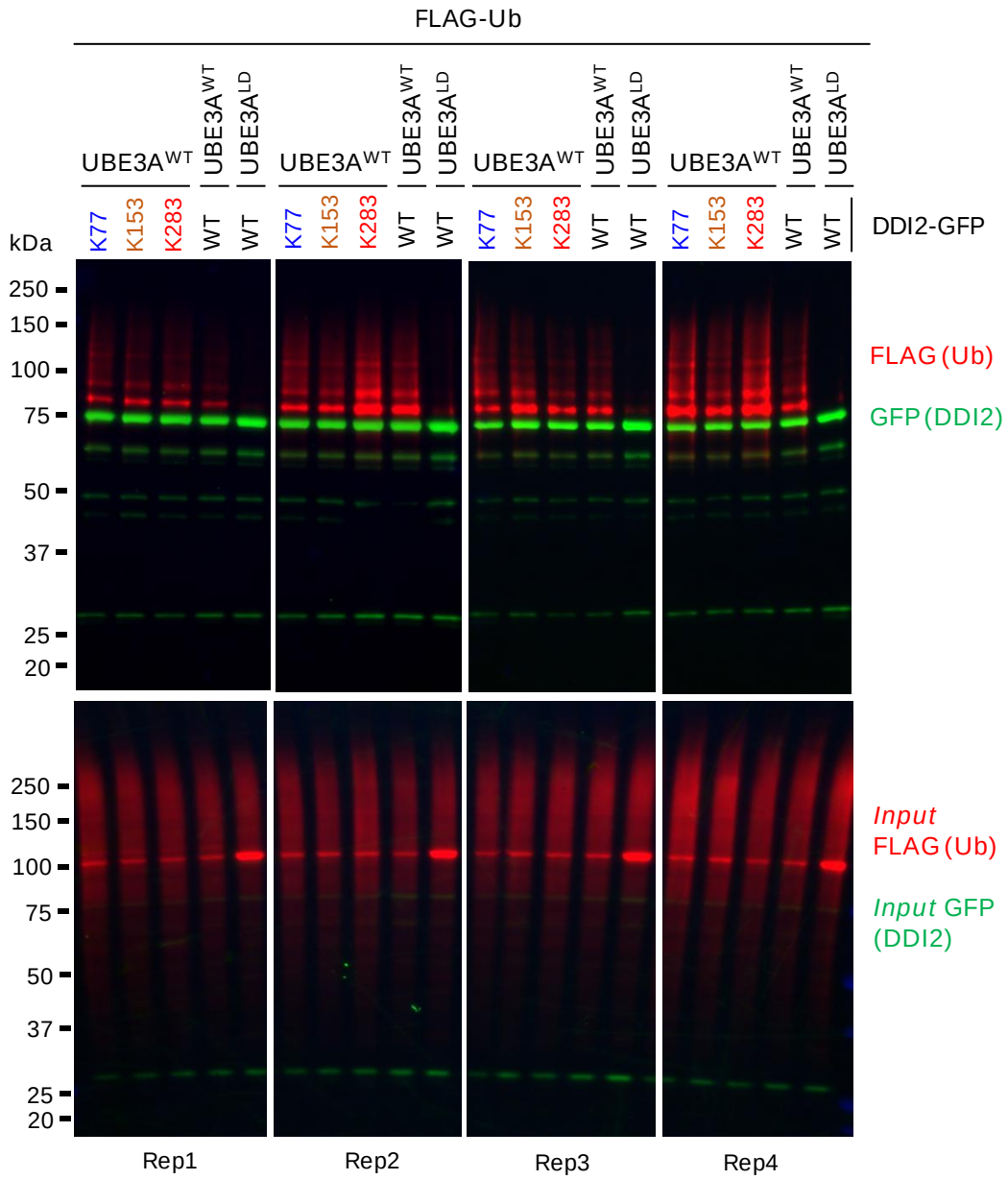

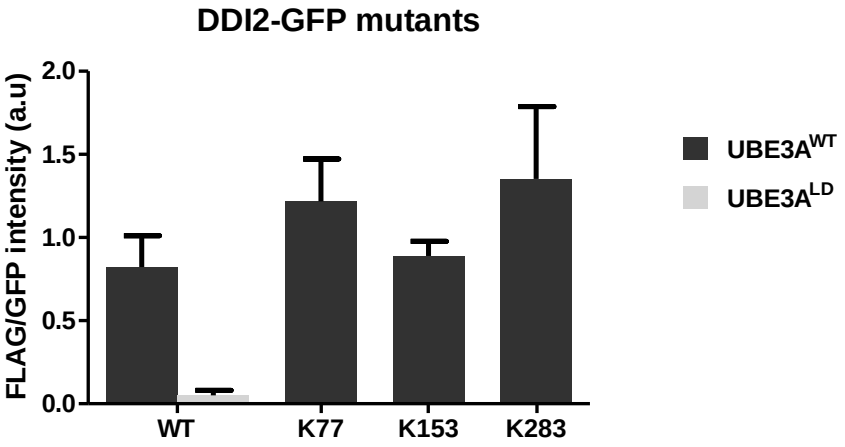

Figure 53. UBE3A-dependent ubiquitination of hDDI2-GFP mutants. Single (K77R, K153R, or K283R) DDI2-GFP mutants were monitored by Western blot after isolating by GFP-pull-down. Anti-FLAG antibody (red) was used to detect ubiquitination pattern of DDI2, while anti-GFP antibody (green) detected the unmodified version of DDI2-GFP. In the whole cell extract UBE3A overexpression was corroborated by anti-UBE3A antibody (Input UBE3A), and FLAG-ubiquitin and GFP-DDI2 were measured as loading controls [Input FLAG (Ub) and Input GFP (DDI2)]. B) Quantification and statistical analysis of the ubiquitination was performed with ImageLab after normalizing FLAG intensities to GFP levels. Mutation on DDI2 lysine K153 decreased ubiquitination by UBE3A^{WT}, although the change was not statistically significant [t-test, p-value > 0.05 (mean±S.E.M., n = 3)].

2.1.4. Ubiquitin chain-types on hDDI2

We next focused on types of ubiquitin linkages formed on hDDI2 by analysing the diGly peptides corresponding to ubiquitin detected by LC-MS/MS (Figure 54, Supplementary Table 2). Ubiquitin K48 was the only chain type detected in hDD2-GFP enriched samples. In addition, quantitative data revealed that K48-containing diGly peptide was two times more abundant in UBE3A^{WT} over-expressing cells with respect to the control sample. The same intensity fold change was measured for ubiquitin itself. Therefore, based on that data, and in agreement with earlier reports (Kim and Huibregtse, 2009), it could be concluded that UBE3A^{WT} overexpression induces K48 ubiquitin chains on hDDI2. However, as with DDI1, no degradation was detected (Figure 31) as being induced by this ubiquitination.

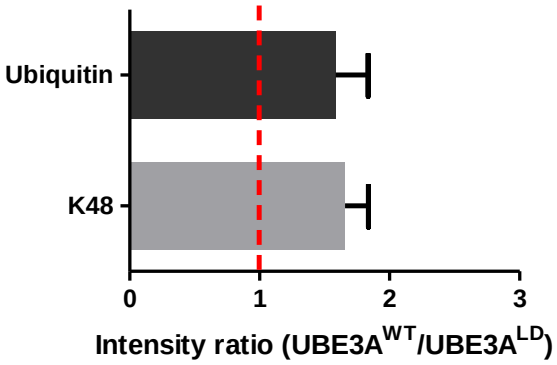

Figure 54. UBE3A forms K48 chains in hDDI2. A single ubiquitin chain-type, K48, was confidently identified and quantified by mass spectrometry. The intensity ratio is given as the ratio of the $UBE3A^{WT}$ overexpressing condition over the intensity recorded for the $UBE3A^{LD}$ sample [t-test, p-value > 0.05, (mean ± S.E.M., n = 3)].

2.1.5. hDDI1 vs hDDI2

Structural and functional analysis of different DDI1 and DDI2 homologues showed domains that are conserved in many species (Sivá et al., 2016). Although different functions have been described for each of the homologues, based on structural similarities, we hypothesized that UBE3A could regulate hDDI1 and hDDI2 through residues located in similar positions within the protein sequence.

In order to compare the location of UBE3A mediated ubiquitination sites on hDDI1 and hDDI2, we first aligned them as previously reported by Siva and colleagues (Sivá et al., 2016) (Figure 55). Alignment showed a sequence similarity of 74% between hDDI1 and hDDI2. More interestingly, from all the lysines detected as ubiquitinated in our experiments three seemed to be conserved in hDDI1 and hDDI2: K77 (same position in both), K161(hDDI1)/K153(hDDI2) and K291(hDDI1)/K283(hDDI2).

Figure 55. Sequence alignment of human DDI1 and DDI2 sequences. Positions of the UBL domain (blue), HDD (orange), RVP domain (green) and catalytic residues (red) are indicated. Modified from Siva et al., 2016.

We previously described that UBE3A regulates hDDI1 ubiquitination through K133, and slightly through K77. However, since K133 is not conserved in hDDI2, we hypothesized that UBE3A mediated regulation of hDDI1 through K133 is transferred to K77 in hDDI2, due to a compensation mechanism.

In summary, in this first Chapter we were able to validate DDI1, DDI2, PSMA5 and MINDY2 proteins as UBE3A substrates in human HEK293T and SH-SY5Y cell lines. We further characterized DDI1 and DDI2 by identifying their ubiquitination sites mediated by UBE3A and the type of ubiquitin-chains formed. Altogether, we successfully stablished an strategy for UBE3A substrate validation and characterization that could be used in future studies with novel UBE3A candidate substrates. Importantly, we have validated that UBE3A ubiquitination of its substrates is preferentially via K48 chains. However, despite that UBE3A mediated ubiquitination might at times result in a reduction of protein levels for its substrates, as observed for MINDY2, and as detected for Rpn10/PSMD4 (Lee et al., 2014; and unpublished data), K48 chains do not always lead to this, as observed for example for hDDI1 and hDDI2.

Chapter 2

Identification and validation of UBE3A counteracting DUBs

Post-translational modifications (PTMs) of proteins are tightly controlled biological processes that occur in response to physiological cues. One such dynamic modulation is ubiquitination. The ubiquitination state of any given protein is reversible and it is determined by the balance between the conjugating action of E3 ubiquitin ligases and their counteracting deubiquitinating (DUB) enzymes. Ubiquitination is crucial for a plethora of physiological processes including cell survival (Chen and Qiu, 2013), differentiation (Suresh et al., 2016) and innate and adaptive immunity (Etzioni et al., 2017), so the regulation of the enzymes modulating protein ubiquitination is crucial for maintaining the appropriate balance of protein modification required for cellular homeostasis. In fact, mutations and dysregulation on ubiquitination-proteasome system elements (E1, E2, E3, DUBs, proteasome) and ubiquitination substrates are implicated in a number of diseases, including cancer (Mansour, 2018; Ruprecht and Lemeer, 2014), Fanconi anemia (van Twest et al., 2017), autoimmune diseases (Moser and Oliver, 2019), neurodegenerative diseases like Alzheimer (Harris et al., 2020) or Parkinson (Pickrell and Youle, 2015), and rare neurological diseases (Osinalde et al., 2018).

Emerging therapeutic strategies are focused on the design of drugs that modify the biological action of enzymes modulating PTMs aiming to restore appropriate cellular PTM levels. In the past two decades, kinase inhibitors have been successfully used to treat cancer and other diseases (Bhullar et al., 2018). At present, great efforts are being made to develop similar strategies to treat diseases caused by altered protein ubiquitination. Due to the dramatic advances in our understanding of DUB functions, mechanisms of action, regulation and disease linkages, together with improvements in DUB biochemical assays and screening technologies, DUBs are emerging as druggable targets, increasing the number of small-molecule DUB inhibitors developed (Harrigan et al., 2018). Attempts have been done to inhibit DUBs in cancer therapy (D'Arcy et al., 2015), aiming to increase ubiquitination, and subsequent degradation of substrates (Pinto-Fernandez and Kessler, 2016). Many DUB inhibitors are now under development for oncology, neurodegeneration and inflammation (Harrigan et al., 2018).

In this context, we propose that modulating protein ubiquitination may represent a therapeutic approach for Angelman syndrome patients that lack

UBE3A activity in the brain. More precisely, inhibition of the DUB counteracting the action of the E3 ligase UBE3A may help restoring non-pathological ubiquitination levels of UBE3A substrates in Angelman syndrome patients.

1. Screening for human UBE3A counteracting DUBs

We previously demonstrated that UBE3A ubiquitinates hDDI1, so we next aimed to discover the DUB capable of deubiquitinating hDDI1. We screened an RNAi library (kindly provided by Dr. J.A. Rodriguez) of multiple human DUBs in order to identify the DUB whose silencing would enhance hDDI1 ubiquitination, and in consequence, act as UBE3A counteracting DUB.

For that purpose, we silenced individually 41 different DUBs in HEK293T cells. More precisely, we silenced 36 members of the USP family, as well as 3 and 2 members of the UCH and OTU families, respectively (Figure 56). After silencing, cells were co-transfected with hDDI1-GFP and FLAG-Ubiquitin. Finally, hDDI1 ubiquitination was monitored using the previously described workflow: GFP-tagged hDDI1 was first isolated by GFP pull-down (s*ee Introduction, Figure 21*), and then ubiquitin and hDDI1-GFP were detected by immunoblot with an anti-FLAG (red signal) and anti-GFP antibodies (green signal), respectively (Figure 56A). Changes in hDDI1 ubiquitination were measured by ImageJ, normalizing the FLAG-Ub signal of each sample against its corresponding GFP signal. Additionally, aiming to compare the results obtained in the several 6-well plate based experiments, we normalized FLAG-Ub/GFP signal obtained for each DUB to the average of the 3 lowest ratios on each dataset of 6 silencing experiments (USPs 1-9; USPs 11-16; USPs 18-24; USPs 25-36; USPs 37-51 and UCHL1-BAP1) (Figure 56B).

As shown in Figure 56B, silencing of most DUBs did not substantially modify the ubiquitination state of hDDI1 (normalized FLAG/GFP intensity between 0.5–2). Interestingly, upon silencing of UCHL-5, OTUD3 and 8 USP family members (2, 3, 7, 8, 9X, 30, 42, and 46), ubiquitination of hDDI1 was enhanced (normalized FLAG/GFP intensity > 2). From those 10 candidates, we focused our attention on the four DUBs having the greatest influence on hDDI1 ubiquination to further validate them: UCHL-5, USP7, USP9X, and USP42.

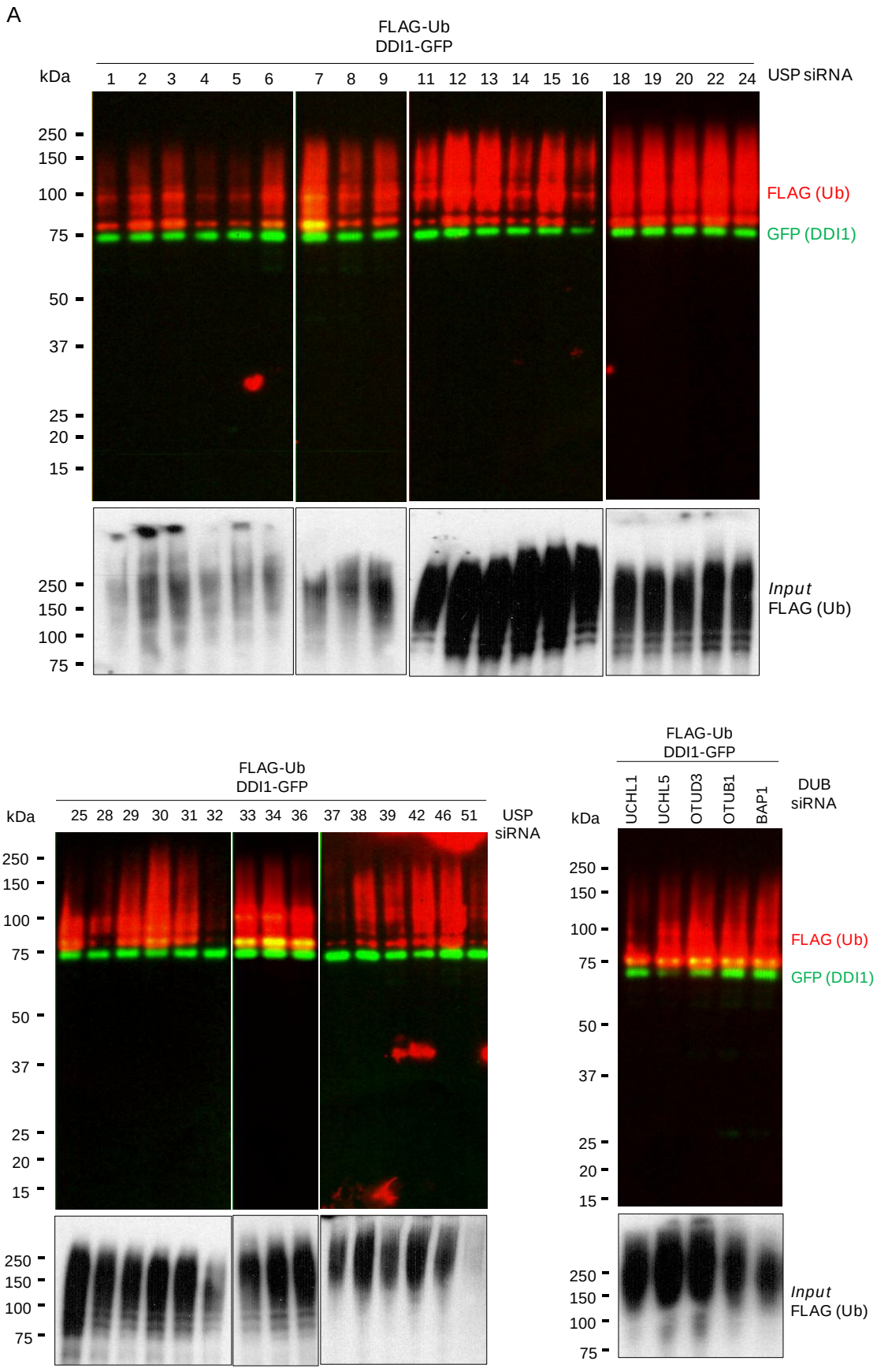
A
FLAG-Ub
DDI1-GFP
kDa
1 2 3 4 5 6 7 8 9 11 12 13 14 15 16 18 19 20 22 24
USP siRNA
250
150
100
75
50
37
25
20
15
FLAG (Ub)
GFP (DDI1)
Input
FLAG (Ub)
FLAG-Ub
DDI1-GFP
kDa
25 28 29 30 31 32 33 34 36 37 38 39 42 46 51
USP
siRNA
FLAG-Ub
DDI1-GFP
UCHL1
UCHL5
OTUD3
OTUB1
BAP1
DUB
siRNA
kDa
FLAG (Ub)
GFP (DDI1)
Input
FLAG (Ub)

B

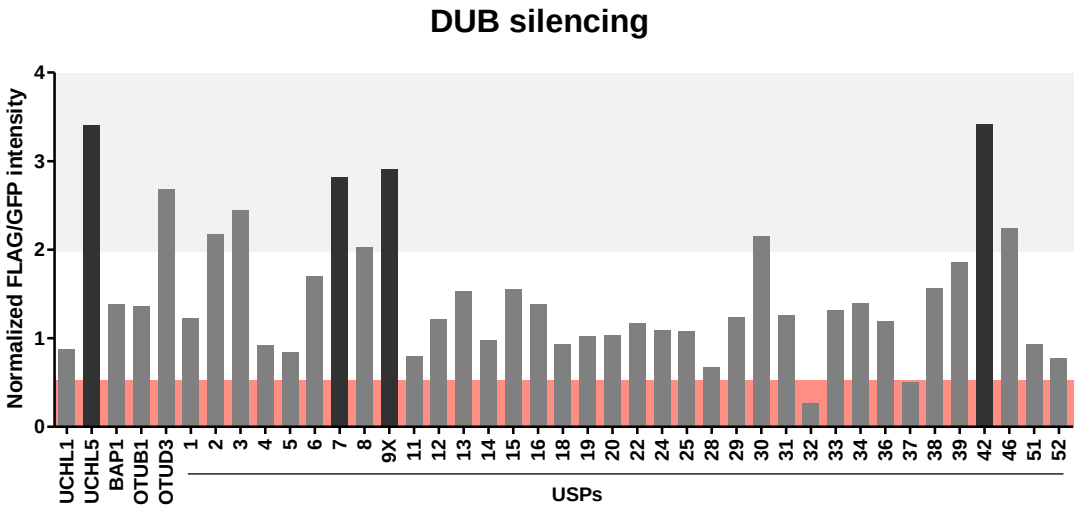

Figure 56. Screening of 41 human DUBs to search for UBE3A counteracting DUBs. A) 41 different human DUBs were silenced using 10 nM siRNAi. After GFP pull-down of DDI1-GFP, anti-GFP and anti-FLAG antibodies were used to detect DDI1-GFP [green, GFP (DDI1)] and its ubiquitinated fraction [red, FLAG(Ub)], respectively. Equivalent ubiquitinated material was quantified in the input or total lysates of each experimental set, using anti-FLAG antibody [Input FLAG (Ub)]. FLAG/GFP intensity ratios were determined in elutions. Those ratios were normalized to the average of three lowest values on each 6-well experimental dataset. B) Graphical plot of the quantifications of DDI1 ubiquitination upon silencing of different DUBs. Silencing of most DUBs did not affect DDI1 ubiquitination (0.5 < fold-change < 2, white). However, upon silencing of some DUBs DDI1 ubiquitination decreased (fold-change < 0.5, red), while upon silencing of some others ubiquitination of DDI1 was enchanced (fold-change > 2, gray). Black bars highlight the DUBs that affect more severely DDI1 ubiquitination (UCHL-5, USP7, USP9X, and USP42).

2. Validation of candidates USP7, USP9X, USP42 and UCH-L5

The DUBs that preliminary appear to counteract UBE3A activity are composed of three members of the USP family (7, 9X and 42) and one member of the UCH family (UCH-L5). All of them, except USP42 have already been described as druggable targets (Harrigan et al., 2018; Peterson et al., 2015; Wang et al., 2020b; Wertz and Murray, 2019), which would increase the possibility of success if we want to use them as targets for Angelman syndrome in the future.

To ensure the preliminary results obtained in the first screening, we aimed to silence the above mentioned four DUBs separately. The silencing of DUBs –UCHL-5, USP7, USP9X and USP42–, was first confirmed by immunoblotting (Figure 57).

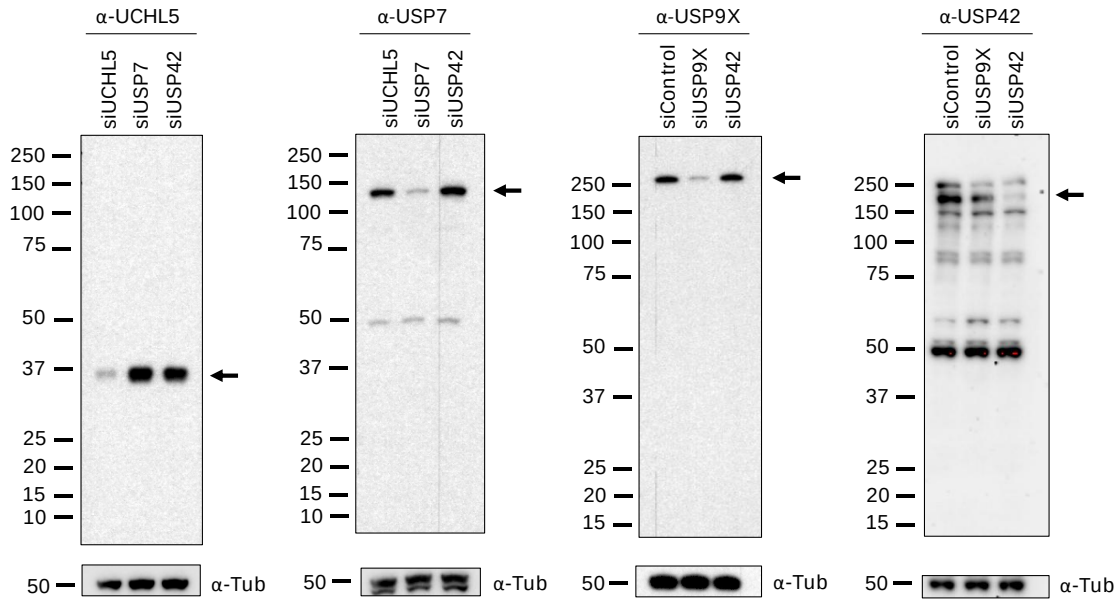

Figure 57. Candidate DUBs are efficiently silenced. Silencing of UCHL-5, USP7, USP9X and USP42 was corroborated using their respective antibodies. Tubulin detection was used as loading control. Black arrows indicate the size of proteins that have been silenced: UCH-L5 (37 kDa), USP7 (128 kDa), USP9X (290 kDa) and USP42 (145 kDa).

Similar to the first screening, in the validation experiment, DUBs were silenced for 24 h, and after silencing, HEK293T cells were co-transfected with hDDI1-GFP and FLAG-Ub. hDDI1-GFP was isolated by GFP pull-down after 48 h incubation, and the ubiquitination of hDDI1 monitored by immunoblotting. Anti-GFP (green signal) was used to detect the non-modified version of hDDI1 and anti-FLAG antibody (red signal) was used to detect its ubiquitination pattern (Figure 58). The experiment was performed in triplicate, and a scramble siRNA was used as a control. Immunobloting results were then quantified using ImageLab software; FLAG intensities were normalized to GFP levels and all the samples were normalized to the control sample containing scramble siRNA. As shown in Figure 58, silencing of neither USP7 nor UCHL-5 had any influence on the ubiquitination state of hDDI1. However, downregulation of USP42showed an increase on hDDI1 ubiquitination, but this increase resulted to be statistically no significant. Importantly, this second round of screening clearly demonstrated that USP9X silencing results in enhanced hDDI1 ubiquitination, and hence, confirms that USP9X is required for deubiquitinating hDDI1 (Figure 58). Consequently, we unveiled and confirmed that USP9X is a UBE3A counteracting DUB.

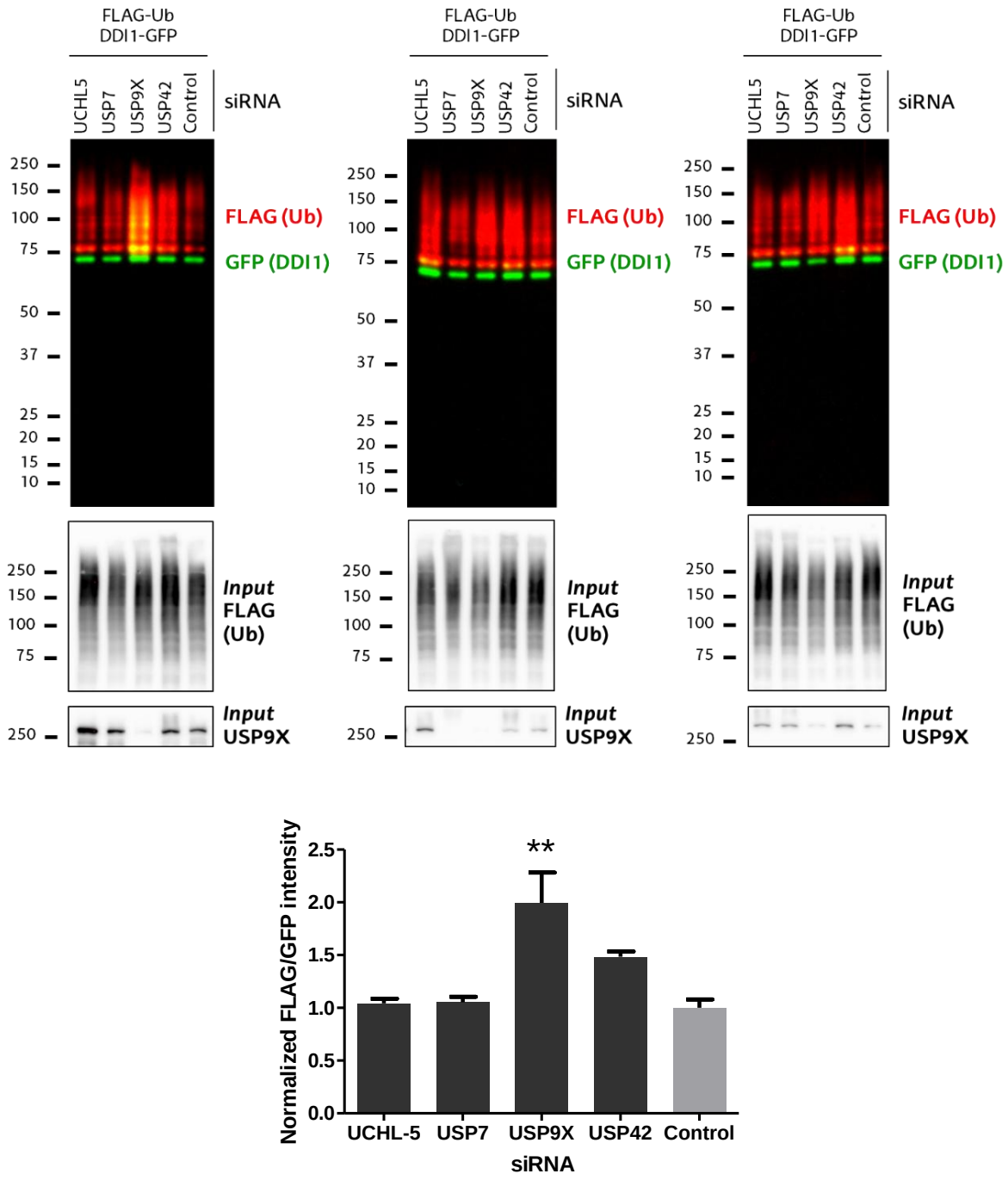

Figure 58. USP9X deubiquitinates hDDI1. Different DUBs were silenced in triplicate – UCHL-5, USP7, USP9X, USP42 – using 10nM siRNAi and compared to the control sample containing scramble siRNAi. DDI1-GFP ubiquitination was detected by Western blot using anti-FLAG antibody (red). Anti-GFP antibody (green) was used to detect non-modified DDI1-GFP levels. Silencing of USP9X was corroborated in whole cell extract using anti-USP9X antibody (Input USP9X), while FLAG-ubiquitin was detected as loading control (Input FLAG-(Ub)). Quantification was performed with Image-J after normalizing FLAG/GFP intensities. USP9X inhibition significantly enhanced DDI1 ubiquitination [one-way ANOVA, **p-value < 0.05, (mean±S.E.M., n = 3)]. DDI1 ubiquitination also increased upon USP42 silencing, but not significantly, while no changes were observed upon UCHL-5 and USP7 depletion.

3. Inhibition of USP9X using WP1130 drug

DUB inhibition has been considered as a potential therapeutic strategy for those diseases on which the function of a given E3 ligase is lost, and certain essential substrates are ubiquitinated at levels below their physiological requirement (Chen et al., 2019; Das et al., 2020; Hanpude et al., 2015). We hypothesized that inhibition of the DUB counteracting the action of the impaired E3 could restore the basal ubiquitination levels of the substrates, and hence, ameliorate the symptoms of the disease.

A compound termed WP1130 has been previously used to experimentally inhibit USP9X (Kapuria et al., 2010; Sun et al., 2011), in addition to USP5, USP14, and UCH37 (Kapuria et al., 2010). Recently, a small molecular inhibitor for USP9X has been developed, FT709 (Clancy et al., 2021), although it is still not commercially available. Since highly selective USP9X inhibitors are not yet available, we tested whether WP1130 would –presumably through USP9X– enhance the ubiquitination of hDDI1.

We first optimized the WP1130 incubation-period to inhibit USP9X in HEK293T and SH-SY5Y cells. Cells were co-transfected with GFP-hDDI1 and FLAG-Ub, and treated with 5 μM WP1130 as previously described by Kapuria and colleagues (Kapuria et al., 2010), for different time periods before harvesting: 30 min, 1 h, 2 h, 4 h and 8 h. Cells treated with DMSO were used as control, as WP1130 had to be solubilized in DSMO. hDDI1 was once again purified through GFP pull-down, and subsequently analyzed by immunobloting. Anti-GFP was used to detect the non-modified hDDI1 and anti-FLAG antibody was used to detect its ubiquitination pattern. Once again, immunobloting results were analyzed and quantified using ImageJ. As shown in Figure 59, in both cell lines the highest hDDI1 ubiquitination levels, indicated as FLAG/GFP intensity, were achieved after 1 hour of WP1130 treatment.

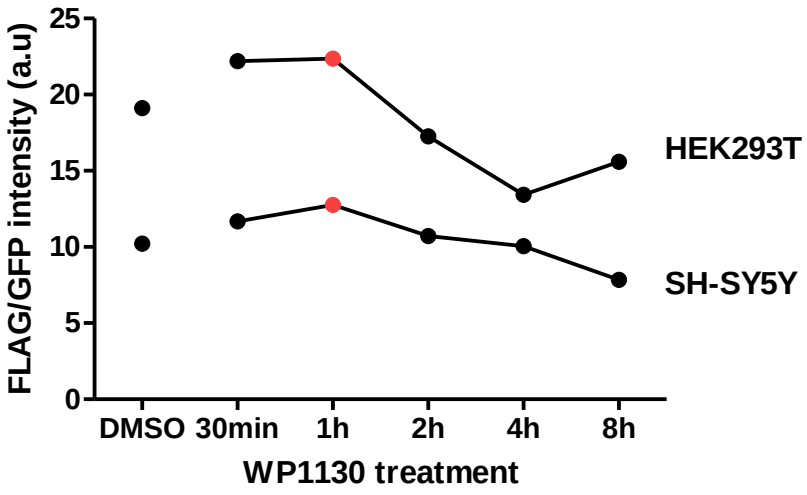

Figure 59. Time course effect of WP1130 treatment in HEK293T and SH-SY5Y cell lines. HEK293T and SH-SY5Y cell lines were co-transfected with FLAG-Ub and GFP-DDI1 and incubated for 48 hours. Before harvesting, cells were treated with 5 μM WP1130 for 8h, 4h, 2h, 1h or 30min. As control, cells were treated 8h with DMSO. After quantifying DDI1 ubiquitination and normalizing to its GFP levels, 1h WP1130 treatment showed the highest increase in DDI1 ubiquitination.

Once established the most effective incubation period for the drug, we repeated the experiment in HEK293T cells in triplicate, and once again observed that hDDI1 ubiquitination was significantly enhanced in cells treated with USP9X inhibitor WP1130 (Figure 60), supporting the earlier observations that DDI1 is an USP9X-regulated substrate. Overall, our data suggest that UBE3A and USP9X are the E3 ligase and DUB, respectively, involved in modulating the ubiquitination of hDDI1.

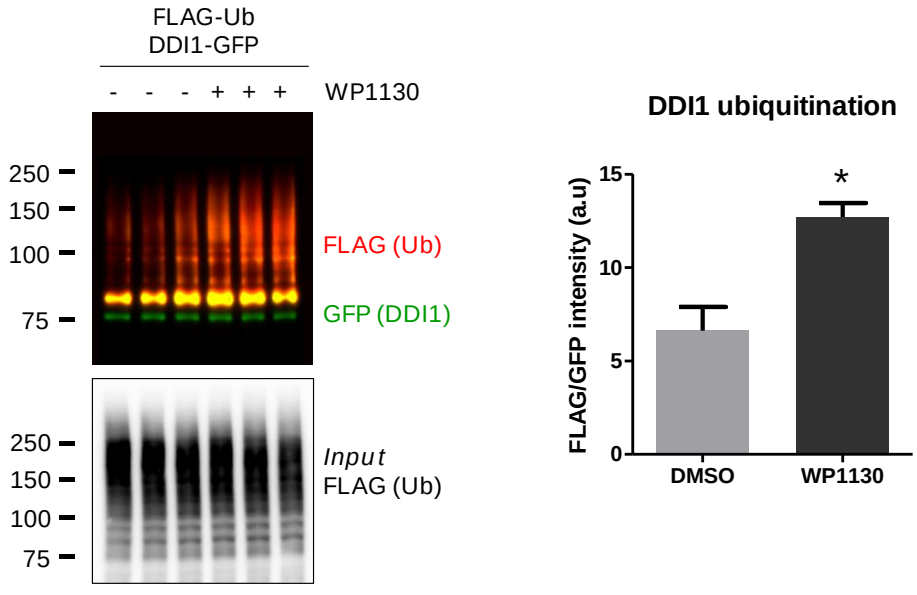

Figure 60. USP9X inhibition by WP1130 enhances DDI1 ubiquitination. Cells expressing GFP-DDI1 and FLAG-Ub were treated with 5 μM WP1130 or DMSO for 1 h. GFP-DDI1 was pulled down and its ubiquitination monitored by Western blot. Anti-GFP antibody was used to detect unmodified GFP-DDI1 levels whereas anti-FLAG antibody was used to detect ubiquitination. The signal of FLAG was normalized to the GFP signal. Equivalent amount of transfected ubiquitin was detected in the cell lysates by measuring FLAG-Ub levels [Input FLAG-(Ub)]. Quantification using Image-J showed a statistically significant increase in DDI1 ubiquitination after WP1130 treatment [t-test, *p-value < 0.05, (mean±S.E.M., n = 3)].

4. WP1130 treatment in *Drosophila melanogaster* flies

Once confirmed that WP1130 treatment in cells results in increased hDDI1 ubiquitination, we next aimed to test if this treatment could ameliorate the Angelman syndrome-like symptoms described for *Ube3a* mutant *Drosophila melanogaster* flies. Previous reports demonstrated that homozygous *Ube3a* mutant *D. melanogaster* flies show a deficient climbing phenotype, meaning that they employ more time climbing the tubes than wild-type flies (Wu et al., 2008). We therefore designed an experiment to test whether the climbing ability of different fly lines changes upon WP1130 treatment. The four fly lines tested were: *Ube3a* homozygous mutant flies (15B), *heterozygous Ube3a* mutant flies (15B/TM6), *faf* (UPS9X fly homolog) mutant flies (BX3/TM6) and wild-type flies (WT).

We employed two tubes for each fly-line, and introduced 10 flies in each of them. In each fly-line, one group was treated with 0.7 mM WP1130 and the other group was treated with DMSO as control. We then measured the time needed for the first fly to climb at least 4 cm on the tube (Palladino et al., 2002). We performed the measurements five times at different drug incubation periods: 0 h, 24 h, 48 h and 72 h. As shown in Figure 61, at 0 h *Ube3a* homozygous mutant flies (15B) showed a climbing deficit, since they needed almost 30 seconds on average to climb 4 cm on a tube, while the rest of the flies (WT, 15B/TM6 and BX3/TM6) needed no more than 10 seconds. After 24 h, 48 h and 72 h, neither WP1130, nor DMSO treated WT, 15B/TM6 and BX3/TM6 flies showed significant differences in their climbing ability. In contrast, *Ube3a* homozygous mutant flies (15B) showed a significant increase in their climbing ability after 24 h, 48 h or even 72 h of WP1130 treatment: the time employed to climb 4 cm on the tube was decreased down to

10 seconds, rescuing the climbing phenotype comparable to wild-type flies (Figure 61).

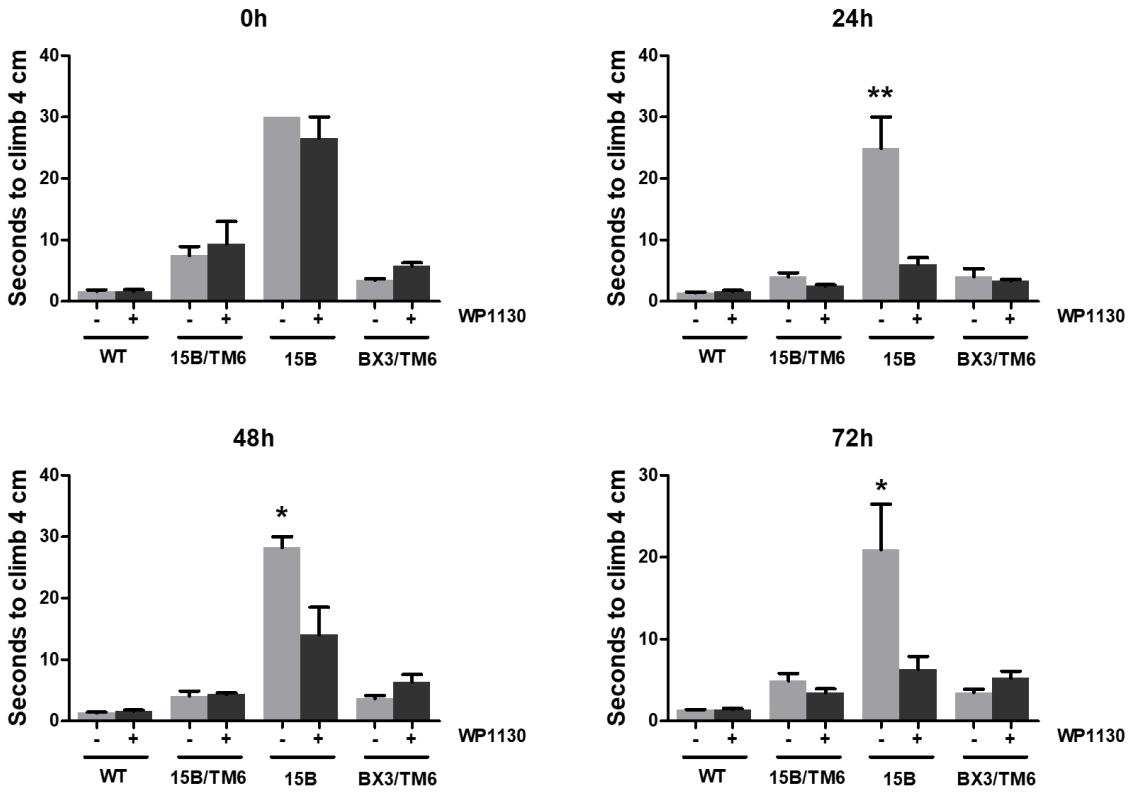

Figure 61. WP1130 treatment in model flies for Angelman syndrome rescues the climbing phenotype. 10 flies were used in each condition (WP1130 and DMSO) and each group: wild-type flies (WT), heterozygous Ube3a deleted flies (15B/TM6), homozygous Ube3a deleted flies (15B) and faf mutant flies (BX3/TM6). Flies were treated with 0.7 mM WP1130 (treatment, dark grey bars) or DMSO (control, light grey bars). The time flies needed to climb 4 cm on a tube was significantly decreased after 24 h treatment [t-test, **p-value < 0.01, (mean ± S.E.M., n=5)] and 48 h and 72 h [t-test, *p-value < 0.05, (mean ± S.E.M., n=5)].

5. Changes in protein ubiquitination upon WP1130 treatment in *Drosophila melanogaster*

WP1130 is a cell-permeable deubiquitinase inhibitor, directly inhibiting DUB activity of USP9X, USP5, USP14, and UCH37 (PubChem). We hypothesized that climbing phenotype of model flies for Angelman syndrome treated with WP1130 was rescued due to a recovery of Rngo (fly homolog for hDDI1) ubiquitination. However, inhibition of different DUBs by WP1130 will affect the

ubiquitination of several other proteins that could also be involved in the rescue of the climbing ability. For example, it has been shown that WP1130 downregulates the antiapoptotic proteins Bcr-Abl and JAK2 (Bartholomeusz et al., 2007b), inducing apoptosis and upregulating proapoptotic proteins, such as MCL-1 and p53 (Kapuria et al., 2010). It also displays potent inhibitory activity against certain tumors (Bartholomeusz et al., 2007a). Therefore, we aimed to elucidate which are the proteins that change their ubiquitination status upon WP1130 treatment, and hence, might be involved in rescuing the climbing phenotype of the Angelman Sydrome model flies.

Comparison of the ubiquitinated proteome of DMSO- and WP1130-treated Drosophila flies should allow the identification of proteins whose ubiquitination is enhanced by the action of the drug. For that purpose, and in order to successfully analyze the ubiquitinated proteins, BioUb flies were employed. Those flies express the BioUb construct under the GMR-GAL4 driver, enabling the purification of the whole ubiquitinated material within the developing eye of the fly.

After treating BioUb flies with 0.7mM WP1130 or DMSO (control) for 48h, biotinylated ubiquitin conjugates formed within the fly photoreceptor neurons were isolated using neutravidin beads (*see Introduction, Figure 20*). The pull-downs were performed on three biological replicates for each of the two conditions analyzed. Silver staining of the 10% of the eluted fractions showed similar amounts of ubiquitinated material between all the replicates, and all the conditions (DMSO and WP1130) (Figure 62A). After fractionation of the remainig sample by SDS-PAGE, endogenously biotinylated carboxilase (~130 KDa) and avidin monomers (~15 KDa) and dimers (~30 KDa) were discarded to avoid very abundant proteins (Figure 2.7b) Each lane of the rest of the gel, was cut into two slices (Figure 62B), and proteins were in-gel digested with trypsin and subsequently analysed by LC-MS/MS.

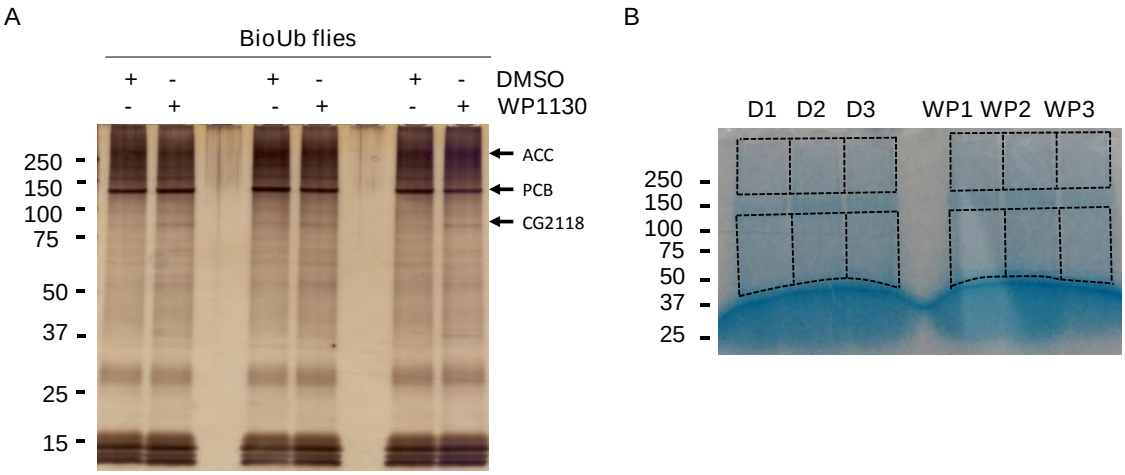

Figure 62. Isolated ubiquitinated material for mass spectomety analyis. A). Silver staining on 10% of the material purified from each biological replicate. Equal amount of WP1130 and DMSO samples from each pull-down replicates were resolved in a 4-15 % gradient gel and stained with silver. Arrowheads indicate the endogenously biotinylated proteins Pyruvate Carboxylase (PCB), acetyl-CoA carboxylase (ACC) and methylcrotonoyl-CoA carboxylase 1 (CG2118). B) Coomassie staining of a gel with equal amounts of WP1130 and DMSO samples. Black dashed lines indicate the gel sections that were analyzed by mass spectrometry, avoiding highly abundant proteins.

In total, 1246 common proteins were identified, 44 proteins exclusively in the DMSO sample and 18 in the WP1130 sample (Figure 63A, Supplementary Table 3). Up to 1000 proteins were identified in all the replicates either for DMSO and WP1130 samples (Figure 63A). As shown in Figure 63B, there was a high correlation of the label-free quantification (LFQ) intensity values (Pearson coefficient > 0.949) both between replicates and across the different conditions. LFQ intensity recorded for the identified proteins among different replicates showed that the most abundant proteins appeared in the three independent replicates (Figure 63C). Moreover, analyzing all the samples together, most abundant proteins, as determined by their LFQ values, were identified in all the replicates in both samples (DMSO and WP1130) (Figure 63D). Those proteins for which LFQ values were not reported by the MaxQuant software on that given experiment, were imputed using random LFQ values from a normal distribution (Tyanova et al., 2016), to simulate expression below the detection limit (Figure 63E).

A

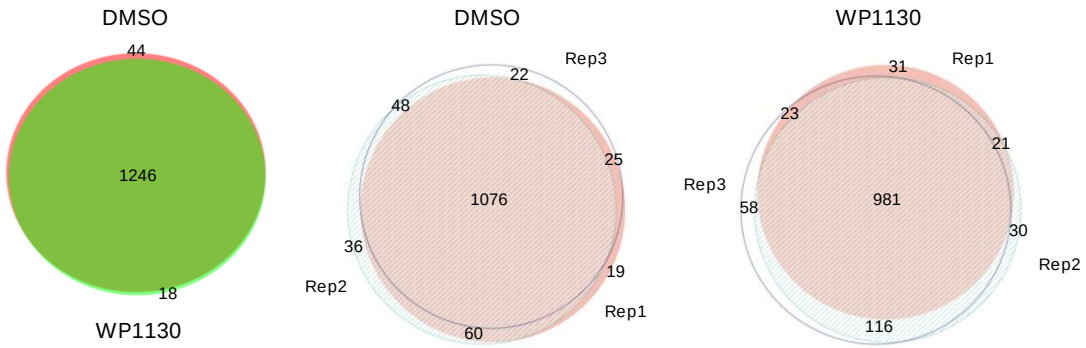
DMSO
44
1246
18
WP1130
DMSO
Rep3
22
48
25
1076
36
19
Rep2
Rep1
60
WP1130
31
Rep1
23
21
Rep3
58
981
30
Rep2
116

B

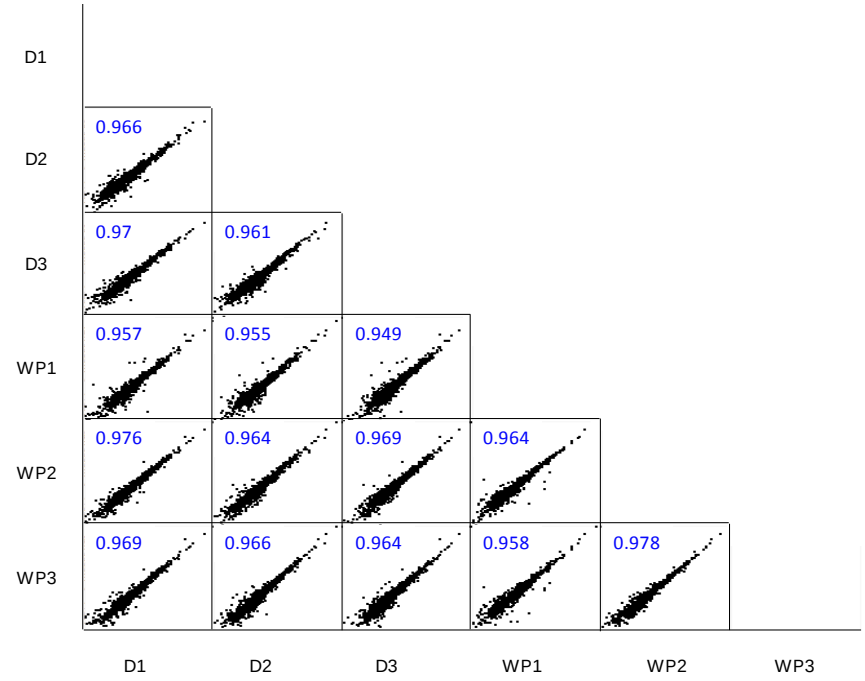
D1
D2
D3
WP1
WP2
WP3
0.966
0.97
0.961
0.957
0.955
0.949
0.976
0.964
0.969
0.964
0.969
0.966
0.964
0.958
0.978
D1
D2
D3
WP1
WP2
WP3

C

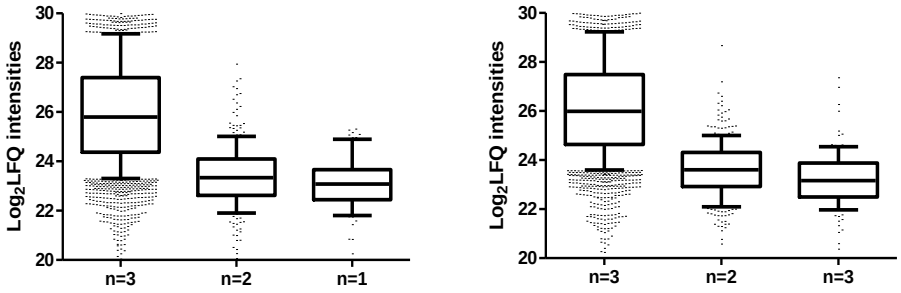
Log2LFQ intensities
30
28
26
24
22
20
n=3
n=2
n=1
Log2LFQ intensities
30
28
26
24
22
20
n=3
n=2
n=3

D

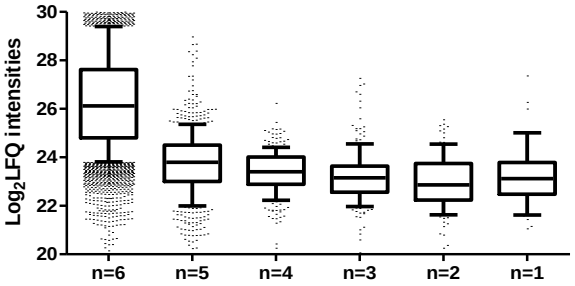

E

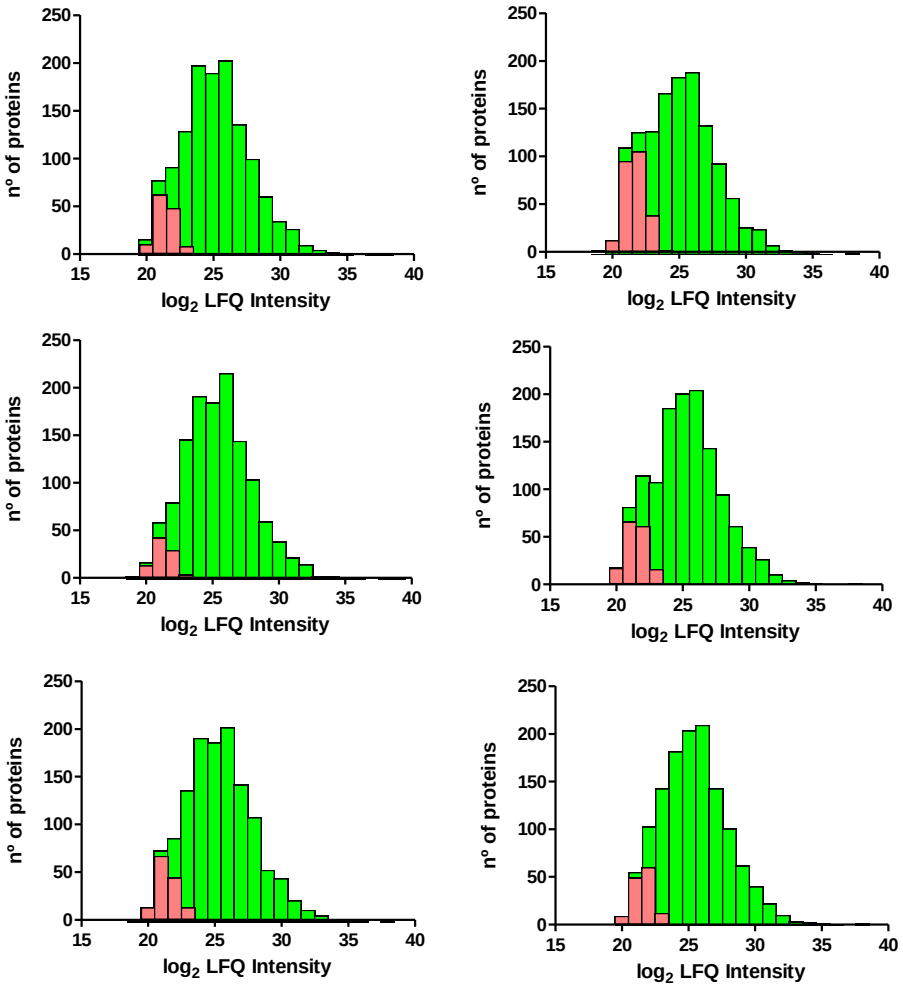

Figure 63. Ubiquitination of several proteins change in BioUb *Drosophila melanogaster* flies upon WP1130 treatment. A) Overlap between proteins identified in the different conditions. Protein identification overlap in the different DMSO and WP1130 replicates, as well as the overall overlap between the two conditions (DMSO vs WP1130) is shown. B) Multicorrelation graphs of LFQ intensities (in log2 scale) of proteins identified across the different pull-downs and replicates. Pearson correlation of each comparison is shown in blue. C) Box plots indicating the positive correlation between the LFQ intensity recorded for the identified proteins among different replicates (Y axis) and the number of independent replicates (X axis) on which those proteins appeared. D) Box plot indicating the correlation between the LFQ intensity for the identified proteins (Y axis) and number

of replicates, all together. E) Frequency histograms showing protein distribution (y axis) according to their LFQ intensity (X axis). Missing LFQ intensity values were replaced with values from a normal distribution (red). LFQ intensities are shown in log2 scale.

In order to identify those proteins more ubiquitinated upon WP1130 treatment, we compared the LFQ intensities of the proteins detected on the WP1130 samples with the ones identified in DMSO samples. More precisely, we calculated the fold-changes (WP1130/DMSO) and significance p-values for all the proteins, and plotted them in a Vulcano plot (Figure 64, Supplementary Table 3).

As expected, most of the proteins detected, including endogenously biotinylated proteins pyruvate carboxylase (PCB), methylcrotonoyl-CoA carboxylase 1 (CG2118) (Chandler and Ballard, 1986), and *faf*, the Drosophila homolog of USP9X, displayed a ratio close to one (log_2 ratio~ 0), (shown with black dots in Figure 64). Acetyl-CoA carboxylase (ACC), another endougenously biotinylated protein, was shifted to the right, but did not reach statistical significance. From the 1308 protein groups identified in total, only two were significantly enriched ($p < 0.05$) at least 2-fold in the WP1130 sample, relative to DMSO sample. One is REST corepressor (CoRest), an essential component of a corepressor complex that represses transcription of neuron-specific genes in non-neuronal cells (Dallman et al., 2004). The other protein identified with a single unique peptide (empty circle) is the metabotropic glutamate receptor (mGluR). It is a G-protein coupled receptor for glutamate; ligand binding causes a conformation change that triggers signaling via guanine nucleotide-binding proteins (G proteins) and modulates the activity of down-stream effectors (Parmentier et al., 1996).

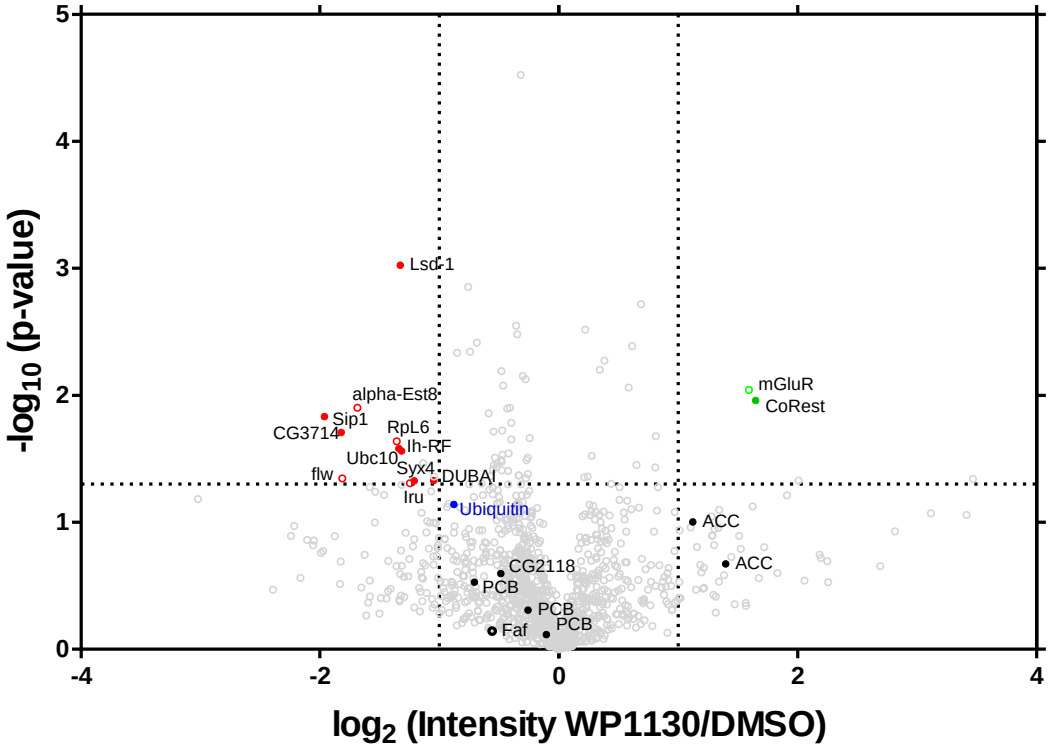

Figure 64. Ubiquitome analysis of WP1130 and DMSO treated Drosophila flies. Comparison of the abundance, determined by their LFQ intensities, of the ubiquitinated proteins identified by MS upon WP1130 treatment relative to DMSO treated flies. The Vulcano plot displays the LFQ WP1130/DMSO ratios in $\log_2$ scale (X-axis) and the t-test p-values in $\log_{10}$ scale (Y-axis). It determines the statistical significance (p-value < 0.05, horizontal black dashed lane) of the fold changes, for each protein. Labelled filled circles represent high confidence proteins found more ubiquitinated in the WP1130 sample than in the DMSO sample. Labelled empty circles are those detected with one unique peptide. Endogenously ubiquitinated proteins (ACC, CG2118 and PCB) and *faf* are shown with filled black dots, and ubiquitin with a filled blue dot.

6. Inhibition of USP9X using FT709 drug

One of the main challenges that drug development faces is the specificity towards the protein of interest. During this Thesis the only drug available for USP9X was WP1130, and as mentioned before, it is not specific for USP9X, because also targets USP5, USP14 and UCH37 (Kapuria et al., 2010). However, FT709 drug has been recently developed, a specific inhibitor for USP9X (Clancy et al., 2021).

We aimed to elucidate if USP9X inhibition using FT709 drug increased hDDI1 ubiquitination. Cells were trasnfected with FLAG-Ub and GFP-hDDI1, and

treated with different concentrations of FT709 diluted in DMSO: 0 µM, 1 µM or 10 µM FT709. No changes were observed in the GFP-hDDI1 mono-ubiquitination band in none of the concentrations (Figure 65). In contrast, statistically significant changes were observed in cells treated with both, 1 µM and 10 µM FT709. These findings, together with the results using WP1130, corroborated that inhibition of USP9X enhanced hDDI1 ubiquitination, so its application to ameliorate the symptoms of the disease needs to be further investigated.

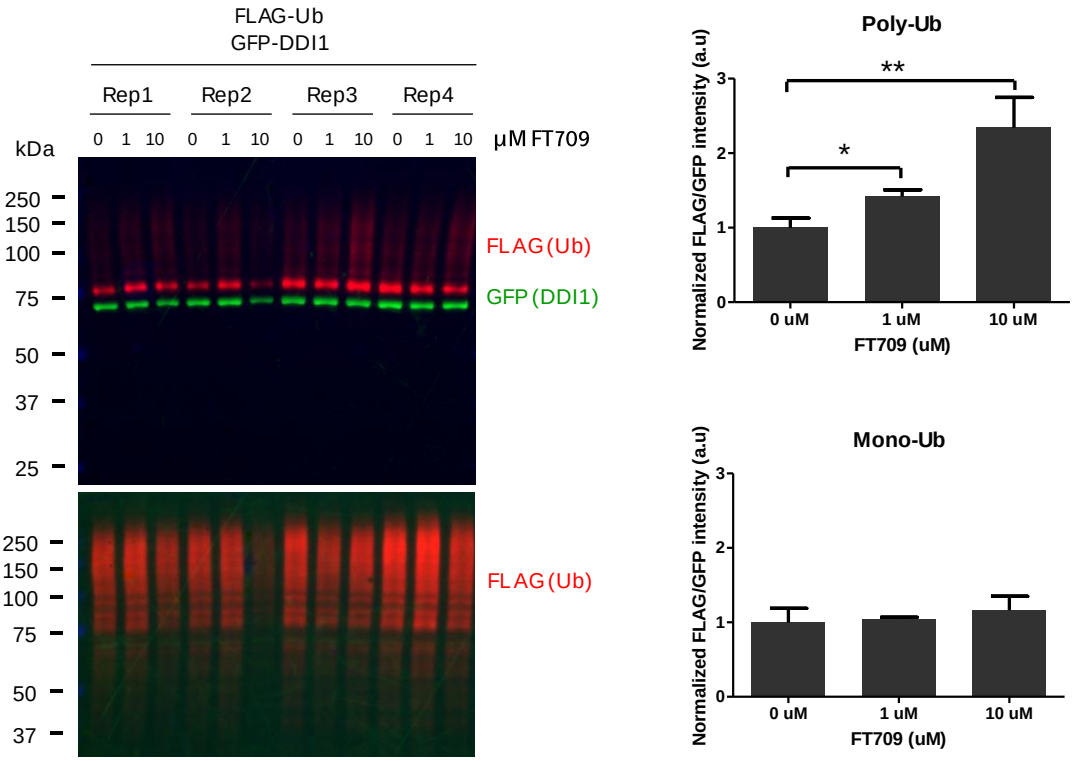

Figure 65. USP9X inhibition by FT709 enhances DDI1 poly-ubiquitination. Cells expressing GFP-DDI1 and FLAG-Ub were treated with 1 µM and 10 µM FT709 or DMSO for 1 h. GFP-DDI1 was pulled down and its ubiquitination monitored by Western blot. Anti-GFP antibody was used to detect unmodified GFP-DDI1 levels whereas anti-FLAG antibody was used to detect ubiquitination. The signal of FLAG was normalized to the GFP signal. Equivalent amount of transfected ubiquitin was detected in the cell lysates by measuring FLAG-Ub levels [Input FLAG-(Ub)]. Quantification using Image-J showed a statistically significant increase in DDI1 poly-ubiquitination after FT709 treatment [t-test, *p-value < 0.05, (mean±S.E.M., n = 3)] (upper panel). In contrast, no differences were observed in DDI1 mono-ubiquitination (bottom panel).

Altogether, findings during Chapter 2 corroborate USP9X as one of the DUBs counteracting UBE3A and mediating DDI1 deubiquitination, and they also show USP9X as an interesting target to improve Angelman syndrome model fly phenotype. However, further work needs to be done to conclude if targeting USP9X could be a viable strategy for Angelman syndrome treatment.

Chapter 3

In vivo identification of UBE3A interactors

The physiology of a cell is determined by thousands of proteins acting in concert to shape a cellular response. Coordination is achieved through proteins interacting with one another, or with other molecules (e.g. DNA, RNA), creating complexes, organelles, and dynamic networks that mediate different cellular processes (Hergovich, 2012; Lou et al., 2020; Yu et al., 2019). For example, UBE3A mediated ubiquitination of proteins is tightly regulated by a protein–protein interaction with the E2 enzyme UbcH7 (Huang et al., 1999).

Due to the central role in biological function, protein interactions also control the mechanisms leading to healthy and disease states in organisms. Diseases are often caused by mutations affecting the binding interface or leading to biochemically dysfunctional allosteric changes in proteins (Baldini et al., 2020; Ryan and Matthews, 2005). For example, signaling receptor mutations avoid the binding of their signaling molecules, causing a variety of human diseases, such as hypercholesterolemia, hyper- or hypothyroidsm or carcinomas (Bertolini et al., 2013; Schöneberg et al., 2004). Mutations in kinases that abolish interactions with their substrates are also involved in immunodeficiencies, cancers and endocrine disorders (Stenberg et al., 2000). Similarly, in Angelman syndrome, mutations on the UBE3A protein usually result in the inability of this protein to interact with its partners (Beasley et al., 2020; Malzac et al., 1998).

Identification of interactors of the disease-causing proteins has the potential to decipher the cellular processes in which those proteins are involved. For example, network analysis of UBE3A interactor proteins revealed the association between UBE3A and cellular processes such as DNA replication, transcription and proteasomal and centrosomal function (Martinez et al., 2018). Therefore, identification of the whole UBE3A interactome could elucidate the molecular basis of Angelman syndrome, which in turn can lead to development of methods for diagnosis and new treatment.

We previously confirmed that UBE3A interacts with its substrates DDI1, DDI2, PSMA5 and MINDY2 (*see Figure 41*). We next aimed to identify UBE3A interactors that are not necessarily substrates, and might be involved in either the regulation of distinct cellular processes and/or UBE3A activity itself. Moreover, we aimed to define if those interactors are full-length, N-terminal or C-terminal UBE3A interactors. For that purpose, we applied the BioID2 strategy (Kim et al., 2016) (*see page 56, BioID2*).

First, we generated three different constructs for human UBE3A protein: (i) full-length UBE3A (UBE3A^{FL}), (ii) N-terminal UBE3A (UBE3A$^{N\text{-}ter}$, Δ501-875) spanning from the AZUL domain up to the start of the HECT domain and (iii) C-terminal UBE3A (UBE3A$^{C\text{-}ter}$, Δ1-476) comprised just by the HECT domain. In all the constructs, UBE3A sequence was linked to the BioID2 through a linker that was previously optimized (data not shown).

To identify UBE3A interactors through BioID2 strategy, HEK293T cells were first transfected with one of the three constructs (UBE3A^{FL}, UBE3A$^{C\text{-}ter}$ or UBE3A$^{N\text{-}ter}$) and supplemented with biotin (50 µg). Immunobloting of cell lysates (Input) show successful biotinylation (Figure 66A, left panel) as well as equal transfection effiency of the constructs (Figure 66A, right panel). Biotinylated material was then purified using streptavidin beads, and immunobloting against biotin of the unbound fraction showed little loss of biotinylated material during the purification protocol (Figure 66B). Finally, analysis of the 10% of the eluted material by immunoblotting with anti-biotin (Figure 66C, left panel) and silver staining (Figure 66C, right panel) showed the amount of material purified in all samples.

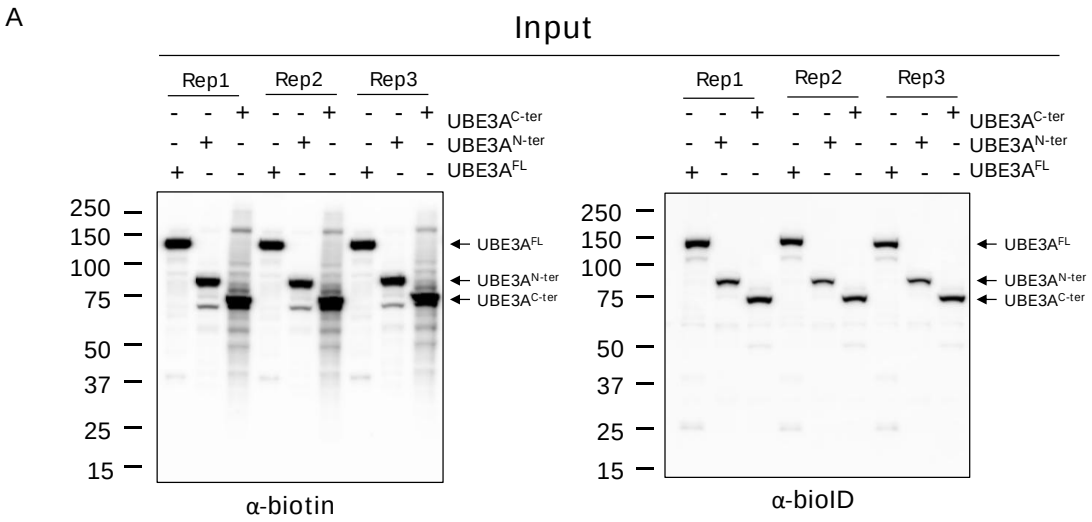

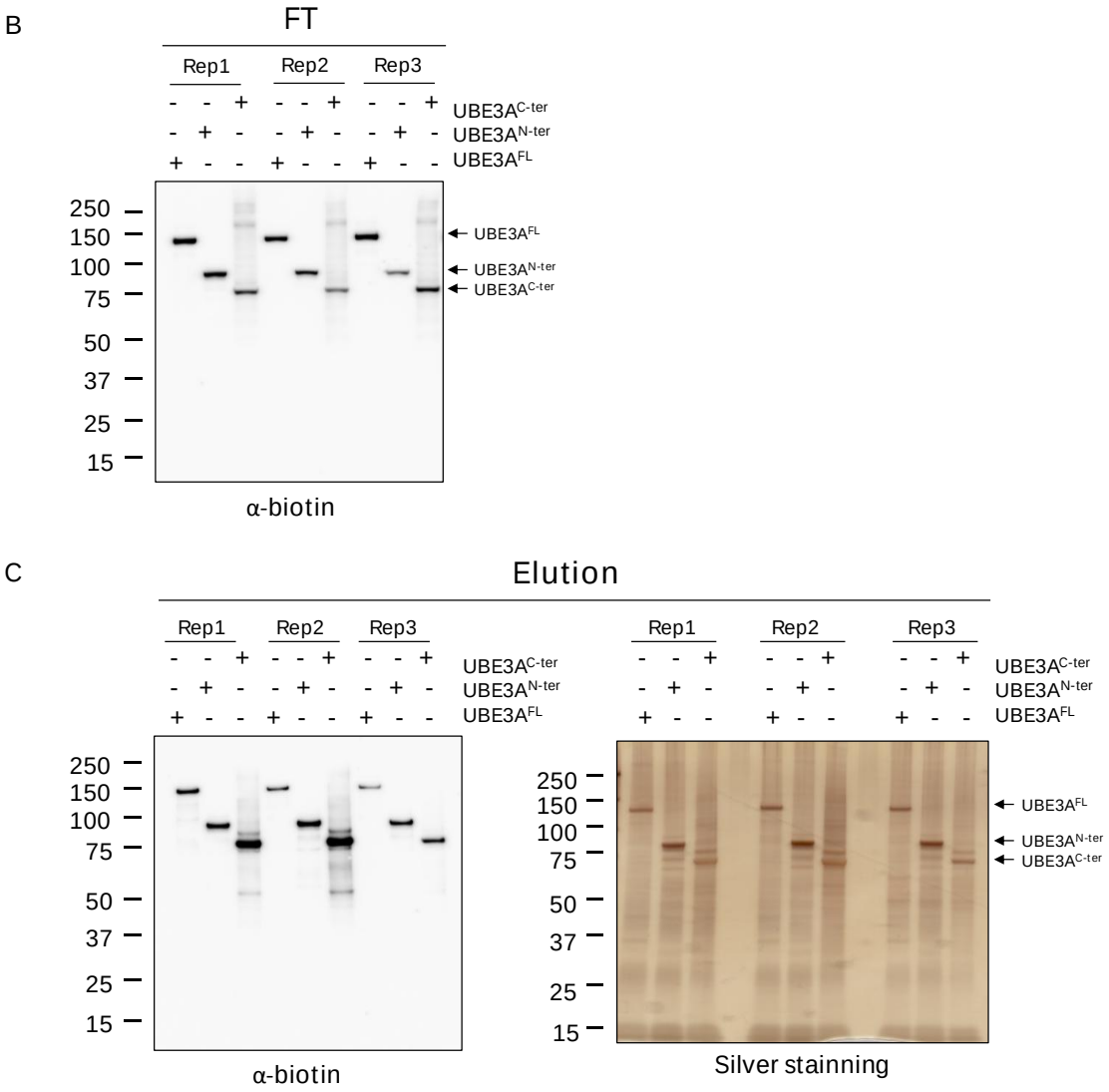

Figure 66. Biotinylated material for mass spectometry analyis. A) Immunobloting of the HEK293T cell lysates (inputs) before biotin pull-down protocol ensured biotinylation through BioID2 (anti-biotin, left panel) and equal transfection efficiency of the constructs (anti-BioID, right panel). B) Immunobloting with anti-biotin of flow-through (FT) samples containing the unbound fraction of the pull-down process, confirmed that majority of the biotinylated material was isolated. C) 10% of the material purified from each of the 9 pull downs performed (3 conditions, 3 biological replicates per condition) were resolved in two 4-15% gradient gels, one was immunoblotted with anti-biotin, while the other was silver stained. Both confirmed the success in purifying biotinylated material.

Once confirmed that the pull-downs were efficient for all the samples, remaining 90% of eluted material was analysed by LC-MS/MS. For that purpose, eluates were run on a SDS-PAGE and each lane was cut into 4 slices (Figure 67). Then, each slice was subjected to in-gel digestion. In brief, proteins were alkylated, reduced and digested with trypsin as described (Ramirez et al., 2018). Finally, resulting peptides were analyzed by LC-MS/MS.

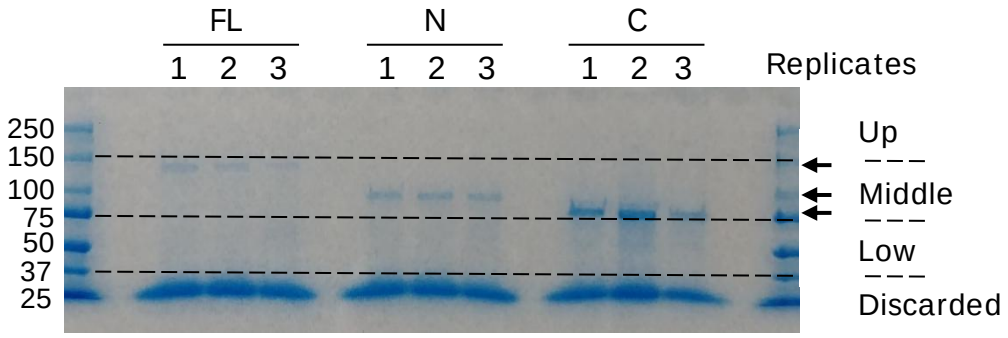

Figure 67. Commassie staining and slicing for mass spectrometry analysis. Commassie staining of the SDS-PAGE for full-length (FL), N-terminal (N) and C-terminal (C) UBE3A-BioID samples after BioID pull-down. Gel was sliced in four parts, indicated with dashed lines; three were prepared for LC-MS/MS analysis (Up, Middle and Low), and the bottom slice containing avidin was discarded to avoid masking the less intense proteins. In the middle slice FL, C and N UBE3A-BioID constructs are highlighted (arrowheads). Three replicates are shown for each of the conditions (1, 2 and 3).

537 proteins were identified for UBE3A$^{N\text{-}ter}$ sample, 618 proteins for UBE3A$^{C\text{-}ter}$ and 609 proteins for UBE3A^{FL}. The overlap of the identified proteins within the three replicates are shown for the three conditions (UBE3A^{FL}, UBE3A$^{N\text{-}ter}$ and UBE3A$^{C\text{-}ter}$) (Figure 68A, Supplementary Table 4). We next combined the list of total proteins identified in each condition, and resulted in a total of 729 proteins confidently identified: 445 proteins were common for all the samples, while 77 proteins were specific for UBE3A$^{C\text{-}ter}$, 10 proteins for UBE3A$^{N\text{-}ter}$, and 52 proteins for UBE3A^{FL} (Figure 68B).

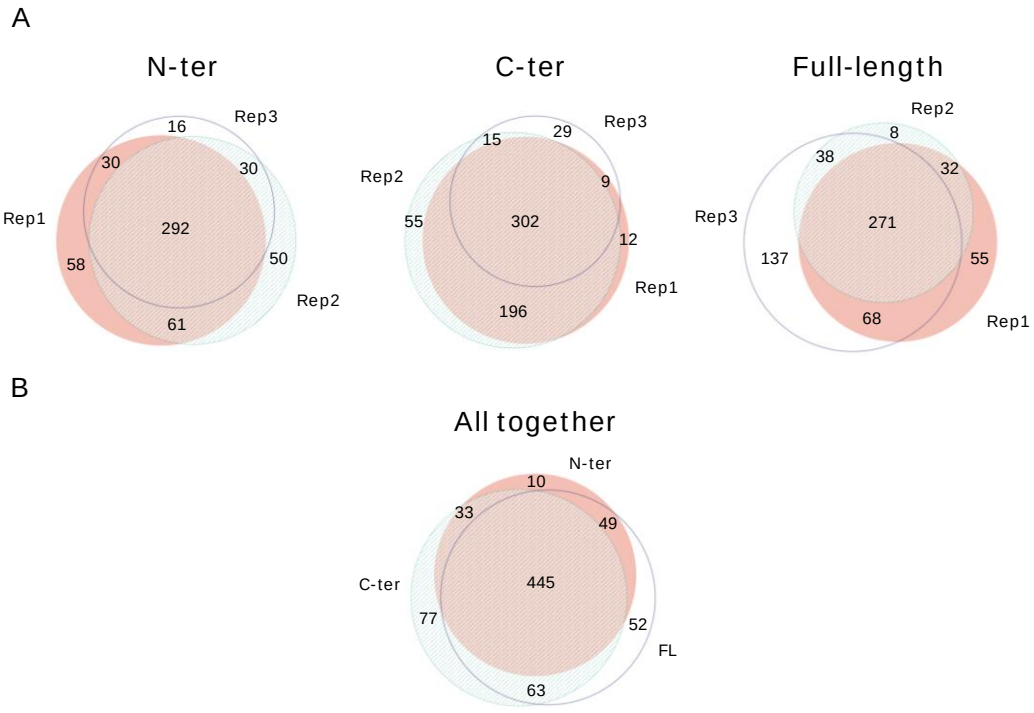

Figure 68. Overlap between proteins identified in the different conditions. Protein identification overlap between the three replicates (rep1, rep2, rep3) of each experimental condition (A), as well as the overlap between UBE3A$^{N\text{-}ter}$, UBE3A$^{C\text{-}ter}$ and UBE3A^{FL} samples (B) are shown through Venn diagrams. Each sample or each replicate has been differently coloured (red, blue and empty circles).

To assess the quality of the experiment, we first performed a multi scatter plot analysis and calculated the Pearson correlation across replicates as well as different samples. The Pearson correlation between replicas was on average 0.862, while across samples the correlation was on average 0.803 (Figure 69).

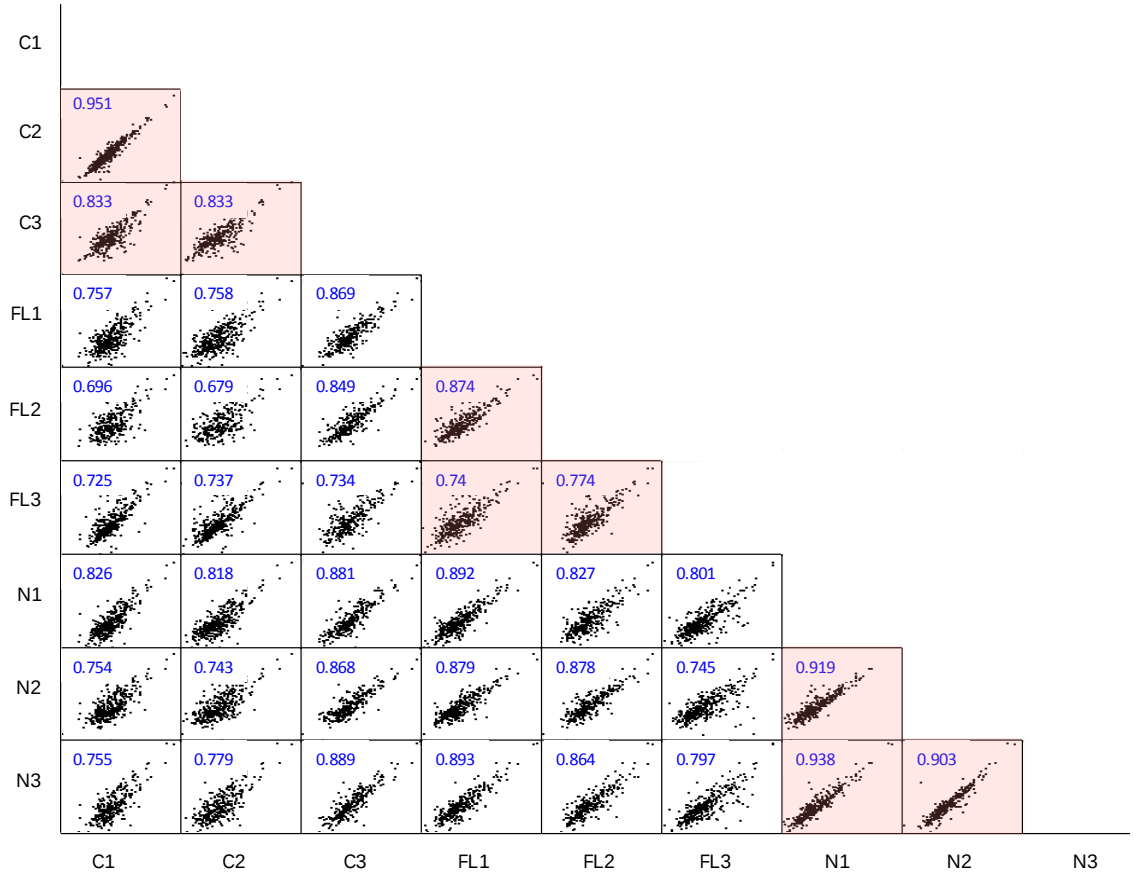

Figure 69. Multi-correlation graphs of LFQ intensities (in log2 scale) of proteins quantified across the different pull-downs and replicates. Pearson correlation of each comparison is shown in blue. Correlation between replicates from the same sample are highlighted in red. C1-2 corresponds to UBE3A$^{C\text{-}ter}$ samples, N1-3 to UBE3A$^{N\text{-}ter}$ samples, and FL1-3 to UBE3A^{FL} samples.

LFQ intensities recorded for the proteins detected in each of the samples showed that most abundant proteins appeared in the three independent replicates, while the less abundant ones appear only in one replica (Figure 70A). Moreover, analyzing all the samples together, most abundant proteins were present across all the samples in the experiment (Figure 70B).

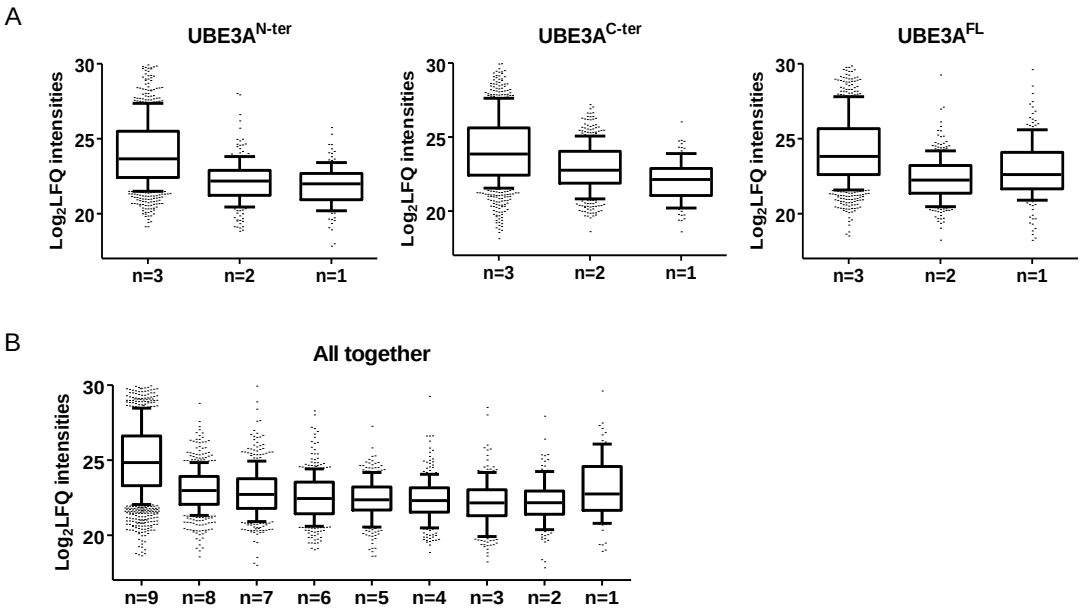

Figure 70. Identification of proteins across different samples. Box plots indicating the positive correlation between the log_2LFQ intensity recorded for the identified proteins among different replicates (Y axis, log_2LFQ intensities) and the number of replicates (X axis, n) on which those proteins appeared. A) The three samples are shown separately ($UBE3A^{N\text{-}ter}$, $UBE3A^{C\text{-}ter}$ and $UBE3A^{FL}$). B) All samples are shown together ($UBE3A^{N\text{-}ter}$, $UBE3A^{C\text{-}ter}$ and $UBE3A^{FL}$).

In order to identify UBE3A interactors and determine if they were full-length, C-terminal or N-terminal interactors, those interactors needed to be quantified. The quantitative data of those proteins for which LFQ values were not reported by the MaxQuant software on that given experiment, were imputed using random LFQ values from a normal distribution (Tyanova et al., 2016), to simulate expression below the detection limit (Figure 71, Supplementary Table 3).

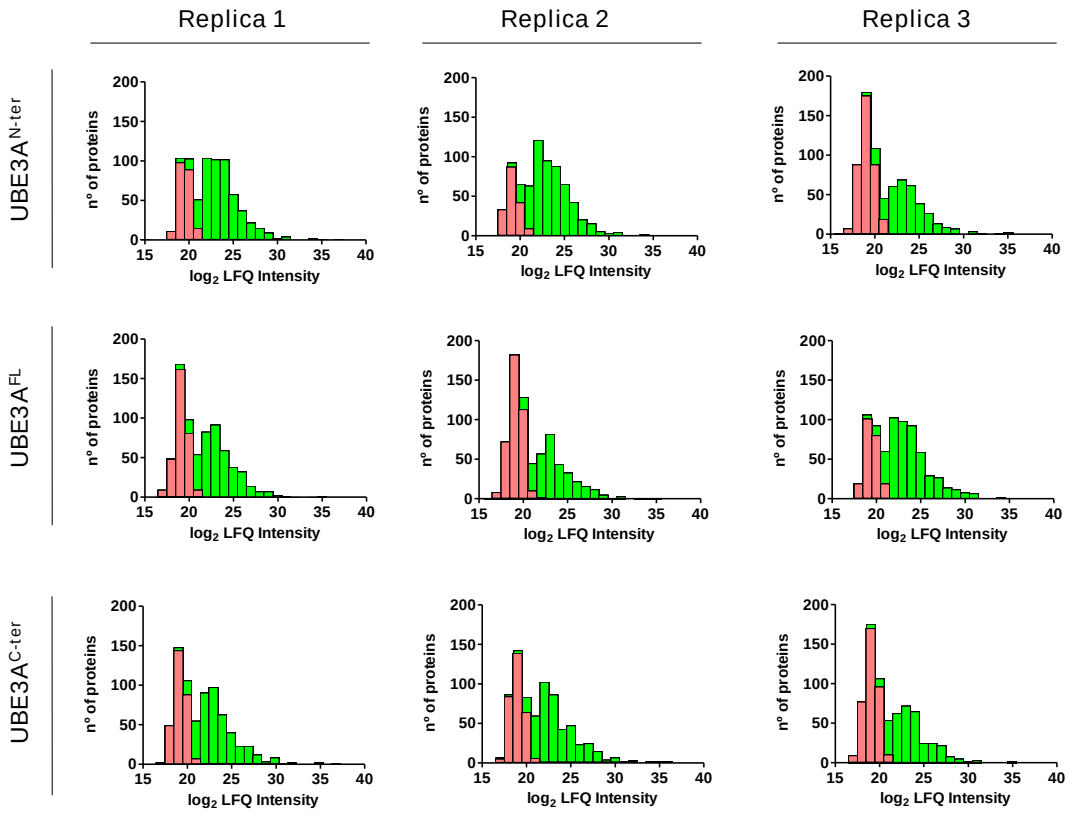

Figure 71. Experimentally recorded and imputed quantitative data. Frequency histograms showing protein distribution (y axis) according to their LFQ intensity (x axis). Missing LFQ intensity values were replaced with values from a normal distribution (red). LFQ intensities are shown in log2 scale. Each sample and each replicate are shown separately (UBE3A$^{N\text{-}ter}$, UBE3A$^{C\text{-}ter}$ and UBE3A^{FL}).

In order to reliably identify UBE3A interactors, several criteria were established; (1) proteins needed to be detected at least in all the replicates of one experimental condition (3-0), or in two out of the three replicates in both samples (2-2), (2) only proteins identified with more than one unique peptide were considered, and (3) proteins need to show a 4-fold change increase in abundance in two different comparisons. For instance, UBE3A$^{N\text{-}ter}$ interactors should not be present in UBE3A$^{C\text{-}ter}$ samples, so in both UBE3A^{FL} vs UBE3A$^{C\text{-}ter}$ and UBE3A$^{N\text{-}ter}$ vs UBE3A$^{C\text{-}ter}$ comparisons, they should show a positive ratio (ratio > 4, $\log_2$ ratio > 2). Similarly, as UBE3A$^{C\text{-}ter}$ interactors should not be present in UBE3A$^{N\text{-}ter}$ samples, they should be highly enriched in UBE3A^{FL} vs UBE3A$^{N\text{-}ter}$ and UBE3A$^{C\text{-}ter}$ vs UBE3A$^{N\text{-}ter}$ comparisons (ratio > 4, $\log_2$ ratio > 2). Finally, if a protein is more abundant in the full length sample (UBE3A^{FL} vs UBE3A$^{C\text{-}ter}$ and UBE3A^{FL} vs UBE3A$^{N\text{-}ter}$) and equally detected or non present in N-term and C-term conditions (UBE3A$^{C\text{-}ter}$ vs UBE3A$^{N\text{-}ter}$), should be considered a full-length interactor.

Quantitative data obtained from the different comparisons are represented in Vulcano plots, where Fold-change (X-axis, log_2Fold-change) and significance p-value (Y-axis, $-log_{10}$p-value) of all proteins detected are plotted (Figure 72). As a quality control of the experiment, we checked the quantitative data of avidin, BioID and the endogenously biotinylated proteins (piruvate carboxilase (PC) and methylcrotonyl-CoA carboxylase (MCCC1)) that, as expected, did not show significant changes in their abundance (-2<log2 ratio<2) (Figure 72), except for the PC and MCCC1carboxylases in the UBE3A N-terminal interactors' analysis (log 2 ratio > 2; p-value<0.05) (Figure 72A).

There were a number of proteins that were significantly more abundant in the full-length samples in comparison to the N-ter or C-ter samples (Figure 72, right part of the plots). From those, only the ones that complied the reliability criteria described above (>1 unique peptide, 3-0 o 2-2, and 4-fold change) were considered as putative substrates, and hence, colored in green filled dots. Finally, proteins identified with a single unique peptide or did not fulfill the 3-0/2-2 criteria were represented with empty dots (Figure 72). Therefore, we considered as putative N-terminal and C-terminal proteins the ones represented with green filled dots in Figure 72A and 72B, respectively. By constrast, following the same criteria, proteins displaying a significantly lower ratio (log2 ratio < -2; p-value<0.05) were highlighted in red.

A

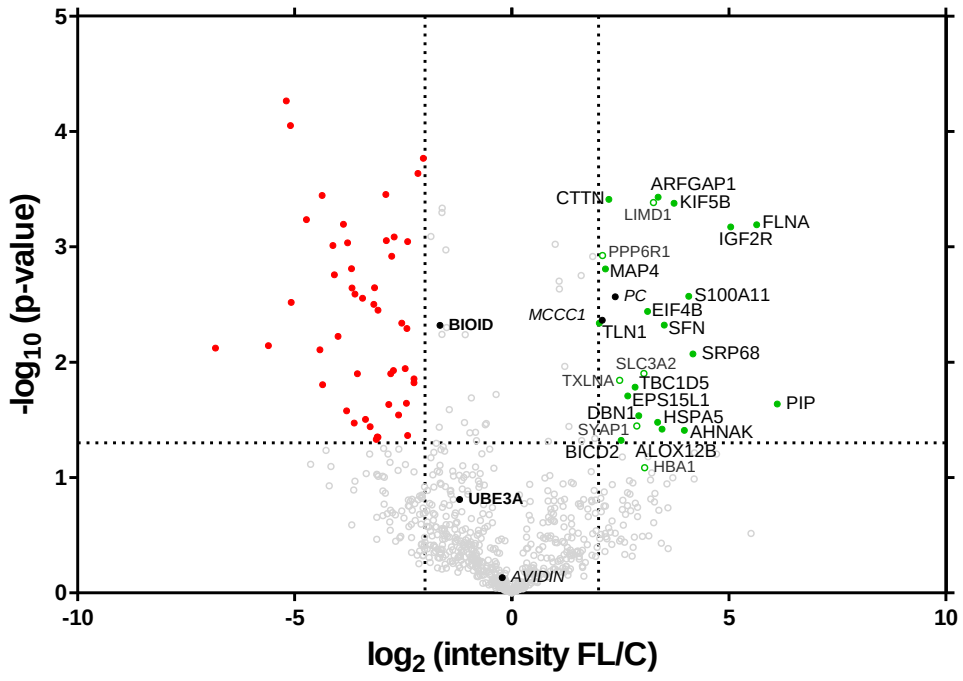

B

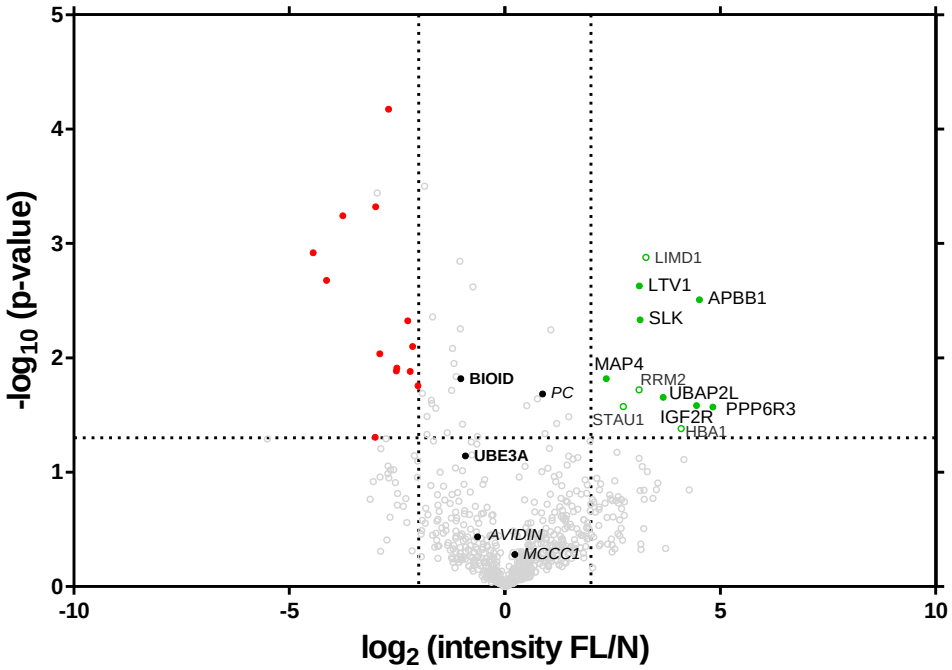

Figure 72. Identification of candidate UBE3A interactors in HEK293T cells. Comparison of the relative abundance of proteins detected by MS in distinct experiment conditions. UBE3A^{FL} over-expression relative to UBE3A$^{N\text{-}ter}$ overexpression (A) and UBE3A^{FL} over-expression relative to UBE3A$^{C\text{-}ter}$ overexpression (B). The Vulcano plots display the LFQ ratios in log2 scale (X-axis) and the t-test p-values in log10 scale (Y-axis). Threshold values are represented: fold-change > 4, vertical dashed line and statistical significance $p < 0.05$, horizontal dashed lane. Labeled filled dots represent confidently identified proteins whereas emply circles indicate proteins that do not comply the reliability criteria (>1 unique peptide + identified in replicates 3-0/2-2). Green and red colors indicate significantly more and less abundant proteins, respectively. Endogenously biotinylated proteins (PC and MCCC1), UBE3A, BioID and Avidin are shown with filled black dots.

In total, 34 UBE3A interactors were detected in the analysis, which are listed in Table 4; 23 N-terminal UBE3A interactors; 7 UBE3A C-terminal interactors and 4 UBE3A full-length interactors. As mentioned previously, we also checked if those UBE3A interactors significantly changed their abundance in the UBE3A$^{C\text{-}ter}$ vs UBE3A$^{N\text{-}ter}$ analysis (Figure 73).

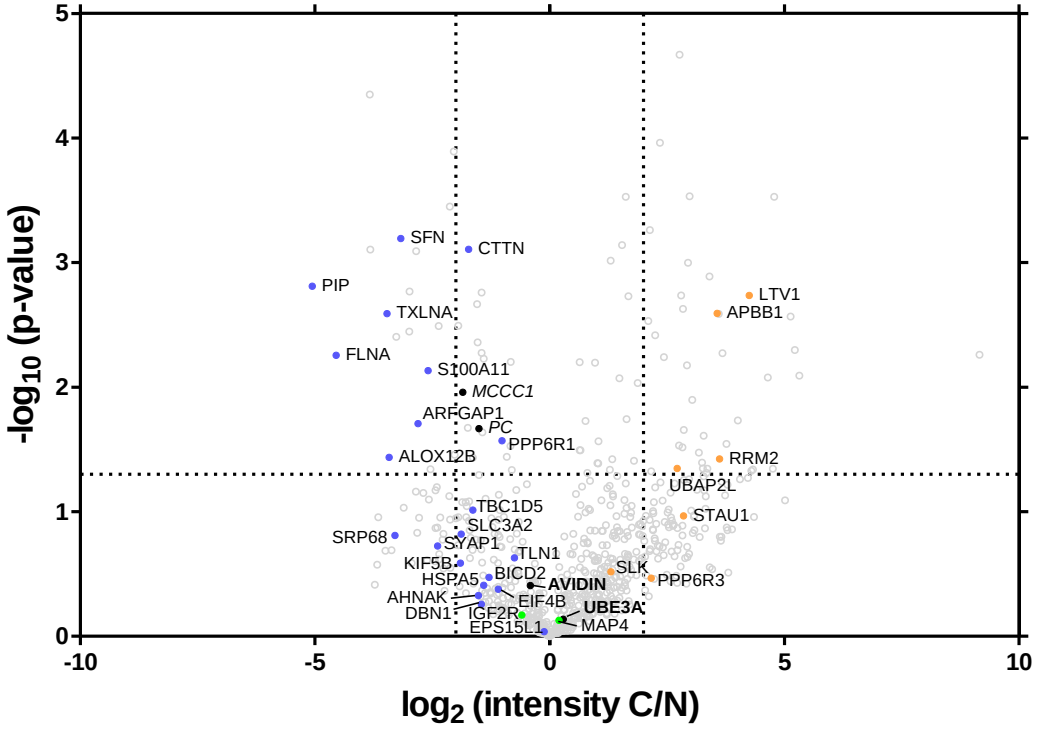

Figure 73. Comparison between UBE3A$^{C\text{-}ter}$ and UBE3A$^{N\text{-}ter}$ conditions to further corroborate UBE3A interactors. Comparison of the relative abundance of proteins detected by MS in UBE3A$^{C\text{-}ter}$ over-expression relative to UBE3A$^{N\text{-}ter}$ overexpression. The Vulcano plots display the LFQ ratios in log2 scale (X-axis) and the t-test p-values in log10 scale (Y-axis). Threshold values are represented: fold-change > 4, vertical dashed line and statistical significance $p < 0.05$, horizontal dashed lane. Labeled filled dots represent confidently identified proteins; N-terminal interactors (blue), C-terminal interactors (orange) and full-length interactors (green). Endogenous carboxylases (PC and MCC1), UBE3A and Avidin (black) are also ploted as controls.

7 out of 23 N-terminal interactors and 4 out of 8 C-terminal interactors showed a 4-fold increase in the UBE3A$^{C\text{-}ter}$ vs UBE3A$^{N\text{-}ter}$ analysis. Hence, those were the proteins considered as strong putative UBE3A interactors, and are listed in bold in Table 6. LIMD1 was only detected in the UBE3A^{FL} sample, meaning that it is a full-length interactor, so it was not present in this comparison.

Table 6. Criteria to consider UBE3A interactors based on different sample comparison (+++ more abundant, --- less abundant and not detected). And putative UBE3A interactors detected by mass spectrometry.

	UBE3A^{FL} vs UBE3A$^{C\text{-}ter}$	UBE3A^{FL} vs UBE3A$^{N\text{-}ter}$	UBE3A$^{C\text{-}ter}$ vs UBE3A$^{N\text{-}ter}$
Full length interactor	+++	+++	Not detected
N-ter interactor	+++	Not detected	---
C-ter interactor	Not detected	+++	+++

	Gene name	log_2 Fold-change	$-log_{10}$ p-value	Exclusion reason
UBE3A N-TERMINAL INTERACTORS	PIP	6,11	1,64	
	FLNA	5,64	3,19	
	SRP68	4,17	2,07	
	S100A11	4,07	2,57	
	AHNAK	3,98	1,41	
	KIF5B	3,74	3,38	
	SFN	3,51	2,32	
	ALOX12B	3,46	1,42	
	ARFGAP1	3,37	3,43	
	HSPA5	3,36	1,48	
	EIF4B	3,13	2,44	
	DBN1	2,92	1,54	
	TBC1D5	2,84	1,78	
	EPS15L1	2,67	1,71	
	BICD2	2,51	1,32	
	CTTN	2,24	3,41	
	TLN1	2,01	2,34	
	SLC3A2	3,04	1,90	1 unique peptide
	SYAP1	2,88	1,45	Not 3-0/2-2
	TXLNA	2,48	1,84	Not 3-0/2-2
	PPP6R1	2,09	2,92	1 unique peptide
UBE3A C-TERMINAL INTERACTORS	APBB1	4,52	2,51	
	PPP6R3	4,82	1,57	
	UBAP2L	3,67	1,65	
	LTV1	3,12	2,63	
	SLK	3,14	2,33	
	RRM2	3,11	1,72	Not 3-0/2-2
	STAU1	2,75	1,57	Not 3-0/2-2
FULL-LENGTH INTERACTORS	IGF2R	5,04	3,17 FL/N-ter	
		4,45	1,58 FL/C-ter	
	MAP4	2,16	2,81 FL/N-ter	
		2,35	1,82 FL/C-ter	
	LIMD1	3,26	3,38 FL/N-ter*	1 unique peptide
		3,27	2,88 FL/C-ter*	1 unique peptide
	HBA1	4,09	1,38 FL/N-ter	Not 3-0/2-2
		3,06	1,08 FL/C-ter*	p-value < 0.05

3-0/2-2 = proteins detected at least in all the replicates of one experimental condition (3-0), or in two out of the three replicates in both samples (2-2).

In order to validate mass spectrometry data, we aimed to perform a co-immunoprecipitation assay by pulling down GFP-tagged LIMD1 and checking if UBE3A was co-purified. Western blot analysis demonstrated that UBE3A was co-purified together with LIMD1, even if GFP-LIMD1 levels were below the detection threshold. PSMA5 (previously described to interact, *Chapter 1*), was used as a positive control. UBE3A did not copurify with the rest of control samples pCDNA, GFP and UBE2L3 (previously described not to interact, *Chapter 1*) (Figure 74).

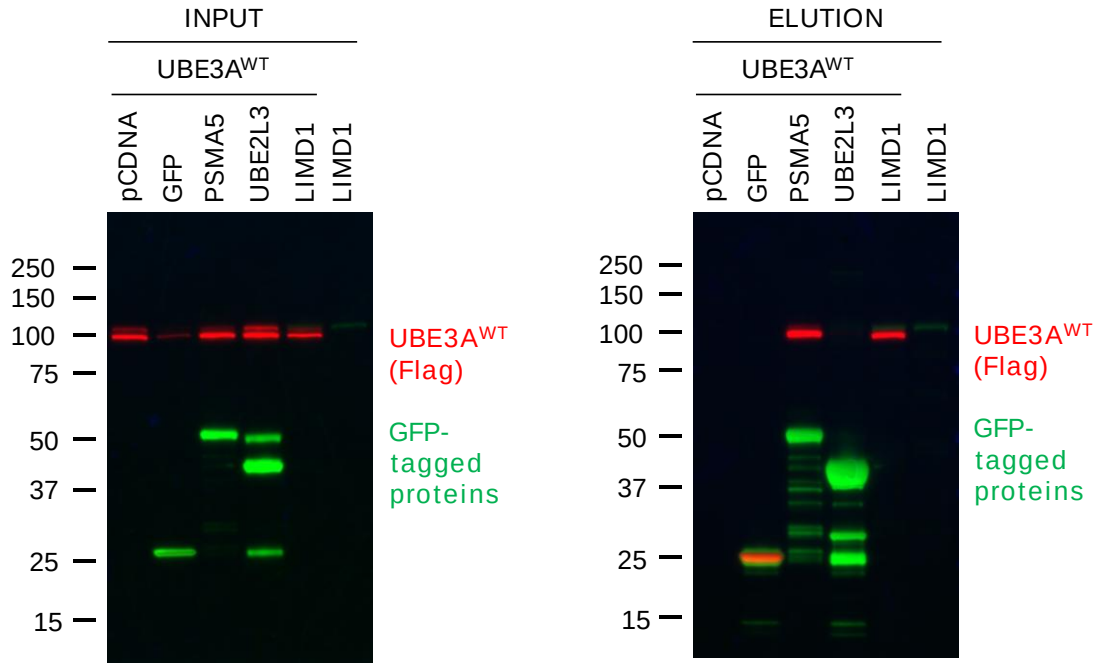

Figure 74. LIMD1 is a UBE3A interactor in HEK293T cells. FLAG-UBE3A (100 kDa) and, GFP (25 kDa) or GFP-tagged substrates PSMA5 (50 kDa), UBE2L3 (40 kDa) or LIMD1 (100 kDa) were co-transfected in HEK293T cells. Whole cells lysates were analysed by immunobloting with anti-FLAG (red) and anti-GFP (green) antibodies, to confirm transfection (Input, left panel). Co-immunoprecipitation of UBE3A putative interactor LIMD1 together with the negative (pCDNA, GFP and UBE2L3) and positive (PSMA5) controls. Co-IP was performed using GFP beads, and eluted samples were immunobloted against anti-GFP, to check substrates, and anti-FLAG to check for UBE3A.

This has been the first time we applied the BioID strategy in our research group, and we have demonstrated that it can be successfully used to identify protein interactors. After validating the strategy in HEK293T cell line, we wanted to move a step forward and apply the BioID strategy in mice. Although our first attempt to generate mice with the BioID transgene failed, our research group is now working on neuronal primary cell cultures in order to successfully identify UBE3A interactors in mice.

Chapter 4

Determination of the human full-length UBE3A structure

UBE3A is an E3 ligase that ubiquitinates its substrates mainly to target them for degradation. It is a member of the HECT type E3 ubiquitin ligases; it interacts with the E2 conjugating enzyme through its HECT domain and it binds ubiquitin to transfers it into substrates. In order to understand the mechanism underlying UBE3A-mediated ubiquitination, many studies focus on resolving the structural domains of UBE3A. The HECT domain located at the C-terminus is well characterized; it consists of two lobes (N and C lobes) with a catalytic site at their junction and an E2-binding site on the N-lobe of the domain (Huang et al., 1999, Lorenz, 2018). The N-terminal sequence contains the AZUL (Amino-terminal Zn-finger of Ube3a) domain, formed by a previously unknown Zn-finger, which may potentially play a role in substrate recognition (Lemak et al., 2011).

Most of the Angelman-associated point mutations lie within the carboxyl-terminal HECT domain of the protein and disrupt its catalytic activity. However, some mutations reported in AS patients locate in one of the conserved cysteines (C44) of the AZUL domain (Lemak et al., 2011) as well as in the non-catalytic amino-terminal portion (residues 1–544). These mutations may affect substrate binding, subcellular localization, or protein stability (Cooper et al. 2004; Bai et al. 2011).

Although HECT and AZUL domains have been characterized, the full-length structure of UBE3A remains unknown. Substrate recognition may be mediated through the amino terminal of UBE3A, and point mutations within this region cause AS. Therefore, it is of vital importance to have the structural information of the full-length UBE3A. It may decipher the mechanism by which UBE3A regulates substrate binding, and in consequence, it may open new therapeutic approaches.

UBE3A encodes 3 isoforms through alternative splicing that differ in length and sequence (Yamamoto et al., 1997). Isoform 1 encodes the shortest polypeptide, with 850 residues. Isoforms 2 and 3 include an additional amino-terminal extension of 23 and 20 residues, respectively. In this study, aiming to decipher the structure of UBE3A, isoform 1, kindly provided by Dr. Tomaic, was used.

The aim of this part of the project is to set up a protocol to resolve the structure of UBE3A. For that purpose, we have collaborated with an expert on the

field, Adriana Rojas, from the Macromolecular Crystallography Platform in CICbioGUNE, Zamudio.

Properties of partial structural regions may differ from the whole protein ones, so although previous studies were considered (Huang et al., 1999; Lemak et al., 2011), we set up our own protocol for human UBE3A full-length expression and purification (Figure 75). We first expressed hUBE3A protein in bacteria. UBE3A was sequentially purified, and then, purified UBE3A was used in a pre-crystallization test to check for the best crystallization condition. Finally, a crystallization experiment was performed.

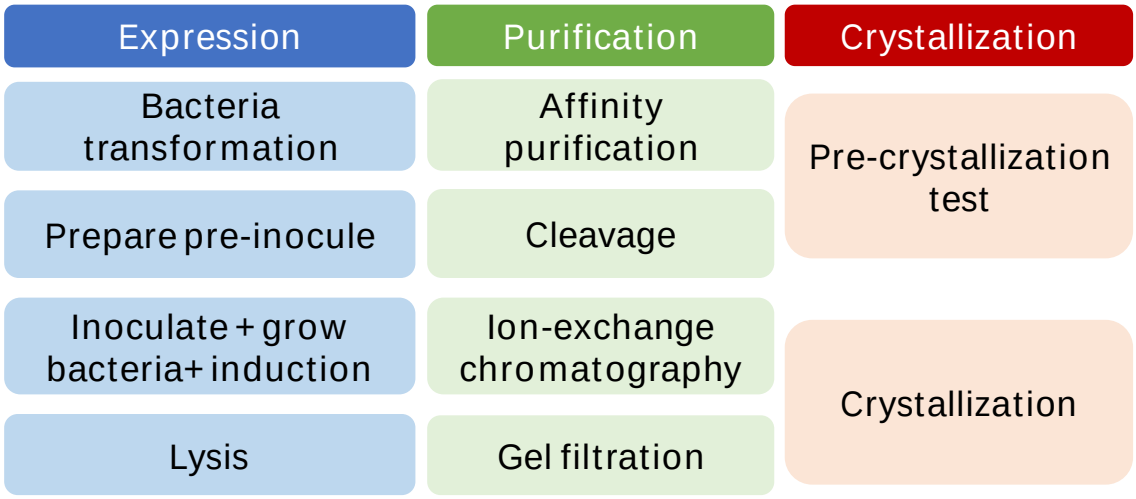

Figure 75. Workflow for hUBE3A purification and crystallization. The three main steps for UBE3A crystallization are highlighted in colours: protein expression (blue), purification (green) and crystallization (red). Different stages in each step are represented.

1. hUBE3A expression in bacteria

To get the best purification efficiency, we used three distinct expression plasmids: His-Parallel2 (HisP2), GST-Parallel2 (GST-P2) and His-SUMO (Sheffield et al., 1999;Walls eta Malakhov et al., 2004). These fusion expression vectors contain the most frequently used affinity tags (His_6 peptide and glutathione S-transferase (GST)) that enable fusion proteins to be efficiently purified. By contrast, His-SUMO expression vector is mainly used to enhance protein solubility and aid purification, since attachment of SUMO to the N-terminus of proteins dramatically enhances their expression and solubility (Malakhov et al., 2004).

We first cloned hUBE3A into His-P2, GST-P2 and His-SUMO vectors, and transformed them into *E.coli* DE3 bacteria, as well as into an improved chemically competent *E.coli* T1R strain. Due to the better transformation efficiency, T1R *E.coli* strain was used for the next steps. After collecting the cells, we lysated and sonicated the sample to crash the bacteria, and centrifuge to discard membrane debris (Figure 76, Pellet, P). Pellet samples were kept for SDS-PAGE, while supernatants were used for next purification steps.

2. Purification

2.1 Affinity purification

Affinity purification is a method of separating a biochemical mixture based on a highly specific interaction between antigen and antibody, enzyme and substrate, receptor and ligand, or protein and nucleic acid (Ninfa et al., 2009). Purification methods using His-P2 and His-SUMO expression vectors are based on the strong interaction between the histidine tag (His_6) and nickel containing agarose resin (Ni-NTA). Ni-NTA agarose uses nitrilotriacetic acid (NTA), a chelating ligand, in an agarose matrix to bind Ni^{2+} ions by its four coordination sites. Similarly, GST-tagged fusion proteins are purified based on the ability of GST (a 26 kDa enzyme) to bind its substrate, glutathione (GSH), which is immobilized to a solid support, such as cross-linked agarose beads.

We loaded the Ni-NTA or glutathione containing agarose resin into a column, and equilibrated them before using for purification. Next, cell lysate was loaded into the column whereas part of it was kept for further analysis by SDS-PAGE (Figure 76, SN). We also collected the flow through (Figure 76, FT) for further analysis of unbound proteins by SDS-PAGE. Then, a washing step was performed to discard the contaminants that may have been interacting non-specifically with the resin. This washing fraction (Figure 76, W) was also kept to check by SDS-PAGE. Moreover, a sample from the resin was taken as control (Figure 76, R). Finally, we eluted the hUBE3A fusion proteins, and part of it was stored for SDS-PAGE analysis (Figure 76, E).

GST-UBE3A can be dissociated and recovered from the column by adding excess of reduced glutathione. The free glutathione competitively displaces the GST fusion protein allowing it to emerge from the affinity column. Likewise, as in His-UBE3A and His-SUMO-UBE3A fusion proteins the electron donor group on the histidine imidazole ring forms bonds with the immobilized Ni^{2+}, adding free imidazole to the column buffer is sufficient to elute both fusion proteins from the column. Once again, after all elutions, a fraction of the sample from the resin was taken to assess by SDS-PAGE the efficiency of the elution (Figure 74, R*).

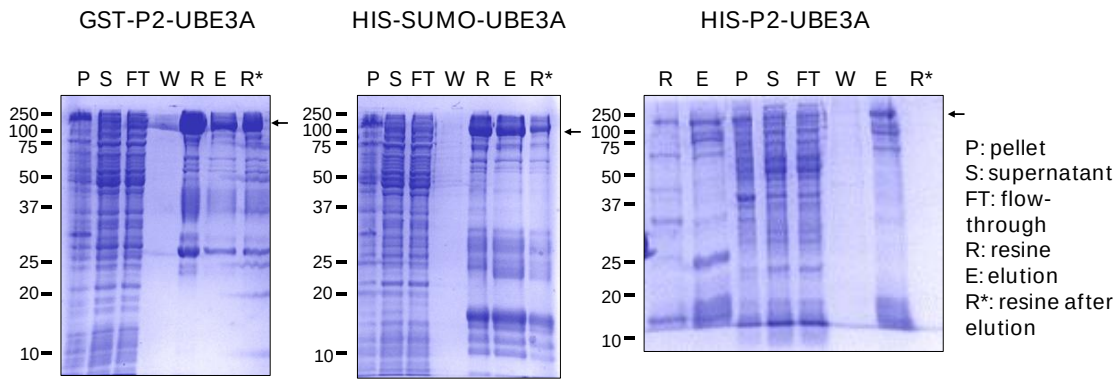

Figure 76. SDS-PAGE for collected samples during the affinity purification protocol. Samples collected during the protocol were run on a SDS-PAGE electrophoresis and the gel was coomassie stained. P, pellet; SN, supernatant; FT, flow-through; R, resin; E, elution; R*, resin after elution. Arrowhead indicates hUBE3A band at 100 kDa.

Coomassie staining of the SDS-PAGE with all the samples collected during the affinity purification indicate that although proteins could be detected in the pellet (P), most of them were present within the soluble fraction (SN) (Figure 76). The vast majority of proteins did not bind to column and hence, were detected in the flow-through (FT). After the washing (W) step, barely any proteins were observed (Figure 76). Samples of resin (R) verified that UBE3A was linked to the resin. Finally, eluted fractions (E) demonstrated that UBE3A was successfully purified, and this was corroborated by checking the resin after elution (R*), which showed only a residual amount of UBE3A still attached. In the GST construct sample, UBE3A protein amount attached to the resin was higher, meaning that the elution was not as efficient as with the other two constructs (His-SUMO and His-P2)(Figure 76). Altogether, these results indicate that, overall, the purification of hUBE3A has been successful.

2.2 Cleaveage

After affinity purification, hUBE3A fusion proteins were cleaved to remove the affinity tag. GST and SUMO tags increase the size of the construct in 27 kDa and 11.5 kDa, respectively, and it is necessary to remove them not to interfere with crystallization. On the contrary, it is not necessary to remove the His-tag, since only adds 6 aminoacids to hUBE3A and it will not affect significantly to UBE3A structure. Therefore, only GST-hUBE3A and SUMO-UBE3A constructs were cleaved. GST-hUBE3A plasmid was cleaved by highly specific Tobacco Etch Viral protease (TEV), while SUMO-UBE3A fusion protein was cleaved by SUMO specific protease 2 (SENP2). We incubated them with their corresponding enzymes overnight on a dialysis buffer, and were loaded again into the column to exclude the tags; tags would be attached to the column, while cleaved samples would be present in the flow-through.

Samples were assessed by SDS-PAGE to verify that the fusion-proteins were successfully cleaved, and that UBE3A was effectively recovered for further purification steps (Figure 77). We first loaded the sample after cleaveage, but before passing it through the column, in order to know the total amount of UBE3A in the samples. In both cases (GST-hUBE3A and SUMO-hUBE3A), we could observe a clear band at 100 kDa, corresponding to the hUBE3A protein (Figure 77, E). GST-hUBE3A construct was successfully cleaved with TEV protease; UBE3A levels remained constant in the flow-through, while contaminant proteins were discarded (Figure 77, FT). This was corroborated by analyzing the resin, which showed a minimal lost of UBE3A protein (Figure 77, R). In contrast, SENP2 cleaveage was less effective and, although UBE3A protein was recovered, high amount of it was detected attached to the column (Figure 77, R in SENP2). TEV (27 kDa) and SENP2 (30 kDa) purified proteins were also run on the SDS-PAGE to identify the band at their corresponding size (Figure 77, C).

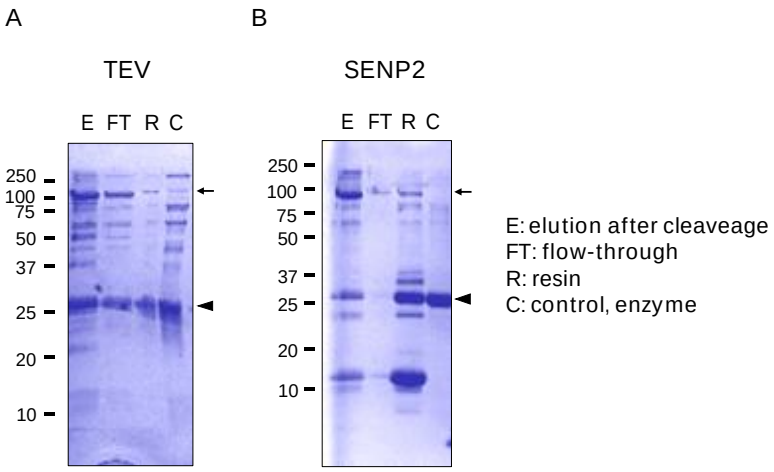

Figure 77. SDS-PAGE for samples before and after tag cleaveage. Samples collected before and after TEV or SENP2 cleaveage were run on a SDS-PAGE electrophoresis and the gel was coomassie stained. E, elution after cleaveage; FT, flow-through; R, resin; C, control (TEV or SENP2). Arrows indicate hUBE3A band at 100 kDa, and triangles indicate the size of the enzymes (TEV and SENP2), around 30 kDa.

2.3 Q-HP: ion-exchange chromatography

We next aimed to enrich purified hUBE3A by ion-exchange chromatography. Ion chromatography separation is based on the reversible interaction between a charged molecule (our protein of interest, hUBE3A) and an oppositely charged chromatography medium. A continuous gradient of NaCl is then used to elute bound substances differentially.

To select conditions for ion-exchange chromatography, we first needed to choose the correct ion exchanger or column. Previous experiments with partial UBE3A proteins demonstrated effective purification using pH 7.5 (Huang et al., 1999). Taking into account that hUBE3A isoelectric point is 5.12 (Protparam web tool), hUBE3A will be negatively charged at pH 7.5. In consequence, we opted for an anion-exchange column that is positively charged (Q-HP column). Another important aspect is to ensure that initial salt concentration allows hUBE3A binding to the column. Therefore, we started with no salt, and continuously increased its concentration up to 1 M NaCl.

Chromatography for hUBE3A (originated from GST-hUBE3A) purification, detected a UV absorbance increase in the flow-through sample, although no protein could be observed by SDS-PAGE (Figure 78, peak 1, fractions X_1 and X_2). During the salt gradient to elute proteins, two main peaks were detected (Figure

78, peak 2 and 3). The bands detected by SDS-PAGE on the second peak (Figure 78, peak 2, fractions B_{10} and B_9) did not correlate with the appropriate size for UBE3A, but mass spectrometry analysis resulted in the detection of hUBE3A, probably because of partial degradation during the purification protocol (data not shown). The third peak (Figure 78, peak 3, fractions C_2 and C_3) visualized a strong band at the size of hUBE3A, and was confirmed by mass spectrometry to be hUBE3A. Therefore, we concluded that hUBE3A elutes at 34 ms/C conductance, with a salt concentration of 300 mM NaCl. Finally, no hUBE3A was significantly detected in the sample eluted upon the final washing step (Figure 78, peak 4, fractions D_3 and D_1).

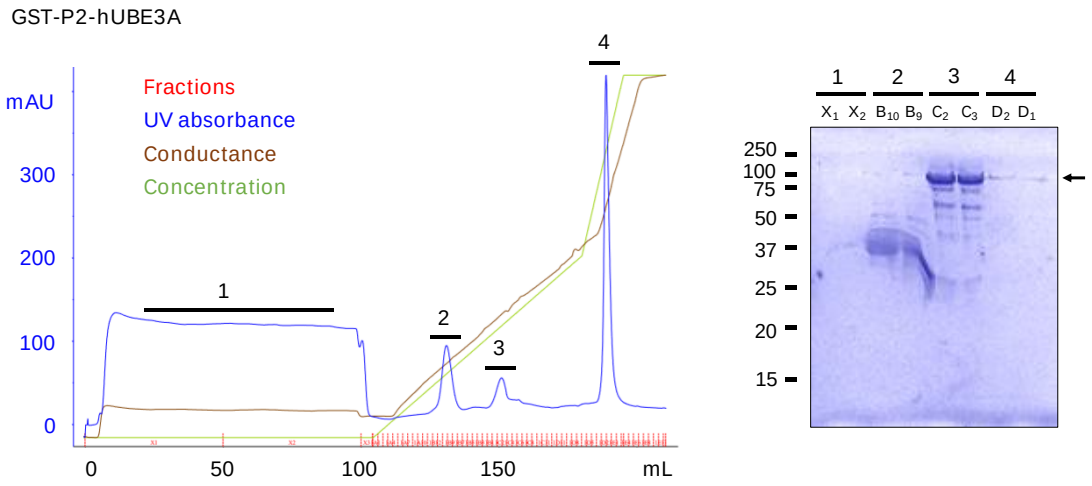

Figure 78. Ion-exchange chromatography of hUBE3A affinity purified from GST-P2 vector. Anion exchange chromatography (5 ml HiTrap Q-HP column). Starting buffer: 25 mM Tris-HCl buffer, pH 7.4; elution saline gradient: 0.0-1 M of sodium chloride in the starting buffer. Flow rate, 2.0 ml/min. Fractions of 2 ml were collected. Four differentiated peaks were detected (1-4), and two fractions were collected from the middle of each peak: X_1 and X_2 (peak 1), B_{10} and B_9 (peak 2), C_2 and C_3 (peak 3), D_2 and D_1 (peak 4). SDS-PAGE and coomassie staining indicate that hUBE3A was mainly detected in the 3rd peak. Blue, UV absorbance (280 nm); red, collected fractions; brown, conductance; green, NaCl concentration.

Purification of hUBE3A (originated from His-SUMO) by anion exchange chromatography resulted in the detection of five peaks (Figure 79, peaks 1-5). SDS-PAGE demonstrated that hUBE3A was not present in the flow-through (Figure 79, fractions X_{1-3}) in the first two peaks, nor in the washing step peak (Figure 79, peak 1 fraction B10, peak 2 fraction B2 and peak 5, fraction D1). It was mainly detected in the 3rd peak (Figure 79, fractions C_{3-5}), although residual amount of the protein could be also observed in the 4th peak (Figure 79, peak 4,

fraction C_9).In line with previous purification results, once again UBE3A eluted at 300 mM NaCl.

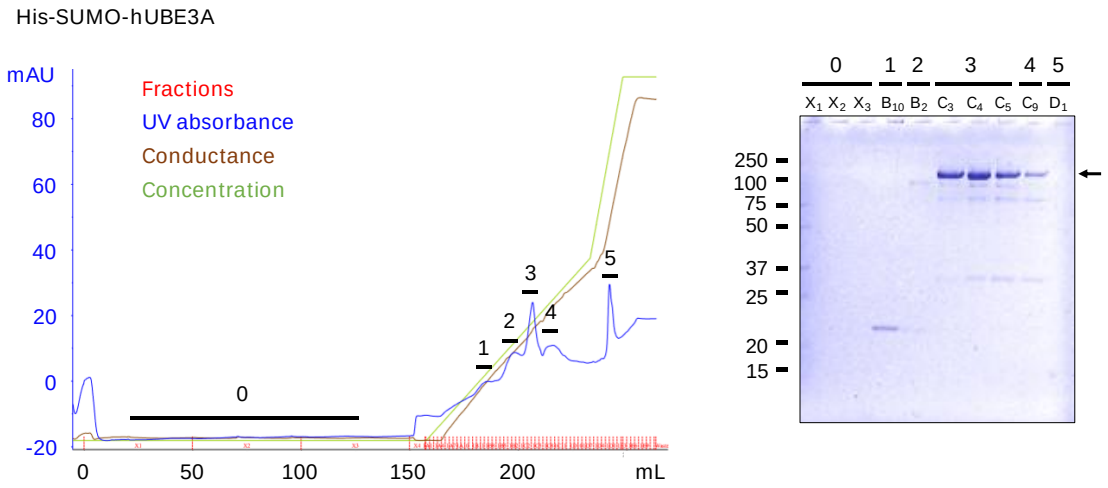

Figure 79. Ion-exchange chromatography of hUBE3A affinity purified from His-SUMO vector. Anion exchange chromatography (5 ml HiTrap Q-HP column). Starting buffer: 25 mM Tris-HCl buffer, pH 7.4; elution saline gradient: 0.0-1 M of sodium chloride in the starting buffer. Flow rate, 2.0 ml/min. Fractions of 2 ml were collected. Five peaks were differentiated, and fractions from each peak were run on a SDS-PAGE and coomassie stained. hUBE3A was mainly detected in the 3rd peak, fractions C_{3-4}. Blue, UV absorbance (280 nm); red, collected fractions; brown, conductance; green, NaCl concentration.

Finally, hUBE3A (originated from His-P2) purification through ion-exchange chromatography discerned four differentiated peaks (Figure 80, peaks 1-4). As shown in Figure 80, peaks 1 and 2, corresponding to the flow through and proteins eluted with low salt concentration, respectively, are rich in proteins but apparently do not contain hUBE3A. By constrast, fractions corresponding to 3th peak, and collected upon elution with 300 mM NaCl, show a band corresponding to the size of UBE3A, but also a further band around 40 kDa (Figure 80, peak 3, fractions C_{3-5}).

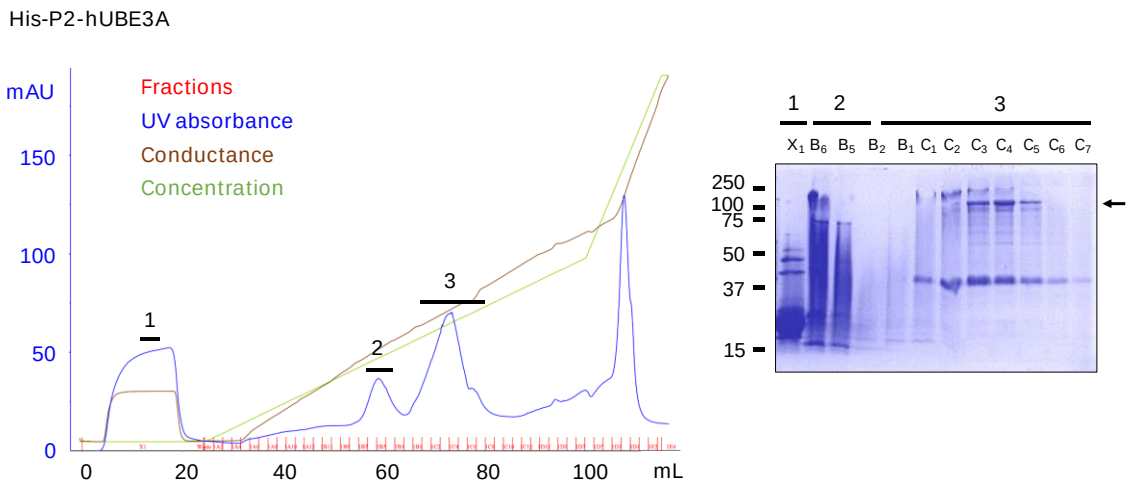

Figure 80. Ion-exchange chromatography of hUBE3A affinity purified from His-P2 vector. Anion exchange chromatography (5 ml HiTrap Q-HP column). Starting buffer: 25 mM Tris-HCl buffer, pH 7.4; elution saline gradient: 0.0-1 M of sodium chloride in the starting buffer. Flow rate, 2.0 ml/min. Fractions of 2 ml were collected. Four main peaks were detected in the chromatography, and SDS-PAGE of the fractions together with coomassie staining showed high amount of proteins in the first two peaks, while UBE3A was detected only in the 3rd peak (fractions C_3-C_5). Blue, UV absorbance (280 nm); red, collected fractions; brown, conductance; green, NaCl concentration.

2.4 Gel filtration chromatography

Size exclusion chromatography (SEC), also known as gel filtration, separates molecules by differences in size as they pass through a resin packed in a column. After ion-exchange chromatography, UBE3A containing fractions derived from the same construct were pooled and run on gel filtration column. Based on UV absorbance of the eluted material, a single prominent peak was detected in GST-P2 and His-SUMO construct-based purifications, indicating that UBE3A was efficiently purified in both cases (Figure 81A and 81B). Moreover, SDS-PAGE and coomassie staining of the eluted fractions demonstrated clear bands at the size of UBE3A (100 kDa) in those prominent peaks, which eluted at 12,5 mL (Figure 81A and 81B). All fractions corresponding to the both hUBE3A protein peaks were pooled and concentrated for crystallization experiments (Figure 81A, fractions B_2-C_1 and Figure 81B, fractions B_2-C_2). On the contrary, purification of His-P2 resulted in the detection of several peaks indicating the presence of contaminants (Figure 81C), as already detected by SDS (Figure 81 inset), so these samples were discarded for further analysis.

A

GST-P2-hUBE3A

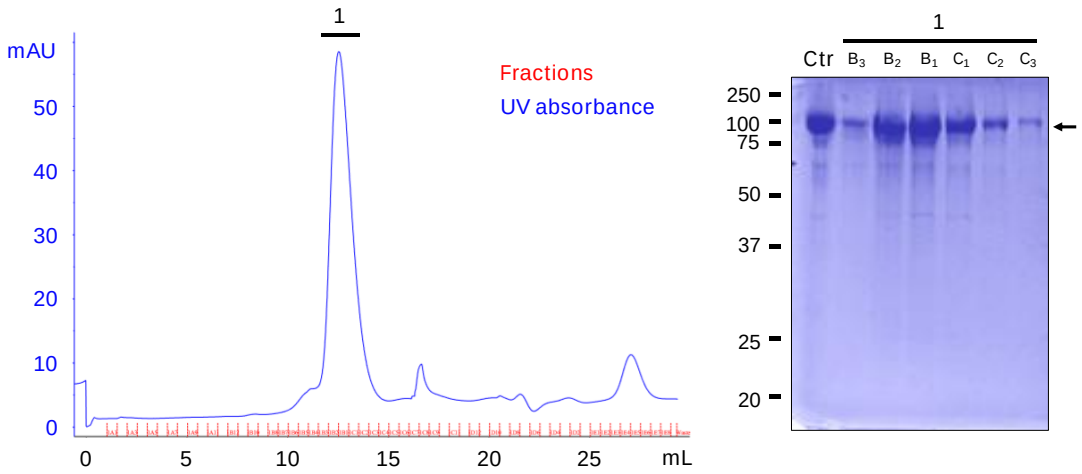

B

His-SUMO-hUBE3A

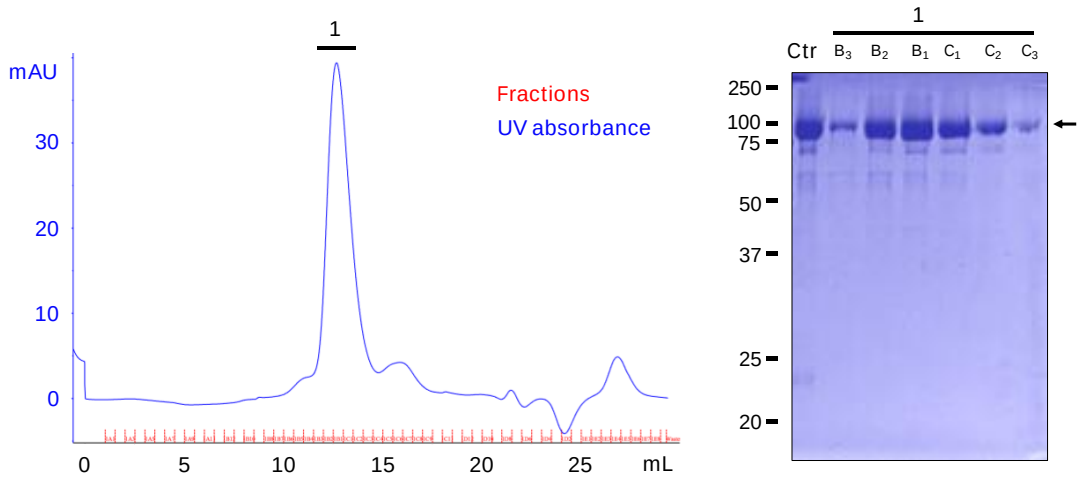

C

His-P2-hUBE3A

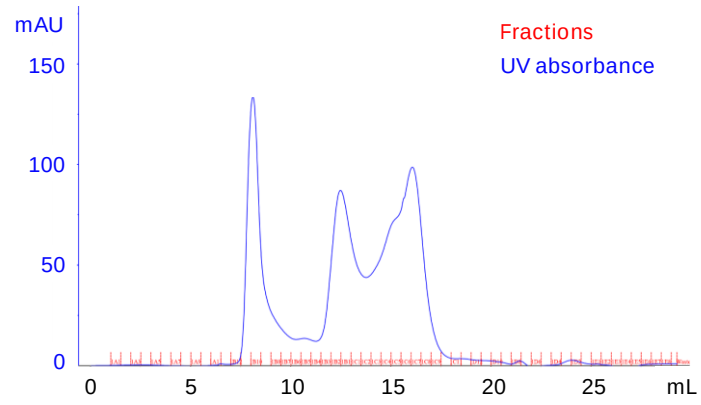

Figure 81. Gel filtration based purification of hUBE3A protein. Elution profile of hUBE3A from a HiLoad 10/30 Superdex 200 Gel Filtration column. Fractions (B_3-C_3) were collected from (A) GST-P2, (B) His-SUMO and (C) His-P2 based purifications, and together with a control sample (Ctr) containing UBE3A protein, they were resolved on a SDS-PAGE and stained with coomassie. hUBE3A protein eluted at 12,5 mL. Blue, UV absorbance (280 nm); red, collected fractions.

3. Crystallization

3.1 Pre-crystallization test

The PCT (Pre-Crystallization Test) is used to determine the appropriate protein concentration for crystallization screening. For that purpose the sample protein is mixed with four different reagents (A1, A2, B1 and B2) provided by the PCT kit. The precipitates formed with each of those unique reagents, indicate if the protein concentration used is appropriate for crystallization. Highly concentrated samples can result in amorphous precipitates, while extremely diluted samples can result in clear drops. According to manufacturer's instructions, the ideal drop should have a microcrystalline or light granular precipitate throughout the drop, and the crystallization screening can be performed if A1/B1 shows a clear drop, together with a light granular precipitate in A2/B2 condition. We tested 2 mg/µL of hUBE3A protein in distinct precipitant solutions (A1, A2, B1 and B2). A1 showed light granular precipitate, while A2 resulted in heavy amorphous precipitate (Figure 82). In contrast, B1 showed a clear drop and B2 resulted in light granular precipitate (Figure 82). Therefore, combination of B1 (clear drop) and B2 (light granular precipitate) demonstrated that 2 mg/µL of hUBE3A protein is suitable for the crystallization experiment. Moreover, granular drops were obtained with reagents containing PEG (polyethylene glycol), meaning that PEG-based packs could be more successful in the crystallization experiment.

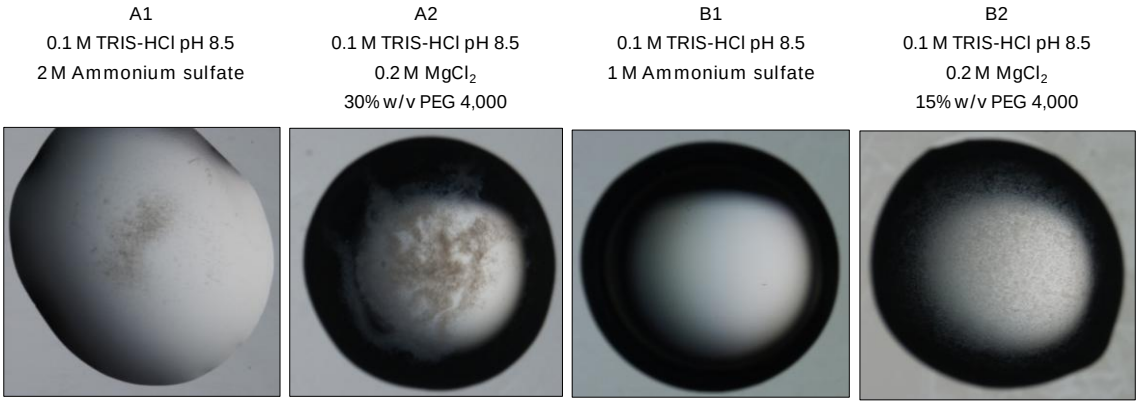

Figure 82. Pre-crystallization test of hUBE3A protein. Hanging-drop vapor diffusion technique was employed at 18 °C by mixing 1 µL purified hUBE3A (2 mg/mL) and 1 µL precipitant solutions: A1 (0.1 M TRIS hydrochloride pH 8.5, 2.0 M Ammonium sulfate), A2 (0.1 M TRIS hydrochloride pH 8.5, 0.2 M Magnesium chloride hexahydrate, 30% w/v Polyethylene glycol 4,000), B1 (0.1 M TRIS hydrochloride pH 8.5, 1.0 M Ammonium sulfate) and B2 (0.1 M TRIS hydrochloride pH 8.5, 0.2 M Magnesium chloride hexahydrate, 15% w/v Polyethylene glycol 4,000). A1 and B2 showed light granular precipitate, A2 showed heavy amorphous precipitate and B1 was clear. Manufacturer's instructions recommend to perform the screen with the established concentration in case A1/B1 is clear, and A2/B2 has light granulated precipitate.

3.2 Screening for crystallization conditions

To achieve diffraction-quality hUBE3A crystals, different crystallization conditions were screened using hanging-drop vapour diffusion technique. 2 mg/uL hUBE3A protein concentration was used and 96-well plates for Morpheus, PACT, Proplex and Ammonium sulphate packs were tested (Supplementary Document 1). Morpheus, PACT and Proplex screening packs contain PEG as precipitant, and they were chosen due to the affinity of hUBE3A for PEG-based reagents in the pre-crystallization test. In addition, ammonium sulphate based pack was also tested. However, none of the 384 conditions tested generated hUBE3A protein crystals for X-ray diffraction analysis. At this point we reconsidered the project, and decided that crystallizing UBE3A together with one of its substrates would be a better approach, since the substrate may stabilize the non-organized regions and enable the crystallization of the full-length structure. In addition to working on the new approach, we attempted to search for UBE3A structure information using a recently developed bioinformatics prediction tool.

3.3 Structure determination

Recently, a AlphaFold protein structure database has been developed by DeepMind and EMBL-EBI (https://alphafold.ebi.ac.uk/). It is an artificial intelligence system that predicts a protein's 3D structure from its amino acid sequence. It regularly achieves accuracy competitive with experiment (Jumper et al., 2021).

Our screening for crystallization conditions did not generate any diffraction-quality hUBE3A crystals. This is in line with the attempts of other research groups, that only managed to solve specific parts of the hUBE3A protein, such as AZUL or HECT domains (Huang et al., 1999; Lemak et al., 2011). Therefore, we employed AlphaFold database to search for human UBE3A predicted structure. As expected, HECT and AZUL domains were successfully predicted, but there was no 3D structure prediction for the rest of the sequence (Figure 83). Crystallization of UBE3A together with one of its substrates may improve its stability, and in consequence, improve the chances of resoluting the full-length crystal structure of human UBE3A, as binding of these unstructured regions might facilitate crystal packing.

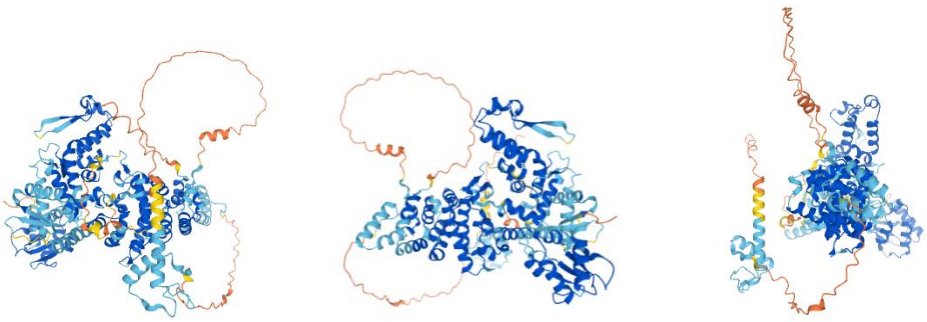

Figure 83. Alphafold human UBE3A full-length predicted structure. AlphaFold produces a per-residue confidence score (pLDDT) between 0 and 100; dark blue (very high, pLDDT>90), light blue (high, 90>pLDDT>70), yellow (low, 70>pLDDT>50) and orange (very low, pLDDT<50). Some regions below 50 pLDDT may be unstructured in isolation. Front, back and side view of human UBE3A structure is shown.

Although we could no achieve the aim of crystallizing UBE3A full-length structure in this Chapter 4, we stablished a successfull purification protocol that will enable the future crystallization experiments planed for UBE3A structure resolution together with its substrates or interactors.

5. Kapitulua

UBE3A gainadierazten duten saguen portaeraren karakterizazioa

Angelman sindromea (AS) gaixotasun neurologikoa da, eta Espektro Autistako gaixotasun (ASD) bezala kontsideratzen da. Beste ASDak bezala, pazienteek komunikazio eta elkarrekintza sozialerako defizita, portaera nahiz interes errepikakorrak, edota arazo sentsorialak azaltzen dituzte (American Psychiatric Association, 2013). UBE3A proteinaren gabezia portaera defizitekin erlazionatu izan da (Mulherkar and Jana, 2010), baina UBE3A genearen gehiegizko dosiak ere autismoaren ezaugarriekin erlazio zuzena duela ikusi dute (Smith et al., 2011; Xu et al., 2018).

ASren aurkako tratamendua lortzeko, beharrezkoa da farmakoen efizientzia testatzea, horretarako fenotipo esanguratsuak azaltzen dituzten sagu modeloak erabiliz. Hori dela eta, beharrezkoa da sagu modelo horien portaera modu sakonean ikertzea. Gure laborategian UBE3A emeki gainadierazten duen sagu modelo bat garatu dugu (UBE3A-OE). Modelo horrek, aldi berean, bioUb sistema ere gainadierazten du, UBE3Aren substratuak identifikatzeko asmoz (84. irudia).

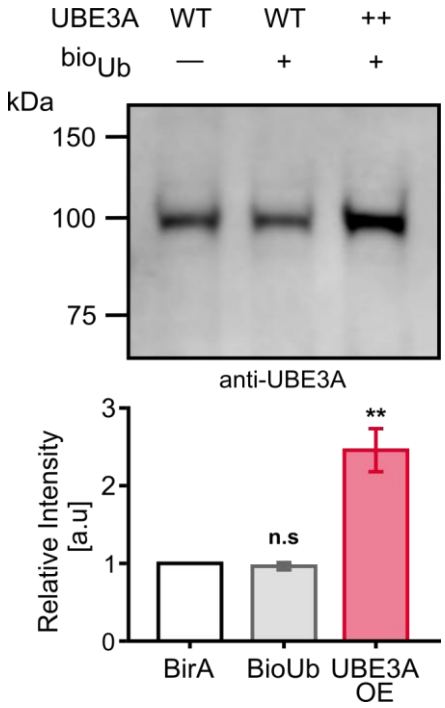

84. irudia. UBE3A-OE saguek UBE3A emeki gainadierazten dute. UBE3A-OE saguen garun osoekin burututako Western plapaketan, anti-UBE3A antigorputzak erakusten du UBE3A proteina emeki gainadierazten dela kontrol saguekin konparatuz. Hiru erreplika independenteren kuantifikazioak erakusten du UBE3Aren seinalea 2,5 aldiz aberastuta dagoela UBE3A-OE saguetan, kontrol saguetako (BirA eta BioUB) UBE3A endogenoarekin konparatuz. Berrikuspenean dagoen eskuizkributik hartutako figura (Lectez et al., 2022).

Hala ere, gaixotasunaren oinarrizko mekanismo molekularrak ulertzeko, eta etorkizunean sagu modelo horretan farmakoak testatu ahal izateko, UBE3A-OE sagu-lerroaren portaeraren karakterizazioa egitea beharrezkoa da. Oraintsu, Angelman sindromearen modelo diren saguentzako portaera test-multzo bat deskribatu dute (Sonzogni et al., 2018). Hala ere, Autismoaren Espektroko gaixotasunak ikertzeko erabiltzen diren portaera test orokorrak burutu ditugu (Kazdoba et al., 2016), gaian aditua den O. Peñagarikano doktorearen ikerketa-taldearekin kolaboratuz.

Portaera esperimentuak burutzeko sagu kontrolak (B6 eta BioUb bikoteak) eta UBE3A-OE saguak (bi UBE3A-OE bikote) erabili ditugu. Lehenik eta behin, portaera sozialak ikertu ditugu; ultrasoinu-bokalizazioak eta elkarrekintza sozialak (elkarganakoa eta orokorra). Jarraian, aktibitate lokomotorea ikertu dugu (abiadura eta distantzia). Azkenik, portaera errepikakorrak (*grooming*) eta minarekiko sentikortasuna aztertu ditugu.

1. Portaera soziala

Isolapenaren ondoriozko ultrasoinu bokalizazioak (UsVs), kumeek amarengandik banatzean igortzen dituzten larritasun-deiak dira. Haur-amaren arteko ahozko komunikazio-portaera ohikoa da, Autismo Espektroko gaixotasunetan garrantzitsua (Crawley, 2007; Shekel et al., 2021). Jaio ondorengo 7. egunean (P7 adinean) 5 minutuz grabatu ditugu ultrasoinu-bokalizazioak. Bokalizazioen zenbaketa eskuz burutu dugu, eta ez dugu atzeman desberdintasunik kontrol eta UBE3A-OE saguen artean (85. irudia).

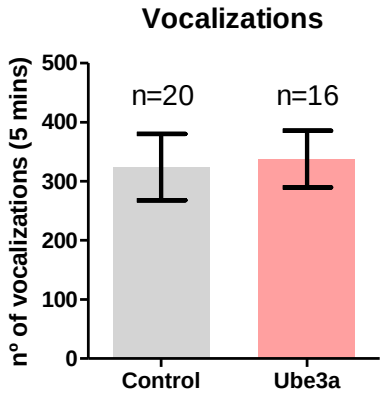

85. irudia. UBE3A-OE saguen ultrasoinu bokalizazio-emisioak normalak dira. P7 saguak soinurik gabeko ganbera batean jarri ditugu, eta ultrasoinu bokalizazioak neurtu ditugu 5 minutuz. Datuak eskuz analizatu ditugu, denbora-tarteko horretako bokalizazio-kopurua zehazteko. Analisi estatistikoak ez du ezberdintasun esanguratsurik erakutsi kontrolen eta UBE3A-OE saguen artean (kontrol saguak n=20, UBE3A-OE saguak n=16, *t*-testa, p-balioa > 0.05).

Jarraian, *Elkarganako elkarrekintza soziala* testaz baliatuz, portaera soziala aztertu dugu. Test horretan sagu bikote bakoitzak elkar aztertzen pasatzen duen denbora neurtzen da (File and Hyde, 1978). 25-28 eguneko adina (P25-P28) duten sagu bi esperimentazio eremu batean kokatzen dira, eta elkarrekintza sozialean (adib. *grooming* egiten, usaintzen...) pasatzen duten denbora eskuz neurtzen da 10 minutuz. Sagu horiek sexu, adin eta genotipo berekoak dira. Emaitzen arteko ezberdintasunak estatistikoki esanguratsuak ez diren arren, UBE3A-OE saguek tendentzia handiagoa erakusten dute sozializatzeko sagu kontrolekin konparatuz (86. irudia).

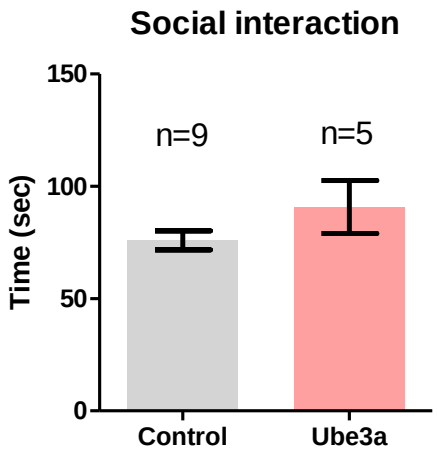

86. irudia. UBE3A-OE saguen elkarrenganako portaera soziala normala da. P25-28 kontrol saguak (zutabe grisa) eta UBE3A-OE saguak (zutabe gorria) esperimentazio eremuan kokatu ditugu, eta elkarrekintzan pasatzen duten denbora (segundutan) neurtu dugu, sagu bikote bakoitzarekin. Ez dugu ezberdintasun estatistikoki esanguratsurik behatu sagu lerro ezberdinen artean (kontrol sagu bikoteak=9, UBE3A-OE sagu bikoteak n=5, *t*-testa, p-balioa > 0.05).

Orokorrean sozializatzeko gaitasuna aztertzeko erabilitako hurrengo metodoa *Hiru ganberako testa* da. Hiru ganberadun kutxa bat erabiltzen da; izkina bateko ganberan ontzi huts bat jartzen da, aldiz, beste izkinako ganberan, ontzi barruan, sagu bat jartzen da. Modu horretan, ikertzen ari garen saguak beste saguarekin edo ingurune berri batekin denbora pasatzeko preferentzia neurtu

daiteke (Nadler et al., 2004). 40-50 eguneko adina duten saguak (P40-50) erabili ditugu esperimentu honetan, eta lerro bakoitzak ganbera bakoitza miatzen pasatzen duen denbora neurtu dugu. Bi sagu lerroek, bai UBE3A-OE eta bai kontrolek, denbora gehiago eman dute sagua dagoen ontzia miatzen, ontzi hutsarekin konparatuz (87A. irudia). Hala ere, ez dago estatistikoki esanguratsua den ezberdintasunik sagu lerro ezberdinen artean, ontzi hutsarekiko edo sozialarekiko preferentziari dagokienez. UBE3A-OE saguek ontzi sozialarekin gutxiago elkarrekiteko tendentzia ikusi daitekeen arren, ez dugu esplorazio-indizean aldaketarik ikusi. (87B. irudia), hortaz, tendentzia hori orokorrean esploratzen denbora gutxiago pasatzearen ondorio da. Esplorazio-indizeak (EI) esperimentu osoan zehar saguek sozializatzen pasatako denbora neurtzen du, eta honela deskribatzen da:

$$EI = \frac{\text{Denbora ontzi soziala esploratzen} - \text{Denbora ontzi hutsa esploratzen}}{\text{Denbora ontzi soziala esploratzen} + \text{Denbora ontzi hutsa esploratzen}}$$

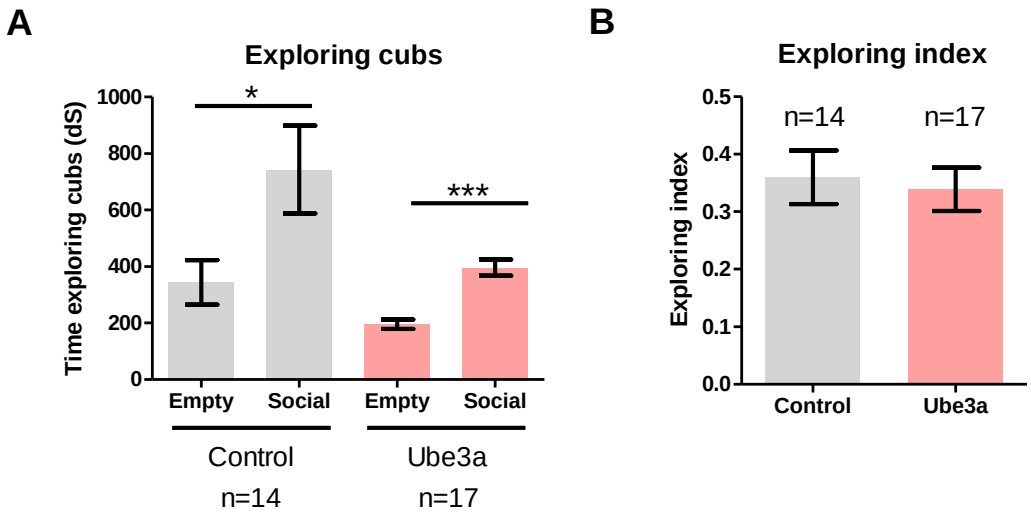

87. irudia. *Hiru Ganberako* testa UBE3A-OE saguen portaera soziala ikertzeko. P40-P50 adineko kontrol saguak (zutabe grisak) eta UBE3A-OE saguak (zutabe gorriak), hiru ganberako kutxa batean jarri ditugu. Izkina bateko ganberan ontzi hutsa, eta beste izkinakoan, ontzi soziala (sagu batekin) kokatu ditugu. A) Saguek ontzietako bakoitza esploratzen emandako denbora (dezisegundotan, dS) neurtu dugu. Sagu lerro bien kasuan, denbora gehiago pasatu dute ontzi soziala esploratzen, ontzi hutsa esploratzen baino (kontrol saguak n=14, UBE3A-OE saguak n=17, *t-testa*, p-balioa < 0.05). Alabaina ez dugu ezberdintasun esanguratsurik aurkitu bi sagu lerroen artean. B) Esplorazio-indizea (EI) neurtu dugu modu honetan: ontzi soziala esploratzen pasatako denborari ontzi hutsarekin pasatako denbora kendu diogu, eta esplorazio-denbora totalarekin (hutsa+soziala) zatitu dugu. Ez dugu ezberdintasun esanguratsurik behatu sagu lerro ezberdinen artean (kontrol saguak n=14, UBE3A-OE saguak n=17, *t*-testa, p-balioa > 0.05).

2. Aktibitate lokomotorea

Angelman sindromearen ezaugarrien artean, ohikoa da aktibitate lokomotorearen disfruntzioa (Angelman, 1965; Williams et al., 2006). Hori dela eta, jarraian, UBE3A-OE saguek mugimendu lokomotorean arazoak dituzten testatu nahi izan dugu. Horretarako, *Eremu irekia* deritzon testa burutu dugu (Hall and Ballachey, 1932): 28-33 eguneko adina (P28-P33) duten saguek eremua batean bidaiatzen duten distantzia eta abiadura neurtu ditugu. Test hori 20 minutuz burutu dugu, eta UBE3A-OE saguek distantzia gehiago egin dute, eta abiadura handiagoan, kontrol saguek baino (88. irudia). Saguen portaera esperimentuetan, fenotipo hori hiperaktibitatearen indikatzaile izaten da.

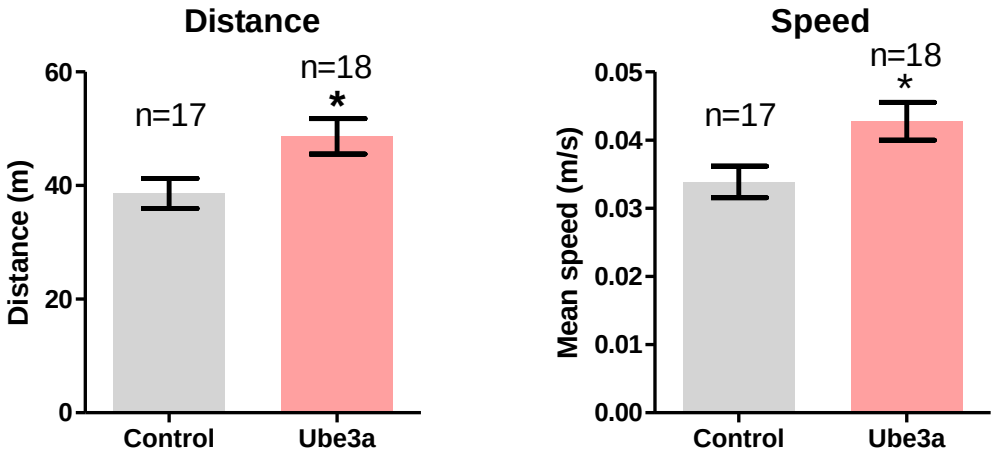

88. irudia. UBE3A-OE saguek distantzia luzeagoak egiten dituzte eta abiadura handiagoan mugitzen dira. P28-P33 adineko kontrol saguak (zutabe grisak) eta UBE3A-OE saguak (zutabe gorriak) *Eremu Irekiko* plakan kokatu ditugu eta 20 minututan zehar zein distantzia burutzen duten (metrotan, m), eta zein abiaduratan (metro/segundu, m/s) mugitzen diren neurtu dugu. UBE3A-OE saguek distantzia luzeagoak eta abiadura handiagoan, egiten dituzte, kontrol saguekin konparatuz (kontrol saguak n=17, UBE3A-OE saguak n=18, *t*-test, p-balioa < 0.05).

Hurrengo helburua antsietate portaerak ikertzea izan da, horretarako *Argi-ilunpe* testa erabiliz. Test hori saguek oso argiztatuta dauden eremuak ekiditeko duten joeran oinarritzen da, eta eremu berriek edo argiak saguen portaeran duten eragina ikertzen du (Bourin and Hascoët, 2003). Horretarako ganbera biko kutxa bat erabiltzen da; ganbera bat ilunpetan dago, bestea berriz, argi indartsua igortzen duen lanpara batek argiztatzen du. Test horretan saguek ganbera batean

edo bestean (argitan edo ilunpetan) pasatzen duten denbora neurtzen da 5 minutuz. Horretarako 50-60 eguneko adina duten saguak (P50-P60) erabili ditugu. Bai UBE3A-OE saguek, baita kontrol saguek ere, denbora gehiago pasatu dute ganbera ilunean, argiztatutakoan baino, baina ez dugu ezberdintasunik aurkitu bi sagu lerroen artean (89A. irudia). Horrez gain, *latentzia trantsizioa* ere neurtu dugu, hau da, saguak argiztatutako eremura lehenengo aldiz pasatzen ematen duen denbora. Kasu horretan, UBE3A-OE saguak azkarrago mugitu dira eremu argira kontrol saguak baino (89B. irudia). Saguen portaera esperimentuetan, latentzia trantsizio-denbora baxuek antsietate-maila baxuak definitzen dituzte, baina kasu honetan kontuan izan behar dugu hiperaktibitateak latentzia trantsizio-denbora horretan eragina izan dezakeela.

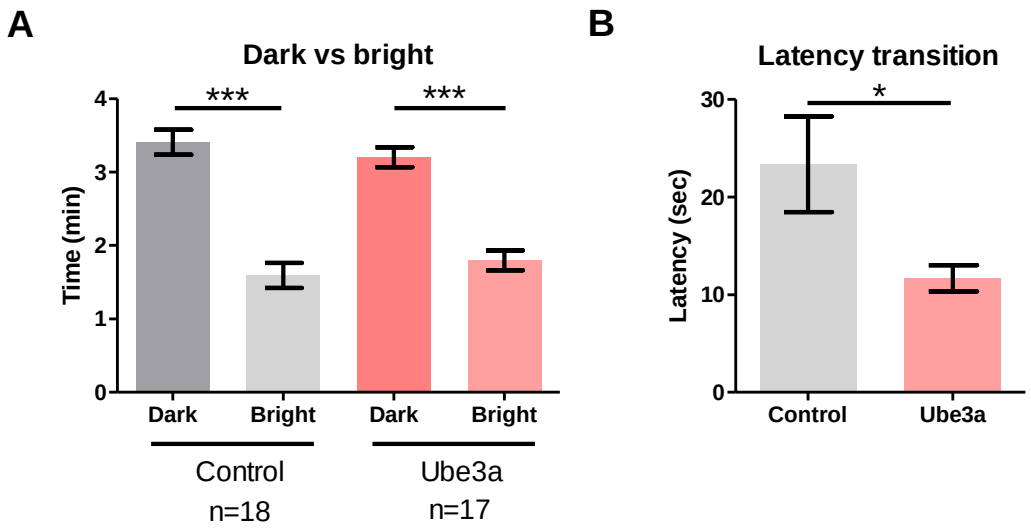

89. irudia. UBE3A-OE saguak lehenago pasatzen dira argiztatutako gunera. P50-P60 adineko kontrol saguak (zutabe grisak) eta UBE3A-OE saguak (zutabe gorriak) ganbera ilun bat eta argiztatutako dituen kutxan kokatu ditugu. A) Saguek ganbera bakoitzean pasatutako denbora (minututan) neurtu dugu 5 minutuz. Bi sagu lerroek denbora gehiago pasatu dute ganbera ilunean, argiztatutakoan baino (kontrol saguak n=18, UBE3A-OE saguak n=17, *t*-test, p-balioa < 0.05), baina ez dugu aldaketa esanguratsurik aurkitu kontrol eta UBE3A-OE saguen artean. B) Latentzia-trantsizioa sagu batek ganbera ilunetik argiztatutakora lehenengo aldiz irtetzeko behar duen denbora da (segundutan). UBE3A-OE saguak lehenago mugitzen dira ganbera argira kontrol saguak baino (kontrol saguak n=18, UBE3A-OE saguak n=17, *t*-test, p-balioa < 0.05).

3. Portaera errepikakorrak

Autismo Espektroko gaixotasunen modelo murino ezberdinek portaera errepikakorrak azaltzen dituzte, horietako bat *grooming*-a izanik (Kazdoba et al., 2016). Portaera hau saguak bere burua miazkatzean edo garbitzean datza. Beraz, gure sagu modeloan portaera errepikakorrak ikertzeko, saguek *grooming* egiten pasatzen duten denbora neurtu dugu, 20 minutuz, eremu zabaleko kutxa batean. UBE3A-OE saguek kontrolek baino tendentzia gehiago azaltzen dute *grooming* egiteko, ezberdintasun hori ia estatitiskoki esanguratsua izanik (p-balioa 0.0519) (90. irudia).

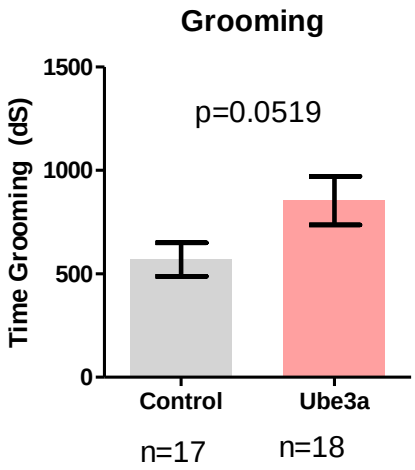

90. irudia. UBE3A-OE saguek *grooming* egiteko tendentzia azaltzen dute. P50-P60 adineko kontrol saguak (zutabe grisak) eta UBE3A-OE saguak (zutabe gorriak) eremu ireki batean kokatu ditugu, eta 20 minutuko jarraipena egin zaie. *Groominig* egiten pasatutako denbora (dezisegundotan (dS) eskuz neurtu dugu. UBE3A-OE saguek grooming egiteko tendentzia handiagoa azaltzen dute (kontrol saguak n=17, UBE3A-OE saguak n=18, *t*-testa, p-balioa = 0.0519)

4. Minarekiko sentikortasuna

Autismo Espektroko gaixotasunen animalia modeloen minarekiko erantzuna ezberdina dela deskribatu izan dute (Woolfe and Macdonald, 1944). Beraz, azkenik, minarekiko sentikortasuna neurtu dugu *Plaka beroa* testa erabiliz. 50 egun baino helduagoak diren saguak (>P50) erabili ditugu esperimentu honetan. 52 ºC-tan dagoen zoru bero batean jarri ditugu, minaren aurkako

portaeraren bat erakutsi duten arte (salto egitea, aurreko hankak miazkatzea...), gehienez 15 segunduz. Ez dugu desberdintasunik kusi UBE3A-OE eta kontrol saguek minarekiko duten sentikortasunen artean (91. irudia).

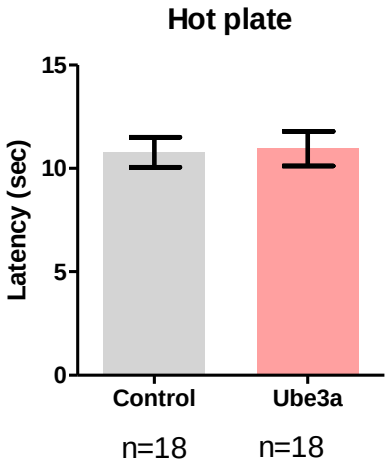

91. irudia. UBE3A-OE saguek minaren aurkako portaera normal dute. P50 adineko kontrol saguak (zutabe grisa) eta UBE3A-OE saguak (zutabe gorriak) 52ºC-tara dagoen plaka beroan jarri ditugu, gehienez 15 segunduz. Minaren aurkako lehen zeinua azaldu arteko denbora (segundutan) neurtu dugu. Ez dugu desberdintasunik aurkitu bi sagu lerroetan artean (kontrol saguak n=18, UBE3A-OE saguak n=18, *t*-testa, p-balioa > 0.05)

Laburbilduz, UBE3A-OE saguen portaeraren karakterizazioak deskribatu du sagu horiek, kontrol saguekin konparatuz, distantzia luzeagoak bidaiatzen dituztela eta abiadura handiagoan mugitzen direla, eta beraz fenotipo hiperaktiboa dutela. Bestalde, antsietate-maila baxuagoak azaltzen dituzte, argiztatutako eremuetarako trantsizio azkarrak erakutsi bezala. Hala ere, neurketa hori hiperaktibitatearen ondorio izan daitekeela kontuan hartu behar da. Gainerako portaera testek ez dute aldaketarik erakutsi gure sagu modeloan, nahiz eta horiek ohikoak izaten diren Autismo Espektroko beste sagu modeloen kasuan.

UBE3A-OE sagu lerroa sortzearen helburu nagusia, proteomika ikerketak burutzea da, ez Angelman sindromearen edo 15q duplikazio sindromearen modelo gisa erabiltzea. 5. Kapitulu honetan burututako UBE3A-OE saguen karakterizazioak erakutsi digu UBE3A mailak ez ditugula esanguratsuki aldatu, eta saguen portaera nahiko normala dela, hiperaktibitateaz gain. Hori ikusirik, modelo hau burutu nahi ditugun ikerketetarako egokia dela bermatzeaz gain, etorkizunean Angelman sindromearen aurkako farmakoek fenotipoan duten eragina testatzeko ere erabili ditzakegula erakutsi dugu.

IX.

DISCUSSION

The characterization of UBE3A E3 ligase is crucial for the deep understanding of the molecular mechanisms by which Angelman syndrome is developed. During this Thesis project we have validated UBE3A candidate substrates previously identified in *Drosophila melanogaster* and mice, employing a modified purification strategy – GFP pull-down–. We have further confirmed that the strategy can be applied for the identification of ubiquitination sites and ubiquitin chain-types mediated by UBE3A, in any given GFP-tagged substrate. In addition, we have performed a screening to identify the UBE3A counteracting DUB, which can greatly contribute to the development of future treatments for AS. We expected changes in the ubiquitination of UBE3A substrates upon UBE3A counteracting DUB inhibition, but we were not sure whether those changes would be sufficient to detect any improvement in the symptoms of the disease. Taking into account that UBE3A has several substrates, and that more than 100 DUBs can co-operate in the cells, changes on a few DUBs, might have not had any effect in the overall ubiquitination landscape, and hence, in AS symptoms. However, treating Angelman syndrome model flies with a specific DUB inhibitor, improved their phenotype. Moreover, mass spectrometry analysis identified proteins that changed their ubiquitination upon drug treatment, and could potentially be responsible for improving the AS fly model phenotype. On the other hand, we have identified several UBE3A interactors in HEK293T cells that may regulate the E3 ligase function, and determined if they are N-terminal, C-terminal or full length interactors. Finally, we have established a protocol for successful UBE3A purification with the aim of resolving its full-length structure, and we have characterized the behavior of our mice model that overexpresses UBE3A.

Altogether, findings during this Thesis project increase the knowledge about proteins that may be affected in AS and proposes a suitable strategy to tackle AS symptoms, opening a new research line for novel therapeutic avenues. In addition, it collects information about the suitability of the UBE3A mice line widely used in our experiments, and it gathers information about the protocol for successful purification of human UBE3A protein.

DDI1/2, PSMA5 and MINDY2 are UBE3A substrates in human HEK293T and SH-SY5Y cell lines

In this Thesis project we applied a modified GFP pull-down strategy to validate in human HEK293T and SH-SY5Y cells (Lee et al., 2014; Elu et al., 2020) putative UBE3A substrates previously identified in *Drosophila melanogaster* (Ramirez et al., 2018) and mice (Lectez et al., 2022, under revision).

UBE3A is a proteasome-associated protein (Jacobson et al., 2014; LaSalle et al., 2015; Martínez-Noël et al., 2018) capable of ubiquitinating several proteasomal subunits in cell culture (Jacobson et al., 2014; Lee et al., 2014; Yi et al., 2017). In line with those studies, many of the putative UBE3A substrates we identified were directly related to the Ubiquitin Proteasome System (UPS). The proteasome regulates dendritic development (Puram et al., 2013), long-term potentiation (Fonseca et al., 2006), long-term depression (Forrest et al., 2013), synaptic plasticity (Dong et al., 2014), synaptic strengthening (Zhao et al., 2003), memory consolidation (Figueiredo et al., 2015), circadian rhythms (van Ooijen et al., 2011) and many other aspects of neuronal function. In addition, UBE3A has been shown to regulate most aspects of neuronal function listed above (Gossan et al., 2014; Jiang et al., 1998; Miao et al., 2013; Pastuzyn and Shepherd, 2017; Pignatelli et al., 2014). Therefore, UBE3A-dependent proteasomal regulation could explain how a single E3 ligase mutation can cause a disorder as complex as AS. In this context, we focused our studies in validating the putative UBE3A substrates related to the UPS (DDI1/2, PSMA5, MINDY, and UBE2L3) as well as other proteins (TAX1BP1 and BMLH) that might be relevant to AS.

Rngo, one of the putative Ube3a substrate candidates identified in *Drosophila melanogaster,* contains both, an UBL and an Ubiquitin-binding domain (UBD), a hallmark of proteasomal shuttles; interacts with the 26S proteasome through its UBL domain (Finley, 2009), and binds to ubiquitin or poly-ubiquitin chains through the UBD domain (Bertolaet et al., 2001). Rngo is also the Drosophila homologue of yeast Ddi1/Vsm1, a protein that binds to several Snc-interacting t-SNAREs (Marash and Gerst, 2003), negatively regulates exocytosis (Lustgarten and Gerst, 1999) and also regulates protein secretion (White et al., 2011). Similarly, the *C. elegans* homologue Ddi1/Vsm1has also been proposed to

regulate synaptic function, with *Vsm-1* mutants displaying a significant increase in synaptic density along the dorsal nerve cord (Guthmueller et al., 2011). Thus, Rngo/DDI1 may have an additional role in synaptic transmission by controlling SNARE-mediated exocytosis. In fact, over-expression of Ube3a, but not its ligase dead form, has been reported to alter neurotransmission at the neuromuscular junction in Drosophila (Valdez et al., 2015).

Two mammalian Rngo homologues have been described, DDI1 and DDI2, but neither of those proteins have to date been functionally characterized. Previous experiments in the lab showed that DDI1 and DDI2 are expressed in the developing brain (Ramirez et al., 2018). Structurally, both proteins contain the characteristic retroviral protease-like domain (RVP) that was recently reported to cleave/activate the Nrf1 transcription factor under proteasome inhibition (Koizumi et al., 2016; Lehrbach and Ruvkun, 2016). Moreover, it is likely that DDI1 is involved in both regulation of synapses and proteasomal function (Guthmueller et al., 2011; Lustgarten and Gerst, 1999; Marash and Gerst, 2003; Nowicka et al., 2015; White et al., 2011) and that both processes are actually misregulated during the genesis of AS.

We confirmed human DDI1 to be an ubiquitination substrate of UBE3A in HEK293T and SH-SY5Y neuroblastoma cells. K48 ubiquitination of hDDI1 by UBE3A is specific, and does not lead to a reduction of hDDI1 protein levels, suggesting rather a non-degradative role. It is not the first time that ubiquitination exerts a non-proteolytic role (Flick et al., 2004). Here we propose a possible DDI1/DDI2 self-regulation mechanism, similar to the one defined for Met4; a UBD was proposed to cap its own K48- linked ubiquitin chain, inactivating the protein and protecting it from degradation (Flick et al., 2006). Something similar could be happening with Rngo/hDDI1. Further work is required to elucidate what the functional role of hDDI1 ubiquitination might be and whether the presence of UBD/UIM/UBA/UBL in ubiquitination substrates might interfere in the canonical role of K48 ubiquitin-linked chains.

PSMA5 is a component of the 20S core proteasome complex involved in the proteolytic degradation of most intracellular proteins (Tomko and Hochstrasser, 2013). The 20S proteasome is mainly defined as a component of the 26S proteasome complex; 20S proteasome associates with one or two 19S regulatory particles to form the 26S proteasome cooperative machinery.

However, evidence demonstrates that degradation by the 20S proteasome does not require ubiquitin tagging or the presence of the 19S regulatory particle, so any change in the ubiquitination status of its components, such as PSMA5, may alter the degradation of proteins in the complex. We observed that mainly PSMA5 poly-ubiquitination and monoubiquitination were increased upon UBE3A overexpression in HEK293T and SH-SY5Y cells, respectively. UBE3A is known to mono- and poly-ubiquitinate substrates (Avagliano Trezza et al., 2021; Elu et al., 2019; Kuhnle et al., 2013; Masuda et al., 2019). Therefore, the differences observed in both cell lines may be tissue specific. In line with our results, it has been described that mono-ubiquitination is more abundant in the brain than in the kidney (Heunis et al., 2020). It has been shown that PSMA5 ubiquitination sites change upon DNA damage, and that the proteolytic activity of the 20S proteasome can be regulated by changes on its core components (Moiseeva et al., 2013). Hence, it is plausible that UBE3A-mediated ubiquitination on PSMA5 alters the activity of the proteasome, and consequently, the fate of a number of proteins that can disrupt cellular homeostasis.

Another candidate UBE3A substrate identified in preliminary experiments with the aforementioned mice (data not shown) is MINDY2, also called FAM63B. MINDY2 is a member of the recently discovered MINDY (Motif interacting with Ub-containing novel DUB family) family of deubiquitinases. GFP pull-down experiment clearly demonstrated an increase in its ubiquitination upon UBE3A overexpression. It has been described that MINDI1/2 is autoinhibited; it is activated through restructuration when it binds K48 chains (Abdul Rehman et al., 2021). If UBE3A mediated ubiquitination regulates MINDY2 conformation, it may alter its deubiquitinase activity. As observed for Drosophila UBE3A substrate Rnp10, and alike other UBE3A substrates, ubiquitination of MINDY2 is increased and the total amount of the protein is decreased, suggesting that UBE3A mediated ubiquitination of MINDY2 drives it into degradation (Lee et al., 2014). K48-linked ubiquitin chains are the canonical degradation signals. Nevertheless, multiple ubiquitin molecules across a single protein can mimic poly-ubiquitination, and hence, provide a degradation signal (Dimova et al., 2012). In line with that, UBE3A-dependent mono-ubiquitination of MINDY2 detected in this study might target the DUB for proteasomal degradation.

Another candidate substrate we tried to validate was the UBE3A cognate E2 UBE2L3 (Huang et al., 1999). However, upon GFP pull-down, we detected no significant differences in the ubiquitination level of UBE2L3 in the presence of wild-type or ligase-dead UBE3A. This could be explained by overall differences in ubiquitination among wild-type and ligase-dead UBE3A samples when overexpressing UBE2L3 and UBE3A at the same time. Total ubiquitination levels are higher in ligase-dead UBE3A samples, so substrate ubiquitination can be underestimated in the wild-type UBE3A sample due to the lower available ubiquitin.

In addition to putative substrates related to UPS, we aimed to validate also those proteins from the preliminary data that, according to literature, might be somehow related with AS symptoms. For instance, BLMH modulates the expression of mouse brain proteins involved in neurodegeneration (Suszynska-Zajczyk et al., 2014) and it is also required for the localization of NUDT12 into cytoplasmic granules. NUDT12 is a protein that regulates circadian clock transcripts in mouse (Wu et al., 2019a), so aberrant ubiquitination of BLMH may affect NUDT12 localization and, hence, explain the circadian symptoms characteristic of Angelman syndrome patients. However, we deteted no changes in BLMH ubiquitination upon UBE3A expression in HEK293T cells, and in SH-SY5Y cell line, since ubiquitin signal was barely undetectable. However, changes upon UBE3A overexpression may not be visible in HEK293T cells considering BLMH role in neurodegeneration (Suszynska-Zajczyk et al., 2014). In addition, there are no studies about human BLMH function, and if the role in circadian rhythm in mouse is conserved in human needs to be further studied.

TAX1BP1 is an autophagy receptor protein, required for the clearance of stress-induced aggregates, promoting viability of neurons (Sarraf et al., 2020). Lack of its regulation may result in the accumulation of cytotoxic proteins, and consequently neuronal death (Sarraf et al., 2020). This may explain several Angelman syndrome symptoms, such as intellectual disability, because precise control of synapse formation and development is essential for correct brain development and function (Verma et al., 2019). Increase in TAX1BP1 ubiquitination upon UBE3A overexpression did not result statistically significant, probably because TAX1BP1 is more specifically expressed in the brain (Sarraf et al., 2020). However, in SH-SY5Y cells the purified material was not enough for

proper analysis. Overall, very little amount of TAX1BP1 was detected in the analysis, mainly because most of the protein was in the non-soluble fraction. TAX1BP1 has been described to localize in aggregates that need to be cleared (Sarraf et al., 2020), and this correlates with the punctuated localization of TAX1BP1 found in our cell culture imaging. The association of TAX1BP1 with the insoluble protein fraction may explain the poor enrichment of this protein in the GFP pull-down assay.

GFP pull-down protocol allows the identification of UBE3A mediated ubiquitination sites on DDI1/DDI2

The GFP pull-down protocol is a powerful tool for the validation of substrates, but we have given a step forward, and optimized the protocol to characterize those substrates. Combining GFP pull-down with mass spectrometry analysis, we generated a protocol for the identification on our proteins of interest the ubiquitination sites and ubiquitin chain-types formed or disrupted as a consequence of the action of an E3 ligase or DUB, respectively (Elu et al., 2020).

Post-translation modifications (PTMs), including protein ubiquitination, play a critical role in essentially all cellular processes by regulating the activity, localization or interactions of proteins, and the position of the PTMs within the protein is of high relevance. For example, ubiquitination of K867 of the human SETDB1 protein enhances its H3K3 methylatransferase activity (Ishimoto et al., 2016) whereas RAS K104 ubiquitination modulates interactions of GEFs (guanine nucleotide exchange factors) (Yin et al., 2019).

Bearing in mind the relevance of PTMs, we postulated that studying in depth the ubiquitination of DDI1, more precisely, depicting DDI1 ubiquitination sites and chain types, may shed light into its regulation and the mechanism by which this proteasomal shuttle could target proteins into degradation.

Proteasomal shuttling proteins contain an N-terminal ubiquitin-like (UBL) domain that interacts with the 26S proteasome (Finley, 2009), and a C-terminal ubiquitin-binding domain (UBD) that binds to ubiquitin or poly-ubiquitin chains

(Bertolaet et al., 2001; Morawe et al., 2011). When ubiquitinated, substrates are captured by the UBD domain, whereas the UBL domain binds to UBL receptors of the proteasome, delivering the substrates for degradation (Finley, 2009). Yeast Ddi1 and Ddi1-like shuttling proteins (e.g., Ddi2) show unique properties among canonical proteasomal shuttles. On the one hand, their UBL domain can bind ubiquitin (Nowicka et al., 2015), and despite having a ubiquitin-like fold, does not interact or very weakly interacts with typical UBL receptors, including Rpn10 (Zhang et al., 2009) and Rpn1 (Rosenzweig et al., 2012). On the other hand, human DDI1 and Ddi1-like proteins lack the UBA domain (a type of UBD), but instead interact with ubiquitin through their UBL domain (Nowicka et al., 2015) or the ubiquitin-interacting motif (UIM) in the case of Ddi1-like proteins (Nowicka et al., 2015; Sivá et al., 2016). In line with this, a novel proteasomal shuttling mechanism has been proposed for yeast Ddi1 (Nowicka et al., 2015). It is feasible that the DDI1 UBL domain, which in yeast Ddi1 is capable of binding ubiquitin (Nowicka et al., 2015), could substitute the role of the UBA domain, a mechanisms that would be facilitated by DDI1's homodimeric conformation. Furthermore, Ddi1 and Ddi1-like proteins contain an additional domain called the retroviral protease-like (RVP) domain (Sirkis et al., 2006) that besides targeting substrates for proteasomal degradation, may exert additional roles in the cell. Thus, further studies are necessary not only to fully understand the shuttling mechanism mediated by DDI1, but also to discover in which other cellular functions DDI1 is involved.

A recent large-scale proteomic study has reported for the first time that human DDI1 is ubiquitinated on K345 and K346, which reside in the retroviral protease domain (RVP) (Akimov et al., 2018). Moreover, studies in rat brain revealed that rat DDI1 K297, also located in the RVP domain, is ubiquitinated (Na et al., 2012). In line with that, we here present the first evidence indicating that its human homolog DDI1 K291, located in the same RVP domain, is also ubiquitinated. As mentioned above, the function of the RVP domain, which is only present in Ddi1 and Ddi1-like proteins, is obscure. Therefore, the recent findings regarding ubiquitination events occurring on human DDI1 RVP domain might provide a baseline for future studies on deciphering the role of this unique domain.

Furthermore, our mass spectrometry-based approach revealed five novel ubiquitination sites in human DDI1: K77 (UBL domain), K133, K161, K213 (HDD

domain) and K382 (C-terminal part). It is likely that ubiquitination of residues located on specific domains may differentially affect hDDI1 function. Hence, future work will be necessary to elucidate the biological significance of each modification.

We are interested in elucidating the molecular mechanisms underlying Angelman syndrome, a rare neurological disease caused by the lack of functional E3 ubiquitin ligase UBE3A in the brain. For that reason, among the six hDDI1 ubiquitination sites detected in the present study, our interest focused on the ones mediated by UBE3A, as it is likely that UBE3A-dependent ubiquitination events are altered in Angelman syndrome patients. Comparing the intensity of the diGly-modified peptides corresponding to hDDI1 in samples overexpressing $UBE3A^{WT}$ and $UBE3A^{LD}$, we found that peptides bearing ubiquitinated K77, K133 and K161 appeared more abundant upon overexpression of $UBE3A^{WT}$. Altogether, these results pointed to the N-terminal region of hDDI1, including the ubiquitin-like domain and the double helical domain (HDD), as a ubiquitination hotspot region, where UBE3A mostly acts. Out of the three putative UBE3A-dependent DDI1 ubiquitination sites detected, K133- and K161-containing peptides reached statistical significance. However, to further corroborate previous results, hDDI1 K77, K133 and K161 were mutated to arginine, both individually or in combination. Upon wild-type UBE3A overexpression, we detected a moderate increase in ubiquitination of hDDI1 K77 and K161 sites. However, the overall ubiquitination status of hDDI1 was not affected upon mutation of K77 and/or K161, probably because the ubiquitination was transferred to an alternative lysine. By contrast, UBE3A-dependent ubiquitination of hDDI1 was significantly reduced when residue K133 was mutated, indicating that undoubtedly UBE3A is responsible for modifying this specific residue. It has been postulated that the HDD domain, in which K133 resides, may play a role in substrate recognition (Trempe et al., 2016). Therefore, it is plausible that UBE3A-dependent ubiquitination of hDDI1 K133 has an influence on such recognition.

The same analysis performed for hDDI2 detected lower ubiquitination levels making mass spectrometry analysis more challenging. 11 ubiquitination sites have been previously described for hDDI2 (K67, K77, K153, K170, K205, K283, K289, K337, K338, K389 and K398). Our mass spectrometry analysis detected four of them (K77, K153, K283 and K289). Except K289, which is not conserved in hDDI1,

the other three ubiquitination sites aligned to K77, K161 and K291 also detected to be ubiquitinated in hDDI1. K133 in hDDI1 is not conserved in hDDI2, but we found that hDDI2 peptides bearing K77 and K153 appeared more abundant upon overexpression of UBE3A^{WT}. However, only K77 reached statistical significance. The low MS/MS counts recorded for lysine 153 in the mass spectrometry analysis could explain why the increase in ubiquitination did not reach statistical significance. Additionally, none of the single point mutations (K77 or K153) affected the ubiquitination levels of DDI2, suggesting that either both sites could simultaneously be regulating DDI2 ubiquitination levels, or that mutation of one site shifts ubiquitination to another site.

UBE3A mediates mainly K48 ubiquitin chains on DDI1/DDI2

The fate of an ubiquitinated protein does not only depend on the specific residue that is modified, but also on the type of ubiquitin linkage that is formed in such residue (Swatek and Komander, 2016). A large variety of ubiquitin linkages differentially modulate proteins and their function in multiple cellular processes. Thus, using a high stringency GFP pull-down protocol, we investigated the ubiquitin chain types specifically and covalently linked to human DDI1 and DDI2.

In both cases, we observed an overall increase in ubiquitin signal upon UBE3A^{WT} overexpression. In parallel, a detailed MS-based analysis revealed that UBE3A predominantly induces the formation of K48-linked ubiquitin chains both in DDI1 and DDI2, and also K11-linked chains specifically in DDI1, suggesting that the increase in ubiquitin signal most likely corresponds to the formation of those chain types.

K48-linked ubiquitin chains have been widely described to direct proteins to degradation via the proteasome (Finley, 2009; Grice and Nathan, 2016). Indeed, several studies have shown that UBE3A forms K48-type linkages, and consequently, modified proteins are predicted to be targeted for degradation (Wang and Pickart, 2005). K11 chains also improve the signal for proteasomal degradation, as evident from the fact that branched K11-linked chains formed by the anaphase-promoting complex (APC/C) increase the efficiency of proteasomal

substrate recognition (Meyer and Rape, 2014). However, and in agreement with our previous work (Ramirez et al., 2018), the unchanged GFP signal clearly indicates that UBE3A-dependent ubiquitination of DDI1 does not target this shuttling protein to degradation, in contrast to what has been seen for Drosophila Rpn10 (Lee et al., 2014), and for his mammalian homologue PSMD4 (unpublished results). One plausible explanation could be that DDI1 ubiquitination leads to a neutralization of this proteasomal shuttle. If the role of DDI1 is to transport K48- or K11-modified proteins to the proteasome, when the client is the shuttle itself, shuttling might be interrupted, by blocking both the proteasomal interaction, as well as the recruitment of further clients. This UBE3A-mediated ubiquitination of DDI1 could thus explain our previous observation that overall proteasomal function is somehow dependent on UBE3A (Lee et al., 2014; Ramirez et al., 2018). Further analysis to decipher the function of K48 and K11 ubiquitin chains in DDI1 *in vivo* is likely to provide more light in this issue.

K29-linked chain type was also slightly more abundant upon UBE3A overexpression. However, since it was only detected in the $UBE3A^{WT}$ and not in $UBE3A^{LD}$ sample, it was assigned the lowest LFQ intensity value among the other chain types in this $UBE3A^{LD}$ set. Therefore, the increase in abundance of K29 needs to be assessed carefully. K27 chains were detected in both conditions ($UBE3A^{WT}$ and $UBE3A^{LD}$) but the localization probability of the lysine ubiquitinated was very low, so it could not be differentiated if the intensity corresponded to K27 or K29 chains. In consequence, K27 was removed from the analysis. It must be noted that both K27 and K29 chains were detected with very few counts.

Mass spectrometry analysis allows the identification of ubiquitin chains and ubiquitin sites but can not conclude if a given mono-ubiquitination event is increased. Recently, it has been described that UBE3A also mediates mono-ubiquitination (Avagliano Trezza et al., 2021). Although mass spectrometry analysis could not detect it, Western blot analysis of DDI1 and DDI2 ubiquitination showed a clear mono-ubiquitination band 10 kDa above the non-modified form, which is increased when overexpressing UBE3A. Therefore, in line with those studies, we concluded that UBE3A also mediates mono-ubiquitination in DDI1/DDI2, suggesting rather a possible non-degradative role (Avagliano Trezza et al., 2021).

USP9X is a UBE3A counteracting DUB

Most PTMs, including ubiquitination, are reversible modifications modulated by the coordinated action of two opposing enzymes: one adding a given chemical group to the protein, the other one removing it. In particular, protein ubiquitination is modulated by E3/DUB pairs. The regulation of the enzymes modulating protein PTMs is crucial for maintaining the appropriate balance of protein modification required for cellular homeostasis. In fact, as already mentioned, deregulation of these enzymes is implicated in a number of diseases, including cancer and rare neurological diseases (Ruprecht and Lemeer, 2014; Osinalde et al., 2018). Therefore, emerging therapeutic strategies are focused on the design of drugs that modify the biological action of these enzymes, and consequently restore appropriate cellular PTM levels. Indeed, in the past two decades, kinase inhibitors have been successfully used to treat cancer (Bhullar et al., 2018; Cohen et al., 2021).

At present, great efforts are being made to develop similar strategies to treat diseases caused by altered protein ubiquitination. More precisely, DUBs are emerging as druggable targets for different diseases. Attempts have been done to inhibit DUBs in cancer therapy (D'Arcy et al., 2015), aiming to increase ubiquitination, and subsequent degradation of substrates (Pinto-Fernandez and Kessler, 2016). In this Thesis we propose that modulating protein ubiquitination may represent a therapeutic approach for Angelman syndrome patients that lack UBE3A activity in the brain. More precisely, inhibition of the DUB counteracting the action of the E3 ligase UBE3A, may help restoring the non-pathological ubiquitination levels of UBE3A substrates in AS patients. So far, there are few studies showing that E3/DUB pairs act in a highly co-ordinated manner to regulate the ubiquitination and, hence, the activity of common substrates (Kee et al., 2005; Xie et al., 2013; Bingol et al., 2014; Sharma et al., 2014). It has been shown that Ubp2 antagonizes Rsp5 E3 ligase activity by forming a complex together with Rsp5 and Rup1, that deubiquitinate Rsp5 substrates (Kee et al., 2005). Additionally, the E3/DUB pair UBR5/DUBA acts to modulate the production of IL-17 in T-cells (Rutz et al., 2015). Nevertheless, the identity of the DUB antagonizing the action of UBE3A has remained elusive, so far. This study is pioneer in revealing USP9X as a DUB counteracting UBE3A. We demonstrate that

siRNA-directed USP9X silencing, as well as treatment with WP1130 (a previously used partially specific USP9x inhibitor) (Kapuria et al., 2010) or FT709 (most recently used USP9X specific drug) (Clancy et al., 2021) significantly enhance human DDI1 ubiquitination. Interestingly, USP9X has been earlier reported to be involved in X-linked intellectual disability (Homan et al., 2014), Huntington's and Alzheimer's disease (Murtaza et al., 2015). Furthermore, USP9X is also known to participate on axonal growth and neuronal cell migration (Homan et al., 2014) as well as in the regulation of seizures (Paemka et al., 2015). This DUB is also known to deubiquitinate α-synuclein, which is central to the pathogenesis of Parkinson disease (PD) (Rott et al., 2011). Consequently, it has been suggested that drugs that modulate the activity of USP9X, together with enhancers of autophagy or proteasomal activity, may help to decrease the levels of α-synuclein and to provide a novel therapeutic strategy to treat α-synucleinopathies. Similarly, based on our results, we propose that attenuating the activity of USP9X may contribute to enhance the ubiquitination levels of UBE3A substrates that might be decreased in Angelman syndrome patients.

USP9X inhibition rescues **Angelman syndrome model flies'** phenotype

Drosophila melanogaster flies are a valuable tool to study different human diseases, such as obesity and aging (Gáliková and Klepsatel, 2018; Ugur et al., 2016), cardiac disease (Bier and Bodmer, 2004), neuromuscular disease (Lloyd and Taylor, 2010) or diabetes (Graham and Pick, 2017). They are widely used also to study neurological diseases such as Alzheimer (Tsuda and Lim, 2018) or Parkinson (Aryal and Lee, 2019). *Ube3a* null mutants for *Drosophila melanogaster* were also developed, and similar to Angelman syndrome patients, flies displayed abnormal locomotive behavior and circadian rhythms, as well as defective long-term memory (Wu et al., 2008). Climbing tests of null *Ube3a* mutants versus wild-type flies demonstrated defective climbing ability due to the loss of function of Ube3a.

We discovered that WP1130 treatment, which inhibits faf, the fly homolog of human UPS9x (Paemka et al., 2015), improved the climbing ability of *Ube3a* homozygous mutant flies, demonstrating amelioration of locomotive Angelman

syndrome-like symptoms. In order to confirm that such improvement is a direct effect of faf inhibition, and not the result of WP1130 targeting additional DUBs, it is necessary to test the effect of the specific drug FT209. Unfortunately, FT709 drug is not commercialized yet, and its little availability made it impossible to further analyze the specific effect of faf inhibition on flies' phenotype. Moreover, we found in the literature that human USP9X targets several proteins (Elu et al., 2022), so we expect that Drosophila faf also targets more proteins in addition to Rngo (fly homolog for DDI1). Therefore, we could not conclude that enhanced ubiquitination of Rngo is responsible for the improvement observed in WP1130-treated *Ube3a* mutant flies.

coREST and mGluR are more ubiquitinated upon WP1130 treatment in *Drosophila melanogaster*

To further characterize the effect of USP9X inhibition in *Drosophila melanogaster*, we aimed to identify the proteins that change their ubiquitination upon WP1130 treatment, and could be responsible for the improvement in the climbing ability of flies. To do so, we used the BioUb strategy successfully applied in many previous studies in our lab (Martinez et al., 2017; Ramirez et al., 2018, 2021).

Among the proteins whose ubiquitination levels were increased upon WP1130 treatment, we identified Rest corepressor (CoRest). It has been reported to be ubiquitinated in many comprehensive proteomic studies (Akimov et al., 2018; Kim et al., 2011; Udeshi et al., 2013). It was first described as a master negative regulator of neuronal gene expression (Chong et al., 1995); it is an essential component of a corepressor complex that represses transcription of neuron-specific genes in non-neuronal cells (Dallman et al., 2004). The variations in CoRest protein structures are responsible for altered protein-protein interactions and thus, differences in transcriptional repressive capacity (Barrios et al., 2014). Moreover, CoRest also plays a role in neuroprotection (Maksour et al., 2020); aberrant expression or altered subcellular localization is associated with a range of neurodegenerative diseases, such as Alzheimer disease (Meyer et al.,

2019), Huntington's disease (Conforti et al., 2013) or Parkinson disease (Huang et al., 2019). Although the regulatory mechanisms governing CoRest protein expression remains obscure, a possible mode of regulation based on SUMOylation has recently been described (Sáez et al., 2018). Here we propose that in the absence of Ube3a, the ubiquitination pattern of CoRest will be altered and consequently, protein-protein interactions or CoRest localization might be affected, ultimately resulting in gene expression deregulation. For example, loss of NUS1 (Guo et al., 2018), SIN3 (Barnes et al., 2014) or Atg6 (Beclin 1) and Pi3K59F autophagy genes (M'Angale and Staveley, 2016) result in defficient climbing ability. It would be interesting to study the link between CoRest and those genes, since changes in the ubiquitination of CoRest may affect the regulation of any of those genes and influence the climbing ability of flies.

The other protein identified by mass spectrometry as more ubiquitinated after WP1130 treatment is the metabotropic glutamate receptor (mGluR), a G-protein coupled receptor for glutamate. mGluR has been related to several symptoms of Angelman syndrome, such as locomotor activity problems, sleep disturbances or epilepsy (Spruyt et al., 2018; Williams et al., 2006). It was previously described a relationship between mGluR receptors and locomotor activity in mice (Iwagaki and Miles, 2011, 2003). mGluR receptor was also described as sleep regulator (Ly and Naidoo, 2019) and it has been related to epileptogenesis (Bianchi et al., 2012), synaptic long-term depression (Lüscher and Huber, 2010) and autism (Lee et al., 2019). Previous studies already demonstrated that metabotropic receptors can be regulated through ubiquitination. For instance, cell surface ubiquitination of metabotropic gamma-aminobutyric acid receptor (GABAR) promotes its endocytosis. USP14 acts as an ubiquitin-binding protein that targets ubiquitinated GABAR to lysosomal degradation and promotes its deubiquitination (Lahaie et al., 2016). Similarly, the Drosophila deubiquitinating enzyme faf (human USP9X) has been shown to regulate Delta/Notch receptor internalization by deubiquitinating Liquid facets, a fly homologue of epsin, a component of the clathrin-endocytic machinery (Chen et al., 2002). Further studies are needed to conclude if indeed USP9X fly homolog faf specifically regulates mGluR, and as a consequence, affect signalling cascades that are important for the expression of genes involved in the climbing ability of Drosophila flies.

BioID strategy successfully identified UBE3A full-length, C-terminal and N-terminal interactors

Cellular processes are typically regulated by protein-protein interactions (PPIs), rather than by individual proteins. They form dynamic networks that are involved in a wide range of cellular processes (Hergovich, 2012; Peng et al., 2016; Yu et al., 2019). They can interact with each other at the same time and place to regulate a cellular process, or each of them can carry out a different biological function in that process (Terentiev et al., 2009). Because of the key relevance of protein-protein interactions in cell homeostasis and proper function, mutations that disrupt links forming protein complexes can result in the development of diseases (Lou et al., 2020; Wanker et al., 2019). Recently, a comprehensive analysis characterized the PPIs that are perturbed by disease mutation (Cheng et al., 2021). Several mutations have also been found in human UBE3A gene (Zhao et al., 2020), and some of them have been directly related to the phenotype of Angelman syndrome (Triono et al., 2021; Weston et al., 2021). It is possible that some of those UBE3A mutations disrupt the link with its interactors. However, there are few studies that describe UBE3A interactors.

The first UBE3A interacting partner described was E6 oncoprotein; the formation of the complex enables the rapid degradation of p53 (Scheffner et al., 1993). Another UBE3A interactor is ASPM (Abnormal spindle-like microcephaly-associated protein), which together with regulate chromosome segregation (Singhmar and Kumar, 2011). HERC2 E3 ligase is also a UBE3A interactor that stimulates its ubiquitin-protein ligase activity (Kühnle et al., 2011). More recently, a proteomic analysis performed in human neuroblastoma SH-SY5Y cell line identified many UBE3A interactors, including numerous proteasomal subunits (Martínez-Noël et al., 2018).

In this Thesis, we aimed to map *in vivo* the UBE3A interactome. Commonly used techniques to study PPIs such as Yeast Two Hybrid (Y2H) (Song and Fields, 1989), antibody-based pull-downs or microarrays (Hall et al., 2007) are not suitable to uncover short-term or transient interactors, neither to detect PPIs *in vivo*. To overcome these limitations, we decided to map *in vivo* the UBE3A interactome applying the improved BioID strategy named BioID2 (Kim et al., 2016) (Roux et al.,

2012). More precisely, we studied the interactome of full-length (FL), C-terminal (C-term) and N-terminal (N-term) UBE3A in order to determine the interacting region of each UBE3A binding protein in HEK293T cells.

Correct protein folding is vital for proper protein function, so partial structures may affect the interacting interface of the protein, and hence disturb its global activity. In order to avoid that, UBE3A partial constructs were designed so that the main functional domains were not affected. The C-terminal UBE3A construct contained the whole catalytic HECT domain, and the N-terminal construct contained the AZUL domain down to the beginning of the HECT domain. Moreover, both constructs shared some residues so their edges overlapped. Using similar constructs, a previous study discovered that some proteasomal proteins interact with these AZUL and HECT regions, demonstrating the ability of partial UBE3A constructs to form PPIs (Kühnle et al., 2018). In addition, our lab tested different types of linkages between the BioID2 tag and UBE3A protein, and checked for the most efficient one (data not shown). The same backbone was used to generate all BioID2-UBE3A constructs; therefore, in principle, similar biotinylation efficiency was expected in all of them.

In general terms, the amount of biotinylated proteins was not as high as expected, and differed substantially depending on the UBE3A construct that we studied, with the C-ter sample having the most biotinylated material. Differences in the abundance of purified material within different UBE3A constructs may happen probably due to; (1) a decrease in the amount of interactors due to the disruption of the interactions when creating the partial UBE3A constructs, (2) differences in the efficiency of BioID2 tag when cloning to different UBE3A sequences, or (3) proteins interacting more with UBE3A N-terminal or C-terminal parts.

Given that the N-terminal part of UBE3A determines substrate specificity (Kühnle et al., 2018), we expected this region to have the highest number of interactors. Indeed, mass spectrometry analysis resulted in the identification of a total of 23 N-terminal, 8 C-terminal, and 3 full-length UBE3A interactors.

The proteins identified as UBE3A interactors in this study (full-length, C-ter and N-ter), did not show enrichment of any cellular process. Nevertheless, many of them are related to autism spectrum disorders and/or neuronal function.

Among the proteins identified as N-terminal UBE3A interactors, two were previously reported; PIP (Prolactin-inducible protein)(Martínez-Noël et al., 2018) and AHNAK (Desmoyokin) (Saez et al., 2018), which was also described as a neurodevelopmental disorder risk gene(Stessman et al., 2017). Pathogenic FLNA (Filamin A) variants have been related to West syndrome, a disease characterized by intellectual disability and epileptic spasms (Hiromoto et al., 2020). Mutations in SRP68 (Signal Recognition Particle 68) gene were found on an individual with autistic traits (Bellanné-Chantelot et al., 2018) whereas HSPA5 (Heat Shock Protein family A member 5) belongs to the "prion diseases" pathway that it is enriched in patients with Autism Spectrum Disorders (Lombardo et al., 2020). EPS15L1 (Epidermal growth factor receptor substrate 15-like 1) and TLN1 (Talin-1) were also identified as ASD candidate genes (Wilfert et al., 2021) and SYAP1 is a synapse associated protein that it is important in motor activity and balance in mice, one of the main characteristics of Angelman syndrome (R. von Collenberg et al., 2019). Some other UBE3A N-terminal interactors identified in our experiment have been related to specific pathways regulating neuronal function. For instance, upregulation of S100A11 (Protein S100-A11) protects against neuronal apoptosis (Xia et al., 2018) and has been related to neurological diseases (Zhang et al., 2021). ARFGAP1 (ADP-ribosylation factor GTPase-activating protein 1) is important for neurite extensions, since regulates the traffic of GAT-1 (GABA Transporter 1) in order to enable synaptic transmission (Reiterer et al., 2008). DBN1 (Debrin) plays a role in dendritic spine morphogenesis and organization, and is involved in memory-related synaptic plasticity in mice hippocampus (Jung et al., 2015). SFN (Stratifin), has been related to ADNP (Activity-dependent neuroprotector homeobox protein), a protein described to regulate cognition (Bend et al., 2019; Gozes, 2018). In addition, reduction of EIF4B (Eukaryotic translation initiation factor 4B) has been related to the down-regulation of the Akt/mTOR pathway in idiopathic autism (Nicolini et al., 2015). In respect to C-terminal interactors, it has been described that RRM2 (Ribonucleoside-diphosphate reductase subunit M2) competes with UBE3A to prevent ANXA1 degradation (Xiong et al., 2021), which is a protein that has a role in the etiology of Autism Spectrum Disorders (Correia et al., 2014). In addition, UBAP2L (Ubiquitin-associated protein 2-like) depletion in a cortical neuronal model of Fragile X Syndrome (FXS) corrects molecular, cellular and electrophysiological defects relevant to Autism Spectrum Disorder (Luo, 2020).

Finally, one of the full length UBE3A interactors, IGF2R (Insulin-like growth factor 2 receptor), plays a critical role in memory consolidation and enhancement by controlling protein metabolism (Yu et al., 2020). The high number of proteins related to neuronal function in our study could explain why the lack of UBE3A results in such severe neurological deficits.

Human full-length UBE3A protein was successfully purified for structure resolution

UBE3A is a HECT type E3 ubiquitin ligase, and although its function has been widely described (Avagliano Trezza et al., 2021; Wang et al., 2019), its full-length structure is still unknown. The structure of the catalytic HECT domain was solved 2 decades ago (Huang et al., 1999), and more recently certain regions at the N-terminal part of UBE3A –AZUL domain and the E6 binding region– have also been described (Lemak et al., 2011; Martinez-Zapien et al., 2016). Neverthless, so far, attempts to solve the full-length structure of UBE3A have failed.

To solve the UBE3A full-length structure, our approach consisted on generating three different UBE3A constructs, each one with a different tag (His, GST or SUMO), in order to purify the E3 ligase with distinct strategies. Affinity chromatography using Histidine tag as bait proved to be the most succesful purification, as the highest enrichment of UBE3A was obtained with a minimal degree of contamination. Besides that, since His label is an small epitope tag, there is no need to remove it for crystallization, and proteins can be purified by a single-step affinity chromatography (Spriestersbach et al., 2015). This feature avoids an extra cutting step, and hence, diminishes the loss of protein during the protocol. By contrast, GST tag is a long protein tag (29 kDa), so it needs to be removed for further analysis, increasing the possibility of sample loss. Scheich et al. stated that the purity of the purified protein is similar using His- or GST-tags, but the protein yield is substantially higher in His-tagged proteins (Scheich et al., 2003). Neverthless, GST tagged UBE3A, which conserves the physiological role of the protein (Harper and Speicher, 2011), was succesfully used to solve the HECT domain structure of the E3 ligase (Huang et al., 1999). Additionally, GST tag, as well

as SUMO tag, is mainly used to enhance the expression of the protein of interest in *E. coli* (Malakhov et al., 2004). Taken into account the previous studies, we decided to test both constructs (His- and GST-tags), and concluded that even though the purity of UBE3A after affinity chromatography was similar, higher yield was obtained with His-tagged UBE3A.

The affinity purification of UBE3A-SUMO showed similar results to GST construct; low enrichment yield, and many contaminant proteins. However, after ion-exchange chromatography, SUMO based-purification showed less degradation products than His- or GST- based purifications. SUMO tag has been described to protect proteins from degradation (Butt et al., 2005), and although the tag is removed before ion-exchange chromatography, the expression of SUMO-UBE3A in *E.coli* may have protected UBE3A from being degraded during the whole purification process. Altogether, our results demonstrate that UBE3A can be successfully purified with any of the above mention purification strategies.

Human full-length UBE3A protein could not be crystallized for structure resolution

Although human UBE3A protein was successfully purified, proper crystal structures for X-ray diffraction experiment were not obtained. There are many factors that can affect the crystallization of a protein, either chemical (pH, precipitant concentration..), physical (temperature, time, surface..) or biochemical (purity of the macromolecule, isoelectric point...) (McPherson and Gavira, 2013). However, the protein itself is the most important and influential variable in the crystallization. As corroborated with Alphafold software (Jumper et al., 2021), UBE3A contains a low organized region between the AZUL and E6 binding domain, probably unstabilizing the whole structure from being crystallized. Polyols are used to stabilize protein structures for crystallization (Sousa, 1995), and even if UBE3A proteins showed a preference for PEG based matrix in the pre-crystallization test, no proper crystals were obtained in our crystallization conditions. We hypothesize that crystallization of UBE3A together with one of its substrates or interactors could stabilize the non-organized region, and enable the

generation of suitable crystal structures for proper X-ray diffraction-based resolution of the full-length structure.

UBE3A mildly-overexpressing mice show a hyperactive phenotype

UBE3A gene is located in the chromosomal region 15q. Deletion or duplication of this region is associated with several neurodevelopmental disorders, including Angelman syndrome and Autism Spectrum Disorders. Although the molecular mechanisms still remain unclear, the UBE3A protein levels strongly correlate with the phenotypes of these disorders. Loss or dysfunction of UBE3A leads to AS, while overexpression of the E3 ligase results in autism (Elgersma, 2015). Therefore, mice models that lack and overexpress UBE3A are both suitable to study AS and ASD, respectively.

Multiple studies focus on generating mouse models of AS by interrupting UBE3A protein function by point mutations, locus deletions, modifications in the imprinting center or paternal allele duplication (Rotaru et al., 2020). Regardless the approach used to disrupt UBE3A function, mice exhibit symptoms similar to human Angelman syndrome patients; reduced locomotor activity, increased anxiety, hypersocial and communicative behaviours and reduced repetitive behaviours (Rotaru et al., 2020).

A number of UBE3A overexpressing mice have also been generated to decipher the pathophysiology of ASD. A mice model with an increased dosage of UBE3A exhibit autism-like symptoms, such as reduced pup communicative behaviours (Copping et al., 2017). Another mice model with a duplication of the 15q region showed defects in social interactions, decreased exploratory activity and increased anxiety (Nakatani et al., 2009), while normal exploratory activity and increased anxiety was shown by the UBE3A isoform 2 overexpression model described above (Copping et al., 2017; Smith et al., 2011). The differences in autism-like symptoms between different mice lines could be probably due to differences in UBE3A overexpression strategies; increased dosage of UBE3A or duplication of the whole 15q region could differentially affect mice behavior.

Our research group developed a mice line that mildly overexpresses UBE3A isoform 1, together with the BioUb system (Lectez et al., 2022, under review). BioUb mice were previously used to study the ubiquitin profiling in liver (Lectez et al., 2014), while UBE3A overexpressing mice were generated to combine them with the BioUb mice, in order to search for UBE3A substrates (Lectez et al., 2022, under review). Although the main goal is not to use these mice as a disease model, it is important to assess the effect of UBE3A overexpression in mice behavior, to confirm that their physiology is not strongly affected. Moreover, if behavioral phenotypes are observed, those could be checked for improvements when testing compounds that target candidate proteins.

As mentioned above, different UBE3A overexpressing mice models exhibit distinct autism-like symptoms (Copping et al., 2017; Nakatani et al., 2009; Smith et al., 2011). Therefore, we performed a behavioral characterization to check those autism-like behaviors in our UBE3A overexpressing mice model. We observed normal social and communicative behaviors, but a more pronounced repetitive behavior, which was barely below the border of statistical significance. Interestingly, hyperactivity, a common comorbid symptom described in about 40-70% of individuals with autism (Antshel and Russo, 2019), was determined based on an increased exploratory behavior in our mice. Reduced anxiety was found in UBE3A overexpressing mice, contrary to what was described for the Dup15q model (Nakatani et al., 2009). The observation of reduced anxiety in our model was not expected, as anxiety usually correlates with autism. However, we cannot rule out that the observed hyperactivity is indeed masking anxiety, given that the test is based on the latency to move out to open space from an enclosed arena. In brief, although, the behavioral characterization of UBE3A overexpressing mice support the role for UBE3A in modulating autism-associated behaviors, the physiology of our UBE3A overexpressing mice is not strongly altered.

In summary, during this Thesis project we have validated UBE3A candidate substrates previously identified in *Drosophila melanogaster* and mice, we have described a strategy to identify ubiquitination sites and ubiquitin chain-types mediated by UBE3A, we have identified USP9X as the UBE3A counteracting DUB, and we have demonstrated that its inhibition could be a suitable approach for the development of future treatments for AS. We have also identified several UBE3A interactors that may regulate the E3 ligase function, and determined if they are N-

terminal, C-terminal or full-length interactors. Finally, we have established a protocol for successful UBE3A purification with the aim of resolving its full-length structure, and we have characterized the behavior of our mice model that overexpresses UBE3A. Although further work needs to be done to deeply understand the molecular mechanisms underlying AS, the investigation reported in this Thesis will open new research lines for future studies.

X.

ONDORIOAK

1. GFP pull-down estrategia modu arrakastatsuan erabili daiteke aurretiaz *Drosophila melanogaster* eulietan identifikatutako substratu kandidatuak giza zeluletan egiaztatzeko.

2. UBE3Ak giza DDI1, DDI2, MINDY2 eta PSMA5 ubikitinatzen ditu HEK293T eta SH-SY5Y lerro zelularretan.

3. UBE3Ak PSMA5 ubikitinatzen du poli-ubikitina kateak sortuz HEK293T zelula lerroan. Aldiz, PSMA5 proteinaren mono-ubikitinazioa gehitzen du SH-SY5Y lerro zelularrean.

4. UBE3A substratu kandidatuak zitoplasman zeharreko kokapen ezberdina azaltzen dute, eta potentzialki giza UBE3A proteinarekin elkarrekin dezakete.

5. Egiaztatutako DDI1, DDI2, PSMA5 eta MINDY2 proteinek UBE3Arekin elkarrekiten dute HEK293T zelulen lerroan.

6. Moldatutako *GFP pull-down* estrategia modu arrakastatsuan erabili daiteke UBE3A proteinak bere substratuetan sortutako ubikitina kate-motak eta ubikitinazio-guneak detektatzeko.

7. UBE3Ak DDI1 eta DDI2 proteinak ubikitinatzen ditu K133 eta K77 hondarretan, hurrenez hurren, eta nagusiki K48 ubikitina kate-mota sortzen du, itxuraz substratu horiek degradaziora bideratu gabe.

8. Giza DDI1 proteinako K133 hondarraren mutazioak, proteina horren UBE3A bidezko ubikitinazioa oztopatzen dute.

9. USP9X deubikitinasaren inhibizioak DDI1 proteinaren ubikitinazio-maila igotzen du, UBE3Aren aurkako funtzioa burutuz.

10. USP9X deubikitinasaren inhibitzailea den WP1130 farmakoak, DDI1en ubikitinazio-maila igotzen du HEK293T zelulen lerroan.

11. WP1130 farmako bidezko tratamenduak *Drosophila melanogaster* Ube3a mutante homozigotoen igotze-ahalmena berreskuratzen du 24 orduren ondoren.

12. WP1130 farmako bidezko tratamenduak *Drosophila melanogaster* eulietan mGluR eta CoRest proteinen ubikitinazio-mailak igotzen ditu.

13. BioID estrategia modu arrakastatsuan erabili da lehenengo aldiz UBE3Aren interaktoreak identifikatzeko, eta horiek proteina osoarekin, amino muturrarekin edo karboxilo muturrarekin elkarrekiten duten deskribatzeko.

14. PIP, FLNA, S100A11, SFN, ALOX12B eta ARFGAP1 proteinek, UBE3Aren amino muturrarekin elkarrekiten dute HEK293T zelulen lerroan.

15. APBB1, UBAP2L eta LTV1 proteinek UBE3Aren karboxilo muturrarekin elkarrekiten dute HEK293T zelulen lerroan.

16. IGF2R eta MAP4 proteinek UBE3Aren egitura osoa behar dute elkarrekintzarako HEK293T zelulen lerroan.

17. LIMD1, UBE3Aren egitura osoarekin elkarrekiten duen proteina kandidatu bat, HEK293T lerro zelularrean UBE3Arekin elkarrekiten du.

18. Giza UBE3A proteinaren purifikaziorako prokotola deskribatu dugu.

19. His-UBE3A, GST-UBE3A eta SUMO-UBE3A plasmidoak arrakastaz erabili daitezke UBE3A proteina purifikatzeko, His-UBE3A delarik denetan efizienteena.

20. UBE3A proteinak, kristalizazio baldintzen artean, polietilenglikolean (PEG) oinarritutako soluzioekiko zaletasuna azaltzen du.

21. UBE3A gainadierazten duten saguek hiperaktibitatea eta antsietate-maila baxuak azaltzen dituzte, distantzia gehiago burutzen baitute, abiadura handiagoan mugitzen baitira, eta argitarako latentzia-trantsizio baxuagoa erakusten baitute.

XI.

REFERENCES

Abdul Rehman, S.A., Armstrong, L.A., Lange, S.M., Kristariyanto, Y.A., Gräwert, T.W., Knebel, A., Svergun, D.I., and Kulathu, Y. (2021). Mechanism of activation and regulation of deubiquitinase activity in MINDY1 and MINDY2. Mol. Cell *81*, 4176-4190.e6. https://doi.org/10.1016/j.molcel.2021.08.024.

Abdul Rehman, S.A., Kristariyanto, Y.A., Choi, S.-Y., Nkosi, P.J., Weidlich, S., Labib, K., Hofmann, K., and Kulathu, Y. (2016). MINDY-1 Is a Member of an Evolutionarily Conserved and Structurally Distinct New Family of Deubiquitinating Enzymes. Mol. Cell *63*, 146–155. https://doi.org/10.1016/j.molcel.2016.05.009.

Adams, M.D., Celniker, S.E., Holt, R.A., Evans, C.A., Gocayne, J.D., Amanatides, P.G., Scherer, S.E., Li, P.W., Hoskins, R.A., Galle, R.F., et al. (2000). The genome sequence of Drosophila melanogaster. Science *287*, 2185–2195. https://doi.org/10.1126/science.287.5461.2185.

Akimov, V., Barrio-Hernandez, I., Hansen, S.V.F., Hallenborg, P., Pedersen, A.-K., Bekker-Jensen, D.B., Puglia, M., Christensen, S.D.K., Vanselow, J.T., Nielsen, M.M., et al. (2018). UbiSite approach for comprehensive mapping of lysine and N-terminal ubiquitination sites. Nat. Struct. Mol. Biol. *25*, 631–640. https://doi.org/10.1038/s41594-018-0084-y.

Alexandrova, A., Petrov, L., and Kirkova, M. (2006). Proteasome activity in experimental diabetes. Cent. Eur. J. Biol. *1*, 289–298. https://doi.org/10.2478/s11535-006-0017-3.

Am, B., M, J., Lm, I., and L, A. (2008). Anatomy of the E2 ligase fold: implications for enzymology and evolution of ubiquitin/Ub-like protein conjugation. J. Struct. Biol. *162*, 205–218. https://doi.org/10.1016/j.jsb.2007.12.006.

American Psychiatric Association (2013). DSM 5 Diagnostic and statistical manual of mental disorders. DSM 5 Diagn. Stat. Man. Ment. Disord. 947 p.-947 p. .

Amerik, A.Y., and Hochstrasser, M. (2004). Mechanism and function of deubiquitinating enzymes. Biochim. Biophys. Acta BBA - Mol. Cell Res. *1695*, 189–207. https://doi.org/10.1016/j.bbamcr.2004.10.003.

Angelman, H. (1965). 'Puppet' Children A Report on Three Cases. Dev. Med. Child Neurol. *7*, 681–688. https://doi.org/10.1111/j.1469-8749.1965.tb07844.x.

Antshel, K.M., and Russo, N. (2019). Autism Spectrum Disorders and ADHD: Overlapping Phenomenology, Diagnostic Issues, and Treatment Considerations. Curr. Psychiatry Rep. *21*, 34. https://doi.org/10.1007/s11920-019-1020-5.

Aravind, L., and Koonin, E.V. (2000). Eukaryote-specific Domains in Translation Initiation Factors: Implications for Translation Regulation and Evolution of the Translation System. Genome Res. *10*, 1172–1184. .

Aryal, B., and Lee, Y. (2019). Disease model organism for Parkinson disease: Drosophila melanogaster. BMB Rep. *52*, 250–258. .

Avagliano Trezza, R., Sonzogni, M., Bossuyt, S.N.V., Zampeta, F.I., Punt, A.M., van den Berg, M., Rotaru, D.C., Koene, L.M.C., Munshi, S.T., Stedehouder, J., et al. (2019). Loss of nuclear UBE3A causes electrophysiological and behavioral deficits in mice and is associated with Angelman syndrome. Nat. Neurosci. *22*, 1235–1247. https://doi.org/10.1038/s41593-019-0425-0.

Avagliano Trezza, R., Punt, A.M., Mientjes, E., van den Berg, M., Zampeta, F.I., de Graaf, I.J., van der Weegen, Y., Demmers, J.A.A., Elgersma, Y., and Distel, B. (2021). Mono-ubiquitination of Rabphilin 3A by UBE3A serves a non-degradative function. Sci. Rep. *11*, 3007. https://doi.org/10.1038/s41598-021-82319-9.

Bailus, B.J., Pyles, B., McAlister, M.M., O'Geen, H., Lockwood, S.H., Adams, A.N., Nguyen, J.T.T., Yu, A., Berman, R.F., and Segal, D.J. (2016). Protein Delivery of an Artificial Transcription Factor Restores Widespread Ube3a Expression in an Angelman Syndrome Mouse Brain. Mol. Ther. *24*, 548–555. https://doi.org/10.1038/mt.2015.236.

Bakke, K.A., Howlin, P., Retterstøl, L., Kanavin, Ø.J., Heiberg, A., and Nærland, T. (2018). Effect of epilepsy on autism symptoms in Angelman syndrome. Mol. Autism *9*. https://doi.org/10.1186/s13229-017-0185-1.

Balakirev, M.Y., Tcherniuk, S.O., Jaquinod, M., and Chroboczek, J. (2003). Otubains: a new family of cysteine proteases in the ubiquitin pathway. EMBO Rep. *4*, 517–522. https://doi.org/10.1038/sj.embor.embor824.

Baldini, R., Mascaro, M., and Meroni, G. (2020). The MID1 gene product in physiology and disease. Gene *747*, 144655. https://doi.org/10.1016/j.gene.2020.144655.

Barghout, S.H., and Schimmer, A.D. (2018). The ubiquitin-activating enzyme, UBA1, as a novel therapeutic target for AML. Oncotarget *9*, 34198–34199. https://doi.org/10.18632/oncotarget.26153.

Barnes, V.L., Bhat, A., Unnikrishnan, A., Heydari, A.R., Arking, R., and Pile, L.A. (2014). SIN3 is critical for stress resistance and modulates adult lifespan. Aging *6*, 645–660. .

Barrios, Á.P., Gómez, A.V., Sáez, J.E., Ciossani, G., Toffolo, E., Battaglioli, E., Mattevi, A., and Andrés, M.E. (2014). Differential Properties of Transcriptional Complexes Formed by the CoREST Family. Mol. Cell. Biol. *34*, 2760–2770. https://doi.org/10.1128/MCB.00083-14.

Bartholomeusz, G., Talpaz, M., Bornmann, W., Kong, L.-Y., and Donato, N.J. (2007a). Degrasyn Activates Proteasomal-Dependent Degradation of c-Myc. Cancer Res. *67*, 3912–3918. https://doi.org/10.1158/0008-5472.CAN-06-4464.

Bartholomeusz, G.A., Talpaz, M., Kapuria, V., Kong, L.Y., Wang, S., Estrov, Z., Priebe, W., Wu, J., and Donato, N.J. (2007b). Activation of a novel Bcr/Abl destruction pathway by WP1130 induces apoptosis of chronic myelogenous leukemia cells. Blood *109*, 3470–3478. https://doi.org/10.1182/blood-2006-02-005579.

Baur, R., and Rape, M. (2020). Getting Close: Insight into the Structure and Function of K11/K48-Branched Ubiquitin Chains. Structure *28*, 1–3. https://doi.org/10.1016/j.str.2019.12.004.

Beasley, S.A., Kellum, C.E., Orlomoski, R.J., Idrizi, F., and Spratt, D.E. (2020). An Angelman syndrome substitution in the HECT E3 ubiquitin ligase C-terminal Lobe of E6AP affects protein stability and activity. PLOS ONE *15*, e0235925. https://doi.org/10.1371/journal.pone.0235925.

Beckett, D., Kovaleva, E., and Schatz, P.J. (1999). A minimal peptide substrate in biotin holoenzyme synthetase-catalyzed biotinylation. Protein Sci. Publ. Protein Soc. *8*, 921–929. https://doi.org/10.1110/ps.8.4.921.

Beehler, B.C., Sleph, P.G., Benmassaoud, L., and Grover, G.J. (2006). Reduction of skeletal muscle atrophy by a proteasome inhibitor in a rat model of denervation. Exp. Biol. Med. Maywood NJ *231*, 335–341. https://doi.org/10.1177/153537020623100315.

Bellanné-Chantelot, C., Schmaltz-Panneau, B., Marty, C., Fenneteau, O., Callebaut, I., Clauin, S., Docet, A., Damaj, G.-L., Leblanc, T., Pellier, I., et al. (2018). Mutations in the SRP54 gene cause severe congenital neutropenia as well as Shwachman-Diamond–like syndrome. Blood *132*, 1318–1331. https://doi.org/10.1182/blood-2017-12-820308.

Bend, E.G., Aref-Eshghi, E., Everman, D.B., Rogers, R.C., Cathey, S.S., Prijoles, E.J., Lyons, M.J., Davis, H., Clarkson, K., Gripp, K.W., et al. (2019). Gene domain-specific DNA methylation episignatures highlight distinct molecular entities of ADNP syndrome. Clin. Epigenetics *11*, 64. https://doi.org/10.1186/s13148-019-0658-5.

Bennett, E.J., and Harper, J.W. (2008). DNA damage: ubiquitin marks the spot. Nat. Struct. Mol. Biol. *15*, 20–22. https://doi.org/10.1038/nsmb0108-20.

Bennett, E.J., Shaler, T.A., Woodman, B., Ryu, K.-Y., Zaitseva, T.S., Becker, C.H., Bates, G.P., Schulman, H., and Kopito, R.R. (2007). Global changes to the ubiquitin system in Huntington's disease. Nature *448*, 704–708. https://doi.org/10.1038/nature06022.

Berndsen, C.E., and Wolberger, C. (2014). New insights into ubiquitin E3 ligase mechanism. Nat. Struct. Mol. Biol. *21*, 301–307. https://doi.org/10.1038/nsmb.2780.

Bertolaet, B.L., Clarke, D.J., Wolff, M., Watson, M.H., Henze, M., Divita, G., and Reed, S.I. (2001). UBA domains of DNA damage-inducible proteins interact with ubiquitin. Nat. Struct. Mol. Biol. *8*, 417. .

Bertolini, S., Pisciotta, L., Rabacchi, C., Cefalù, A.B., Noto, D., Fasano, T., Signori, A., Fresa, R., Averna, M., and Calandra, S. (2013). Spectrum of mutations and phenotypic expression in patients with autosomal dominant hypercholesterolemia identified in Italy. Atherosclerosis *227*, 342–348. https://doi.org/10.1016/j.atherosclerosis.2013.01.007.

Besche, H.C., Sha, Z., Kukushkin, N.V., Peth, A., Hock, E.-M., Kim, W., Gygi, S., Gutierrez, J.A., Liao, H., Dick, L., et al. (2014). Autoubiquitination of the 26S Proteasome on Rpn13 Regulates Breakdown of Ubiquitin Conjugates. EMBO J. *33*, 1159–1176. https://doi.org/10.1002/embj.201386906.

Beygo, J., Buiting, K., Ramsden, S.C., Ellis, R., Clayton-Smith, J., and Kanber, D. (2019). Update of the EMQN/ACGS best practice guidelines for molecular analysis of Prader-Willi and Angelman syndromes. Eur. J. Hum. Genet. *27*, 1326–1340. https://doi.org/10.1038/s41431-019-0435-0.

Beygo, J., Grosser, C., Kaya, S., Mertel, C., Buiting, K., and Horsthemke, B. (2020). Common genetic variation in the Angelman syndrome imprinting centre affects the imprinting of chromosome 15. Eur. J. Hum. Genet. 1–5. https://doi.org/10.1038/s41431-020-0595-y.

Bhullar, K.S., Lagarón, N.O., McGowan, E.M., Parmar, I., Jha, A., Hubbard, B.P., and Rupasinghe, H.P.V. (2018). Kinase-targeted cancer therapies: progress, challenges and future directions. Mol. Cancer *17*. https://doi.org/10.1186/s12943-018-0804-2.

Bi, X., Sun, J., Ji, A.X., and Baudry, M. (2016). Potential therapeutic approaches for Angelman syndrome. Expert Opin. Ther. Targets *20*, 601–613. https://doi.org/10.1517/14728222.2016.1115837.

Bianchi, M., Crinelli, R., Giacomini, E., Carloni, E., Radici, L., Scarpa, E.-S., Tasini, F., and Magnani, M. (2019). A negative feedback mechanism links UBC gene expression to ubiquitin levels by affecting RNA splicing rather than transcription. Sci. Rep. *9*, 1–19. https://doi.org/10.1038/s41598-019-54973-7.

Bianchi R, Wong RKS, Merlin LR. Glutamate Receptors in Epilepsy: Group I mGluR-Mediated Epileptogenesis. In: Noebels JL, Avoli M, Rogawski MA, Olsen RW, Delgado-Escueta AV, editors. Jasper's Basic Mechanisms of the Epilepsies [Internet]. 4th ed. Bethesda (MD): National Center for Biotechnology Information (US); 2012. PMID: 22787676.

Bier, E., and Bodmer, R. (2004). Drosophila, an emerging model for cardiac disease. Gene *342*, 1–11. https://doi.org/10.1016/j.gene.2004.07.018.

Bindels-de Heus, K.G.C.B., Mous, S.E., ten Hooven-Radstaake, M., van Iperen-Kolk, B.M., Navis, C., Rietman, A.B., ten Hoopen, L.W., Brooks, A.S., Elgersma, Y., Moll, H.A., et al. (2020). An overview of health issues and development in a large clinical cohort of children with Angelman syndrome. Am. J. Med. Genet. A. *182*, 53–63. https://doi.org/10.1002/ajmg.a.61382.

Bird, L.M. (2014). Angelman syndrome: review of clinical and molecular aspects. Appl. Clin. Genet. *7*, 93–104. https://doi.org/10.2147/TACG.S57386.

Bird, L.M., Tan, W.H., Bacino, C.A., Peters, S.U., Skinner, S.A., Anselm, I., Barbieri-Welge, R., Bauer-Carlin, A., Gentile, J.K., Glaze, D.G., et al. (2011). A therapeutic trial of pro-methylation dietary supplements in Angelman syndrome. Am. J. Med. Genet. A. *155A*, 2956–2963. https://doi.org/10.1002/ajmg.a.34297.

Born, H.A., Dao, A.T., Levine, A.T., Lee, W.L., Mehta, N.M., Mehra, S., Weeber, E.J., and Anderson, A.E. (2017). Strain-dependence of the Angelman Syndrome phenotypes in Ube3a maternal deficiency mice. Sci. Rep. *7*. https://doi.org/10.1038/s41598-017-08825-x.

Bourin, M., and Hascoët, M. (2003). The mouse light/dark box test. Eur. J. Pharmacol. *463*, 55–65. https://doi.org/10.1016/S0014-2999(03)01274-3.

Brand, A.H., and Perrimon, N. (1993). Targeted gene expression as a means of altering cell fates and generating dominant phenotypes. Dev. Camb. Engl. *118*, 401–415. .

Branon, T.C., Bosch, J.A., Sanchez, A.D., Udeshi, N.D., Svinkina, T., Carr, S.A., Feldman, J.L., Perrimon, N., and Ting, A.Y. (2018). Efficient proximity labeling in living cells and organisms with TurboID. Nat. Biotechnol. *36*, 880–887. https://doi.org/10.1038/nbt.4201.

Brimer, N., Lyons, C., Vande Pol, SB. (2007). Association of E6AP (UBE3A) with human papillomavirus type 11 E6 protein. Virology. *358*, 303-10. doi: 10.1016/j.virol.2006.08.038.

Broca, C., Varin, E., Armanet, M., Tourrel-Cuzin, C., Bosco, D., Dalle, S., and Wojtusciszyn, A. (2014). Proteasome Dysfunction Mediates High Glucose-Induced Apoptosis in Rodent Beta Cells and Human Islets. PLOS ONE *9*, e92066. https://doi.org/10.1371/journal.pone.0092066.

Budny, B., Badura-Stronka, M., Materna-Kiryluk, A., Tzschach, A., Raynaud, M., Latos-Bielenska, A., and Ropers, H.H. (2010). Novel missense mutations in the ubiquitination-related gene UBE2A cause a recognizable X-linked mental retardation syndrome. Clin. Genet. *77*, 541–551. https://doi.org/10.1111/j.1399-0004.2010.01429.x.

Buel, G.R., Chen, X., Chari, R., O'Neill, M.J., Ebelle, D.L., Jenkins, C., Sridharan, V., Tarasov, S.G., Tarasova, N.I., Andresson, T., et al. (2020). Structure of E3 ligase E6AP with a proteasome-binding site provided by substrate receptor hRpn10. Nat. Commun. *11*, 1291. https://doi.org/10.1038/s41467-020-15073-7.

Buiting, K., Saitoh, S., Gross, S., Dittrich, B., Schwartz, S., Nicholls, R.D., and Horsthemke, B. (1995). Inherited microdeletions in the Angelman and Prader-Willi syndromes define an imprinting centre on human chromosome 15. Nat. Genet. *9*, 395–400. https://doi.org/10.1038/ng0495-395.

Buiting, K., Gross, S., Lich, C., Gillessen-Kaesbach, G., el-Maarri, O., and Horsthemke, B. (2003). Epimutations in Prader-Willi and Angelman syndromes: a molecular study of 136 patients with an imprinting defect. Am. J. Hum. Genet. *72*, 571–577. https://doi.org/10.1086/367926.

Buiting, K., Clayton-Smith, J., Driscoll, D.J., Gillessen-Kaesbach, G., Kanber, D., Schwinger, E., Williams, C., and Horsthemke, B. (2015). Clinical utility gene card for: Angelman Syndrome. Eur. J. Hum. Genet. *23*. https://doi.org/10.1038/ejhg.2014.93.

Buiting, K., Williams, C., and Horsthemke, B. (2016). Angelman syndrome — insights into a rare neurogenetic disorder. Nat. Rev. Neurol. *12*, 584–593. https://doi.org/10.1038/nrneurol.2016.133.

Burnett, B., Li, F., and Pittman, R.N. (2003). The polyglutamine neurodegenerative protein ataxin-3 binds polyubiquitylated proteins and has ubiquitin protease activity. Hum. Mol. Genet. *12*, 3195–3205. https://doi.org/10.1093/hmg/ddg344.

Butland, S.L., Sanders, S.S., Schmidt, M.E., Riechers, S.P., Lin, D.T.S., Martin, D.D.O., Vaid, K., Graham, R.K., Singaraja, R.R., Wanker, E.E., et al. (2014). The palmitoyl acyltransferase HIP14 shares a high proportion of interactors with huntingtin: implications for a role in the pathogenesis of Huntington's disease. Hum. Mol. Genet. *23*, 4142–4160. https://doi.org/10.1093/hmg/ddu137.

Butt, T.R., Edavettal, S.C., Hall, J.P., and Mattern, M.R. (2005). SUMO fusion technology for difficult-to-express proteins. Protein Expr. Purif. *43*, 1–9. https://doi.org/10.1016/j.pep.2005.03.016.

Caron, A.Z., Haroun, S., Leblanc, É., Trensz, F., Guindi, C., Amrani, A., and Grenier, G. (2011). The proteasome inhibitor MG132 reduces immobilization-induced skeletal muscle

atrophy in mice. BMC Musculoskelet. Disord. *12*, 185. https://doi.org/10.1186/1471-2474-12-185.

Castle, W.E. (1906). Inbreeding, cross-breeding and sterility in Drosophila. Science *23*, 153. https://doi.org/10.1126/science.23.578.153.

Chandler, C.S., and Ballard, F.J. (1985). Distribution and degradation of biotin-containing carboxylases in human cell lines. Biochem. J. *232*, 385–393. .

Chandler, C.S., and Ballard, F.J. (1986). Multiple biotin-containing proteins in 3T3-L1 cells. Biochem. J. *237*, 123–130. .

Chastagner, P., Israël, A., and Brou, C. (2006). Itch/AIP4 mediates Deltex degradation through the formation of K29-linked polyubiquitin chains. EMBO Rep. *7*, 1147–1153. https://doi.org/10.1038/sj.embor.7400822.

Chen, Y.S., and Qiu, X.B. (2013). Ubiquitin at the crossroad of cell death and survival. Chin. J. Cancer *32*, 640–647. https://doi.org/10.5732/cjc.012.10283.

Chen, R.H., Chen, Y.H., and Huang, T.Y. (2019). Ubiquitin-mediated regulation of autophagy. J. Biomed. Sci. *26*, 80. https://doi.org/10.1186/s12929-019-0569-y.

Chen, X., Zhang, B., and Fischer, J.A. (2002). A specific protein substrate for a deubiquitinating enzyme: Liquid facets is the substrate of Fat facets. Genes Dev. *16*, 289–294. https://doi.org/10.1101/gad.961502.

Chen, Y., Zhang, Y., and Guo, X. (2017). Proteasome dysregulation in human cancer: implications for clinical therapies. Cancer Metastasis Rev. *36*, 703–716. https://doi.org/10.1007/s10555-017-9704-y.

Chen, Y.H., Huang, T.Y., Lin, Y.T., Lin, S.Y., Li, W.H., Hsiao, H.J., Yan, R.L., Tang, H.W., Shen, Z.Q., Chen, G.C., et al. (2021). VPS34 K29/K48 branched ubiquitination governed by UBE3C and TRABID regulates autophagy, proteostasis and liver metabolism. Nat. Commun. *12*. https://doi.org/10.1038/s41467-021-21715-1.

Chen, Y.S., Hong, Z.X., Lin, S.Z., and Harn, H.J. (2020). Identifying Therapeutic Targets for Spinocerebellar Ataxia Type 3/Machado–Joseph Disease through Integration of Pathological Biomarkers and Therapeutic Strategies. Int. J. Mol. Sci. *21*, 3063. https://doi.org/10.3390/ijms21093063.

Cheng, F., Zhao, J., Wang, Y., Lu, W., Liu, Z., Zhou, Y., Martin, W.R., Wang, R., Huang, J., Hao, T., et al. (2021). Comprehensive characterization of protein-protein interactions perturbed by disease mutations. Nat. Genet. *53*, 342–353. https://doi.org/10.1038/s41588-020-00774-y.

Cheng, J., Fan, Y.-H., Xu, X., Zhang, H., Dou, J., Tang, Y., Zhong, X., Rojas, Y., Yu, Y., Zhao, Y., et al. (2014). A small-molecule inhibitor of UBE2N induces neuroblastoma cell death via activation of p53 and JNK pathways. Cell Death Dis. *5*, e1079. https://doi.org/10.1038/cddis.2014.54.

Chew, E.H., Poobalasingam, T., Hawkey, C.J., and Hagen, T. (2007). Characterization of cullin-based E3 ubiquitin ligases in intact mammalian cells-evidence for cullin dimerization. Cell. Signal. *19*, 1071–1080. https://doi.org/10.1016/j.cellsig.2006.12.002.

Choi, S.Y., Jang, H., Roe, J.S., Kim, S.T., Cho, E.J., and Youn, H.D. (2013). Phosphorylation and ubiquitination-dependent degradation of CABIN1 releases p53 for transactivation upon genotoxic stress. Nucleic Acids Res. *41*, 2180–2190. https://doi.org/10.1093/nar/gks1319.

Chojnowski, A., Sobota, R.M., Ong, P.F., Xie, W., Wong, X., Dreesen, O., Burke, B., and Stewart, C.L. (2018). 2C-BioID: An Advanced Two Component BioID System for Precision Mapping of Protein Interactomes. IScience *10*, 40–52. https://doi.org/10.1016/j.isci.2018.11.023.

Chong, J.A., Tapia-Ramirez, J., Kim, S., Toledo-Aral, J.J., Zheng, Y., Boutros, M.C., Altshuller, Y.M., Frohman, M.A., Kraner, S.D., and Mandel, G. (1995). REST: A mammalian silencer protein that restricts sodium channel gene expression to neurons. Cell *80*, 949–957. https://doi.org/10.1016/0092-8674(95)90298-8.

Choo, Y.Y., and Hagen, T. (2012). Mechanism of Cullin3 E3 Ubiquitin Ligase Dimerization. PLoS ONE *7*. https://doi.org/10.1371/journal.pone.0041350.

Chung, L., Bey, A.L., Towers, A.J., Cao, X., Kim, I.H., and Jiang, Y. (2018). Lovastatin suppresses hyperexcitability and seizure in Angelman syndrome model. Neurobiol. Dis. *110*, 12–19. https://doi.org/10.1016/j.nbd.2017.10.016.

Ciarlone, S.L., Wang, X., Rogawski, M.A., and Weeber, E.J. (2016). Effects of the synthetic neurosteroid ganaxolone on seizure activity and behavioral deficits in an Angelman syndrome mouse model. Neuropharmacology *116*, 142–150. https://doi.org/10.1016/j.neuropharm.2016.12.009.

Ciechanover, A. (2013). Intracellular protein degradation: From a vague idea through the lysosome and the ubiquitin–proteasome system and onto human diseases and drug targeting. Bioorg. Med. Chem. *21*, 3400–3410. https://doi.org/10.1016/j.bmc.2013.01.056.

Ciechanover, A., and Ben-Saadon, R. (2004). N-terminal ubiquitination: more protein substrates join in. 4. .

Ciechanover, A., Heller, H., Katz-Etzion, R., and Hershko, A. (1981). Activation of the heat-stable polypeptide of the ATP-dependent proteolytic system. Proc. Natl. Acad. Sci. U. S. A. *78*, 761–765. .

Clague, M.J., Urbé, S., and Komander, D. (2019). Breaking the chains: deubiquitylating enzyme specificity begets function. Nat. Rev. Mol. Cell Biol. *20*, 338–352. https://doi.org/10.1038/s41580-019-0099-1.

Clancy, A., Heride, C., Pinto-Fernández, A., Elcocks, H., Kallinos, A., Kayser-Bricker, K.J., Wang, W., Smith, V., Davis, S., Fessler, S., et al. (2021). The deubiquitylase USP9X controls ribosomal stalling. J. Cell Biol. *220*. https://doi.org/10.1083/jcb.202004211.

Clute, P., and Pines, J. (1999). Temporal and spatial control of cyclin B1 destruction in metaphase. Nat. Cell Biol. *1*, 82–87. https://doi.org/10.1038/10049.

Cohen, P., Cross, D., and Jänne, P.A. (2021). Kinase drug discovery 20 years after imatinib: progress and future directions. Nat. Rev. Drug Discov. *20*, 551–569. https://doi.org/10.1038/s41573-021-00195-4.

Conforti, P., Zuccato, C., Gaudenzi, G., Ieraci, A., Camnasio, S., Buckley, N.J., Mutti, C., Cotelli, F., Contini, A., and Cattaneo, E. (2013). Binding of the repressor complex REST-mSIN3b by small molecules restores neuronal gene transcription in Huntington's disease models. J. Neurochem. *127*, 22–35. https://doi.org/10.1111/jnc.12348.

Cope, G.A., Suh, G.S.B., Aravind, L., Schwarz, S.E., Zipursky, S.L., Koonin, E.V., and Deshaies, R.J. (2002). Role of predicted metalloprotease motif of Jab1/Csn5 in cleavage of Nedd8 from Cul1. Science *298*, 608–611. https://doi.org/10.1126/science.1075901.

Copping, N.A., Christian, S.G., Ritter, D.J., Islam, M.S., Buscher, N., Zolkowska, D., Pride, M.C., Berg, E.L., LaSalle, J.M., and Ellegood, J. (2017). Neuronal overexpression of Ube3a isoform 2 causes behavioral impairments and neuroanatomical pathology relevant to 15q11. 2-q13. 3 duplication syndrome. Hum. Mol. Genet. *26*, 3995–4010.

Cornwell, M.J., Thomson, G.J., Coates, J., Belotserkovskaya, R., Waddell, I.D., Jackson, S.P., and Galanty, Y. (2019). Small-Molecule Inhibition of UBE2T/FANCL-Mediated Ubiquitylation in the Fanconi Anemia Pathway. ACS Chem. Biol. *14*, 2148–2154. https://doi.org/10.1021/acschembio.9b00570.

Correia, C.T., Conceição, I.C., Oliveira, B., Coelho, J., Sousa, I., Sequeira, A.F., Almeida, J., Café, C., Duque, F., Mouga, S., et al. (2014). Recurrent duplications of the annexin A1 gene (ANXA1) in autism spectrum disorders. Mol. Autism *5*, 28. https://doi.org/10.1186/2040-2392-5-28.

Crawley, J.N. (2007). Mouse Behavioral Assays Relevant to the Symptoms of Autism*. Brain Pathol. *17*, 448–459. https://doi.org/10.1111/j.1750-3639.2007.00096.x.

Daily, J.L., Nash, K., Jinwal, U., Golde, T., Rogers, J., Peters, M.M., Burdine, R.D., Dickey, C., Banko, J.L., and Weeber, E.J. (2011). Adeno-Associated Virus-Mediated Rescue of the Cognitive Defects in a Mouse Model for Angelman Syndrome. PLoS ONE *6*. https://doi.org/10.1371/journal.pone.0027221.

Dallman, J.E., Allopenna, J., Bassett, A., Travers, A., and Mandel, G. (2004). A Conserved Role But Different Partners for the Transcriptional Corepressor CoREST in Fly and Mammalian Nervous System Formation. J. Neurosci. *24*, 7186–7193. https://doi.org/10.1523/JNEUROSCI.0238-04.2004.

Dambacher, C.M., Worden, E.J., Herzik, M.A., Martin, A., and Lander, G.C. Atomic structure of the 26S proteasome lid reveals the mechanism of deubiquitinase inhibition. ELife *5*. https://doi.org/10.7554/eLife.13027.

Dantuma, N.P., Groothuis, T.A.M., Salomons, F.A., and Neefjes, J. (2006). A dynamic ubiquitin equilibrium couples proteasomal activity to chromatin remodeling. J. Cell Biol. *173*, 19–26. https://doi.org/10.1083/jcb.200510071.

D'Arcy, P., Wang, X., and Linder, S. (2015). Deubiquitinase inhibition as a cancer therapeutic strategy. Pharmacol. Ther. *147*, 32–54. https://doi.org/10.1016/j.pharmthera.2014.11.002.

Das, S., Ramakrishna, S., and Kim, K.-S. (2020). Critical Roles of Deubiquitinating Enzymes in the Nervous System and Neurodegenerative Disorders. Mol. Cells *43*, 203–214. https://doi.org/10.14348/molcells.2020.2289.

David, Y., Ziv, T., Admon, A., and Navon, A. (2010). The E2 Ubiquitin-conjugating Enzymes Direct Polyubiquitination to Preferred Lysines. J. Biol. Chem. *285*, 8595–8604. https://doi.org/10.1074/jbc.M109.089003.

van Delft, S., Govers, R., Strous, G.J., Verkleij, A.J., and van Bergen en Henegouwen, P.M. (1997). Epidermal growth factor induces ubiquitination of Eps15. J. Biol. Chem. *272*, 14013–14016. https://doi.org/10.1074/jbc.272.22.14013.

Deng, L., Wang, C., Spencer, E., Yang, L., Braun, A., You, J., Slaughter, C., Pickart, C., and Chen, Z.J. (2000). Activation of the IkappaB kinase complex by TRAF6 requires a dimeric ubiquitin-conjugating enzyme complex and a unique polyubiquitin chain. Cell *103*, 351–361. https://doi.org/10.1016/s0092-8674(00)00126-4.

Deng, L., Meng, T., Chen, L., Wei, W., and Wang, P. (2020). The role of ubiquitination in tumorigenesis and targeted drug discovery. Signal Transduct. Target. Ther. *5*, 1–28. https://doi.org/10.1038/s41392-020-0107-0.

Deshaies, R.J., and Joazeiro, C.A.P. (2009). RING domain E3 ubiquitin ligases. Annu. Rev. Biochem. *78*, 399–434. https://doi.org/10.1146/annurev.biochem.78.101807.093809.

Deveraux, Q., Ustrell, V., Pickart, C., and Rechsteiner, M. (1994). A 26 S protease subunit that binds ubiquitin conjugates. J. Biol. Chem. *269*, 7059–7061. .

Di Fiore, P.P., Polo, S., and Hofmann, K. (2003). When ubiquitin meets ubiquitin receptors: a signalling connection. Nat. Rev. Mol. Cell Biol. *4*, 491–497. https://doi.org/10.1038/nrm1124.

Dikic, I., Wakatsuki, S., and Walters, K.J. (2009). Ubiquitin-binding domains — from structures to functions. Nat. Rev. Mol. Cell Biol. *10*, 659–671. https://doi.org/10.1038/nrm2767.

Dimova, N.V., Hathaway, N.A., Lee, B.-H., Kirkpatrick, D.S., Berkowitz, M.L., Gygi, S.P., Finley, D., and King, R.W. (2012). APC/C-mediated multiple monoubiquitination provides an alternative degradation signal for cyclin B1. Nat. Cell Biol. *14*, 168–176. https://doi.org/10.1038/ncb2425.

Dirac-Svejstrup, A.B., Walker, J., Faull, P., Encheva, V., Akimov, V., Puglia, M., Perkins, D., Kümper, S., Hunjan, S.S., Blagoev, B., et al. (2020). DDI2 Is a Ubiquitin-Directed Endoprotease Responsible for Cleavage of Transcription Factor NRF1. Mol. Cell *79*, 332-341.e7. https://doi.org/10.1016/j.molcel.2020.05.035.

Dodge, A., Peters, M.M., Greene, H.E., Dietrick, C., Botelho, R., Chung, D., Willman, J., Nenninger, A.W., Ciarlone, S., Kamath, S.G., et al. (2020). Generation of a Novel Rat Model of Angelman Syndrome with a Complete Ube3a Gene Deletion. Autism Res. *13*, 397–409. https://doi.org/10.1002/aur.2267.

Domon, B., and Aebersold, R. (2006). Mass spectrometry and protein analysis. Science *312*, 212–217. https://doi.org/10.1126/science.1124619.

Doncaster, L. (1916). The mechanism of mendelian heredity. Eugen. Rev. *8*, 164–166. .

Dong, C., Bach, S.V., Haynes, K.A., and Hegde, A.N. (2014). Proteasome Modulates Positive and Negative Translational Regulators in Long-Term Synaptic Plasticity. J. Neurosci. *34*, 3171–3182. https://doi.org/10.1523/JNEUROSCI.3291-13.2014.

Durcan, T.M., Tang, M.Y., Pérusse, J.R., Dashti, E.A., Aguileta, M.A., McLelland, G.-L., Gros, P., Shaler, T.A., Faubert, D., Coulombe, B., et al. (2014). USP8 regulates mitophagy by removing K6-linked ubiquitin conjugates from parkin. EMBO J. *33*, 2473–2491. https://doi.org/10.15252/embj.201489729.

de Duve, C., Pressman, B.C., Gianetto, R., Wattiaux, R., and Appelmans, F. (1955). Tissue fractionation studies. 6. Intracellular distribution patterns of enzymes in rat-liver tissue. Biochem. J. *60*, 604–617. .

Dynek, J.N., Goncharov, T., Dueber, E.C., Fedorova, A.V., Izrael-Tomasevic, A., Phu, L., Helgason, E., Fairbrother, W.J., Deshayes, K., Kirkpatrick, D.S., et al. (2010). c-IAP1 and UbcH5 promote K11-linked polyubiquitination of RIP1 in TNF signalling. EMBO J. *29*, 4198–4209. https://doi.org/10.1038/emboj.2010.300.

Eddins, M.J., Varadan, R., Fushman, D., Pickart, C.M., and Wolberger, C. (2007). Crystal structure and solution NMR studies of Lys48-linked tetraubiquitin at neutral pH. J. Mol. Biol. *367*, 204–211. https://doi.org/10.1016/j.jmb.2006.12.065.

Egan, M., Farrell, K., Hoey, E., McGuire, B.E., and Lydon, H.K. (2020). Interventions to improve sleep for individuals with Angelman syndrome: A systematic review. Res. Dev. Disabil. *97*, 103554. https://doi.org/10.1016/j.ridd.2019.103554.

Eisenhaber, B., Chumak, N., Eisenhaber, F., and Hauser, M.T. (2007). The ring between ring fingers (RBR) protein family. Genome Biol. *8*, 209. https://doi.org/10.1186/gb-2007-8-3-209.

Elgersma, Y. (2015). Neurodevelopmental disease: A molecular tightrope. Nature *526*, 50–51. https://doi.org/10.1038/526050b.

Elia, A.E.H., Boardman, A.P., Wang, D.C., Huttlin, E.L., Everley, R.A., Dephoure, N., Zhou, C., Koren, I., Gygi, S.P., and Elledge, S.J. (2015). Quantitative Proteomic Atlas of Ubiquitination and Acetylation in the DNA Damage Response. Mol. Cell *59*, 867–881. https://doi.org/10.1016/j.molcel.2015.05.006.

Elu, N., Osinalde, N., Beaskoetxea, J., Ramirez, J., Lectez, B., Aloria, K., Rodriguez, J.A., Arizmendi, J.M., and Mayor, U. (2019). Detailed Dissection of UBE3A-Mediated DDI1 Ubiquitination. Front. Physiol. *10*. https://doi.org/10.3389/fphys.2019.00534.

Elu, N., Osinalde, N., Ramirez, J., Presa, N., Rodriguez, J.A., Prieto, G. and Mayor, U. (2022). Identification of substrates for human deubiquitinating enzymes (DUBs): An up-to-date review and a case study for neurodevelopmental disorders. Semin Cell Dev Biol. *15*:S1084-9521(22)00003-9. doi: 10.1016/j.semcdb.2022.01.001.

Elu, N., Lectez, B., Ramirez, J., Osinalde, N., and Mayor, U. (2020). Mass Spectrometry-Based Characterization of Ub- and UbL-Modified Proteins. Methods Mol. Biol. Clifton NJ *2051*, 265–276. https://doi.org/10.1007/978-1-4939-9744-2_11.

Emmerich, C.H., Ordureau, A., Strickson, S., Arthur, J.S.C., Pedrioli, P.G.A., Komander, D., and Cohen, P. (2013). Activation of the canonical IKK complex by K63/M1-linked

hybrid ubiquitin chains. Proc. Natl. Acad. Sci. *110*, 15247–15252. https://doi.org/10.1073/pnas.1314715110.

Emmerich, C.H., Bakshi, S., Kelsall, I.R., Ortiz-Guerrero, J., Shpiro, N., and Cohen, P. (2016). Lys63/Met1-hybrid ubiquitin chains are commonly formed during the activation of innate immune signalling. Biochem. Biophys. Res. Commun. *474*, 452–461. https://doi.org/10.1016/j.bbrc.2016.04.141.

Etlinger, J.D., and Goldberg, A.L. (1977). A soluble ATP-dependent proteolytic system responsible for the degradation of abnormal proteins in reticulocytes. Proc. Natl. Acad. Sci. *74*, 54–58. https://doi.org/10.1073/pnas.74.1.54.

Etzioni, A., Ciechanover, A., and Pikarsky, E. (2017). Immune defects caused by mutations in the ubiquitin system. J. Allergy Clin. Immunol. *139*, 743–753. https://doi.org/10.1016/j.jaci.2016.11.031.

Evans, P.C., Smith, T.S., Lai, M.J., Williams, M.G., Burke, D.F., Heyninck, K., Kreike, M.M., Beyaert, R., Blundell, T.L., and Kilshaw, P.J. (2003). A novel type of deubiquitinating enzyme. J. Biol. Chem. *278*, 23180–23186. https://doi.org/10.1074/jbc.M301863200.

Evers, M.M., Tran, H.D., Zalachoras, I., Pepers, B.A., Meijer, O.C., den Dunnen, J.T., van Ommen, G.-J.B., Aartsma-Rus, A., and van Roon-Mom, W.M.C. (2013). Ataxin-3 protein modification as a treatment strategy for spinocerebellar ataxia type 3: Removal of the CAG containing exon. Neurobiol. Dis. *58*, 49–56. https://doi.org/10.1016/j.nbd.2013.04.019.

Evers, M.M., Toonen, L.J.A., and van Roon-Mom, W.M.C. (2014). Ataxin-3 Protein and RNA Toxicity in Spinocerebellar Ataxia Type 3: Current Insights and Emerging Therapeutic Strategies. Mol. Neurobiol. *49*, 1513–1531. https://doi.org/10.1007/s12035-013-8596-2.

Fei, C., Li, Z., Li, C., Chen, Y., Chen, Z., He, X., Mao, L., Wang, X., Zeng, R., and Li, L. (2013). Smurf1-Mediated Lys29-Linked Nonproteolytic Polyubiquitination of Axin Negatively Regulates Wnt/ -Catenin Signaling. Mol. Cell. Biol. *33*, 4095–4105. https://doi.org/10.1128/MCB.00418-13.

Feist, E., Burmester, G.R., and Krüger, E. (2016). The proteasome - victim or culprit in autoimmunity. Clin. Immunol. Orlando Fla *172*, 83–89. https://doi.org/10.1016/j.clim.2016.07.018.

Fenn, J.B., Mann, M., Meng, C.K., Wong, S.F., and Whitehouse, C.M. (1989). Electrospray ionization for mass spectrometry of large biomolecules. Science *246*, 64–71. https://doi.org/10.1126/science.2675315.

Fiesel, F.C., Moussaud-Lamodière, E.L., Ando, M., and Springer, W. (2014). A specific subset of E2 ubiquitin-conjugating enzymes regulate Parkin activation and mitophagy differently. J. Cell Sci. *127*, 3488–3504. https://doi.org/10.1242/jcs.147520.

Figueiredo, L.S., Dornelles, A.S., Petry, F.S., Falavigna, L., Dargél, V.A., Köbe, L.M., Aguzzoli, C., Roesler, R., and Schröder, N. (2015). Two waves of proteasome-dependent protein degradation in the hippocampus are required for recognition memory consolidation. Neurobiol. Learn. Mem. *120*, 1–6. https://doi.org/10.1016/j.nlm.2015.02.005.

File, S.E., and Hyde, J.R. (1978). Can social interaction be used to measure anxiety? Br. J. Pharmacol. *62*, 19–24. .

Finehout, E.J., and Lee, K.H. (2004). An introduction to mass spectrometry applications in biological research. Biochem. Mol. Biol. Educ. Bimon. Publ. Int. Union Biochem. Mol. Biol. *32*, 93–100. https://doi.org/10.1002/bmb.2004.494032020331.

Finley, D. (2009). Recognition and Processing of Ubiquitin-Protein Conjugates by the Proteasome. Annu. Rev. Biochem. *78*, 477–513. https://doi.org/10.1146/annurev.biochem.78.081507.101607.

Finley, D., Bartel, B., and Varshavsky, A. (1989). The tails of ubiquitin precursors are ribosomal proteins whose fusion to ubiquitin facilitates ribosome biogenesis. Nature *338*, 394–401. https://doi.org/10.1038/338394a0.

Finley, D., Chen, X., and Walters, K.J. (2016). Gates, channels, and switches: elements of the proteasome machine. Trends Biochem. Sci. *41*, 77–93. https://doi.org/10.1016/j.tibs.2015.10.009.

Fischer, J.A., Giniger, E., Maniatis, T., and Ptashne, M. (1988). GAL4 activates transcription in Drosophila. Nature *332*, 853–856. https://doi.org/10.1038/332853a0.

Flick, K., Ouni, I., Wohlschlegel, J.A., Capati, C., McDonald, W.H., Yates, J.R., and Kaiser, P. (2004). Proteolysis-independent regulation of the transcription factor Met4 by a single Lys 48-linked ubiquitin chain. Nat. Cell Biol. *6*, 634–641. https://doi.org/10.1038/ncb1143.

Flick, K., Raasi, S., Zhang, H., Yen, J.L., and Kaiser, P. (2006). A ubiquitin-interacting motif protects polyubiquitinated Met4 from degradation by the 26S proteasome. Nat. Cell Biol. *8*, 509–515. https://doi.org/10.1038/ncb1402.

Fonseca, R., Vabulas, R.M., Hartl, F.U., Bonhoeffer, T., and Nägerl, U.V. (2006). A Balance of Protein Synthesis and Proteasome-Dependent Degradation Determines the Maintenance of LTP. Neuron *52*, 239–245. https://doi.org/10.1016/j.neuron.2006.08.015.

Forrest, C.M., Darlington, L.G., and Stone, T.W. (2013). Involvement of the proteasome and caspase activation in hippocampal long-term depression induced by the serine protease subtilisin. Neuroscience *231*, 233–246. https://doi.org/10.1016/j.neuroscience.2012.11.029.

Franco, M., Seyfried, N.T., Brand, A.H., Peng, J., and Mayor, U. (2011). A novel strategy to isolate ubiquitin conjugates reveals wide role for ubiquitination during neural development. Mol. Cell. Proteomics MCP *10*, M110.002188. https://doi.org/10.1074/mcp.M110.002188.

French, M.E., Klosowiak, J.L., Aslanian, A., Reed, S.I., Yates, J.R., and Hunter, T. (2017). Mechanism of ubiquitin chain synthesis employed by a HECT domain ubiquitin ligase. J. Biol. Chem. *292*, 10398–10413. https://doi.org/10.1074/jbc.M117.789479.

Fu, Z., Lu, C., Zhang, C., and Qiao, B. (2019). PSMA5 promotes the tumorigenic process of prostate cancer and is related to bortezomib resistance. Anticancer. Drugs *30*, e0773. https://doi.org/10.1097/CAD.0000000000000773.

Fuchs, G., and Oren, M. (2014). Writing and reading H2B monoubiquitylation. Biochim. Biophys. Acta *1839*, 694–701. https://doi.org/10.1016/j.bbagrm.2014.01.002.

Gabriely, G., Kama, R., Gelin-Licht, R., and Gerst, J.E. (2008). Different domains of the UBL-UBA ubiquitin receptor, Ddi1/Vsm1, are involved in its multiple cellular roles. Mol. Biol. Cell *19*, 3625–3637. .

Gáliková, M., and Klepsatel, P. (2018). Obesity and Aging in the Drosophila Model. Int. J. Mol. Sci. *19*. https://doi.org/10.3390/ijms19071896.

Gatto, C.L., and Broadie, K. (2011). Drosophila Modeling of Heritable Neurodevelopmental Disorders. Curr. Opin. Neurobiol. *21*, 834–841. https://doi.org/10.1016/j.conb.2011.04.009.

Geisler, S., Vollmer, S., Golombek, S., and Kahle, P.J. (2014). The ubiquitin-conjugating enzymes UBE2N, UBE2L3 and UBE2D2/3 are essential for Parkin-dependent mitophagy. J. Cell Sci. *127*, 3280–3293. https://doi.org/10.1242/jcs.146035.

George, A.J., Hoffiz, Y.C., Charles, A.J., Zhu, Y., and Mabb, A.M. (2018). A Comprehensive Atlas of E3 Ubiquitin Ligase Mutations in Neurological Disorders. Front. Genet. *9*. https://doi.org/10.3389/fgene.2018.00029.

Gerlach, B., Cordier, S.M., Schmukle, A.C., Emmerich, C.H., Rieser, E., Haas, T.L., Webb, A.I., Rickard, J.A., Anderton, H., Wong, W.W.-L., et al. (2011). Linear ubiquitination prevents inflammation and regulates immune signalling. Nature *471*, 591–596. https://doi.org/10.1038/nature09816.

Glassman, L.W., Grocott, O.R., Kunz, P.A., Larson, A.M., Zella, G., Ganguli, K., and Thibert, R.L. (2017). Prevalence of gastrointestinal symptoms in Angelman syndrome. Am. J. Med. Genet. A. *173*, 2703–2709. https://doi.org/10.1002/ajmg.a.38401.

Glickman, M.H., and Ciechanover, A. (2002). The Ubiquitin-Proteasome Proteolytic Pathway: Destruction for the Sake of Construction. Physiol. Rev. *82*, 373–428. https://doi.org/10.1152/physrev.00027.2001.

Goldberg, A.L., and St. John, A.C. (1976). Intracellular Protein Degradation in Mammalian and Bacterial Cells: Part 2. Annu. Rev. Biochem. *45*, 747–804. https://doi.org/10.1146/annurev.bi.45.070176.003531.

Gomes, A.V., Waddell, D.S., Siu, R., Stein, M., Dewey, S., Furlow, J.D., and Bodine, S.C. (2012). Upregulation of proteasome activity in muscle RING finger 1-null mice following denervation. FASEB J. Off. Publ. Fed. Am. Soc. Exp. Biol. *26*, 2986–2999. https://doi.org/10.1096/fj.12-204495.

Goodrich, J.S., Clouse, K.N., and Schüpbach, T. (2004). Hrb27C, Sqd and Otu cooperatively regulate gurken RNA localization and mediate nurse cell chromosome dispersion in Drosophila oogenesis. Development *131*, 1949–1958. https://doi.org/10.1242/dev.01078.

Goru, S.K., Pandey, A., and Gaikwad, A.B. (2016). E3 ubiquitin ligases as novel targets for inflammatory diseases. Pharmacol. Res. *106*, 1–9. https://doi.org/10.1016/j.phrs.2016.02.006.

Gossan, N.C., Zhang, F., Guo, B., Jin, D., Yoshitane, H., Yao, A., Glossop, N., Zhang, Y.Q., Fukada, Y., and Meng, Q.-J. (2014). The E3 ubiquitin ligase UBE3A is an integral component of the molecular circadian clock through regulating the BMAL1 transcription factor. Nucleic Acids Res. *42*, 5765–5775. https://doi.org/10.1093/nar/gku225.

Gozes, I. (2018). ADNP Regulates Cognition: A Multitasking Protein. Front. Neurosci. *12*, 873. https://doi.org/10.3389/fnins.2018.00873.

Graham, P., and Pick, L. (2017). Drosophila as a Model for Diabetes and Diseases of Insulin Resistance. Curr. Top. Dev. Biol. *121*, 397–419. https://doi.org/10.1016/bs.ctdb.2016.07.011.

Greer, P.L., Hanayama, R., Bloodgood, B.L., Mardinly, A.R., Lipton, D.M., Flavell, S.W., Kim, T.K., Griffith, E.C., Waldon, Z., Maehr, R., et al. (2010). The Angelman Syndrome protein Ube3A regulates synapse development by ubiquitinating arc. Cell *140*, 704–716. https://doi.org/10.1016/j.cell.2010.01.026.

Grice, G.L., and Nathan, J.A. (2016). The recognition of ubiquitinated proteins by the proteasome. Cell. Mol. Life Sci. *73*, 3497–3506. https://doi.org/10.1007/s00018-016-2255-5.

Groen, E.J.N., and Gillingwater, T.H. (2015). UBA1: At the Crossroads of Ubiquitin Homeostasis and Neurodegeneration. Trends Mol. Med. *21*, 622–632. https://doi.org/10.1016/j.molmed.2015.08.003.

Groll, M., Ditzel, L., Löwe, J., Stock, D., Bochtler, M., Bartunik, H.D., and Huber, R. (1997). Structure of 20S proteasome from yeast at 2.4Å resolution. Nature *386*, 463–471. https://doi.org/10.1038/386463a0.

Grou, C.P., Pinto, M.P., Mendes, A.V., Domingues, P., and Azevedo, J.E. (2015). The de novo synthesis of ubiquitin: identification of deubiquitinases acting on ubiquitin precursors. Sci. Rep. *5*, 12836. https://doi.org/10.1038/srep12836.

Gu, B., Zhu, M., Glass, M.R., Rougié, M., Nikolova, V.D., Moy, S.S., Carney, P.R., and Philpot, B.D. (2019). Cannabidiol attenuates seizures and EEG abnormalities in Angelman syndrome model mice. J. Clin. Invest. *129*, 5462–5467. https://doi.org/10.1172/JCI130419.

Gu, B., Carstens, K.E., Judson, M.C., Dalton, K.A., Rougié, M., Clark, E.P., Dudek, S.M., and Philpot, B.D. Ube3a reinstatement mitigates epileptogenesis in Angelman syndrome model mice. J. Clin. Invest. *129*, 163–168. https://doi.org/10.1172/JCI120816.

Guo, J., Zhang, L., Li, K., Mei, J., Xue, J., Chen, J., Tang, X., Shen, L., Jiang, H., Chen, C., et al. (2018). Coding mutations in NUS1 contribute to Parkinson's disease. Proc. Natl. Acad. Sci. U. S. A. *115*, 11567–11572. https://doi.org/10.1073/pnas.1809969115.

Guthmueller, K.L., Yoder, M.L., and Holgado, A.M. (2011). Determining Genetic Expression Profiles in C. elegans Using Microarray and Real-time PCR. J. Vis. Exp. JoVE 2777. https://doi.org/10.3791/2777.

Haas, A.L., Warms, J.V., Hershko, A., and Rose, I.A. (1982). Ubiquitin-activating enzyme. Mechanism and role in protein-ubiquitin conjugation. J. Biol. Chem. *257*, 2543–2548. .

Haglund, K., Sigismund, S., Polo, S., Szymkiewicz, I., Di Fiore, P.P., and Dikic, I. (2003). Multiple monoubiquitination of RTKs is sufficient for their endocytosis and degradation. Nat. Cell Biol. *5*, 461–466. https://doi.org/10.1038/ncb983.

Hall, C., and Ballachey, E.L. (1932). A study of the rat's behavior in a field. A contribution to method in comparative psychology. Univ. Calif. Publ. Psychol. *6*, 1–12. .

Hall, D.A., Ptacek, J., and Snyder, M. (2007). Protein microarray technology. Mech. Ageing Dev. *128*, 161–167. https://doi.org/10.1016/j.mad.2006.11.021.

Han, J.W., Zheng, H.F., Cui, Y., Sun, L.D., Ye, D.Q., Hu, Z., Xu, J.H., Cai, Z.M., Huang, W., Zhao, G.P., et al. (2009). Genome-wide association study in a Chinese Han population identifies nine new susceptibility loci for systemic lupus erythematosus. Nat. Genet. *41*, 1234–1237. https://doi.org/10.1038/ng.472.

Hanpude, P., Bhattacharya, S., Dey, A.K., and Maiti, T.K. (2015). Deubiquitinating enzymes in cellular signaling and disease regulation. IUBMB Life *67*, 544–555. https://doi.org/10.1002/iub.1402.

Hanzlik, E., Klinger, S.A., Carson, R., and Duis, J. (2020). Mirtazapine for Sleep Disturbances in Angelman Syndrome: A retrospective chart review of eight pediatric cases. J. Clin. Sleep Med. JCSM Off. Publ. Am. Acad. Sleep Med. https://doi.org/10.5664/jcsm.8284.

Harper, S., and Speicher, D.W. (2011). Purification of proteins fused to glutathione S-tranferase. Methods Mol. Biol. Clifton NJ *681*, 259–280. https://doi.org/10.1007/978-1-60761-913-0_14.

Harrigan, J.A., Jacq, X., Martin, N.M., and Jackson, S.P. (2018). Deubiquitylating enzymes and drug discovery: emerging opportunities. Nat. Rev. Drug Discov. *17*, 57–78. https://doi.org/10.1038/nrd.2017.152.

Harris, L.D., Jasem, S., and Licchesi, J.D.F. (2020). The Ubiquitin System in Alzheimer's Disease. In Proteostasis and Disease, (Springer, Cham), pp. 195–221.

Hartmann-Petersen, R., and Gordon, C. (2004). Integral UBL domain proteins: a family of proteasome interacting proteins. Semin. Cell Dev. Biol. *15*, 247–259. https://doi.org/10.1016/j.semcdb.2003.12.006.

Hergovich, A. (2012). Mammalian Hippo signalling: a kinase network regulated by protein-protein interactions. Biochem. Soc. Trans. *40*, 124–128. https://doi.org/10.1042/BST20110619.

Hershko, A., Ciechanover, A., Heller, H., Haas, A.L., and Rose, I.A. (1980). Proposed role of ATP in protein breakdown: conjugation of protein with multiple chains of the polypeptide of ATP-dependent proteolysis. Proc. Natl. Acad. Sci. U. S. A. *77*, 1783. https://doi.org/10.1073/pnas.77.4.1783.

Hershko, A., Heller, H., Elias, S., and Ciechanover, A. (1983). Components of ubiquitin-protein ligase system. Resolution, affinity purification, and role in protein breakdown. J. Biol. Chem. *258*, 8206–8214. .

Heunis, T., Lamoliatte, F., Marín-Rubio, J.L., Dannoura, A., and Trost, M. (2020). Technical report: Targeted proteomic analysis reveals enrichment of atypical ubiquitin chains in contractile murine tissues. J. Proteomics *229*. https://doi.org/10.1016/j.jprot.2020.103963.

Hicke, L. (2001). Ubiquitin and proteasomes: Protein regulation by monoubiquitin. Nat. Rev. Mol. Cell Biol. *2*, 195–201. https://doi.org/10.1038/35056583.

Hira, A., Yoshida, K., Sato, K., Okuno, Y., Shiraishi, Y., Chiba, K., Tanaka, H., Miyano, S., Shimamoto, A., Tahara, H., et al. (2015). Mutations in the Gene Encoding the E2 Conjugating Enzyme UBE2T Cause Fanconi Anemia. Am. J. Hum. Genet. *96*, 1001–1007. https://doi.org/10.1016/j.ajhg.2015.04.022.

Hiromoto, Y., Azuma, Y., Suzuki, Y., Hoshina, M., Uchiyama, Y., Mitsuhashi, S., Miyatake, S., Mizuguchi, T., Takata, A., Miyake, N., et al. (2020). Hemizygous FLNA variant in West syndrome without periventricular nodular heterotopia. Hum. Genome Var. *7*, 1–5. https://doi.org/10.1038/s41439-020-00131-9.

Hitchcock, A.L., Auld, K., Gygi, S.P., and Silver, P.A. (2003). A subset of membrane-associated proteins is ubiquitinated in response to mutations in the endoplasmic reticulum degradation machinery. Proc. Natl. Acad. Sci. U. S. A. *100*, 12735–12740. https://doi.org/10.1073/pnas.2135500100.

Hoege, C., Pfander, B., Moldovan, G.L., Pyrowolakis, G., and Jentsch, S. (2002). RAD6-dependent DNA repair is linked to modification of PCNA by ubiquitin and SUMO. Nature *419*, 135–141. https://doi.org/10.1038/nature00991.

Hu, C.F., Liao, X.Y., Xu, D.D., Ruan, Y.B., and Gao, F.G. (2021). K48-Linked Ubiquitination Contributes to Nicotine-Augmented Bone Marrow-Derived Dendritic-Cell-Mediated Adaptive Immunity. Vaccines *9*. https://doi.org/10.3390/vaccines9030278.

Hu, M., Li, P., Li, M., Li, W., Yao, T., Wu, J.W., Gu, W., Cohen, R.E., and Shi, Y. (2002). Crystal structure of a UBP-family deubiquitinating enzyme in isolation and in complex with ubiquitin aldehyde. Cell *111*, 1041–1054. https://doi.org/10.1016/s0092-8674(02)01199-6.

Hu, M., Li, P., Song, L., Jeffrey, P.D., Chenova, T.A., Wilkinson, K.D., Cohen, R.E., and Shi, Y. (2005). Structure and mechanisms of the proteasome-associated deubiquitinating enzyme USP14. EMBO J. *24*, 3747–3756. https://doi.org/10.1038/sj.emboj.7600832.

Hu, Y., Cui, Y., Fan, X., WU, Q., Li, W., and Wang, W. (2016). Prenatal diagnosis and genetic counseling in a fetus associated with risk of Angelman syndrome with a small supernumerary marker chromosome derived from chromosome 22. Mol. Cytogenet. *9*. https://doi.org/10.1186/s13039-016-0248-6.

Huang, D., Li, Q., Wang, Y., Liu, Z., Wang, Z., Li, H., Wang, J., Su, J., Ma, Y., Yu, M., et al. (2019). Brain-specific NRSF deficiency aggravates dopaminergic neurodegeneration and

impairs neurogenesis in the MPTP mouse model of Parkinson's disease. Aging *11*, 3280–3297. https://doi.org/10.18632/aging.101979.

Huang, H.-S., Allen, J.A., Mabb, A.M., King, I.F., Miriyala, J., Taylor-Blake, B., Sciaky, N., Dutton, J.W., Lee, H.-M., Chen, X., et al. (2011). Topoisomerase inhibitors unsilence the dormant allele of Ube3a in neurons. Nature *481*, 185–189. https://doi.org/10.1038/nature10726.

Huang, L., Kinnucan, E., Wang, G., Beaudenon, S., Howley, P.M., Huibregtse, J.M., and Pavletich, N.P. (1999). Structure of an E6AP-UbcH7 complex: insights into ubiquitination by the E2-E3 enzyme cascade. Science *286*, 1321–1326. https://doi.org/10.1126/science.286.5443.1321.

Huibregtse, J.M., Scheffner, M., and Howley, P.M. (1991). A cellular protein mediates association of p53 with the E6 oncoprotein of human papillomavirus types 16 or 18. EMBO J. *10*, 4129–4135. .

Huibregtse, J.M., Scheffner, M., Beaudenon, S., and Howley, P.M. (1995). A family of proteins structurally and functionally related to the E6-AP ubiquitin-protein ligase. Proc. Natl. Acad. Sci. U. S. A. *92*, 2563–2567. .

Husnjak, K., and Dikic, I. (2012). Ubiquitin-Binding Proteins: Decoders of Ubiquitin-Mediated Cellular Functions. Annu. Rev. Biochem. *81*, 291–322. https://doi.org/10.1146/annurev-biochem-051810-094654.

Husnjak, K., Elsasser, S., Zhang, N., Chen, X., Randles, L., Shi, Y., Hofmann, K., Walters, K.J., Finley, D., and Dikic, I. (2008). Proteasome subunit Rpn13 is a novel ubiquitin receptor. Nature *453*, 481–488. https://doi.org/10.1038/nature06926.

Hyer, M.L., Milhollen, M.A., Ciavarri, J., Fleming, P., Traore, T., Sappal, D., Huck, J., Shi, J., Gavin, J., Brownell, J., et al. (2018). A small-molecule inhibitor of the ubiquitin activating enzyme for cancer treatment. Nat. Med. *24*, 186–193. https://doi.org/10.1038/nm.4474.

Ishimoto, K., Kawamata, N., Uchihara, Y., Okubo, M., Fujimoto, R., Gotoh, E., Kakinouchi, K., Mizohata, E., Hino, N., Okada, Y., et al. (2016). Ubiquitination of Lysine 867 of the Human SETDB1 Protein Upregulates Its Histone H3 Lysine 9 (H3K9) Methyltransferase Activity. PLOS ONE *11*, e0165766. https://doi.org/10.1371/journal.pone.0165766.

Itoh, Y., and Suzuki, M. (2018). Design, synthesis, and biological evaluation of novel ubiquitin-activating enzyme inhibitors. Bioorg. Med. Chem. Lett. *28*, 2723–2727. https://doi.org/10.1016/j.bmcl.2018.03.004.

Iwagaki, N., and Miles, G.B. (2011). Activation of group I metabotropic glutamate receptors modulates locomotor-related motoneuron output in mice. J. Neurophysiol. *105*, 2108–2120. https://doi.org/10.1152/jn.01037.2010.

Jackson, G.R. (2008). Guide to Understanding Drosophila Models of Neurodegenerative Diseases. PLoS Biol. *6*. https://doi.org/10.1371/journal.pbio.0060053.

Jacobson, A.D., MacFadden, A., Wu, Z., Peng, J., and Liu, C.-W. (2014). Autoregulation of the 26S proteasome by in situ ubiquitination. Mol. Biol. Cell *25*, 1824–1835. https://doi.org/10.1091/mbc.E13-10-0585.

Jensen, L., Farook, M.F., and Reiter, L.T. (2013). Proteomic Profiling in Drosophila Reveals Potential Dube3a Regulation of the Actin Cytoskeleton and Neuronal Homeostasis. PLoS ONE *8*. https://doi.org/10.1371/journal.pone.0061952.

Jiang, Y., Armstrong, D., Albrecht, U., Atkins, C.M., Noebels, J.L., Eichele, G., Sweatt, J.D., and Beaudet, A.L. (1998). Mutation of the Angelman Ubiquitin Ligase in Mice Causes Increased Cytoplasmic p53 and Deficits of Contextual Learning and Long-Term Potentiation. Neuron *21*, 799–811. https://doi.org/10.1016/S0896-6273(00)80596-6.

Jumper, J., Evans, R., Pritzel, A., Green, T., Figurnov, M., Ronneberger, O., Tunyasuvunakool, K., Bates, R., Žídek, A., Potapenko, A., et al. (2021). Highly accurate protein structure prediction with AlphaFold. Nature *596*, 583–589. https://doi.org/10.1038/s41586-021-03819-2.

Jung, G., Kim, E.J., Cicvaric, A., Sase, S., Gröger, M., Höger, H., Sialana, F.J., Berger, J., Monje, F.J., and Lubec, G. (2015). Drebrin depletion alters neurotransmitter receptor levels in protein complexes, dendritic spine morphogenesis and memory-related synaptic plasticity in the mouse hippocampus. J. Neurochem. *134*, 327–339. https://doi.org/10.1111/jnc.13119.

Kaiser, S.E., Riley, B.E., Shaler, T.A., Trevino, R.S., Becker, C.H., Schulman, H., and Kopito, R.R. (2011). Protein standard absolute quantification (PSAQ) method for the measurement of cellular ubiquitin pools. Nat. Methods *8*, 691–696. https://doi.org/10.1038/nmeth.1649.

Kalsner, L., and Chamberlain, S.J. (2015). Prader-Willi, Angelman, and 15q11-q13 Duplication Syndromes. Pediatr. Clin. North Am. *62*, 587–606. https://doi.org/10.1016/j.pcl.2015.03.004.

Kaphzan, H., Buffington, S.A., Jung, J.I., Rasband, M.N., and Klann, E. (2011). Alterations in intrinsic membrane properties and the axon initial segment in a mouse model of Angelman syndrome. J. Neurosci. Off. J. Soc. Neurosci. *31*, 17637–17648. https://doi.org/10.1523/JNEUROSCI.4162-11.2011.

Kaplun, L., Tzirkin, R., Bakhrat, A., Shabek, N., Ivantsiv, Y., and Raveh, D. (2005). The DNA Damage-Inducible UbL-UbA Protein Ddi1 Participates in Mec1-Mediated Degradation of Ho Endonuclease. Mol. Cell. Biol. *25*, 5355–5362. https://doi.org/10.1128/MCB.25.13.5355-5362.2005.

Kapuria, V., Peterson, L.F., Fang, D., Bornmann, W.G., Talpaz, M., and Donato, N.J. (2010). Deubiquitinase Inhibition by Small-Molecule WP1130 Triggers Aggresome Formation and Tumor Cell Apoptosis. Cancer Res. *70*, 9265–9276. https://doi.org/10.1158/0008-5472.CAN-10-1530.

Karas, M., and Hillenkamp, F. (1988). Laser desorption ionization of proteins with molecular masses exceeding 10,000 daltons. Anal. Chem. *60*, 2299–2301. https://doi.org/10.1021/ac00171a028.

Kawano, O., Egawa, K., and Shiraishi, H. (2020). Perampanel for nonepileptic myoclonus in Angelman syndrome. Brain Dev. *0*. https://doi.org/10.1016/j.braindev.2020.02.007.

Kazdoba, T.M., Leach, P.T., and Crawley, J.N. (2016). Behavioral phenotypes of genetic mouse models of autism. Genes Brain Behav. *15*, 7–26. https://doi.org/10.1111/gbb.12256.

Khatri, N., and Man, H.-Y. (2019). The Autism and Angelman Syndrome Protein Ube3A/E6AP: The Gene, E3 Ligase Ubiquitination Targets and Neurobiological Functions. Front. Mol. Neurosci. *12*. https://doi.org/10.3389/fnmol.2019.00109.

Kim, H.C., and Huibregtse, J.M. (2009). Polyubiquitination by HECT E3s and the Determinants of Chain Type Specificity. Mol. Cell. Biol. *29*, 3307–3318. https://doi.org/10.1128/MCB.00240-09.

Kim, D.I., Jensen, S.C., Noble, K.A., KC, B., Roux, K.H., Motamedchaboki, K., and Roux, K.J. (2016). An improved smaller biotin ligase for BioID proximity labeling. Mol. Biol. Cell *27*, 1188–1196. https://doi.org/10.1091/mbc.E15-12-0844.

Kim, W., Bennett, E.J., Huttlin, E.L., Guo, A., Li, J., Possemato, A., Sowa, M.E., Rad, R., Rush, J., Comb, M.J., et al. (2011). Systematic and quantitative assessment of the ubiquitin-modified proteome. Mol. Cell *44*, 325–340. https://doi.org/10.1016/j.molcel.2011.08.025.

Kimura, Y., and Tanaka, K. (2010). Regulatory mechanisms involved in the control of ubiquitin homeostasis. J. Biochem. (Tokyo) *147*, 793–798. https://doi.org/10.1093/jb/mvq044.

Kishino, T., and Wagstaff, J. (1998). Genomic Organization of theUBE3A/E6-AP Gene and Related Pseudogenes. Genomics *47*, 101–107. https://doi.org/10.1006/geno.1997.5093.

Kishino, T., Lalande, M., and Wagstaff, J. (1997). UBE3A/E6-AP mutations cause Angelman syndrome. Nat. Genet. *15*, 70–73. https://doi.org/10.1038/ng0197-70.

Kitajima, Y., Yoshioka, K., and Suzuki, N. (2020). The ubiquitin–proteasome system in regulation of the skeletal muscle homeostasis and atrophy: from basic science to disorders. J. Physiol. Sci. *70*, 40. https://doi.org/10.1186/s12576-020-00768-9.

Kliza, K., and Husnjak, K. (2020). Resolving the Complexity of Ubiquitin Networks. Front. Mol. Biosci. *7*. https://doi.org/10.3389/fmolb.2020.00021.

Kliza, K., Taumer, C., Pinzuti, I., Franz-Wachtel, M., Kunzelmann, S., Stieglitz, B., Macek, B., and Husnjak, K. (2017). Internally tagged ubiquitin: a tool to identify linear polyubiquitin-modified proteins by mass spectrometry. Nat. Methods *14*, 504–512. https://doi.org/10.1038/nmeth.4228.

Knoll, J.H., Nicholls, R.D., Magenis, R.E., Graham, J.M., Lalande, M., and Latt, S.A. (1989). Angelman and Prader-Willi syndromes share a common chromosome 15 deletion but differ in parental origin of the deletion. Am. J. Med. Genet. *32*, 285–290. https://doi.org/10.1002/ajmg.1320320235.

Kobayashi, F., Nishiuchi, T., Takaki, K., and Konno, H. (2018). Ubiquitin chain specificities of E6AP E3 ligase and its HECT domain. Biochem. Biophys. Res. Commun. *496*, 686–692. https://doi.org/10.1016/j.bbrc.2017.12.076.

Koizumi, S., Irie, T., Hirayama, S., Sakurai, Y., Yashiroda, H., Naguro, I., Ichijo, H., Hamazaki, J., and Murata, S. (2016). The aspartyl protease DDI2 activates Nrf1 to compensate for proteasome dysfunction. ELife *5*, e18357. https://doi.org/10.7554/eLife.18357.

Komander, D. (2009). The emerging complexity of protein ubiquitination. Biochem. Soc. Trans. *37*, 937–953. https://doi.org/10.1042/BST0370937.

Komander, D., and Barford, D. (2008). Structure of the A20 OTU domain and mechanistic insights into deubiquitination. Biochem. J. *409*, 77–85. https://doi.org/10.1042/BJ20071399.

Komander, D., and Rape, M. (2012). The Ubiquitin Code. Annu. Rev. Biochem. *81*, 203–229. https://doi.org/10.1146/annurev-biochem-060310-170328.

Kondratiev, N.V., Alfimova, M.V., and Golimbet, V.E. (2017). [A search of target regions for association studies between DNA methylation and cognitive impairment in schizophrenia]. Zh. Nevrol. Psikhiatr. Im. S. S. Korsakova *117*, 72–75. https://doi.org/10.17116/jnevro20171178172-75.

Kühne, C., and Banks, L. (1998). E3-Ubiquitin Ligase/E6-AP Links Multicopy Maintenance Protein 7 to the Ubiquitination Pathway by a Novel Motif, the L2G Box. J. Biol. Chem. *273*, 34302–34309. https://doi.org/10.1074/jbc.273.51.34302.

Kühnle, S., Kogel, U., Glockzin, S., Marquardt, A., Ciechanover, A., Matentzoglu, K., and Scheffner, M. (2011). Physical and Functional Interaction of the HECT Ubiquitin-protein Ligases E6AP and HERC2. J. Biol. Chem. *286*, 19410–19416. https://doi.org/10.1074/jbc.M110.205211.

Kuhnle, S., Mothes, B., Matentzoglu, K., and Scheffner, M. (2013). Role of the ubiquitin ligase E6AP/UBE3A in controlling levels of the synaptic protein Arc. Proc. Natl. Acad. Sci. *110*, 8888–8893. https://doi.org/10.1073/pnas.1302792110.

Kühnle, S., Martínez-Noël, G., Leclere, F., Hayes, S.D., Harper, J.W., and Howley, P.M. (2018). Angelman syndrome–associated point mutations in the Zn2+-binding N-terminal (AZUL) domain of UBE3A ubiquitin ligase inhibit binding to the proteasome. J. Biol. Chem. *293*, 18387–18399. https://doi.org/10.1074/jbc.RA118.004653.

Kumar, S., Talis, A.L., and Howley, P.M. (1999). Identification of HHR23A as a substrate for E6-associated protein-mediated ubiquitination. J. Biol. Chem. *274*, 18785–18792. https://doi.org/10.1074/jbc.274.26.18785.

Kumar, V., Joshi, T., Vatsa, N., Singh, B.K., and Jana, N.R. (2019). Simvastatin Restores HDAC1/2 Activity and Improves Behavioral Deficits in Angelman Syndrome Model Mouse. Front. Mol. Neurosci. *12*. https://doi.org/10.3389/fnmol.2019.00289.

Lafarga, M., Berciano, M.T., Pena, E., Mayo, I., Castaño, J.G., Bohmann, D., Rodrigues, J.P., Tavanez, J.P., and Carmo-Fonseca, M. (2002). Clastosome: A Subtype of Nuclear Body Enriched in 19S and 20S Proteasomes, Ubiquitin, and Protein Substrates of Proteasome. Mol. Biol. Cell *13*, 2771–2782. https://doi.org/10.1091/mbc.E02-03-0122.

Lahaie, N., Kralikova, M., Prézeau, L., Blahos, J., and Bouvier, M. (2016). Post-endocytotic Deubiquitination and Degradation of the Metabotropic γ-Aminobutyric Acid

Receptor by the Ubiquitin-specific Protease 14. J. Biol. Chem. *291*, 7156–7170. https://doi.org/10.1074/jbc.M115.686907.

Lambertson, D., Chen, L., and Madura, K. (1999). Pleiotropic defects caused by loss of the proteasome-interacting factors Rad23 and Rpn10 of Saccharomyces cerevisiae. Genetics *153*, 69–79. .

Lander, G.C., Estrin, E., Matyskiela, M.E., Bashore, C., Nogales, E., and Martin, A. (2012). Complete subunit architecture of the proteasome regulatory particle. Nature *482*, 186–191. https://doi.org/10.1038/nature10774.

Landré, V., Revi, B., Mir, M.G., Verma, C., Hupp, T.R., Gilbert, N., and Ball, K.L. (2017). Regulation of transcriptional activators by DNA-binding domain ubiquitination. Cell Death Differ. *24*, 903–916. https://doi.org/10.1038/cdd.2017.42.

Larsen, C.N., Krantz, B.A., and Wilkinson, K.D. (1998). Substrate specificity of deubiquitinating enzymes: ubiquitin C-terminal hydrolases. Biochemistry *37*, 3358–3368. https://doi.org/10.1021/bi972274d.

LaSalle, J.M., Reiter, L.T., and Chamberlain, S.J. (2015). Epigenetic regulation of UBE3A and roles in human neurodevelopmental disorders. Epigenomics *7*, 1213–1228. https://doi.org/10.2217/epi.15.70.

Lectez, B., Migotti, R., Lee, S.Y., Ramirez, J., Beraza, N., Mansfield, B., Sutherland, J.D., Martinez-Chantar, M.L., Dittmar, G., and Mayor, U. (2014). Ubiquitin Profiling in Liver Using a Transgenic Mouse with Biotinylated Ubiquitin. J. Proteome Res. *13*, 3016–3026. https://doi.org/10.1021/pr5001913.

Lee, K., Vyas, Y., Garner, C.C., and Montgomery, J.M. (2019). Autism-associated Shank3 mutations alter mGluR expression and mGluR-dependent but not NMDA receptor-dependent long-term depression. Synapse *73*, e22097. https://doi.org/10.1002/syn.22097.

Lee, S.Y., Ramirez, J., Franco, M., Lectez, B., Gonzalez, M., Barrio, R., and Mayor, U. (2014). Ube3a, the E3 ubiquitin ligase causing Angelman syndrome and linked to autism, regulates protein homeostasis through the proteasomal shuttle Rpn10. Cell. Mol. Life Sci. *71*, 2747–2758. https://doi.org/10.1007/s00018-013-1526-7.

de Leeuw, N., Bulk, S., Green, A., Jaeckle-Santos, L., Baker, L.A., Zinn, A.R., Kleefstra, T., van der Smagt, J.J., Vianne Morgante, A.M., de Vries, B.B.A., et al. (2010). UBE2A deficiency syndrome: Mild to severe intellectual disability accompanied by seizures, absent speech, urogenital, and skin anomalies in male patients. Am. J. Med. Genet. A. *152A*, 3084–3090. https://doi.org/10.1002/ajmg.a.33743.

Lehrbach, N.J., and Ruvkun, G. (2016). Proteasome dysfunction triggers activation of SKN-1A/Nrf1 by the aspartic protease DDI-1. ELife *5*, e17721. https://doi.org/10.7554/eLife.17721.

Leidecker, O., Matic, I., Mahata, B., Pion, E., and Xirodimas, D.P. (2012). The ubiquitin E1 enzyme Ube1 mediates NEDD8 activation under diverse stress conditions. Cell Cycle *11*, 1142–1150. https://doi.org/10.4161/cc.11.6.19559.

Lemaitre, B., Nicolas, E., Michaut, L., Reichhart, J.M., and Hoffmann, J.A. (1996). The dorsoventral regulatory gene cassette spätzle/Toll/cactus controls the potent

antifungal response in Drosophila adults. Cell *86*, 973–983. https://doi.org/10.1016/s0092-8674(00)80172-5.

Lemak, A., Yee, A., Bezsonova, I., Dhe-Paganon, S., and Arrowsmith, C.H. (2011). Zn-binding AZUL domain of human ubiquitin protein ligase Ube3A. J. Biomol. NMR *51*, 185–190. https://doi.org/10.1007/s10858-011-9552-y.

Lewis, E.B. (1978). A gene complex controlling segmentation in Drosophila. Nature *276*, 565–570. https://doi.org/10.1038/276565a0.

Li, M., Chen, D., Shiloh, A., Luo, J., Nikolaev, A.Y., Qin, J., and Gu, W. (2002). Deubiquitination of p53 by HAUSP is an important pathway for p53 stabilization. Nature *416*, 648–653. https://doi.org/10.1038/nature737.

Li, W., Bengtson, M.H., Ulbrich, A., Matsuda, A., Reddy, V.A., Orth, A., Chanda, S.K., Batalov, S., and Joazeiro, C.A.P. (2008). Genome-Wide and Functional Annotation of Human E3 Ubiquitin Ligases Identifies MULAN, a Mitochondrial E3 that Regulates the Organelle's Dynamics and Signaling. PLoS ONE *3*. https://doi.org/10.1371/journal.pone.0001487.

Li, W., Yao, A., Zhi, H., Kaur, K., Zhu, Y., Jia, M., Zhao, H., Wang, Q., Jin, S., Zhao, G., et al. (2016a). Angelman Syndrome Protein Ube3a Regulates Synaptic Growth and Endocytosis by Inhibiting BMP Signaling in Drosophila. PLoS Genet. *12*. https://doi.org/10.1371/journal.pgen.1006062.

Li, X., Liu, H., Fischhaber, P.L., and Tang, T.-S. (2015). Toward therapeutic targets for SCA3: Insight into the role of Machado-Joseph disease protein ataxin-3 in misfolded proteins clearance. Prog. Neurobiol. *132*, 34–58. https://doi.org/10.1016/j.pneurobio.2015.06.004.

Li, Y., Huang, J., Sun, J., Xiang, S., Yang, D., Ying, X., Lu, M., Li, H., and Ren, G. (2016b). The transcription levels and prognostic values of seven proteasome alpha subunits in human cancers. Oncotarget *8*, 4501–4519. https://doi.org/10.18632/oncotarget.13885.

Liang, K., Volk, A.G., Haug, J.S., Marshall, S.A., Woodfin, A.R., Bartom, E.T., Gilmore, J.M., Florens, L., Washburn, M.P., Sullivan, K.D., et al. (2017). Therapeutic Targeting of MLL Degradation Pathways in MLL-Rearranged Leukemia. Cell *168*, 59-72.e13. https://doi.org/10.1016/j.cell.2016.12.011.

Ling, L., and Goeddel, D.V. (2000). T6BP, a TRAF6-interacting protein involved in IL-1 signaling. Proc. Natl. Acad. Sci. U. S. A. *97*, 9567–9572. https://doi.org/10.1073/pnas.170279097.

Liu, J., Shaik, S., Dai, X., Wu, Q., Zhou, X., Wang, Z., and Wei, W. (2015). Targeting the ubiquitin pathway for cancer treatment. Biochim. Biophys. Acta *1855*, 50–60. https://doi.org/10.1016/j.bbcan.2014.11.005.

Liu, Y., Johe, K., Sun, J., Hao, X., Wang, Y., Bi, X., and Baudry, M. (2019). Enhancement of synaptic plasticity and reversal of impairments in motor and cognitive functions in a mouse model of Angelman Syndrome by a small neurogenic molecule, NSI-189. Neuropharmacology *144*, 337–344. https://doi.org/10.1016/j.neuropharm.2018.10.038.

Lloyd, T.E., and Taylor, J.P. (2010). Flightless flies: Drosophila models of neuromuscular disease. Ann. N. Y. Acad. Sci. *1184*, e1-20. https://doi.org/10.1111/j.1749-6632.2010.05432.x.

Lombardo, S.D., Battaglia, G., Petralia, M.C., Mangano, K., Basile, M.S., Bruno, V., Fagone, P., Bella, R., Nicoletti, F., and Cavalli, E. (2020). Transcriptomic Analysis Reveals Abnormal Expression of Prion Disease Gene Pathway in Brains from Patients with Autism Spectrum Disorders. Brain Sci. *10*, 200. https://doi.org/10.3390/brainsci10040200.

Lopez, S.J., Segal, D.J., and LaSalle, J.M. (2019). UBE3A: An E3 Ubiquitin Ligase With Genome-Wide Impact in Neurodevelopmental Disease. Front. Mol. Neurosci. *11*. https://doi.org/10.3389/fnmol.2018.00476.

Lopez-Castejon, G., and Edelmann, M.J. (2016). Deubiquitinases: Novel Therapeutic Targets in Immune Surveillance? (Hindawi).

Lopitz-Otsoa, F., Rodriguez-Suarez, E., Aillet, F., Casado-Vela, J., Lang, V., Matthiesen, R., Elortza, F., and Rodriguez, M.S. (2012). Integrative analysis of the ubiquitin proteome isolated using Tandem Ubiquitin Binding Entities (TUBEs). J. Proteomics *75*, 2998–3014. https://doi.org/10.1016/j.jprot.2011.12.001.

Lorenz, S. (2018). Structural mechanisms of HECT-type ubiquitin ligases. Biol. Chem. *399*, 127–145. https://doi.org/10.1515/hsz-2017-0184.

Lou, J., Hao, Y., Lin, K., Lyu, Y., Chen, M., Wang, H., Zou, D., Jiang, X., Wang, R., Jin, D., et al. (2020). Circular RNA CDR1as disrupts the p53/MDM2 complex to inhibit Gliomagenesis. Mol. Cancer *19*, 138. https://doi.org/10.1186/s12943-020-01253-y.

Low, D., and Chen, K.S. (2011). UBE3A regulates MC1R expression: a link to hypopigmentation in Angelman syndrome: UBE3A activates MC1R promoter. Pigment Cell Melanoma Res. *24*, 944–952. https://doi.org/10.1111/j.1755-148X.2011.00884.x.

Lowe, J., Stock, D., Jap, B., Zwickl, P., Baumeister, W., and Huber, R. (1995). Crystal structure of the 20S proteasome from the archaeon T. acidophilum at 3.4 A resolution. Science *268*, 533–539. https://doi.org/10.1126/science.7725097.

Luo, E.C. (2020). Large-scale activity assignment of RNA-interacting proteins identifies a functional antagonist to fragile X mental retardation protein.

Luo, H., Qin, Y., Reu, F., Ye, S., Dai, Y., Huang, J., Wang, F., Zhang, D., Pan, L., Zhu, H., et al. (2016). Microarray-based analysis and clinical validation identify ubiquitin-conjugating enzyme E2E1 (UBE2E1) as a prognostic factor in acute myeloid leukemia. J. Hematol. Oncol.J Hematol Oncol *9*, 125. https://doi.org/10.1186/s13045-016-0356-0.

Lüscher, C., and Huber, K.M. (2010). Group 1 mGluR-dependent synaptic long-term depression (mGluR-LTD): mechanisms and implications for circuitry & disease. Neuron *65*, 445–459. https://doi.org/10.1016/j.neuron.2010.01.016.

Lustgarten, V., and Gerst, J.E. (1999). Yeast VSM1 encodes a v-SNARE binding protein that may act as a negative regulator of constitutive exocytosis. Mol. Cell. Biol. *19*, 4480–4494. https://doi.org/10.1128/mcb.19.6.4480.

Ly, S., and Naidoo, N. (2019). Loss of DmGluRA exacerbates age-related sleep disruption and reduces lifespan. Neurobiol. Aging *80*, 83–90. https://doi.org/10.1016/j.neurobiolaging.2019.04.004.

Mabb, A.M., Je, H.S., Wall, M.J., Robinson, C.G., Larsen, R.S., Qiang, Y., Corrêa, S.A.L., and Ehlers, M.D. (2014). Triad3A regulates synaptic strength by ubiquitination of Arc. Neuron *82*, 1299–1316. https://doi.org/10.1016/j.neuron.2014.05.016.

Madura, K. (2004). Rad23 and Rpn10: perennial wallflowers join the melee. Trends Biochem. Sci. *29*, 637–640. https://doi.org/10.1016/j.tibs.2004.10.008.

Magenis, R.E., Brown, M.G., Lacy, D.A., Budden, S., LaFranchi, S., Opitz, J.M., Reynolds, J.F., and Ledbetter, D.H. (1987). Is angelman syndrome an alternate result of del(15)(qllql3)? Am. J. Med. Genet. *28*, 829–838. https://doi.org/10.1002/ajmg.1320280407.

Magenis, R.E., Toth-Fejel, S., Allen, L.J., Black, M., Brown, M.G., Budden, S., Cohen, R., Friedman, J.M., Kalousek, D., and Zonana, J. (1990). Comparison of the 15q deletions in Prader-Willi and Angelman syndromes: specific regions, extent of deletions, parental origin, and clinical consequences. Am. J. Med. Genet. *35*, 333–349. https://doi.org/10.1002/ajmg.1320350307.

Makarova, K.S., Aravind, L., and Koonin, E.V. (2000). A novel superfamily of predicted cysteine proteases from eukaryotes, viruses and Chlamydia pneumoniae. Trends Biochem. Sci. *25*, 50–52. https://doi.org/10.1016/s0968-0004(99)01530-3.

Maksour, S., Ooi, L., and Dottori, M. (2020). More than a Corepressor: The Role of CoREST Proteins in Neurodevelopment. ENeuro *7*. https://doi.org/10.1523/ENEURO.0337-19.2020.

Malakhov, M.P., Mattern, M.R., Malakhova, O.A., Drinker, M., Weeks, S.D., and Butt, T.R. (2004). SUMO fusions and SUMO-specific protease for efficient expression and purification of proteins. J. Struct. Funct. Genomics *5*, 75–86. https://doi.org/10.1023/B:JSFG.0000029237.70316.52.

Malzac, P., Webber, H., Moncla, A., Graham, J.M., Kukolich, M., Williams, C., Pagon, R.A., Ramsdell, L.A., Kishino, T., and Wagstaff, J. (1998). Mutation analysis of UBE3A in Angelman syndrome patients. Am. J. Hum. Genet. *62*, 1353–1360. .

M'Angale, P.G., and Staveley, B.E. (2016). Inhibition of Atg6 and Pi3K59F autophagy genes in neurons decreases lifespan and locomotor ability in Drosophila melanogaster. Genet. Mol. Res. *15*. https://doi.org/10.4238/gmr15048953.

Mani, A., Oh, A.S., Bowden, E.T., Lahusen, T., Lorick, K.L., Weissman, A.M., Schlegel, R., Wellstein, A., and Riegel, A.T. (2006). E6AP Mediates Regulated Proteasomal Degradation of the Nuclear Receptor Coactivator Amplified in Breast Cancer 1 in Immortalized Cells. Cancer Res. *66*, 8680–8686. https://doi.org/10.1158/0008-5472.CAN-06-0557.

Mansour, M.A. (2018). Ubiquitination: Friend and foe in cancer. Int J Biochem Cell Biol. *101*, 80-93. doi: 10.1016/j.biocel.2018.06.001.

Mao, Y., Senic-Matuglia, F., Di Fiore, P.P., Polo, S., Hodsdon, M.E., and De Camilli, P. (2005). Deubiquitinating function of ataxin-3: Insights from the solution structure of the

Josephin domain. Proc. Natl. Acad. Sci. U. S. A. *102*, 12700–12705. https://doi.org/10.1073/pnas.0506344102.

Maranga, C., Fernandes, T.G., Bekman, E., and Rocha, S.T. da Angelman syndrome: a journey through the brain. FEBS J. *287*, 2154-2175. https://doi.org/10.1111/febs.15258.

Marash, M., and Gerst, J.E. (2003). Phosphorylation of the Autoinhibitory Domain of the Sso t-SNAREs Promotes Binding of the Vsm1 SNARE Regulator in Yeast. Mol. Biol. Cell *14*, 3114–3125. https://doi.org/10.1091/mbc.E02-12-0804.

Margolis, S.S., Salogiannis, J., Lipton, D.M., Mandel-Brehm, C., Wills, Z.P., Mardinly, A.R., Hu, L., Greer, P.L., Bikoff, J.B., Ho, H.-Y.H., et al. (2010). EphB-mediated degradation of the RhoA GEF Ephexin5 relieves a developmental brake on excitatory synapse formation. Cell *143*, 442–455. https://doi.org/10.1016/j.cell.2010.09.038.

Margolis, S.S., Sell, G.L., Zbinden, M.A., and Bird, L.M. (2015). Angelman Syndrome. Neurotherapeutics *12*, 641–650. https://doi.org/10.1007/s13311-015-0361-y.

Marmorstein, R., Carey, M., Ptashne, M., and Harrison, S.C. (1992). DNA recognition by GAL4: structure of a protein-DNA complex. Nature *356*, 408–414. https://doi.org/10.1038/356408a0.

Martinez, A., Lectez, B., Ramirez, J., Popp, O., Sutherland, J.D., Urbé, S., Dittmar, G., Clague, M.J., and Mayor, U. (2017). Quantitative proteomic analysis of Parkin substrates in Drosophila neurons. Mol. Neurodegener. *12*. https://doi.org/10.1186/s13024-017-0170-3.

Martinez, A., Ramirez, J., Osinalde, N., Arizmendi, J.M., and Mayor, U. (2018). Neuronal Proteomic Analysis of the Ubiquitinated Substrates of the Disease-Linked E3 Ligases Parkin and Ube3a. BioMed Res. Int. *2018*, 3180413. https://doi.org/10.1155/2018/3180413.

Martínez-Noël, G., Luck, K., Kühnle, S., Desbuleux, A., Szajner, P., Galligan, J.T., Rodriguez, D., Zheng, L., Boyland, K., Leclere, F., et al. (2018). Network analysis of UBE3A/E6AP-associated proteins provides connections to several distinct cellular processes. J. Mol. Biol. *430*, 1024–1050. https://doi.org/10.1016/j.jmb.2018.01.021.

Martinez-Zapien, D., Ruiz, F.X., Poirson, J., Mitschler, A., Ramirez, J., Forster, A., Cousido-Siah, A., Masson, M., Vande Pol, S., Podjarny, A., et al. (2016). Structure of the E6/E6AP/p53 complex required for HPV-mediated degradation of p53. Nature *529*, 541–545. https://doi.org/10.1038/nature16481.

Marttila, A.T., Laitinen, O.H., Airenne, K.J., Kulik, T., Bayer, E.A., Wilchek, M., and Kulomaa, M.S. (2000). Recombinant NeutraLite avidin: a non-glycosylated, acidic mutant of chicken avidin that exhibits high affinity for biotin and low non-specific binding properties. FEBS Lett. *467*, 31–36. https://doi.org/10.1016/s0014-5793(00)01119-4.

Masuda, Y., Saeki, Y., Arai, N., Kawai, H., Kukimoto, I., Tanaka, K., and Masutani, C. (2019). Stepwise multipolyubiquitination of p53 by the E6AP-E6 ubiquitin ligase complex. J. Biol. Chem. *294*, 14860–14875. https://doi.org/10.1074/jbc.RA119.008374.

Matsui, S., Sandberg, A.A., Negoro, S., Seon, B.K., and Goldstein, G. (1982). Isopeptidase: a novel eukaryotic enzyme that cleaves isopeptide bonds. Proc. Natl. Acad. Sci. U. S. A. *79*, 1535–1539. .

Matsumoto, M., Hatakeyama, S., Oyamada, K., Oda, Y., Nishimura, T., and Nakayama, K.I. (2005). Large-scale analysis of the human ubiquitin-related proteome. Proteomics *5*, 4145–4151. https://doi.org/10.1002/pmic.200401280.

Matsuura, T., Sutcliffe, J.S., Fang, P., Galjaard, R.J., Jiang, Y.H., Benton, C.S., Rommens, J.M., and Beaudet, A.L. (1997). De novo truncating mutations in E6-AP ubiquitin-protein ligase gene (UBE3A) in Angelman syndrome. Nat. Genet. *15*, 74–77. https://doi.org/10.1038/ng0197-74.

Matthews, W., Driscoll, J., Tanaka, K., Ichihara, A., and Goldberg, A.L. (1989). Involvement of the proteasome in various degradative processes in mammalian cells. Proc. Natl. Acad. Sci. *86*, 2597–2601. https://doi.org/10.1073/pnas.86.8.2597.

Matthiesen, R., and Bunkenborg, J. (2020). Introduction to Mass Spectrometry-Based Proteomics. Methods Mol. Biol. Clifton NJ *2051*, 1–58. https://doi.org/10.1007/978-1-4939-9744-2_1.

Maurer, T., and Wertz, I.E. (2016). Length Matters: MINDY Is a New Deubiquitinase Family that Preferentially Cleaves Long Polyubiquitin Chains. Mol. Cell *63*, 4–6. https://doi.org/10.1016/j.molcel.2016.06.027.

Mayor, U., and Peng, J. (2012). Deciphering Tissue-specific Ubiquitination by Mass Spectrometry. Methods Mol. Biol. Clifton NJ *832*, 65–80. https://doi.org/10.1007/978-1-61779-474-2_3.

Mayor, T., Graumann, J., Bryan, J., MacCoss, M.J., and Deshaies, R.J. (2007). Quantitative profiling of ubiquitylated proteins reveals proteasome substrates and the substrate repertoire influenced by the Rpn10 receptor pathway. Mol. Cell. Proteomics MCP *6*, 1885–1895. https://doi.org/10.1074/mcp.M700264-MCP200.

McClellan, A.J., Laugesen, S.H., and Ellgaard, L. (2019). Cellular functions and molecular mechanisms of non-lysine ubiquitination. Open Biol. *9*. https://doi.org/10.1098/rsob.190147.

McDougle, C.J., and Keary, C.J. (2020). Sleep and EEG biomarkers as avenues toward new treatment approaches in Angelman syndrome. Neuropsychopharmacology *45*, 238–239. https://doi.org/10.1038/s41386-019-0517-2.

McGrath, J.P., Jentsch, S., and Varshavsky, A. (1991). UBA 1: an essential yeast gene encoding ubiquitin-activating enzyme. EMBO J. *10*, 227–236. https://doi.org/10.1002/j.1460-2075.1991.tb07940.x.

McPherson, A., and Gavira, J.A. (2013). Introduction to protein crystallization. Acta Crystallogr. Sect. F Struct. Biol. Commun. *70*, 2–20. https://doi.org/10.1107/S2053230X13033141.

Meng, L., Ward, A.J., Chun, S., Bennett, C.F., Beaudet, A.L., and Rigo, F. (2015). Towards a therapy for Angelman syndrome by targeting a long non-coding RNA. Nature *518*, 409–412. https://doi.org/10.1038/nature13975.

Messick, T.E., Russell, N.S., Iwata, A.J., Sarachan, K.L., Shiekhattar, R., Shanks, J.R., Reyes-Turcu, F.E., Wilkinson, K.D., and Marmorstein, R. (2008). Structural Basis for Ubiquitin Recognition by the Otu1 Ovarian Tumor Domain Protein. J. Biol. Chem. *283*, 11038–11049. https://doi.org/10.1074/jbc.M704398200.

Metzger, M.B., Pruneda, J.N., Klevit, R.E., and Weissman, A.M. (2014). RING-type E3 ligases: Master manipulators of E2 ubiquitin-conjugating enzymes and ubiquitination. Biochim. Biophys. Acta *1843*, 47–60. https://doi.org/10.1016/j.bbamcr.2013.05.026.

Meyer, H.-J., and Rape, M. (2014). Enhanced Protein Degradation by Branched Ubiquitin Chains. Cell *157*, 910–921. https://doi.org/10.1016/j.cell.2014.03.037.

Meyer, K., Feldman, H.M., Lu, T., Drake, D., Lim, E.T., Ling, K.H., Bishop, N.A., Pan, Y., Seo, J., Lin, Y.-T., et al. (2019). REST and Neural Gene Network Dysregulation in iPSC Models of Alzheimer's Disease. Cell Rep. *26*, 1112-1127.e9. https://doi.org/10.1016/j.celrep.2019.01.023.

Miao, S., Chen, R., Ye, J., Tan, G.H., Li, S., Zhang, J., Jiang, Y., and Xiong, Z.-Q. (2013). The Angelman Syndrome Protein Ube3a Is Required for Polarized Dendrite Morphogenesis in Pyramidal Neurons. J. Neurosci. *33*, 327–333. https://doi.org/10.1523/JNEUROSCI.2509-12.2013.

Michel, M.A., Elliott, P.R., Swatek, K.N., Simicek, M., Pruneda, J.N., Wagstaff, J.L., Freund, S.M.V., and Komander, D. (2015). Assembly and Specific Recognition of K29- and K33-Linked Polyubiquitin. Mol. Cell *58*, 95–109. https://doi.org/10.1016/j.molcel.2015.01.042.

Michelle, C., Vourc'h, P., Mignon, L., and Andres, C.R. (2009). What Was the Set of Ubiquitin and Ubiquitin-Like Conjugating Enzymes in the Eukaryote Common Ancestor? J. Mol. Evol. *68*, 616–628. https://doi.org/10.1007/s00239-009-9225-6.

Milazzo, C., Mientjes, E.J., Wallaard, I., Rasmussen, S.V., Erichsen, K.D., Kakunuri, T., van der Sman, A.S.E., Kremer, T., Miller, M.T., Hoener, M.C., et al. (2021). Antisense oligonucleotide treatment rescues UBE3A expression and multiple phenotypes of an Angelman syndrome mouse model. JCI Insight *6*. https://doi.org/10.1172/jci.insight.145991.

Miller, D.E., Cook, K.R., and Hawley, R.S. (2019). The joy of balancers. PLoS Genet. *15*. https://doi.org/10.1371/journal.pgen.1008421.

Min, M., Mayor, U., and Lindon, C. (2013). Ubiquitination site preferences in anaphase promoting complex/cyclosome (APC/C) substrates. Open Biol. *3*. https://doi.org/10.1098/rsob.130097.

Min, M., Mayor, U., Dittmar, G., and Lindon, C. (2014). Using in vivo biotinylated ubiquitin to describe a mitotic exit ubiquitome from human cells. Mol. Cell. Proteomics MCP *13*, 2411–2425. https://doi.org/10.1074/mcp.M113.033498.

Misaghi, S., Galardy, P.J., Meester, W.J.N., Ovaa, H., Ploegh, H.L., and Gaudet, R. (2005). Structure of the ubiquitin hydrolase UCH-L3 complexed with a suicide substrate. J. Biol. Chem. *280*, 1512–1520. https://doi.org/10.1074/jbc.M410770200.

Mishra, A., Godavarthi, S.K., and Jana, N.R. (2009). UBE3A/E6-AP regulates cell proliferation by promoting proteasomal degradation of p27. Neurobiol. Dis. *36*, 26–34. https://doi.org/10.1016/j.nbd.2009.06.010.

Moiseeva, T.N., Bottrill, A., Melino, G., and Barlev, N.A. (2013). DNA damage-induced ubiquitylation of proteasome controls its proteolytic activity. Oncotarget *4*, 1338–1348. .

Morawe, T., Honemann-Capito, M., von Stein, W., and Wodarz, A. (2011). Loss of the extraproteasomal ubiquitin receptor Rings lost impairs ring canal growth in Drosophila oogenesis. J. Cell Biol. *193*, 71–80. https://doi.org/10.1083/jcb.201009142.

Morgan, T.H. (1910). Sex limited inheritance in Drosophila. Science *32*, 120–122. https://doi.org/10.1126/science.32.812.120.

Morreale, F.E., and Walden, H. (2016). Types of Ubiquitin Ligases. Cell *165*, 248-248.e1. https://doi.org/10.1016/j.cell.2016.03.003.

Morreale, F.E., Bortoluzzi, A., Chaugule, V.K., Arkinson, C., Walden, H., and Ciulli, A. (2017). Allosteric Targeting of the Fanconi Anemia Ubiquitin-Conjugating Enzyme Ube2T by Fragment Screening. J. Med. Chem. *60*, 4093–4098. https://doi.org/10.1021/acs.jmedchem.7b00147.

Moser, E., and Oliver, P.M. (2019). Special Issue: E3 ubiquitin ligases, the match makers and grim reapers of immune cells. Cell. Immunol. *340*, 103924. https://doi.org/10.1016/j.cellimm.2019.103924.

Mótyán, J.A., Miczi, M., and Tőzsér, J. (2020). Dimer Interface Organization is a Main Determinant of Intermonomeric Interactions and Correlates with Evolutionary Relationships of Retroviral and Retroviral-Like Ddi1 and Ddi2 Proteases. Int. J. Mol. Sci. *21*. https://doi.org/10.3390/ijms21041352.

Mulder, G.J. (1839). Ueber die Zusammensetzung einiger thierischen Substanzen. J. Fr. Prakt. Chem. *16*, 129–152. https://doi.org/10.1002/prac.18390160137.

Mulherkar, S.A., and Jana, N.R. (2010). Loss of dopaminergic neurons and resulting behavioural deficits in mouse model of Angelman syndrome. Neurobiol. Dis. *40*, 586–592. https://doi.org/10.1016/j.nbd.2010.08.002.

Muller, H.J. (1918). Genetic Variability, Twin Hybrids and Constant Hybrids, in a Case of Balanced Lethal Factors. Genetics *3*, 422–499. .

Muller, H.J. (1927). Artificial transmutation of the gene. Science *66*, 84–87. https://doi.org/10.1126/science.66.1699.84.

Munter, S.D., Görnemann, J., Derua, R., Lesage, B., Qian, J., Heroes, E., Waelkens, E., Eynde, A.V., Beullens, M., and Bollen, M. (2017). Split-BioID: a proximity biotinylation assay for dimerization-dependent protein interactions. FEBS Lett. *591*, 415–424. https://doi.org/10.1002/1873-3468.12548.

Murtaza, M., Jolly, L.A., Gecz, J., and Wood, S.A. (2015). La FAM fatale: USP9X in development and disease. Cell. Mol. Life Sci. *72*, 2075–2089. https://doi.org/10.1007/s00018-015-1851-0.

Na, C.H., Jones, D.R., Yang, Y., Wang, X., Xu, Y., and Peng, J. (2012). Synaptic protein ubiquitination in rat brain revealed by antibody-based ubiquitome analysis. J. Proteome Res. *11*, 4722–4732. https://doi.org/10.1021/pr300536k.

Nadler, J.J., Moy, S.S., Dold, G., and Simmons, N., Perez, A., Young, N.B., Barbaro, R.P., Piven, J., Magnuson, T.R., and Crawley, J.N. (2004). Automated apparatus for quantitation of social approach behaviors in mice. Genes Brain Behav. *3*, 303–314. https://doi.org/10.1111/j.1601-183X.2004.00071.x.

Nakatani, J., Tamada, K., Hatanaka, F., Ise, S., Ohta, H., Inoue, K., Tomonaga, S., Watanabe, Y., Chung, Y.J., Banerjee, R., et al. (2009). Abnormal Behavior in a Chromosome-Engineered Mouse Model for Human 15q11-13 Duplication Seen in Autism. Cell *137*, 1235–1246. https://doi.org/10.1016/j.cell.2009.04.024.

Nanao, M.H., Tcherniuk, S.O., Chroboczek, J., Dideberg, O., Dessen, A., and Balakirev, M.Y. (2004). Crystal structure of human otubain 2. EMBO Rep. *5*, 783–788. https://doi.org/10.1038/sj.embor.7400201.

Narayanan, S., Cai, C.Y., Assaraf, Y.G., Guo, H.Q., Cui, Q., Wei, L., Huang, J.J., Ashby, C.R., and Chen, Z.S. (2020). Targeting the ubiquitin-proteasome pathway to overcome anti-cancer drug resistance. Drug Resist. Updat. *48*, 100663. https://doi.org/10.1016/j.drup.2019.100663.

Nascimento, R.M.P., Otto, P.A., Brouwer, A.P.M. de, and Vianna-Morgante, A.M. (2006). UBE2A, Which Encodes a Ubiquitin-Conjugating Enzyme, Is Mutated in a Novel X-Linked Mental Retardation Syndrome. Am. J. Hum. Genet. *79*, 549–555. https://doi.org/10.1086/507047.

Nawaz, Z., Lonard, D.M., Smith, C.L., Lev-Lehman, E., Tsai, S.Y., Tsai, M.J., and O'Malley, B.W. (1999). The Angelman syndrome-associated protein, E6-AP, is a coactivator for the nuclear hormone receptor superfamily. Mol. Cell. Biol. *19*, 1182–1189. https://doi.org/10.1128/mcb.19.2.1182.

Newton, K., Matsumoto, M.L., Wertz, I.E., Kirkpatrick, D.S., Lill, J.R., Tan, J., Dugger, D., Gordon, N., Sidhu, S.S., Fellouse, F.A., et al. (2008). Ubiquitin chain editing revealed by polyubiquitin linkage-specific antibodies. Cell *134*, 668–678. https://doi.org/10.1016/j.cell.2008.07.039.

Nicastro, G., Menon, R.P., Masino, L., Knowles, P.P., McDonald, N.Q., and Pastore, A. (2005). The solution structure of the Josephin domain of ataxin-3: Structural determinants for molecular recognition. Proc. Natl. Acad. Sci. U. S. A. *102*, 10493–10498. https://doi.org/10.1073/pnas.0501732102.

Nicholls, R.D., Pai, G.S., Gottlieb, W., and Cantú, E.S. (1992). Paternal uniparental disomy of chromosome 15 in a child with Angelman syndrome. Ann. Neurol. *32*, 512–518. https://doi.org/10.1002/ana.410320406.

Nicolini, C., Ahn, Y., Michalski, B., Rho, J.M., and Fahnestock, M. (2015). Decreased mTOR signaling pathway in human idiopathic autism and in rats exposed to valproic acid. Acta Neuropathol. Commun. *3*, 3. https://doi.org/10.1186/s40478-015-0184-4.

Nijman, S.M.B., Luna-Vargas, M.P.A., Velds, A., Brummelkamp, T.R., Dirac, A.M.G., Sixma, T.K., and Bernards, R. (2005). A Genomic and Functional Inventory of

Deubiquitinating Enzymes. Cell *123*, 773–786. https://doi.org/10.1016/j.cell.2005.11.007.

Noor, A., Dupuis, L., Mittal, K., Lionel, A.C., Marshall, C.R., Scherer, S.W., Stockley, T., Vincent, J.B., Mendoza-Londono, R., and Stavropoulos, D.J. (2015). 15q11.2 Duplication Encompassing Only the UBE3A Gene Is Associated with Developmental Delay and Neuropsychiatric Phenotypes. Hum. Mutat. *36*, 689–693. https://doi.org/10.1002/humu.22800.

Nowicka, U., Zhang, D., Walker, O., Krutauz, D., Castañeda, C.A., Chaturvedi, A., Chen, T.Y., Reis, N., Glickman, M.H., and Fushman, D. (2015). DNA-Damage-Inducible 1 Protein (Ddi1) Contains an Uncharacteristic Ubiquitin-like Domain that Binds Ubiquitin. Structure *23*, 542–557. https://doi.org/10.1016/j.str.2015.01.010.

Nuber, U., Schwarz, S., Kaiser, P., Schneider, R., and Scheffner, M. (1996). Cloning of human ubiquitin-conjugating enzymes UbcH6 and UbcH7 (E2-F1) and characterization of their interaction with E6-AP and RSP5. J. Biol. Chem. *271*, 2795–2800. https://doi.org/10.1074/jbc.271.5.2795.

Nuber, U., Schwarz, S.E., and Scheffner, M. (1998). The ubiquitin-protein ligase E6-associated protein (E6-AP) serves as its own substrate. Eur. J. Biochem. *254*, 643–649. https://doi.org/10.1046/j.1432-1327.1998.2540643.x.

Nüsslein-Volhard, C., and Wieschaus, E. (1980). Mutations affecting segment number and polarity in Drosophila. Nature *287*, 795–801. https://doi.org/10.1038/287795a0.

Oda, H., Kumar, S., and Howley, P.M. (1999). Regulation of the Src family tyrosine kinase Blk through E6AP-mediated ubiquitination. Proc. Natl. Acad. Sci. *96*, 9557–9562. https://doi.org/10.1073/pnas.96.17.9557.

Ohi, M.D., Vander Kooi, C.W., Rosenberg, J.A., Chazin, W.J., and Gould, K.L. (2003). Structural insights into the U-box, a domain associated with multi-ubiquitination. Nat. Struct. Biol. *10*, 250–255. https://doi.org/10.1038/nsb906.

Ohtake, F., Saeki, Y., Ishido, S., Kanno, J., and Tanaka, K. (2016). The K48-K63 Branched Ubiquitin Chain Regulates NF-κB Signaling. Mol. Cell *64*, 251–266. https://doi.org/10.1016/j.molcel.2016.09.014.

Ohtake, F., Tsuchiya, H., Saeki, Y., and Tanaka, K. (2018). K63 ubiquitylation triggers proteasomal degradation by seeding branched ubiquitin chains. Proc. Natl. Acad. Sci. U. S. A. *115*, E1401–E1408. https://doi.org/10.1073/pnas.1716673115.

Olabarria, M., Pasini, S., Corona, C., Robador, P., Song, C., Patel, H., and Lefort, R. (2019). Dysfunction of the ubiquitin ligase E3A Ube3A/E6-AP contributes to synaptic pathology in Alzheimer's disease. Commun. Biol. *2*, 1–14. https://doi.org/10.1038/s42003-019-0350-5.

de Oliveira, J.F., do Prado, P.F.V., da Costa, S.S., Sforça, M.L., Canateli, C., Ranzani, A.T., Maschietto, M., de Oliveira, P.S.L., Otto, P.A., Klevit, R.E., et al. (2019). Mechanistic insights revealed by a UBE2A mutation linked to intellectual disability. Nat. Chem. Biol. *15*, 62–70. https://doi.org/10.1038/s41589-018-0177-2.

Olsen, J.V., Ong, S.-E., and Mann, M. (2004). Trypsin cleaves exclusively C-terminal to arginine and lysine residues. Mol. Cell. Proteomics MCP *3*, 608–614. https://doi.org/10.1074/mcp.T400003-MCP200.

O'Neill, M.F., Heron-Maxwell, C., Conway, M.W., Monn, J.A. and Ornstein, P. (2003). Group II metabotropic glutamate receptor antagonists LY341495 and LY366457 increase locomotor activity in mice. Neuropharmacology. *5*, 565-574. doi: 10.1016/s0028-3908(03)00232-6.

Osinalde, N., Duarri, A., Ramirez, J., Barrio, R., Perez de Nanclares, G., and Mayor, U. (2018). Impaired proteostasis in rare neurological diseases. Semin. Cell Dev. Biol. https://doi.org/10.1016/j.semcdb.2018.10.007.

Otoda, T., Yuasa, T., and Aihara, K. (2018). Evaluating the Ubiquitin–proteasome System as a Therapeutic Target in Diabetic Kidney Disease. *2*, 5. .

Paemka, L., Mahajan, V.B., Ehaideb, S.N., Skeie, J.M., Tan, M.C., Wu, S., Cox, A.J., Sowers, L.P., Gecz, J., Jolly, L., et al. (2015). Seizures Are Regulated by Ubiquitin-specific Peptidase 9 X-linked (USP9X), a De-Ubiquitinase. PLOS Genet. *11*, e1005022. https://doi.org/10.1371/journal.pgen.1005022.

Palladino, M.J., Hadley, T.J., and Ganetzky, B. (2002). Temperature-sensitive paralytic mutants are enriched for those causing neurodegeneration in Drosophila. Genetics *161*, 1197–1208. https://doi.org/10.1093/genetics/161.3.1197.

Pandey, U.B., and Nichols, C.D. (2011). Human Disease Models in Drosophila melanogaster and the Role of the Fly in Therapeutic Drug Discovery. Pharmacol. Rev. *63*, 411–436. https://doi.org/10.1124/pr.110.003293.

Parmentier, M.L., Pin, J.P., Bockaert, J., and Grau, Y. (1996). Cloning and Functional Expression of a DrosophilaMetabotropic Glutamate Receptor Expressed in the Embryonic CNS. J. Neurosci. *16*, 6687–6694. https://doi.org/10.1523/JNEUROSCI.16-21-06687.1996.

Pastuzyn, E.D., and Shepherd, J.D. (2017). Activity-Dependent Arc Expression and Homeostatic Synaptic Plasticity Are Altered in Neurons from a Mouse Model of Angelman Syndrome. Front. Mol. Neurosci. *10*. .

Paulson, H., Shakkottai, V. (1998). Spinocerebellar Ataxia Type 3. In: Adam MP, Ardinger HH, Pagon RA, Wallace SE, Bean LJH, Gripp KW, Mirzaa GM, Amemiya A, editors. GeneReviews® [Internet]. Seattle (WA): University of Washington, Seattle; 1993–2022. PMID: 20301375.

Pelzer, C., Kassner, I., Matentzoglu, K., Singh, R.K., Wollscheid, H.P., Scheffner, M., Schmidtke, G., and Groettrup, M. (2007). UBE1L2, a Novel E1 Enzyme Specific for Ubiquitin. J. Biol. Chem. *282*, 23010–23014. https://doi.org/10.1074/jbc.C700111200.

Peng, J., Schwartz, D., Elias, J.E., Thoreen, C.C., Cheng, D., Marsischky, G., Roelofs, J., Finley, D., and Gygi, S.P. (2003). A proteomics approach to understanding protein ubiquitination. Nat. Biotechnol. *21*, 921–926. https://doi.org/10.1038/nbt849.

Peng, X., Wang, J., Peng, W., Wu, F.X., and Pan, Y. (2016). Protein–protein interactions: detection, reliability assessment and applications. Brief. Bioinform. bbw066. https://doi.org/10.1093/bib/bbw066.

Pereira, P.C., Fernandes, R., and Ramalho, J. (2006). Oxidative Stress Up–Regulates Ubiquitin Proteasome System in Retinal Endothelial Cells. Invest. Ophthalmol. Vis. Sci. *47*, 2093–2093. .

Perteguer, M.J., Gómez-Puertas, P., Cañavate, C., Dagger, F., Gárate, T., and Valdivieso, E. (2013). Ddi1-like protein from Leishmania major is an active aspartyl proteinase. Cell Stress Chaperones *18*, 171–181. https://doi.org/10.1007/s12192-012-0368-9.

Peters, J.M., Franke, W.W., and Kleinschmidt, J.A. (1994). Distinct 19 S and 20 S subcomplexes of the 26 S proteasome and their distribution in the nucleus and the cytoplasm. J. Biol. Chem. *269*, 7709–7718. .

Peters, S.U., Bird, L.M., Kimonis, V., Glaze, D.G., Shinawi, U.M., Bichell, T.J., Barbieri-Welge, R., Nespeca, M., Anselm, I., Waisbren, S., et al. (2010). Double-Blind Therapeutic Trial in Angelman Syndrome Using Betaine and Folic Acid. Am. J. Med. Genet. A. *152A*, 1994–2001. https://doi.org/10.1002/ajmg.a.33509.

Peterson, L.F., Sun, H., Liu, Y., Potu, H., Kandarpa, M., Ermann, M., Courtney, S.M., Young, M., Showalter, H.D., Sun, D., et al. (2015). Targeting deubiquitinase activity with a novel small-molecule inhibitor as therapy for B-cell malignancies. Blood *125*, 3588–3597. https://doi.org/10.1182/blood-2014-10-605584.

Petroski, M.D., and Deshaies, R.J. (2005). Function and regulation of cullin-RING ubiquitin ligases. Nat. Rev. Mol. Cell Biol. *6*, 9–20. https://doi.org/10.1038/nrm1547.

Pham, A.D., and Sauer, F. (2000). Ubiquitin-Activating/Conjugating Activity of TAFII250, a Mediator of Activation of Gene Expression in Drosophila. Science *289*, 2357–2360. https://doi.org/10.1126/science.289.5488.2357.

Pickrell, A.M., and Youle, R.J. (2015). The roles of PINK1, parkin, and mitochondrial fidelity in Parkinson's disease. Neuron *85*, 257–273. https://doi.org/10.1016/j.neuron.2014.12.007.

Pignatelli, M., Piccinin, S., Molinaro, G., Di Menna, L., Riozzi, B., Cannella, M., Motolese, M., Vetere, G., Catania, M.V., Battaglia, G., et al. (2014). Changes in mGlu5 Receptor-Dependent Synaptic Plasticity and Coupling to Homer Proteins in the Hippocampus of Ube3A Hemizygous Mice Modeling Angelman Syndrome. J. Neurosci. *34*, 4558–4566. https://doi.org/10.1523/JNEUROSCI.1846-13.2014.

Pinto-Fernandez, A., and Kessler, B.M. (2016). DUBbing Cancer: Deubiquitylating Enzymes Involved in Epigenetics, DNA Damage and the Cell Cycle As Therapeutic Targets. Front. Genet. *7*. https://doi.org/10.3389/fgene.2016.00133.

Polge, C., Attaix, D., and Taillandier, D. (2015). Role of E2-Ub-conjugating enzymes during skeletal muscle atrophy. Front. Physiol. *6*. https://doi.org/10.3389/fphys.2015.00059.

Popovic, D., Vucic, D., and Dikic, I. (2014). Ubiquitination in disease pathogenesis and treatment. Nat. Med. *20*, 1242–1253. https://doi.org/10.1038/nm.3739.

Powis, R.A., Karyka, E., Boyd, P., Côme, J., Jones, R.A., Zheng, Y., Szunyogova, E., Groen, E.J.N., Hunter, G., Thomson, D., et al. (2016). Systemic restoration of UBA1 ameliorates disease in spinal muscular atrophy. JCI Insight *1*. https://doi.org/10.1172/jci.insight.87908.

de Pril, R., Fischer, D.F., Roos, R.A.C., and van Leeuwen, F.W. (2007). Ubiquitin-conjugating enzyme E2-25K increases aggregate formation and cell death in polyglutamine diseases. Mol. Cell. Neurosci. *34*, 10–19. https://doi.org/10.1016/j.mcn.2006.09.006.

Pruneda, J.N., Smith, F.D., Daurie, A., Swaney, D.L., Villén, J., Scott, J.D., Stadnyk, A.W., Le Trong, I., Stenkamp, R.E., Klevit, R.E., et al. (2014). E2~Ub conjugates regulate the kinase activity of Shigella effector OspG during pathogenesis. EMBO J. *33*, 437–449. https://doi.org/10.1002/embj.201386386.

Puram, S.V., Kim, A.H., Park, H.Y., Anckar, J., and Bonni, A. (2013). The Ubiquitin Receptor S5a/Rpn10 Links Centrosomal Proteasomes with Dendrite Development in the Mammalian Brain. Cell Rep. *4*, 19–30. https://doi.org/10.1016/j.celrep.2013.06.006.

Purbeck, C., Eletr, Z.M., and Kuhlman, B. (2010). Kinetics of the transfer of ubiquitin from UbcH7 to E6AP. Biochemistry *49*, 1361–1363. https://doi.org/10.1021/bi9014693.

R. von Collenberg, C., Schmitt, D., Rülicke, T., Sendtner, M., Blum, R., and Buchner, E. (2019). An essential role of the mouse synapse-associated protein Syap1 in circuits for spontaneous motor activity and rotarod balance. Biol. Open *8*, bio042366. https://doi.org/10.1242/bio.042366.

Raasi, S., Varadan, R., Fushman, D., and Pickart, C.M. (2005). Diverse polyubiquitin interaction properties of ubiquitin-associated domains. Nat. Struct. Mol. Biol. *12*, 708–714. https://doi.org/10.1038/nsmb962.

Ramatenki, V., Dumpati, R., Vadija, R., Vellanki, S., Potlapally, S.R., Rondla, R., and Vuruputuri, U. (2016). Targeting the ubiquitin-conjugating enzyme E2D4 for cancer drug discovery–a structure-based approach. J. Chem. Biol. *10*, 51–67. https://doi.org/10.1007/s12154-016-0164-6.

Ramirez, J., Martinez, A., Lectez, B., Lee, S.Y., Franco, M., Barrio, R., Dittmar, G., and Mayor, U. (2015). Proteomic Analysis of the Ubiquitin Landscape in the Drosophila Embryonic Nervous System and the Adult Photoreceptor Cells. PloS One *10*, e0139083. https://doi.org/10.1371/journal.pone.0139083.

Ramirez, J., Min, M., Barrio, R., Lindon, C., and Mayor, U. (2016). Isolation of Ubiquitinated Proteins to High Purity from In Vivo Samples. In Proteostasis: Methods and Protocols, R. Matthiesen, ed. (New York, NY: Springer New York), pp. 193–202.

Ramirez, J., Lectez, B., Osinalde, N., Sivá, M., Elu, N., Aloria, K., Procházková, M., Perez, C., Martínez-Hernández, J., Barrio, R., et al. (2018). Quantitative proteomics reveals neuronal ubiquitination of Rngo/Ddi1 and several proteasomal subunits by Ube3a, accounting for the complexity of Angelman syndrome. Hum. Mol. Genet. *27*, 1955–1971. https://doi.org/10.1093/hmg/ddy103.

Ramirez, J., Prieto, G., Olazabal-Herrero, A., Borràs, E., Fernandez-Vigo, E., Alduntzin, U., Osinalde, N., Beaskoetxea, J., Lectez, B., Aloria, K., et al. (2021). A Proteomic Approach for Systematic Mapping of Substrates of Human Deubiquitinating Enzymes. Int. J. Mol. Sci. *22*. https://doi.org/10.3390/ijms22094851.

van Ree, J.H., Jeganathan, K.B., Malureanu, L., and van Deursen, J.M. (2010). Overexpression of the E2 ubiquitin–conjugating enzyme UbcH10 causes chromosome missegregation and tumor formation. J. Cell Biol. *188*, 83–100. https://doi.org/10.1083/jcb.200906147.

Reiter, L.T., Potocki, L., Chien, S., Gribskov, M., and Bier, E. (2001). A systematic analysis of human disease-associated gene sequences in Drosophila melanogaster. Genome Res. *11*, 1114–1125. https://doi.org/10.1101/gr.169101.

Reiter, L.T., Seagroves, T.N., Bowers, M., and Bier, E. (2006). Expression of the Rho-GEF Pbl/ECT2 is regulated by the UBE3A E3 ubiquitin ligase. Hum. Mol. Genet. *15*, 2825–2835. https://doi.org/10.1093/hmg/ddl225.

Reiterer, V., Maier, S., Sitte, H.H., Kriz, A., Rüegg, M.A., Hauri, H.-P., Freissmuth, M., and Farhan, H. (2008). Sec24- and ARFGAP1-Dependent Trafficking of GABA Transporter-1 Is a Prerequisite for Correct Axonal Targeting. J. Neurosci. *28*, 12453–12464. https://doi.org/10.1523/JNEUROSCI.3451-08.2008.

Renatus, M., Parrado, S.G., D'Arcy, A., Eidhoff, U., Gerhartz, B., Hassiepen, U., Pierrat, B., Riedl, R., Vinzenz, D., Worpenberg, S., et al. (2006). Structural Basis of Ubiquitin Recognition by the Deubiquitinating Protease USP2. Structure *14*, 1293–1302. https://doi.org/10.1016/j.str.2006.06.012.

Ries, L.K., Sander, B., Deol, K.K., Letzelter, M.-A., Strieter, E.R., and Lorenz, S. (2019). Analysis of ubiquitin recognition by the HECT ligase E6AP provides insight into its linkage specificity. J. Biol. Chem. *294*, 6113–6129. https://doi.org/10.1074/jbc.RA118.007014.

Ries, L.K., Liess, A.K.L., Feiler, C.G., Spratt, D.E., Lowe, E.D., and Lorenz, S. Crystal structure of the catalytic C-lobe of the HECT-type ubiquitin ligase E6AP. Protein Sci. *29*, 1550-1554. https://doi.org/10.1002/pro.3832.

Riise, R., Odqvist, L., Mattsson, J., Monkley, S., Abdillahi, S.M., Tyrchan, C., Muthas, D., and Yrlid, L.F. (2019). Bleomycin hydrolase regulates the release of chemokines important for inflammation and wound healing by keratinocytes. Sci. Rep. *9*. https://doi.org/10.1038/s41598-019-56667-6.

Rinetti, G.V., and Schweizer, F.E. (2010). Ubiquitination acutely regulates presynaptic neurotransmitter release in mammalian neurons. J. Neurosci. Off. J. Soc. Neurosci. *30*, 3157–3166. https://doi.org/10.1523/JNEUROSCI.3712-09.2010.

Rittinger, K., and Ikeda, F. (2017). Linear ubiquitin chains: enzymes, mechanisms and biology. Open Biol. *7*. https://doi.org/10.1098/rsob.170026.

Roberts, D.B. (2006). Drosophila melanogaster: the model organism. Entomol. Exp. Appl. *121*, 93–103. https://doi.org/10.1111/j.1570-8703.2006.00474.x.

Ronchi, V.P., Klein, J.M., Edwards, D.J., and Haas, A.L. (2014). The active form of E6-associated protein (E6AP)/UBE3A ubiquitin ligase is an oligomer. J. Biol. Chem. *289*, 1033–1048. https://doi.org/10.1074/jbc.M113.517805.

Rose, I.A., and Warms, J.V. (1983). An enzyme with ubiquitin carboxy-terminal esterase activity from reticulocytes. Biochemistry *22*, 4234–4237. https://doi.org/10.1021/bi00287a012.

Rosenzweig, R., Bronner, V., Zhang, D., Fushman, D., and Glickman, M.H. (2012). Rpn1 and Rpn2 Coordinate Ubiquitin Processing Factors at Proteasome. J. Biol. Chem. *287*, 14659–14671. https://doi.org/10.1074/jbc.M111.316323.

Rotaru, D.C., van Woerden, G.M., Wallaard, I., and Elgersma, Y. (2018). Adult Ube3a Gene Reinstatement Restores the Electrophysiological Deficits of Prefrontal Cortex Layer 5 Neurons in a Mouse Model of Angelman Syndrome. J. Neurosci. Off. J. Soc. Neurosci. *38*, 8011–8030. https://doi.org/10.1523/JNEUROSCI.0083-18.2018.

Rotaru, D.C., Mientjes, E.J., and Elgersma, Y. (2020). Angelman Syndrome: From Mouse Models to Therapy. Neuroscience *445*, 172–189. https://doi.org/10.1016/j.neuroscience.2020.02.017.

Roux, K.J., Kim, D.I., Raida, M., and Burke, B. (2012). A promiscuous biotin ligase fusion protein identifies proximal and interacting proteins in mammalian cells. J. Cell Biol. *196*, 801–810. https://doi.org/10.1083/jcb.201112098.

Ruprecht, B., and Lemeer, S. (2014). Proteomic analysis of phosphorylation in cancer. Expert Rev. Proteomics *11*, 259–267. https://doi.org/10.1586/14789450.2014.901156.

Ryan, D.P., and Matthews, J.M. (2005). Protein–protein interactions in human disease. Curr. Opin. Struct. Biol. *15*, 441–446. https://doi.org/10.1016/j.sbi.2005.06.001.

Ryu, K.Y., Maehr, R., Gilchrist, C.A., Long, M.A., Bouley, D.M., Mueller, B., Ploegh, H.L., and Kopito, R.R. (2007). The mouse polyubiquitin gene UbC is essential for fetal liver development, cell-cycle progression and stress tolerance. EMBO J. *26*, 2693–2706. https://doi.org/10.1038/sj.emboj.7601722.

Ryu, K.Y., Garza, J.C., Lu, X.Y., Barsh, G.S., and Kopito, R.R. (2008a). Hypothalamic neurodegeneration and adult-onset obesity in mice lacking the Ubb polyubiquitin gene. Proc. Natl. Acad. Sci. *105*, 4016–4021. https://doi.org/10.1073/pnas.0800096105.

Ryu, K.Y., Sinnar, S.A., Reinholdt, L.G., Vaccari, S., Hall, S., Garcia, M.A., Zaitseva, T.S., Bouley, D.M., Boekelheide, K., Handel, M.A., et al. (2008b). The Mouse Polyubiquitin Gene Ubb Is Essential for Meiotic Progression. Mol. Cell. Biol. *28*, 1136–1146. https://doi.org/10.1128/MCB.01566-07.

Sachdeva, R., Donkers, S.J., and Kim, S.Y. (2016). Angelman syndrome: A review highlighting musculoskeletal and anatomical aberrations. Clin. Anat. N. Y. N *29*, 561–567. https://doi.org/10.1002/ca.22659.

Sadikovic, B., Fernandes, P., Zhang, V.W., Ward, P.A., Miloslavskaya, I., Rhead, W., Rosenbaum, R., Gin, R., Roa, B., and Fang, P. (2014). Mutation Update for UBE3A Variants in Angelman Syndrome. Hum. Mutat. *35*, 1407–1417. https://doi.org/10.1002/humu.22687.

Saez, I., Koyuncu, S., Gutierrez-Garcia, R., Dieterich, C., and Vilchez, D. (2018). Insights into the ubiquitin-proteasome system of human embryonic stem cells. Sci. Rep. *8*, 4092. https://doi.org/10.1038/s41598-018-22384-9.

Sáez, J.E., Arredondo, C., Rivera, C., and Andrés, M.E. (2018). PIASγ controls stability and facilitates SUMO-2 conjugation to CoREST family of transcriptional co-repressors. Biochem. J. *475*, 1441–1454. https://doi.org/10.1042/BCJ20170983.

Sahoo, T., Bacino, C.A., German, J.R., Shaw, C.A., Bird, L.M., Kimonis, V., Anselm, I., Waisbren, S., Beaudet, A.L., and Peters, S.U. (2007). Identification of novel deletions of 15q11q13 in Angelman syndrome by array-CGH: molecular characterization and genotype-phenotype correlations. Eur. J. Hum. Genet. EJHG *15*, 943–949. https://doi.org/10.1038/sj.ejhg.5201859.

Sailer, C., Offensperger, F., Julier, A., Kammer, K.-M., Walker-Gray, R., Gold, M.G., Scheffner, M., and Stengel, F. (2018). Structural dynamics of the E6AP/UBE3A-E6-p53 enzyme-substrate complex. Nat. Commun. *9*. https://doi.org/10.1038/s41467-018-06953-0.

Sala-Gaston, J., Martinez-Martinez, A., Pedrazza, L., Lorenzo-Martín, L.F., Caloto, R., Bustelo, X.R., Ventura, F., and Rosa, J.L. (2020). HERC Ubiquitin Ligases in Cancer. Cancers *12*. https://doi.org/10.3390/cancers12061653.

Samanta, D. (2021). Epilepsy in Angelman syndrome: A scoping review. Brain Dev. *43*, 32–44. https://doi.org/10.1016/j.braindev.2020.08.014.

Sang, T.K., and Jackson, G.R. (2005). Drosophila Models of Neurodegenerative Disease. NeuroRx *2*, 438–446. .

Sang, L., Miller, J.J., Corbit, K.C., Giles, R.H., Brauer, M.J., Otto, E.A., Baye, L.M., Wen, X., Scales, S.J., Kwong, M., et al. (2011). Mapping the NPHP-JBTS-MKS protein network reveals ciliopathy disease genes and pathways. Cell *145*, 513–528. https://doi.org/10.1016/j.cell.2011.04.019.

Sarraf, S.A., Raman, M., Guarani-Pereira, V., Sowa, M.E., Huttlin, E.L., Gygi, S.P., and Harper, J.W. (2013). Landscape of the PARKIN-dependent ubiquitylome in response to mitochondrial depolarization. Nature *496*, 372–376. https://doi.org/10.1038/nature12043.

Sarraf, S.A., Shah, H.V., Kanfer, G., Pickrell, A.M., Holtzclaw, L.A., Ward, M.E., and Youle, R.J. (2020). Loss of TAX1BP1-Directed Autophagy Results in Protein Aggregate Accumulation in the Brain. Mol. Cell *80*, 779-795.e10. https://doi.org/10.1016/j.molcel.2020.10.041.

Scheel, H., Tomiuk, S., and Hofmann, K. (2003). Elucidation of ataxin-3 and ataxin-7 function by integrative bioinformatics. Hum. Mol. Genet. *12*, 2845–2852. https://doi.org/10.1093/hmg/ddg297.

Scheffner, M., and Kumar, S. (2014). Mammalian HECT ubiquitin-protein ligases: Biological and pathophysiological aspects. Biochim. Biophys. Acta BBA - Mol. Cell Res. *1843*, 61–74. https://doi.org/10.1016/j.bbamcr.2013.03.024.

Scheffner, M., Huibregtse, J.M., Vierstra, R.D., and Howley, P.M. (1993). The HPV-16 E6 and E6-AP complex functions as a ubiquitin-protein ligase in the ubiquitination of p53. Cell *75*, 495–505. https://doi.org/10.1016/0092-8674(93)90384-3.

Scheich, C., Sievert, V., and Büssow, K. (2003). An automated method for high-throughput protein purification applied to a comparison of His-tag and GST-tag

affinity chromatography. BMC Biotechnol. *3*, 12. https://doi.org/10.1186/1472-6750-3-12.

Schmidt, T.G., and Skerra, A. (2007). The Strep-tag system for one-step purification and high-affinity detection or capturing of proteins. Nat. Protoc. *2*, 1528–1535. https://doi.org/10.1038/nprot.2007.209.

Schoenheimer, R., Ratner, S., and Rittenberg, D. (1939). Studies in protein metabolism x. the metabolic activity of body proteins investigated with l (-)-leucine containing two isotopes. J. Biol. Chem *130*, 703–732. .

Schöneberg, T., Schulz, A., Biebermann, H., Hermsdorf, T., Römpler, H., and Sangkuhl, K. (2004). Mutant G-protein-coupled receptors as a cause of human diseases. Pharmacol. Ther. *104*, 173–206. https://doi.org/10.1016/j.pharmthera.2004.08.008.

Schulman, B.A., and Harper, J.W. (2009). Ubiquitin-like protein activation by E1 enzymes: the apex for downstream signalling pathways. Nat. Rev. Mol. Cell Biol. *10*, 319–331. https://doi.org/10.1038/nrm2673.

Sell, G.L., and Margolis, S.S. (2015). From UBE3A to Angelman syndrome: a substrate perspective. Front. Neurosci. *9*. https://doi.org/10.3389/fnins.2015.00322.

Serbyn, N., Noireterre, A., Bagdiul, I., Plank, M., Michel, A.H., Loewith, R., Kornmann, B., and Stutz, F. (2020). The Aspartic Protease Ddi1 Contributes to DNA-Protein Crosslink Repair in Yeast. Mol. Cell *77*, 1066-1079.e9. https://doi.org/10.1016/j.molcel.2019.12.007.

Shaughnessy, N., Forman, E.B., O'Rourke, D., Lynch, S.A., and Lynch, B. (2020). X-linked infantile spinal muscular atrophy (SMAX2) caused by novel c.1681G>A substitution in the UBA1 gene, expanding the phenotype. Neuromuscul. Disord. NMD *30*, 35–37. https://doi.org/10.1016/j.nmd.2019.11.004.

Shekel, I., Giladi, S., Raykin, E., Weiner, M., Chalifa-Caspi, V., Lederman, D., Kofman, O., and Golan, H.M. (2021). Isolation-Induced Ultrasonic Vocalization in Environmental and Genetic Mice Models of Autism. Front. Neurosci. *15,* 769670. doi: 10.3389/fnins.2021.769670.

Shimoji, T., Murakami, K., Sugiyama, Y., Matsuda, M., Inubushi, S., Nasu, J., Shirakura, M., Suzuki, T., Wakita, T., Kishino, T., et al. (2009). Identification of annexin A1 as a novel substrate for E6AP-mediated ubiquitylation. J. Cell. Biochem. *106*, 1123–1135. https://doi.org/10.1002/jcb.22096.

Shimura, H., Hattori, N., Kubo, S. i, Mizuno, Y., Asakawa, S., Minoshima, S., Shimizu, N., Iwai, K., Chiba, T., Tanaka, K., et al. (2000). Familial Parkinson disease gene product, parkin, is a ubiquitin-protein ligase. Nat. Genet. *25*, 302–305. https://doi.org/10.1038/77060.

Silva-Santos, S., van Woerden, G.M., Bruinsma, C.F., Mientjes, E., Jolfaei, M.A., Distel, B., Kushner, S.A., and Elgersma, Y. (2015). Ube3a reinstatement identifies distinct developmental windows in a murine Angelman syndrome model. J. Clin. Invest. *125*, 2069–2076. https://doi.org/10.1172/JCI80554.

Simchi, L., and Kaphzan, H. (2021). Aberrant aggressive behavior in a mouse model of Angelman syndrome. Sci. Rep. *11*, 1–12. https://doi.org/10.1038/s41598-020-79984-7.

Sims, J.J., and Cohen, R.E. (2009). Linkage-specific avidity defines the lysine 63-linked polyubiquitin binding preference of Rap80. Mol. Cell *33*, 775–783. https://doi.org/10.1016/j.molcel.2009.02.011.

Singhmar, P., and Kumar, A. (2011). Angelman Syndrome Protein UBE3A Interacts with Primary Microcephaly Protein ASPM, Localizes to Centrosomes and Regulates Chromosome Segregation. PLoS ONE *6*. https://doi.org/10.1371/journal.pone.0020397.

Sirkis, R., Gerst, J.E., and Fass, D. (2006). Ddi1, a Eukaryotic Protein With the Retroviral Protease Fold. J. Mol. Biol. *364*, 376–387. https://doi.org/10.1016/j.jmb.2006.08.086.

Sirois, C.L., Bloom, J.E., Fink, J.J., Gorka, D., Keller, S., Germain, N.D., Levine, E.S., and Chamberlain, S.J. (2020). Abundance and localization of human UBE3A protein isoforms. BioRxiv 2020.03.30.016857. https://doi.org/10.1101/2020.03.30.016857.

Sivá, M., Svoboda, M., Veverka, V., Trempe, J.F., Hofmann, K., Kožíšek, M., Hexnerová, R., Sedlák, F., Belza, J., Brynda, J., et al. (2016). Human DNA-Damage-Inducible 2 Protein Is Structurally and Functionally Distinct from Its Yeast Ortholog. Sci. Rep. *6*. https://doi.org/10.1038/srep30443.

Smith, S.E.P., Zhou, Y.D., Zhang, G., Jin, Z., Stoppel, D.C., and Anderson, M.P. (2011). Increased gene dosage of Ube3a results in autism traits and decreased glutamate synaptic transmission in mice. Sci. Transl. Med. *3*, 103ra97. https://doi.org/10.1126/scitranslmed.3002627.

Song, O., and Fields, S. (1989). A novel genetic system to detect protein-protein interactions. Nature *340*. https://doi.org/10.1038/340245a0.

Sonzogni, M., Wallaard, I., Santos, S.S., Kingma, J., du Mee, D., van Woerden, G.M., and Elgersma, Y. (2018). A behavioral test battery for mouse models of Angelman syndrome: a powerful tool for testing drugs and novel Ube3a mutants. Mol. Autism *9*. https://doi.org/10.1186/s13229-018-0231-7.

Sousa, R. (1995). Use of glycerol, polyols and other protein structure stabilizing agents in protein crystallization. Acta Crystallogr. D Biol. Crystallogr. *51*, 271–277. https://doi.org/10.1107/S0907444994014009.

Spit, M., Rieser, E., and Walczak, H. (2019). Linear ubiquitination at a glance. J. Cell Sci. *132*. https://doi.org/10.1242/jcs.208512.

Spriestersbach, A., Kubicek, J., Schäfer, F., Block, H., and Maertens, B. (2015). Chapter One - Purification of His-Tagged Proteins. In Methods in Enzymology, J.R. Lorsch, ed. (Academic Press), pp. 1–15.

Spruyt, K., Braam, W., and Curfs, L.MG. (2018). Sleep in Angelman syndrome: A review of evidence. Sleep Med. Rev. *37*, 69–84. https://doi.org/10.1016/j.smrv.2017.01.002.

Stahl, E.A., Raychaudhuri, S., Remmers, E.F., Xie, G., Eyre, S., Thomson, B.P., Li, Y., Kurreeman, F.A.S., Zhernakova, A., Hinks, A., et al. (2010). Genome-wide

association study meta-analysis identifies seven new rheumatoid arthritis risk loci. Nat. Genet. *42*, 508–514. https://doi.org/10.1038/ng.582.

Starnawska, A., Demontis, D., McQuillin, A., O'Brien, N.L., Staunstrup, N.H., Mors, O., Nielsen, A.L., Børglum, A.D., and Nyegaard, M. (2016). Hypomethylation of FAM63B in bipolar disorder patients. Clin. Epigenetics *8*, 52. https://doi.org/10.1186/s13148-016-0221-6.

Steen, H., and Mann, M. (2004). The ABC's (and XYZ's) of peptide sequencing. Nat. Rev. Mol. Cell Biol. *5*, 699–711. https://doi.org/10.1038/nrm1468.

Stegmeier, F., Rape, M., Draviam, V.M., Nalepa, G., Sowa, M.E., Ang, X.L., McDonald, E.R., Li, M.Z., Hannon, G.J., Sorger, P.K., et al. (2007). Anaphase initiation is regulated by antagonistic ubiquitination and deubiquitination activities. Nature *446*, 876–881. https://doi.org/10.1038/nature05694.

Steinhauer, W.R., Walsh, R.C., and Kalfayan, L.J. (1989). Sequence and structure of the Drosophila melanogaster ovarian tumor gene and generation of an antibody specific for the ovarian tumor protein. Mol. Cell. Biol. *9*, 5726–5732. .

Stenberg, K.A.E., Riikonen, P.T., and Vihinen, M. (2000). KinMutBase, a database of human disease-causing protein kinase mutations. Nucleic Acids Res. *28*, 369–371. .

Stessman, H.A.F., Xiong, B., Coe, B.P., Wang, T., Hoekzema, K., Fenckova, M., Kvarnung, M., Gerdts, J., Trinh, S., Cosemans, N., et al. (2017). Targeted sequencing identifies 91 neurodevelopmental disorder risk genes with autism and developmental disability biases. Nat. Genet. *49*, 515–526. https://doi.org/10.1038/ng.3792.

Stoltze, L., Schirle, M., Schwarz, G., Schröter, C., Thompson, M.W., Hersh, L.B., Kalbacher, H., Stevanovic, S., Rammensee, H.G., and Schild, H. (2000). Two new proteases in the MHC class I processing pathway. Nat. Immunol. *1*, 413–418. https://doi.org/10.1038/80852.

Sun, S.C. (2008). Deubiquitylation and regulation of the immune response. Nat. Rev. Immunol. *8*, 501–511. https://doi.org/10.1038/nri2337.

Sun, H., Kapuria, V., Peterson, L.F., Fang, D., Bornmann, W.G., Bartholomeusz, G., Talpaz, M., and Donato, N.J. (2011). Bcr-Abl ubiquitination and Usp9x inhibition block kinase signaling and promote CML cell apoptosis. Blood *117*, 3151–3162. https://doi.org/10.1182/blood-2010-03-276477.

Sun, J., Liu, Y., Jia, Y., Hao, X., Lin, W. ju, Tran, J., Lynch, G., Baudry, M., and Bi, X. (2018). UBE3A-mediated p18/LAMTOR1 ubiquitination and degradation regulate mTORC1 activity and synaptic plasticity. ELife *7*, e37993. https://doi.org/10.7554/eLife.37993.

Suresh, B., Lee, J., Kim, H., and Ramakrishna, S. (2016). Regulation of pluripotency and differentiation by deubiquitinating enzymes. Cell Death Differ. *23*, 1257–1264. https://doi.org/10.1038/cdd.2016.53.

Suszynska-Zajczyk, J., Łuczak, M., Marczak, Ł., and Jakubowski, H. (2014). Hyperhomocysteinemia and Bleomycin Hydrolase Modulate the Expression of Mouse Brain Proteins Involved in Neurodegeneration. J. Alzheimers Dis. *40*, 713–726. https://doi.org/10.3233/JAD-132033.

Swatek, K.N., and Komander, D. (2016). Ubiquitin modifications. Cell Res. *26*, 399–422. https://doi.org/10.1038/cr.2016.39.

Tan, W.H., and Bird, L.M. (2017). Pharmacological therapies for Angelman syndrome. Wien. Med. Wochenschr. *167*, 205–218. https://doi.org/10.1007/s10354-015-0408-z.

Tan, W.H., Bacino, C.A., Skinner, S.A., Anselm, I., Barbieri-Welge, R., Bauer-Carlin, A., Beaudet, A.L., Bichell, T.J., Gentile, J.K., Glaze, D.G., et al. (2011). Angelman Syndrome: Mutations Influence Features in Early Childhood. Am. J. Med. Genet. A. *155A*, 81–90. https://doi.org/10.1002/ajmg.a.33775.

Terentiev, A.A., Moldogazieva, N.T., and Shaitan, K.V. (2009). Dynamic proteomics in modeling of the living cell. Protein-protein interactions. Biochem. Mosc. *74*, 1586–1607. https://doi.org/10.1134/S0006297909130112.

Terrell, J., Shih, S., Dunn, R., and Hicke, L. (1998). A Function for Monoubiquitination in the Internalization of a G Protein–Coupled Receptor. Mol. Cell *1*, 193–202. https://doi.org/10.1016/S1097-2765(00)80020-9.

Thibaudeau, T.A., Anderson, R.T., and Smith, D.M. (2018). A common mechanism of proteasome impairment by neurodegenerative disease-associated oligomers. Nat. Commun. *9*, 1097. https://doi.org/10.1038/s41467-018-03509-0.

Thomas, M., and Banks, L. (1998). Inhibition of Bak-induced apoptosis by HPV-18 E6. Oncogene *17*, 2943–2954. https://doi.org/10.1038/sj.onc.1202223.

Thrower, J.S., Hoffman, L., Rechsteiner, M., and Pickart, C.M. (2000). Recognition of the polyubiquitin proteolytic signal. EMBO J. *19*, 94–102. https://doi.org/10.1093/emboj/19.1.94.

Tirard, M., Hsiao, H.H., Nikolov, M., Urlaub, H., Melchior, F., and Brose, N. (2012). In vivo localization and identification of SUMOylated proteins in the brain of His6-HA-SUMO1 knock-in mice. Proc. Natl. Acad. Sci. U. S. A. *109*, 21122–21127. https://doi.org/10.1073/pnas.1215366110.

Tokunaga, F., Sakata, S., Saeki, Y., Satomi, Y., Kirisako, T., Kamei, K., Nakagawa, T., Kato, M., Murata, S., Yamaoka, S., et al. (2009). Involvement of linear polyubiquitylation of NEMO in NF-κB activation. Nat. Cell Biol. *11*, 123–132. https://doi.org/10.1038/ncb1821.

Tomko, R.J., and Hochstrasser, M. (2013). Molecular Architecture and Assembly of the Eukaryotic Proteasome. Annu. Rev. Biochem. *82*. https://doi.org/10.1146/annurev-biochem-060410-150257.

Tomko, R.J., Funakoshi, M., Schneider, K., Wang, J., and Hochstrasser, M. (2010). Heterohexameric Ring Arrangement of the Eukaryotic Proteasomal ATPases: Implications for Proteasome Structure and Assembly. Mol. Cell *38*, 393–403. https://doi.org/10.1016/j.molcel.2010.02.035.

Tonazzini, I., Van Woerden, G.M., Masciullo, C., Mientjes, E.J., Elgersma, Y., and Cecchini, M. (2019). The role of ubiquitin ligase E3A in polarized contact guidance and rescue strategies in UBE3A-deficient hippocampal neurons. Mol. Autism *10*, 41. https://doi.org/10.1186/s13229-019-0293-1.

Tong, L. (2013). Structure and function of biotin-dependent carboxylases. Cell. Mol. Life Sci. CMLS *70*, 863–891. https://doi.org/10.1007/s00018-012-1096-0.

Traven, A., Jelicic, B., and Sopta, M. (2006). Yeast Gal4: a transcriptional paradigm revisited. EMBO Rep. *7*, 496–499. https://doi.org/10.1038/sj.embor.7400679.

Trempe, J.F., Brown, N.R., Lowe, E.D., Gordon, C., Campbell, I.D., Noble, M.E.M., and Endicott, J.A. (2005). Mechanism of Lys48-linked polyubiquitin chain recognition by the Mud1 UBA domain. EMBO J. https://doi.org/10.1038/sj.emboj.7600797.

Triono, A., Iskandar, K., Nugrahanto, A.P., Hadiyanto, M.L., Gunadi, and Herini, E.S. (2021). The role of whole exome sequencing in the UBE3A point mutation of Angelman Syndrome: A case report. Ann. Med. Surg. *73*, 103170. https://doi.org/10.1016/j.amsu.2021.103170.

Tsirigotis, M., Zhang, M., Chiu, R.K., Wouters, B.G., and Gray, D.A. (2001). Sensitivity of Mammalian Cells Expressing Mutant Ubiquitin to Protein-damaging Agents. J. Biol. Chem. *276*, 46073–46078. https://doi.org/10.1074/jbc.M109023200.

Tsuda, L., and Lim, Y.-M. (2018). Alzheimer's Disease Model System Using Drosophila. Adv. Exp. Med. Biol. *1076*, 25–40. https://doi.org/10.1007/978-981-13-0529-0_3.

Tsurusaki, Y., Ohashi, I., Enomoto, Y., Naruto, T., Mitsui, J., Aida, N., and Kurosawa, K. (2017). A novel UBE2A mutation causes X-linked intellectual disability type Nascimento. Hum. Genome Var. *4*, 17019. https://doi.org/10.1038/hgv.2017.19.

van Twest, S., Murphy, V.J., Hodson, C., Tan, W., Swuec, P., O'Rourke, J.J., Heierhorst, J., Crismani, W., and Deans, A.J. (2017). Mechanism of Ubiquitination and Deubiquitination in the Fanconi Anemia Pathway. Mol. Cell *65*, 247–259. https://doi.org/10.1016/j.molcel.2016.11.005.

Tyanova, S., Temu, T., Sinitcyn, P., Carlson, A., Hein, M.Y., Geiger, T., Mann, M., and Cox, J. (2016). The Perseus computational platform for comprehensive analysis of (prote)omics data. Nat. Methods *13*, 731–740. https://doi.org/10.1038/nmeth.3901.

Udeshi, N.D., Svinkina, T., Mertins, P., Kuhn, E., Mani, D.R., Qiao, J.W., and Carr, S.A. (2013). Refined preparation and use of anti-diglycine remnant (K-ε-GG) antibody enables routine quantification of 10,000s of ubiquitination sites in single proteomics experiments. Mol. Cell. Proteomics MCP *12*, 825–831. https://doi.org/10.1074/mcp.O112.027094.

Ugur, B., Chen, K., and Bellen, H.J. (2016). Drosophila tools and assays for the study of human diseases. Dis. Model. Mech. *9*, 235–244. https://doi.org/10.1242/dmm.023762.

Uhlén, M., Fagerberg, L., Hallström, B.M., Lindskog, C., Oksvold, P., Mardinoglu, A., Sivertsson, Å., Kampf, C., Sjöstedt, E., Asplund, A., et al. (2015). Proteomics. Tissue-based map of the human proteome. Science *347*, 1260419. https://doi.org/10.1126/science.1260419.

Urraca, N., Cleary, J., Brewer, V., Pivnick, E.K., McVicar, K., Thibert, R.L., Schanen, N.C., Esmer, C., Lamport, D., and Reiter, L.T. (2013). The Interstitial Duplication 15q11.2-q13 Syndrome Includes Autism, Mild Facial Anomalies and a Characteristic EEG Signature. Autism Res. *6*, 268–279. https://doi.org/10.1002/aur.1284.

Valdez, C., Scroggs, R., Chassen, R., and Reiter, L.T. (2015). Variation in Dube3a expression affects neurotransmission at the Drosophila neuromuscular junction. Biol. Open *4*, 776–782. https://doi.org/10.1242/bio.20148045.

Valluy, J., Bicker, S., Aksoy-Aksel, A., Lackinger, M., Sumer, S., Fiore, R., Wüst, T., Seffer, D., Metge, F., Dieterich, C., et al. (2015). A coding-independent function of an alternative Ube3a transcript during neuronal development. Nat. Neurosci. *18*, 666–673. https://doi.org/10.1038/nn.3996.

van Ooijen, G., Dixon, L.E., Troein, C., and Millar, A.J. (2011). Proteasome Function Is Required for Biological Timing throughout the Twenty-Four Hour Cycle. Curr. Biol. *21*, 869–875. https://doi.org/10.1016/j.cub.2011.03.060.

Varnaitė, R., and MacNeill, S.A. (2016). Meet the neighbors: Mapping local protein interactomes by proximity-dependent labeling with BioID. Proteomics *16*, 2503–2518. https://doi.org/10.1002/pmic.201600123.

Vasilescu, J., Smith, J.C., Ethier, M., and Figeys, D. (2005). Proteomic analysis of ubiquitinated proteins from human MCF-7 breast cancer cells by immunoaffinity purification and mass spectrometry. J. Proteome Res. *4*, 2192–2200. https://doi.org/10.1021/pr050265i.

Vatsa, N., and Jana, N.R. (2018). UBE3A and Its Link With Autism. Front. Mol. Neurosci. *11*. https://doi.org/10.3389/fnmol.2018.00448.

Verbrugge, S.E., Scheper, R.J., Lems, W.F., de Gruijl, T.D., and Jansen, G. (2015). Proteasome inhibitors as experimental therapeutics of autoimmune diseases. Arthritis Res. Ther. *17*. https://doi.org/10.1186/s13075-015-0529-1.

Verma, R. (2002). Role of Rpn11 Metalloprotease in Deubiquitination and Degradation by the 26S Proteasome. Science *298*, 611–615. https://doi.org/10.1126/science.1075898.

Verma, V., Paul, A., Amrapali Vishwanath, A., Vaidya, B., and Clement, J.P. (2019). Understanding intellectual disability and autism spectrum disorders from common mouse models: synapses to behaviour. Open Biol. *9*, 180265. https://doi.org/10.1098/rsob.180265.

Vila, I.K., Yao, Y., Kim, G., Xia, W., Kim, H., Kim, S.J., Park, M.K., Hwang, J.P., Billalabeitia, E.G., Hung, M.-C., et al. (2017). A UBE2O-AMPKα2 Axis That Promotes Tumor Initiation and Progression Offers Opportunities for Therapy. Cancer Cell *31*, 208–224. https://doi.org/10.1016/j.ccell.2017.01.003.

Vu, T.H., and Hoffman, A.R. (1997). Imprinting of the Angelman syndrome gene, UBE3A , is restricted to brain. Nat. Genet. *17*, 12–13. https://doi.org/10.1038/ng0997-12.

Wagner, S.A., Beli, P., Weinert, B.T., Nielsen, M.L., Cox, J., Mann, M., and Choudhary, C. (2011). A Proteome-wide, Quantitative Survey of In Vivo Ubiquitylation Sites Reveals Widespread Regulatory Roles. Mol. Cell. Proteomics MCP *10*. https://doi.org/10.1074/mcp.M111.013284.

Wagner, S.A., Beli, P., Weinert, B.T., Schölz, C., Kelstrup, C.D., Young, C., Nielsen, M.L., Olsen, J.V., Brakebusch, C., and Choudhary, C. (2012). Proteomic analyses reveal

divergent ubiquitylation site patterns in murine tissues. Mol. Cell. Proteomics MCP *11*, 1578–1585. https://doi.org/10.1074/mcp.M112.017905.

Wang, M., and Pickart, C.M. (2005). Different HECT domain ubiquitin ligases employ distinct mechanisms of polyubiquitin chain synthesis. EMBO J. *24*, 4324–4333. https://doi.org/10.1038/sj.emboj.7600895.

Wang, B., Zeng, L., Merillat, S.A., Fischer, S., Ochaba, J., Thompson, L.M., Barmada, S.J., Scaglione, K.M., and Paulson, H.L. (2018a). The ubiquitin conjugating enzyme Ube2W regulates solubility of the Huntington's disease protein, huntingtin. Neurobiol. Dis. *109*, 127–136. https://doi.org/10.1016/j.nbd.2017.10.002.

Wang, J., Lou, S.S., Wang, T., Wu, R.J., Li, G., Zhao, M., Lu, B., Li, Y.Y., Zhang, J., Cheng, X., et al. (2019). UBE3A-mediated PTPA ubiquitination and degradation regulate PP2A activity and dendritic spine morphology. Proc. Natl. Acad. Sci. U. S. A. *116*, 12500–12505. https://doi.org/10.1073/pnas.1820131116.

Wang, M., Dai, W., Ke, Z., and Li, Y. (2020a). Functional roles of E3 ubiquitin ligases in gastric cancer (Review). Oncol. Lett. *20*, 1–1. https://doi.org/10.3892/ol.2020.11883.

Wang, P.Y., Chang, K.T., Lin, Y.M., Kuo, T.Y., and Wang, G.S. (2018b). Ubiquitination of MBNL1 Is Required for Its Cytoplasmic Localization and Function in Promoting Neurite Outgrowth. Cell Rep. *22*, 2294–2306. https://doi.org/10.1016/j.celrep.2018.02.025.

Wang, X., Herr, R.A., and Hansen, T.H. (2012). Ubiquitination of Substrates by Esterification. Traffic Cph. Den. *13*, 19–24. https://doi.org/10.1111/j.1600-0854.2011.01269.x.

Wang, X., Meul, T., and Meiners, S. (2020b). Exploring the proteasome system: A novel concept of proteasome inhibition and regulation. Pharmacol. Ther. 107526. https://doi.org/10.1016/j.pharmthera.2020.107526.

Wanker, E.E., Ast, A., Schindler, F., Trepte, P., and Schnoegl, S. (2019). The pathobiology of perturbed mutant huntingtin protein-protein interactions in Huntington's disease. J. Neurochem. *151*, 507–519. https://doi.org/10.1111/jnc.14853.

Wauer, T., and Komander, D. (2014). The JAMM in the proteasome. Nat. Struct. Mol. Biol. *21*, 346–348. https://doi.org/10.1038/nsmb.2800.

Wertz, I.E., and Murray, J.M. (2019). Structurally-defined deubiquitinase inhibitors provide opportunities to investigate disease mechanisms. Drug Discov. Today Technol. *31*, 109–123. https://doi.org/10.1016/j.ddtec.2019.02.003.

Weston, K.P., Gao, X., Zhao, J., Kim, K.S., Maloney, S.E., Gotoff, J., Parikh, S., Leu, Y.C., Wu, K.P., Shinawi, M., et al. (2021). Identification of disease-linked hyperactivating mutations in UBE3A through large-scale functional variant analysis. Nat. Commun. *12*, 6809. https://doi.org/10.1038/s41467-021-27156-0.

Whitcomb, E.A., Tsai, Y.C., Basappa, J., Liu, K., Le Feuvre, A.K., Weissman, A.M., and Taylor, A. (2019). Stabilization of p27Kip1/CDKN1B by UBCH7/UBE2L3 catalyzed ubiquitinylation: a new paradigm in cell-cycle control. FASEB J. Off. Publ. Fed. Am. Soc. Exp. Biol. *33*, 1235–1247. https://doi.org/10.1096/fj.201800960R.

White, R.E., Dickinson, J.R., Semple, C.A.M., Powell, D.J., and Berry, C. (2011). The retroviral proteinase active site and the N-terminus of Ddi1 are required for repression of protein secretion. FEBS Lett. *585*, 139–142. https://doi.org/10.1016/j.febslet.2010.11.026.

Wickliffe, K.E., Williamson, A., Meyer, H.J., Kelly, A., and Rape, M. (2011). K11-linked ubiquitin chains as novel regulators of cell division. Trends Cell Biol. *21*, 656–663. https://doi.org/10.1016/j.tcb.2011.08.008.

Wijk, S.J.L., and Timmers, H.T.M. (2010). The family of ubiquitin-conjugating enzymes (E2s): deciding between life and death of proteins. FASEB J. *24*, 981–993. https://doi.org/10.1096/fj.09-136259.

Wilfert, A.B., Turner, T.N., Murali, S.C., Hsieh, P., Sulovari, A., Wang, T., Coe, B.P., Guo, H., Hoekzema, K., Bakken, T.E., et al. (2021). Recent ultra-rare inherited variants implicate new autism candidate risk genes. Nat. Genet. *53*, 1125–1134. https://doi.org/10.1038/s41588-021-00899-8.

Wilkinson, K.D., Urban, M.K., and Haas, A.L. (1980). Ubiquitin is the ATP-dependent proteolysis factor I of rabbit reticulocytes. J. Biol. Chem. *255*, 7529–7532. .

Williams, C.A., Beaudet, A.L., Clayton-Smith, J., Knoll, J.H., Kyllerman, M., Laan, L.A., Magenis, R.E., Moncla, A., Schinzel, A.A., Summers, J.A., et al. (2006). Angelman syndrome 2005: Updated consensus for diagnostic criteria. Am. J. Med. Genet. A. *140A*, 413–418. https://doi.org/10.1002/ajmg.a.31074.

Williams, C.A., Driscoll, D.J., and Dagli, A.I. (2010). Clinical and genetic aspects of Angelman syndrome. Genet. Med. Off. J. Am. Coll. Med. Genet. *12*, 385–395. https://doi.org/10.1097/GIM.0b013e3181def138.

Wójcik, C., and DeMartino, G.N. (2003). Intracellular localization of proteasomes. Int. J. Biochem. Cell Biol. *35*, 579–589. https://doi.org/10.1016/s1357-2725(02)00380-1.

Woolfe, G., and Macdonald, A.D. (1944). The Evaluation of the Analgesic Action of Pethidine Hydrochloride (demerol). J. Pharmacol. Exp. Ther. *80*, 300–307. .

Wu, H., Li, L., Chen, K.M., Homolka, D., Gos, P., Fleury-Olela, F., McCarthy, A.A., and Pillai, R.S. (2019a). Decapping Enzyme NUDT12 Partners with BLMH for Cytoplasmic Surveillance of NAD-Capped RNAs. Cell Rep. *29*, 4422-4434.e13. https://doi.org/10.1016/j.celrep.2019.11.108.

Wu, X., Lei, C., Xia, T., Zhong, X., Yang, Q., and Shu, H.B. (2019b). Regulation of TRIF-mediated innate immune response by K27-linked polyubiquitination and deubiquitination. Nat. Commun. *10*, 4115. https://doi.org/10.1038/s41467-019-12145-1.

Wu, Y., Bolduc, F.V., Bell, K., Tully, T., Fang, Y., Sehgal, A., and Fischer, J.A. (2008). A Drosophila model for Angelman syndrome. Proc. Natl. Acad. Sci. U. S. A. *105*, 12399–12404. https://doi.org/10.1073/pnas.0805291105.

Xia, Q., Li, X., Zhou, H., Zheng, L., and Shi, J. (2018). S100A11 protects against neuronal cell apoptosis induced by cerebral ischemia via inhibiting the nuclear translocation of annexin A1. Cell Death Dis. *9*, 657. https://doi.org/10.1038/s41419-018-0686-7.

Xiao, F., Lin, X., Tian, J., Wang, X., Chen, Q., Rui, K., Ma, J., Wang, S., Wang, Q., Wang, X., et al. (2017). Proteasome inhibition suppresses Th17 cell generation and ameliorates autoimmune development in experimental Sjögren's syndrome. Cell. Mol. Immunol. *14*, 924–934. https://doi.org/10.1038/cmi.2017.8.

Xiao, Y., Wu, Q.Q., Duan, M.X., Liu, C., Yuan, Y., Yang, Z., Liao, H.H., Fan, D., and Tang, Q.Z. (2018). TAX1BP1 overexpression attenuates cardiac dysfunction and remodeling in STZ-induced diabetic cardiomyopathy in mice by regulating autophagy. Biochim. Biophys. Acta Mol. Basis Dis. *1864*, 1728–1743. https://doi.org/10.1016/j.bbadis.2018.02.012.

Xiong, W., Zhang, B., Yu, H., Zhu, L., Yi, L., and Jin, X. (2021). RRM2 Regulates Sensitivity to Sunitinib and PD-1 Blockade in Renal Cancer by Stabilizing ANXA1 and Activating the AKT Pathway. Adv. Sci. *8*, 2100881. https://doi.org/10.1002/advs.202100881.

Xu, G., Paige, J.S., and Jaffrey, S.R. (2010a). Global analysis of lysine ubiquitination by ubiquitin remnant immunoaffinity profiling. Nat. Biotechnol. *28*, 868–873. https://doi.org/10.1038/nbt.1654.

Xu, G.W., Ali, M., Wood, T.E., Wong, D., Maclean, N., Wang, X., Gronda, M., Skrtic, M., Li, X., Hurren, R., et al. (2010b). The ubiquitin-activating enzyme E1 as a therapeutic target for the treatment of leukemia and multiple myeloma. Blood *115*, 2251–2259. https://doi.org/10.1182/blood-2009-07-231191.

Xu, P., Duong, D.M., Seyfried, N.T., Cheng, D., Xie, Y., Robert, J., Rush, J., Hochstrasser, M., Finley, D., and Peng, J. (2009). Quantitative proteomics reveals the function of unconventional ubiquitin chains in proteasomal degradation. Cell *137*, 133–145. https://doi.org/10.1016/j.cell.2009.01.041.

Xu, X., Li, C., Gao, X., Xia, K., Guo, H., Li, Y., Hao, Z., Zhang, L., Gao, D., Xu, C., et al. (2018). Excessive UBE3A dosage impairs retinoic acid signaling and synaptic plasticity in autism spectrum disorders. Cell Res. *28*, 48–68. https://doi.org/10.1038/cr.2017.132.

Yamamoto, Y., Huibregtse, J.M., and Howley, P.M. (1997). The HumanE6-APGene (UBE3A) Encodes Three Potential Protein Isoforms Generated by Differential Splicing. Genomics *41*, 263–266. https://doi.org/10.1006/geno.1997.4617.

Yang, Y., Kitagaki, J., Dai, R.-M., Tsai, Y.C., Lorick, K.L., Ludwig, R.L., Pierre, S.A., Jensen, J.P., Davydov, I.V., Oberoi, P., et al. (2007). Inhibitors of ubiquitin-activating enzyme (E1), a new class of potential cancer therapeutics. Cancer Res. *67*, 9472–9481. https://doi.org/10.1158/0008-5472.CAN-07-0568.

Yao, H., and Xu, J. (2020). Regulation of Cancer Immune Checkpoint: Mono- and Poly-Ubiquitination: Tags for Fate. In Regulation of Cancer Immune Checkpoints: Molecular and Cellular Mechanisms and Therapy, J. Xu, ed. (Singapore: Springer), pp. 295–324.

Yao, T., and Cohen, R.E. (2002). A cryptic protease couples deubiquitination and degradation by the proteasome. Nature *419*, 403–407. https://doi.org/10.1038/nature01071.

Yates, J.R., Ruse, C.I., and Nakorchevsky, A. (2009). Proteomics by mass spectrometry: approaches, advances, and applications. Annu. Rev. Biomed. Eng. *11*, 49–79. https://doi.org/10.1146/annurev-bioeng-061008-124934.

Yau, R.G., Doerner, K., Castellanos, E.R., Haakonsen, D.L., Werner, A., Wang, N., Yang, X.W., Martinez-Martin, N., Matsumoto, M.L., Dixit, V.M., et al. (2017). Assembly and Function of Heterotypic Ubiquitin Chains in Cell Cycle and Protein Quality Control. Cell *171*, 918-933.e20. https://doi.org/10.1016/j.cell.2017.09.040.

Ye, Y., and Rape, M. (2009). Building ubiquitin chains: E2 enzymes at work. Nat. Rev. Mol. Cell Biol. *10*, 755–764. https://doi.org/10.1038/nrm2780.

Yi, J.J., Berrios, J., Newbern, J.M., Snider, W.D., Philpot, B.D., Hahn, K.M., and Zylka, M.J. (2015). An autism-linked mutation disables phosphorylation control of UBE3A. Cell *162*, 795–807. https://doi.org/10.1016/j.cell.2015.06.045.

Yi, J.J., Paranjape, S.R., Walker, M.P., Choudhury, R., Wolter, J.M., Fragola, G., Emanuele, M.J., Major, M.B., and Zylka, M.J. (2017). The autism-linked UBE3A T485A mutant E3 ubiquitin ligase activates the Wnt/β-catenin pathway by inhibiting the proteasome. J. Biol. Chem. *292*, 12503–12515. https://doi.org/10.1074/jbc.M117.788448.

Yin, Q., Han, T., Fang, B., Zhang, G., Zhang, C., Roberts, E.R., Izumi, V., Zheng, M., Jiang, S., Yin, X., et al. (2019). K27-linked ubiquitination of BRAF by ITCH engages cytokine response to maintain MEK-ERK signaling. Nat. Commun. *10*. https://doi.org/10.1038/s41467-019-09844-0.

Yip, M.C.J., Bodnar, N.O., and Rapoport, T.A. (2020). Ddi1 is a ubiquitin-dependent protease. Proc. Natl. Acad. Sci. U. S. A. *117*, 7776–7781. https://doi.org/10.1073/pnas.1902298117.

Young, M.J., Hsu, K.C., Lin, T.E., Chang, W.C., and Hung, J.J. (2019). The role of ubiquitin-specific peptidases in cancer progression. J. Biomed. Sci. *26*. https://doi.org/10.1186/s12929-019-0522-0.

Young, P., Deveraux, Q., Beal, R.E., Pickart, C.M., and Rechsteiner, M. (1998). Characterization of two polyubiquitin binding sites in the 26 S protease subunit 5a. J. Biol. Chem. *273*, 5461–5467. https://doi.org/10.1074/jbc.273.10.5461.

Yu, X.-W., Pandey, K., Katzman, A.C., and Alberini, C.M. (2020). A role for CIM6P/IGF2 receptor in memory consolidation and enhancement. ELife *9*, e54781. https://doi.org/10.7554/eLife.54781.

Yu, Y., Zhang, L., Chen, Y., Li, Y., Wang, Z., Li, G., Wang, G., and Xin, J. (2019). GroEL Protein (Heat Shock Protein 60) of Mycoplasma gallisepticum Induces Apoptosis in Host Cells by Interacting with Annexin A2. Infect. Immun. *87*. https://doi.org/10.1128/IAI.00248-19.

Yuan, T., Yan, F., Ying, M., Cao, J., He, Q., Zhu, H., and Yang, B. (2018). Inhibition of Ubiquitin-Specific Proteases as a Novel Anticancer Therapeutic Strategy. Front. Pharmacol. *9*. https://doi.org/10.3389/fphar.2018.01080.

Zaaroor-Regev, D., de Bie, P., Scheffner, M., Noy, T., Shemer, R., Heled, M., Stein, I., Pikarsky, E., and Ciechanover, A. (2010). Regulation of the polycomb protein

Ring1B by self-ubiquitination or by E6-AP may have implications to the pathogenesis of Angelman syndrome. Proc. Natl. Acad. Sci. U. S. A. *107*, 6788–6793. https://doi.org/10.1073/pnas.1003108107.

Zeng, C., Zhao, C., Ge, F., Li, Y., Cao, J., Ying, M., Lu, J., He, Q., Yang, B., Dai, X., et al. (2020). Machado-Joseph Deubiquitinases: From Cellular Functions to Potential Therapy Targets. Front. Pharmacol. *11*. https://doi.org/10.3389/fphar.2020.01311.

Zhang, D., Raasi, S., and Fushman, D. (2008). Affinity makes the difference: non-selective interaction of the UBA domain of ubiquilin-1 with monomeric ubiquitin and polyubiquitin chains. J. Mol. Biol. *377*, 162–180. https://doi.org/10.1016/j.jmb.2007.12.029.

Zhang, L., Zhu, T., Miao, H., and Liang, B. (2021). The Calcium Binding Protein S100A11 and Its Roles in Diseases. Front. Cell Dev. Biol. *9*, 693262. https://doi.org/10.3389/fcell.2021.693262.

Zhang, X., Linder, S., and Bazzaro, M. (2020). Drug Development Targeting the Ubiquitin–Proteasome System (UPS) for the Treatment of Human Cancers. Cancers *12*. https://doi.org/10.3390/cancers12040902.

Zhang, Y., Zhou, X., Zhao, L., Li, C., Zhu, H., Xu, L., Shan, L., Liao, X., Guo, Z., and Huang, P. (2011). UBE2W interacts with FANCL and regulates the monoubiquitination of Fanconi anemia protein FANCD2. Mol. Cells *31*, 113–122. https://doi.org/10.1007/s10059-011-0015-9.

Zhao, G.Y., Sonoda, E., Barber, L.J., Oka, H., Murakawa, Y., Yamada, K., Ikura, T., Wang, X., Kobayashi, M., Yamamoto, K., et al. (2007). A critical role for the ubiquitin-conjugating enzyme Ubc13 in initiating homologous recombination. Mol. Cell *25*, 663–675. https://doi.org/10.1016/j.molcel.2007.01.029.

Zhao, X., Zhang, R., and Yu, S. (2020). Mutation screening of the UBE3A gene in Chinese Han population with autism. BMC Psychiatry *20*, 589. https://doi.org/10.1186/s12888-020-03000-5.

Zhao, Y., Hegde, A.N., and Martin, K.C. (2003). The Ubiquitin Proteasome System Functions as an Inhibitory Constraint on Synaptic Strengthening. Curr. Biol. *13*, 887–898. https://doi.org/10.1016/S0960-9822(03)00332-4.

Zhou, Y., Chen, R., Luo, X., Zhang, W.D., and Qin, J.J. (2020). The E2 ubiquitin-conjugating enzyme UbcH5c: an emerging target in cancer and immune disorders. Drug Discov. Today https://doi.org/10.1016/j.drudis.2020.09.015.

Zhuang, J., Shirazi, F., Singh, R.K., Kuiatse, I., Wang, H., Lee, H.C., Berkova, Z., Berger, A., Hyer, M., Chattopadhyay, N., et al. (2019). Ubiquitin-activating enzyme inhibition induces an unfolded protein response and overcomes drug resistance in myeloma. Blood *133*, 1572–1584. https://doi.org/10.1182/blood-2018-06-859686.

Zientara-Rytter, K., and Subramani, S. (2019). The Roles of Ubiquitin-Binding Protein Shuttles in the Degradative Fate of Ubiquitinated Proteins in the Ubiquitin-Proteasome System and Autophagy. Cells *8*. https://doi.org/10.3390/cells8010040.

Zimny, J., Sikora, M., Guranowski, A., and Jakubowski, H. (2006). Protective mechanisms against homocysteine toxicity: the role of bleomycin hydrolase. J. Biol. Chem. *281*, 22485–22492. https://doi.org/10.1074/jbc.M603656200.

Zylka, M.J. (2020). Prenatal treatment path for angelman syndrome and other neurodevelopmental disorders. Autism Res. *13*, 11–17. https://doi.org/10.1002/aur.2203.